NAM

Special Report on the Earthquakes near Uithuizen in August, September & October 2022

Datum October 2022

Editors

An earlier version of this Special Report has been shared with SodM on Friday 7th October 2022. This version of this report covered seven earthquakes in August and September 2020 that all had their epicentre in a small area near the village of Uithuizen.

The earthquake of 11th October 2022, also with an epicentre near Uithuizen, increased the earthquake density to 0.46 earthquakes / (year * km^2). With this last earthquake the monitoring level for 'Strong Seismicity' was exceeded.

The current version of the report has been updated to include the earthquake on 11th October 2022.

Contents

Summary and Conclusions

In August, September and October 2022 eight earthquakes occurred with an epicentre in a 500m by 150 m area near the village of Uithuizen.

Despite being 9 days apart, the first two of these earthquakes had almost identical epicentres. The comparison of their source mechanism also indicated these earthquakes occurred at the same fault.

These eight earthquakes with an epicentre in a very small area had a large impact on the highest observed earthquake density. On 24th September 2022 the monitoring level of the highest earthquake density for 'increased seismicity' was exceeded, when earthquake density reached 0.38 earthquake events per (year * km^2). With the earthquake on 11th October 2022, this monitoring level reached 0.46 earthquake events per (year * km^2) exceeding the monitoring level for 'strong seismicity'.

The motions recorded for the earthquakes near Uithuizen are broadly consistent with the predictions from the empirical PGV GMPE's used in damage assessment.

1 Introduction

1.1 Reason for this Special Report

When a threshold level of the monitoring protocol is exceeded, NAM publishes a report within two weeks after the event and shared this with SodM and the ministry of Economic Affairs and Climate Policy. To date thirteen of these reports have been published.

Title	Date
Rapportage recente aardbevingen Wirdum en Garsthuizen 2016/2017	Mar 2017
Ground Motions from the M_L 2.6 Slochteren Earthquake of 27th May 2017	June 2017
Special Report on the earthquake density and activity rate following the earthquakes in Appingedam (M_L=1.8) and Scharmer (M_L=1.5) in August 2017	Sept 2017
Special Report on the Loppersum Earthquakes – December 2017	Dec 2017
Special Report on the Zeerijp Earthquake	Jan 2018
Short Special Report Exceedance Activity Rate - February 2018	Feb 2018
Special Report - Westerwijtwerd Earthquake - 22nd May 2019	May 2019
Analyse overschrijding MRP-grenswaarde Aardbevingsdichtheid 9 september 2019	Sept 2019
Analyse overschrijding aardbevingsdichtheid - 3 december 2019	Dec 2019
Special Report on the Zijldijk M_L = 2.5 Earthquake of 2nd May 2020	May 2020
Special Report on the Loppersum M_L=2.7 Earthquake of 14th June 2020	Aug 2020
Special Report on the Zeerijp Earthquake Swarm starting 4th October 2021 (with a separate supplement)	Nov 2021
Special Report on the Garrelsweer Earthquake 16th November 2021 with Magnitude ML = 3.2	Nov 2021

Table 1.1 Reports analysing remarkable events in the earthquake record.

Additionally, NAM published twice a year a half-yearly seismic monitoring report to SodM and the ministry of Economic Affairs and Climate Policy.

Title	Date
Analyse seismiciteit	Nov 2016
Rapportage Seismiciteit Groningen - November 2017	Nov 2017
Rapportage Seismiciteit Groningen - Juni 2018	July 2018
Rapportage Seismiciteit Groningen - November 2018	Nov 2018
Rapportage Seismiciteit Groningen - Mei 2019	May 2019
Rapportage Seismiciteit Groningen - November 2019	Nov 2019
Rapportage Seismiciteit Groningen - Mei 2020	Apr 2020
Rapportage Seismiciteit Groningen - November 2020	Nov 2021
Rapportage Seismiciteit Groningen - Mei 2021	June 2021
Rapportage Seismiciteit Groningen - November 2021	Nov 2021
Rapportage Seismiciteit Groningen - Mei 2022	May 2022

Table 1.2 Half-yearly surveillance reports issued by NAM to SodM and published on the NAM onderzoeksrapporten-webpage.

1.2 Content of this Special Report

The current report describes aspects of the earthquakes near Uithuizen in August, September and October 2022. On 24th September 2022 the largest earthquake density increased to 0.38 earthquake events per (year *km^2) and exceeded the monitoring level for 'increased seismicity'.

With the earthquake of 11th October 2022 also with an epicentre near Uithuizen the earthquake density increased to 0.46 earthquakes / (year * km2). With this last earthquake the monitoring level for 'Strong Seismicity' was exceeded.

2 Analysis of recent earthquakes near Uithuizen

2.1 Introduction

A total of eight earthquakes occurred near the village of Uithuizen in the Groningen field between August and October 2022, with local magnitudes ranging from 0.7 to 2.7. The largest event occurred on Saturday 24th September 2022 at 10:20 am (UTC; 12:20 local time) and is the first event of local magnitude greater than 2.5—the smallest magnitude considered in the Groningen Hazard and Risk Assessment—to occur since the 16th November 2021 M_L3.2 Zeerijp earthquake.

2.2 Event rate

Since 2014, the number of earthquakes shows a declining trend. From a peak of more than 60 earthquakes per year (with magnitude larger than 1.2 on the Richter-scale) in September and October 2011, the earthquake rate has dropped to around 10 earthquakes per year in July 2022 (Fig. 2.1). More recently it has increased to 20 earthquakes per year.

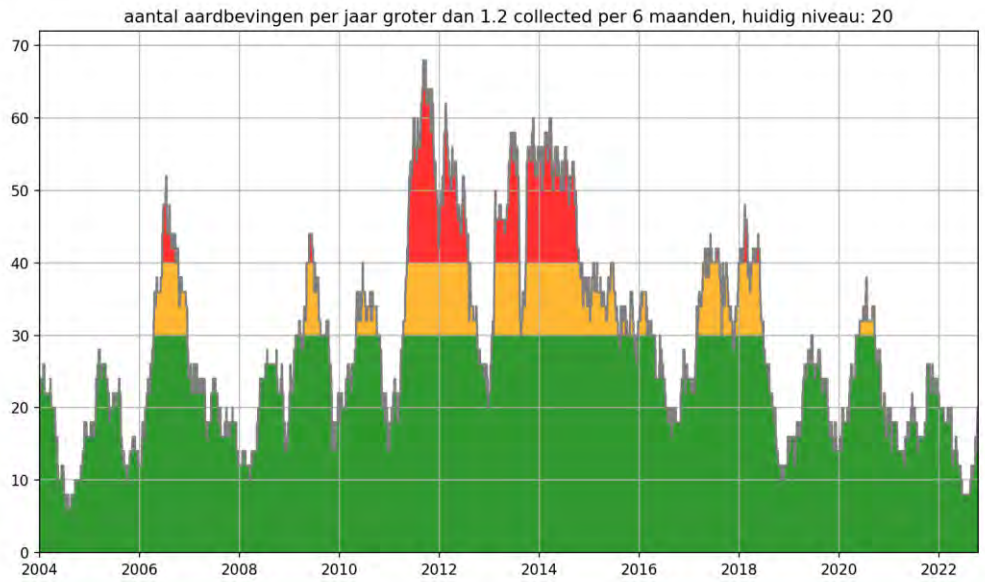

Figure 2.1 Number of earthquakes per year as stipulated in the Mijnbouwregeling artikel 1.3a.5. These are earthquakes with a magnitude larger than $M_L \geq 1,2$ during the previous 6 months converted to an annual basis.

2.3 Epicentres

In August, September and October 2022, eight earthquakes occurred with an epicentre near the village of Uithuizen. Table 2.1 lists the timing, location and magnitude of these earthquakes.

No	Date	Time	Location	Northing	Easting	Depth	Magnitude
42	11-Oct-22	15:36:40	Uithuizen	602600	241550	3050	1.3
39	24-Sep-22	11:37:30	Uithuizen	602500	241600	3250	1.7
38	24-Sep-22	10:20:39	Uithuizen	602100	241650	2950	2.7
35*	19-Sep-22	08:02:56	Uithuizen	602100	241550	2950	0.7
34	18-Sep-22	04:10:01	Uithuizen	602150	240750	3000	0.8
33	09-Sep-22	00:39:12	Uithuizen	602300	241600	3050	2.3
32	28-Aug-22	03:18:59	Uithuizen	602350	241700	3250	1.3
31	19-Aug-22	05:49:14	Uithuizen	602400	241700	3200	1.9

*very noisy result due to poor field records

Table 2.1 Timing, location and magnitude of earthquakes in August, September and October 2022 near the village of Uithuizen.

2.4 Earthquake Density

The first two of these earthquakes occurred 9 days apart, but their epicentres were separated by only 50 m. As this is within the accuracy of the determination of the epicentres, for all practical purposes, these epicentres overlap. The epicentre of the earthquake on 9th September, almost three weeks after the first earthquake, is separated from this earthquake by some 140 m. Seven of these eight earthquakes had their epicentre within a 500 by 150 area near Uithuizen (Fig. 2.4). The epicentre of the earthquake on the 18th September 2022 (with magnitude 0.8) was located at about a kilometre distance from this area. While these earthquakes are separated too far apart in time to be considered after-shocks, the close proximity of their epicentres is remarkable.

Based on the pressure equilibration currently in progress in the reservoir, the remaining earthquakes are expected to have epicentres predominantly around the village of Loppersum and the area to the North-West of Loppersum. This trend is also reflected in the observed earthquake density. Despite the lower earthquake event rate and smaller area where earthquakes occur, the decline in the maximum earthquake density is less pronounced. This is caused by the smaller area where the earthquakes occur and the observed clustering of the earthquakes in this remaining area; in October 2021 near Zeerijp (Ref. 25) and near Uithuizen.

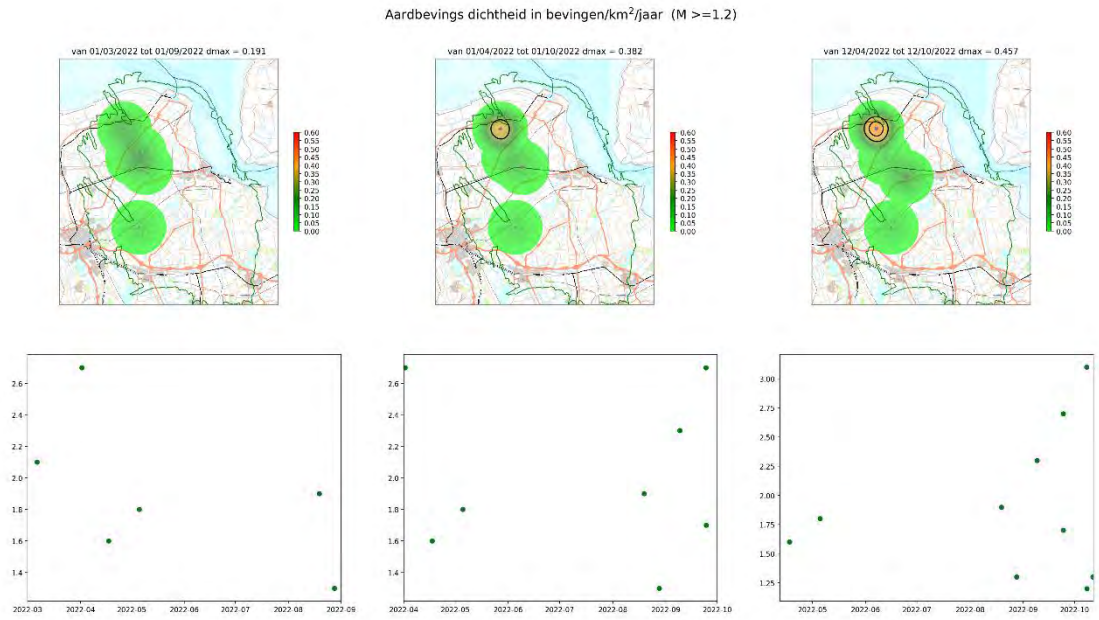

Figure 2.2 Top: Earthquake density maps for earthquakes with a magnitude larger ML ≥ 1,2 during the previous six months. The earthquake density is shown as an annual density. Bottom: Graphs of earthquake magnitude versus date. Left map shows the earthquake density at 1st September 2022. The middle map shows earthquake density at 1st October 2022 and the right map at 12st October 2022.

On 24th September 2022 the monitoring level of the highest earthquake density for 'increased seismicity' was exceeded, when earthquake density reached 0.38 earthquake events per (year * km^2). This monitoring level increased on 11th October 2022 to 0.46 earthquake events per (year * km^2), exceeding the monitoring level for 'strong seismicity'.

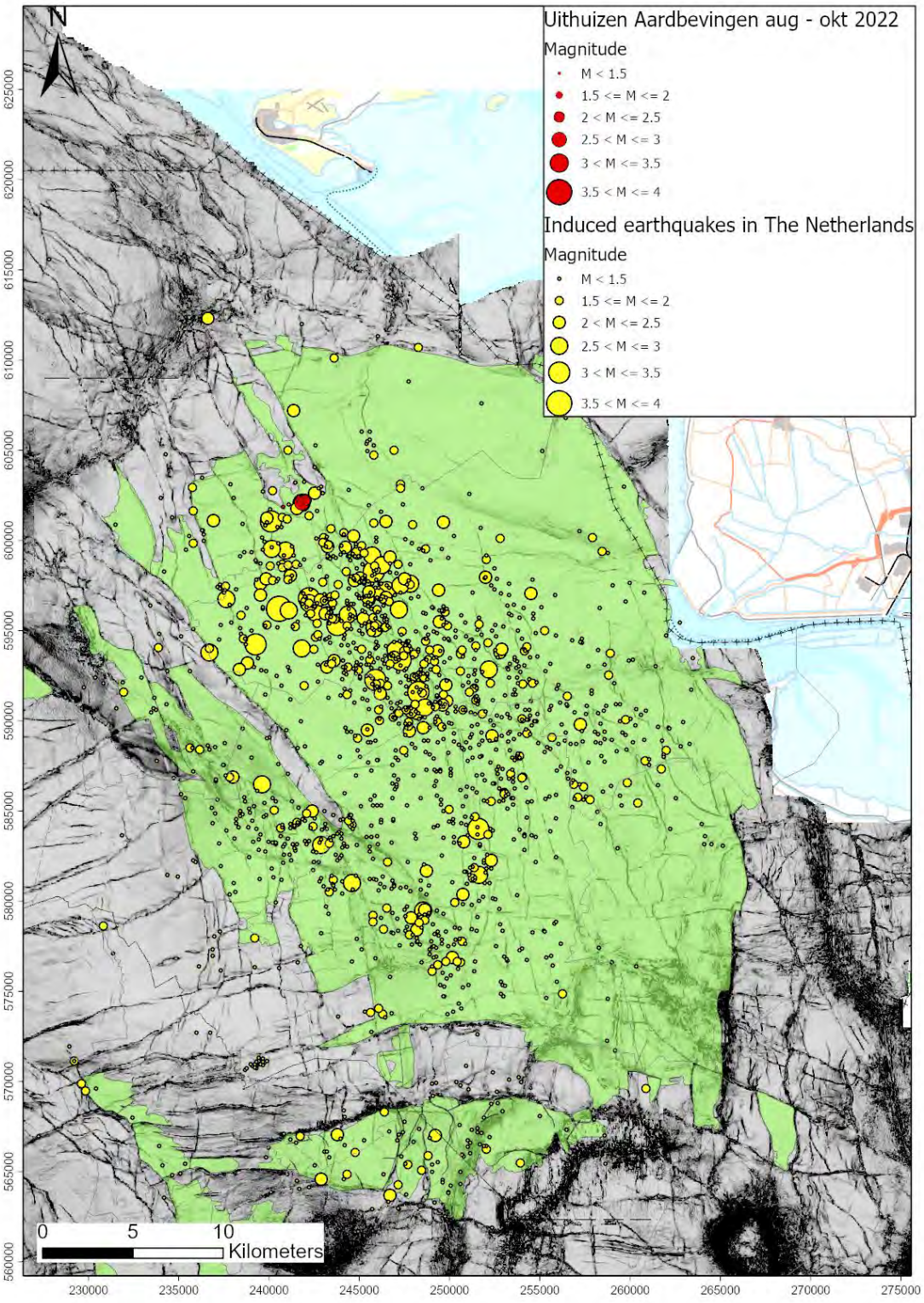

Figure 2.3 Map of the deep subsurface with in green the Groningen gas field and surrounding gas fields. The red dot shows the location of the earthquake near Uithuizen on 9th September 2022. All other earthquakes before 1st September 2022 have been indicated as yellow dots. The size of the dot is an indication of the magnitude of the earthquake.

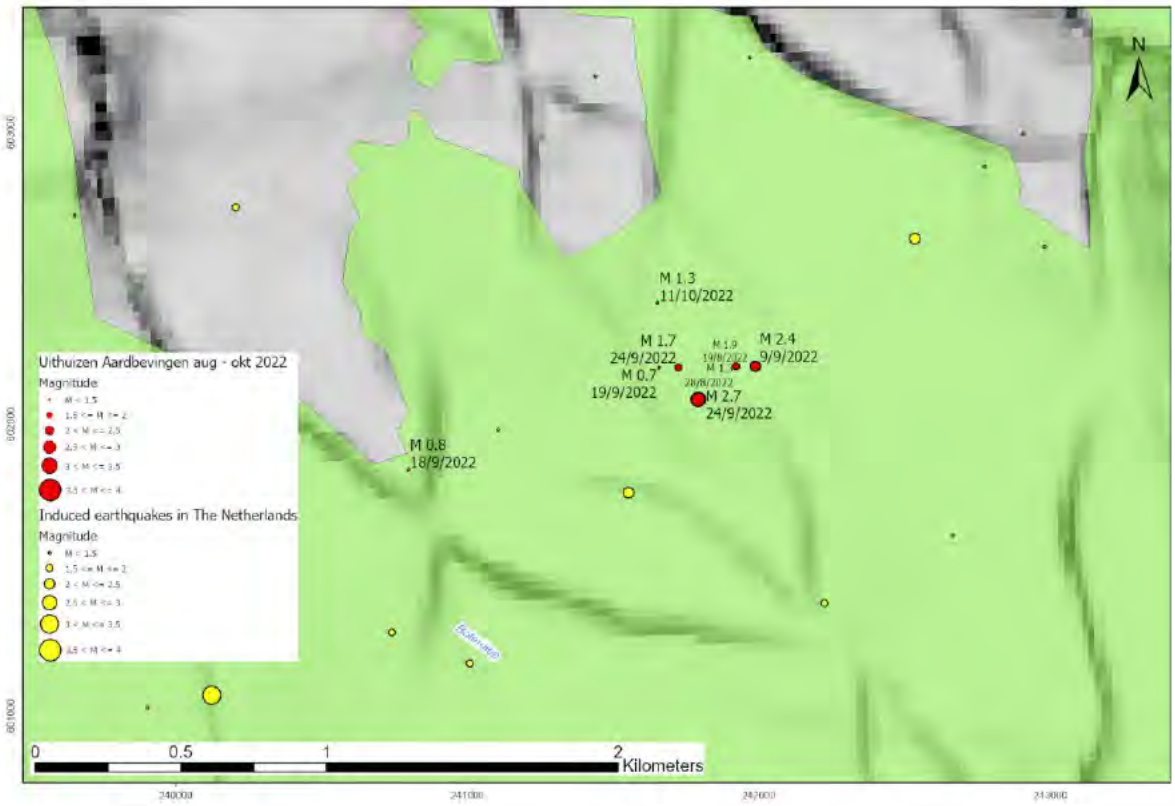

Figure 2.4 Enlargement of figure 2.3 showing the location of the earthquakes in August, September and October 2022 near Uithuizen.

2.5 Source Mechanism

Table 2.2 summarises the source mechanism (double couple part) for the earthquakes near Uithuizen. More details van be found in appendices A to G. A comparison of the strike angle for these earthquakes also indicates that the first two earthquakes, on the 19th August and 28th August 2022, probably occurred at the same fault.

No	Date	Time	Location	Strike	Dip	Rake	Magnitude
42	11-Oct-22	15:36:40	Uithuizen	133.22	45.91	-110.01	1.3
39	24-Sep-22	11:37:30	Uithuizen	150.27	41.00	-92.95	1.7
38	24-Sep-22	10:20:39	Uithuizen	298.10	40.89	-117.84	2.7
35*	19-Sep-22	08:03:56	Uithuizen	321.79	32.59	87.89	0.7
34	18-Sep-22	04:10:01	Uithuizen	319.65	50.16	-122.02	0.8
33	09-Sep-22	00:39:12	Uithuizen	317.67	48.81	-110.22	2.3
32	28-Aug-22	03:18:59	Uithuizen	127.65	42.01	-103.37	1.3
31	19-Aug-22	05:49:14	Uithuizen	130.87	46.25	-95.89	1.9

*very noisy result due to poor field records

Table 2.2 Source mechanism of earthquakes in August, September and October 2022.

Moment tensor solutions are presented in Figure 2.5 and 2.6. The first two events show almost perfect normal faulting, while the oblique component increases in the other events. The combination of strikes and rakes point to maximum horizontal stress direction close to 130°.

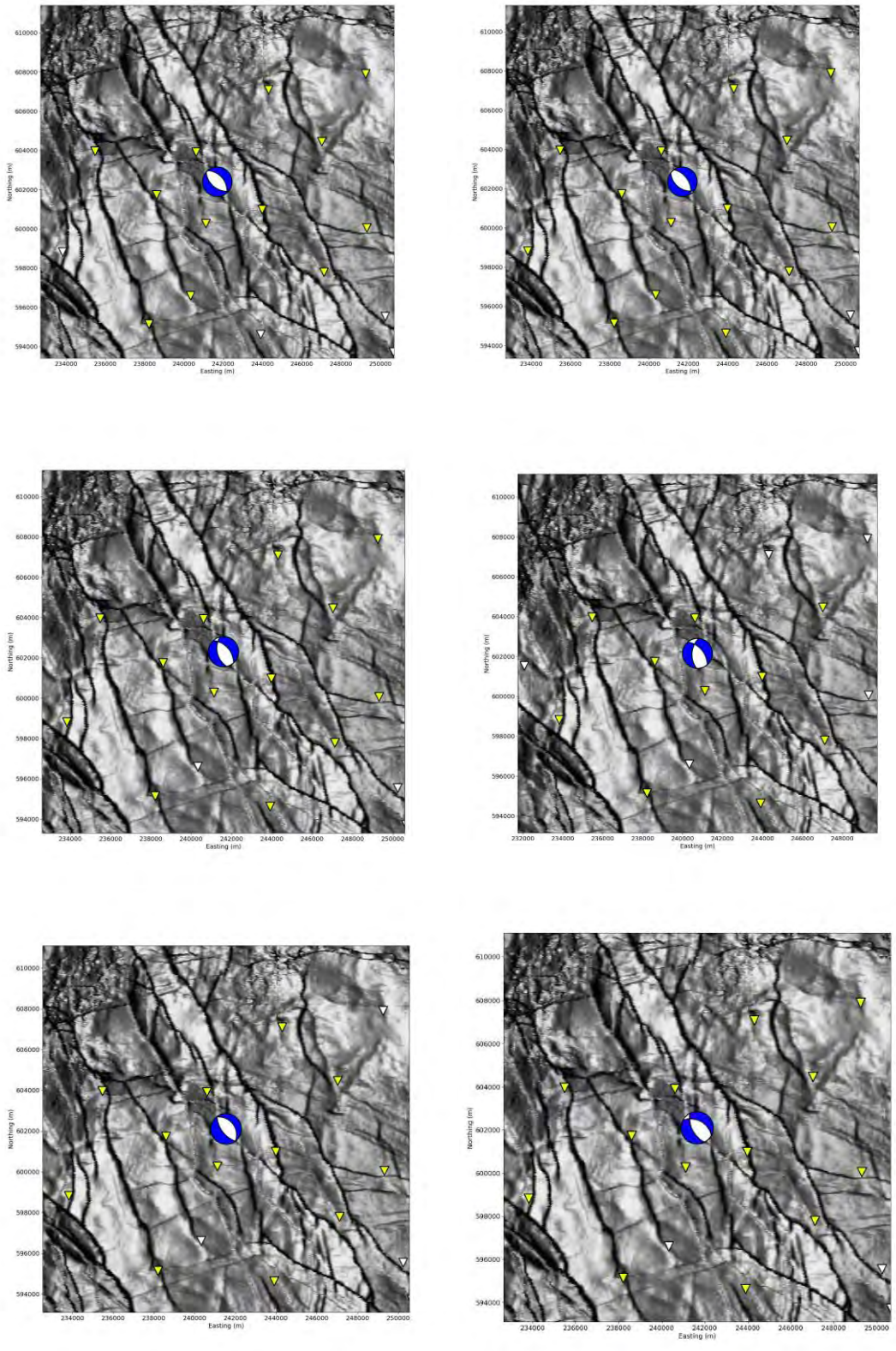

Figure 2.5 Moment tensor solutions for the double-coupled parts (left to right, top to bottom: events 31, 32, 33, 34, 35 and 38.

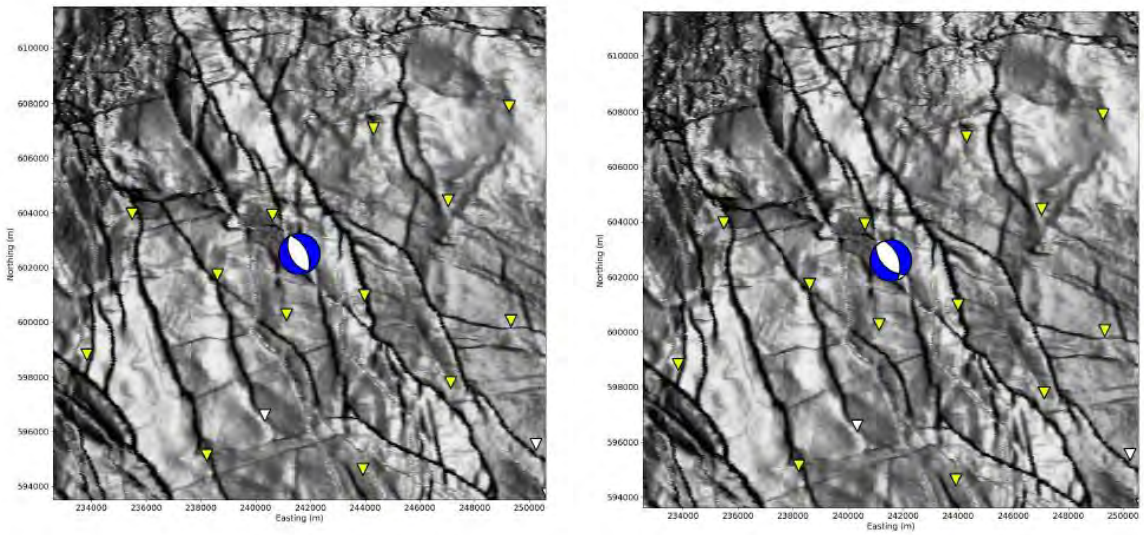

Figure 2.6 Moment tensor solutions for the double-coupled parts (left to right: events 39 and 42.

3 Analysis of the Surface Ground-Motions recorded during the M_L 1.3-2.7 Uithuizen Earthquakes

3.1 Introduction

In this chapter of the report the ground-motions recorded for the earthquakes near Uithuizen will be presented and discussed. The locations of the epicentres with respect to the B-network and G-network, the two strong-motion networks operated by the KNMI in the Groningen field (Ref. 44 and 46), are as shown in Figure 3.1.

The purpose of this report is to provide an overview of the ground-motions recorded during the six largest events in table 2.1 and 2.2, all of which occurred near Uithuizen, in terms of their amplitudes and durations, and compare the recorded amplitudes of motion with predictions from the current empirical Ground-Motion Prediction Equations (GMPEs; Ref. 42) used to estimate values of peak ground velocity (PGV) due to earthquakes in the Groningen field, as well as the V6 and V7 Groningen Ground-Motion Models (GMMs; Ref. 41, 42 and 43). The smallest two events are not included in the analysis because of the very small amplitudes of their ground-motions.

A total of 83 records from each of the six events were accessed from the online portal of the KNMI (KNMI, 1993; http://rdsa.knmi.nl/dataportal/), corresponding to 74 records from the surface accelerographs of the G-network and nine records from the B-network. The records were processed as described by Edwards and Ntinalexis (2021); the total number of usable records for each event, as well as the distance ranges covered by the records, are presented in Table 3.1. Figure 3.2 shows the usable recordings in the magnitude-distance occupied by the database of Ntinalexis *et al*. (Ref. 47).

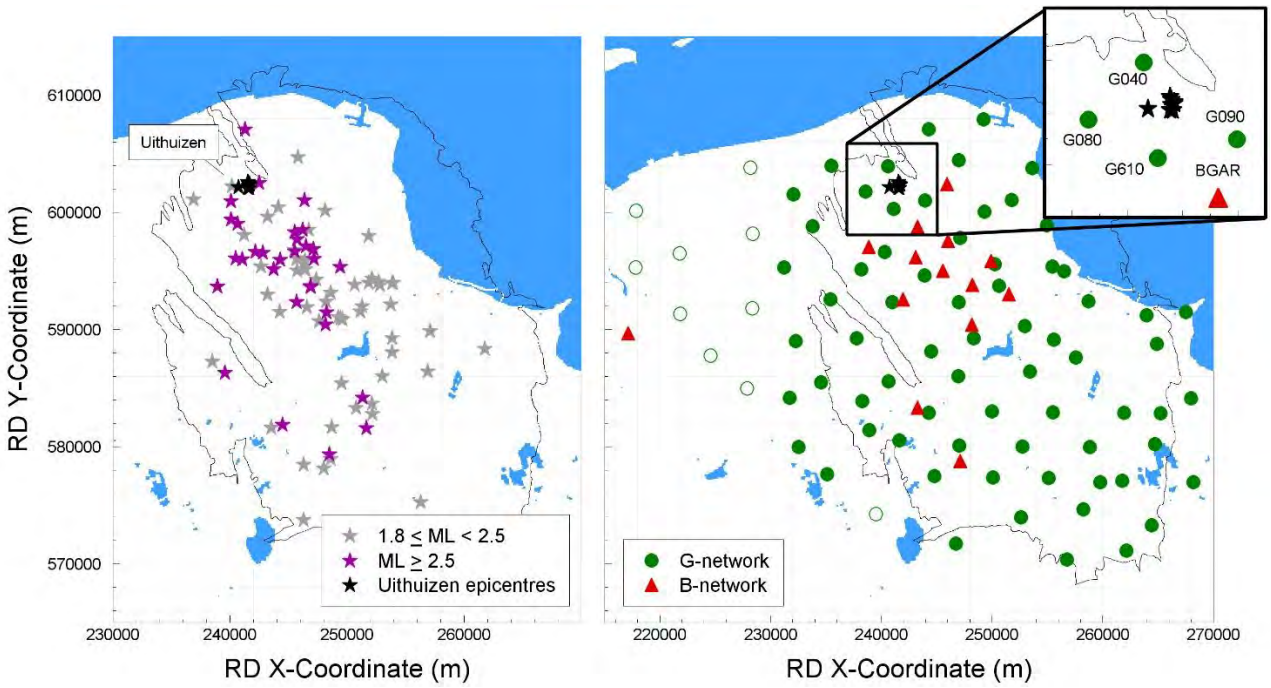

Figure 3.1 Left: Epicentres of the nine earthquakes (black star) together with epicentres of previous earthquakes of $M_L \geq 2.5$ (magenta stars) and of M_L 1.8-2.4 (grey stars). Right: G-network (green) and B-network (red) stations; open circles indicate G-stations without borehole geophones.

ID	M_L	No. Recs	Smallest R_{epi} (km)	Largest R_{epi} (km)
42	1.3	3	2.37	9.54
39	1.7	5	2.20	9.96
38	2.7	46	1.90	31.80
33	2.3	57	1.90	31.02
32	1.3	4	2.16	5.99
31	1.9	21	2.20	19.67

Table 3.1 Numbers of usable records for each event and their distance ranges

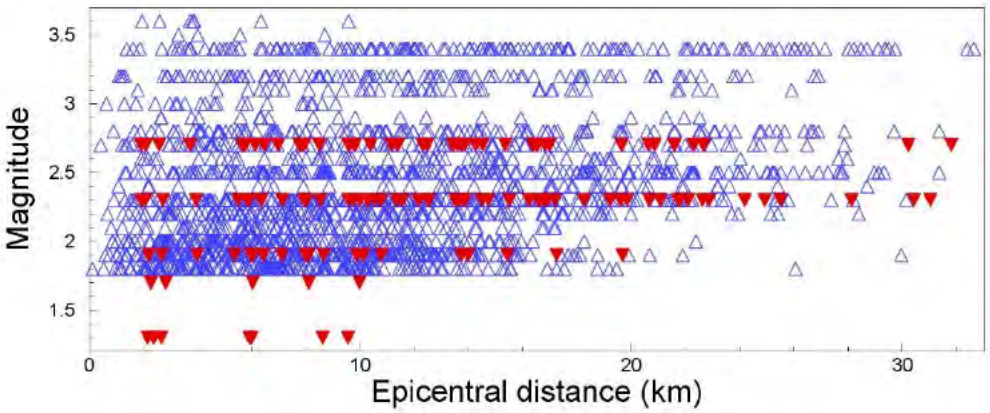

Figure 3.2 Magnitude-distance distribution of the recordings presented in Table 3.1 (red) and of the Ntinalexis et al. (Ref. 47) database (blue)

3.2 Peak Ground Accelerations and Velocities

Figure 3.3 shows the geometric mean horizontal components of PGA and PGV plotted against magnitude together with the corresponding values from the complete database of Ntinalexis *et al.* (Ref. 47). Figures 3.4 and 3.5 show the horizontal values of PGA and PGV of three component definitions from each recording obtained during the Uithuizen earthquakes plotted against the distance of the recording site from the epicentre. The definitions shown are a) the geometric mean component (GM), which is the geometric-mean of the values corresponding to each as-recorded horizontal component, b) the larger component, which corresponds to the larger of the two values recorded by the horizontal components and c) maximum-rotated component (MaxRot) or vector component, which is the largest value that can be obtained by rotating the two horizontal components through all angles. Overall, the motions appear to have, on average, smaller amplitudes than those observed in previous earthquakes, albeit with a similar amplitude range. At the same time, the largest PGA values recorded for the M_L2.3 and M_L2.7 events are also the largest that have been recorded to date for those magnitudes.

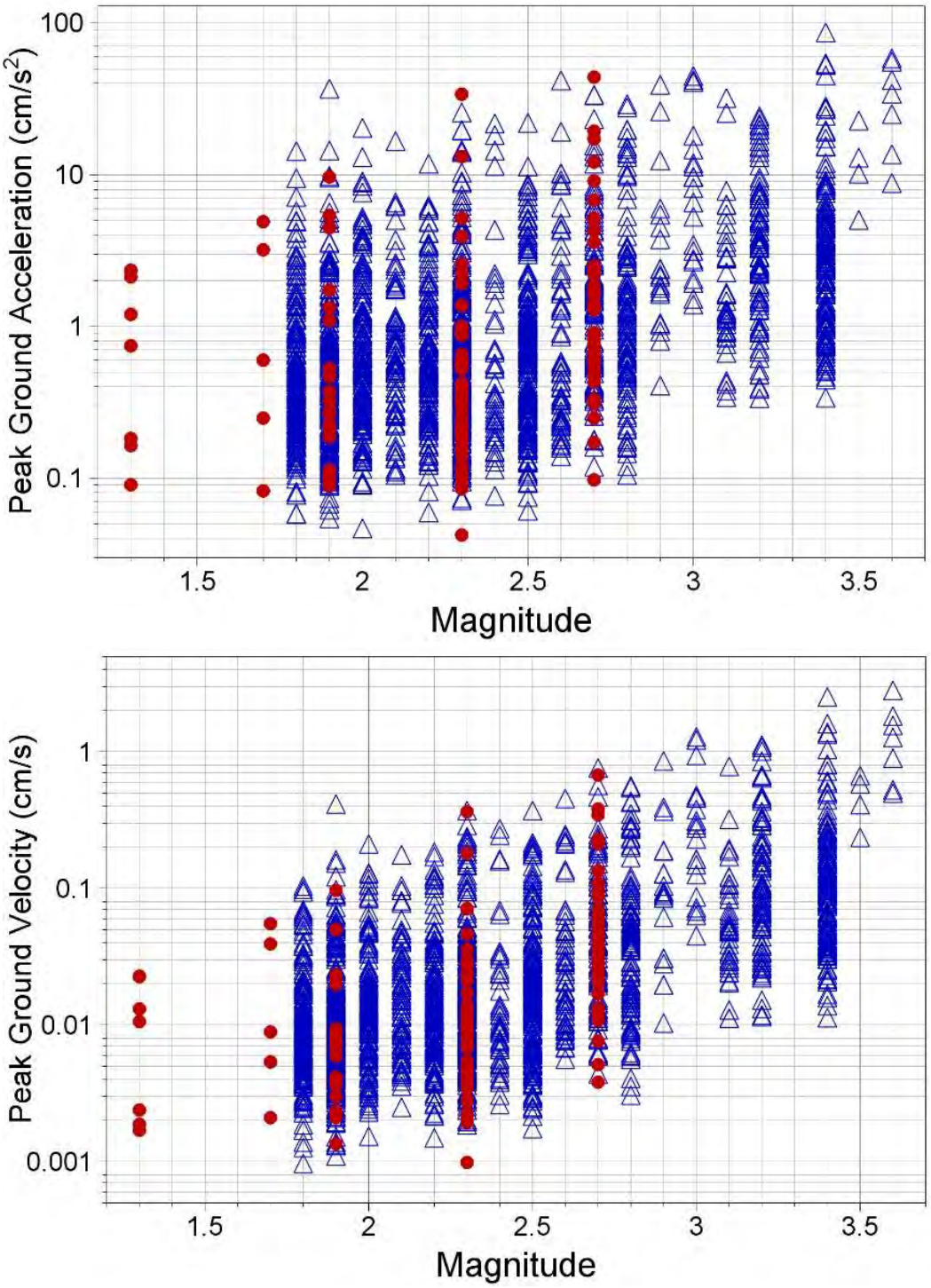

Figure 3.3 Geometric mean horizontal components of PGA (upper) and PGV (lower) recorded during the six Uithuizen earthquakes (red) and in previous earthquakes (blue) plotted against local magnitude

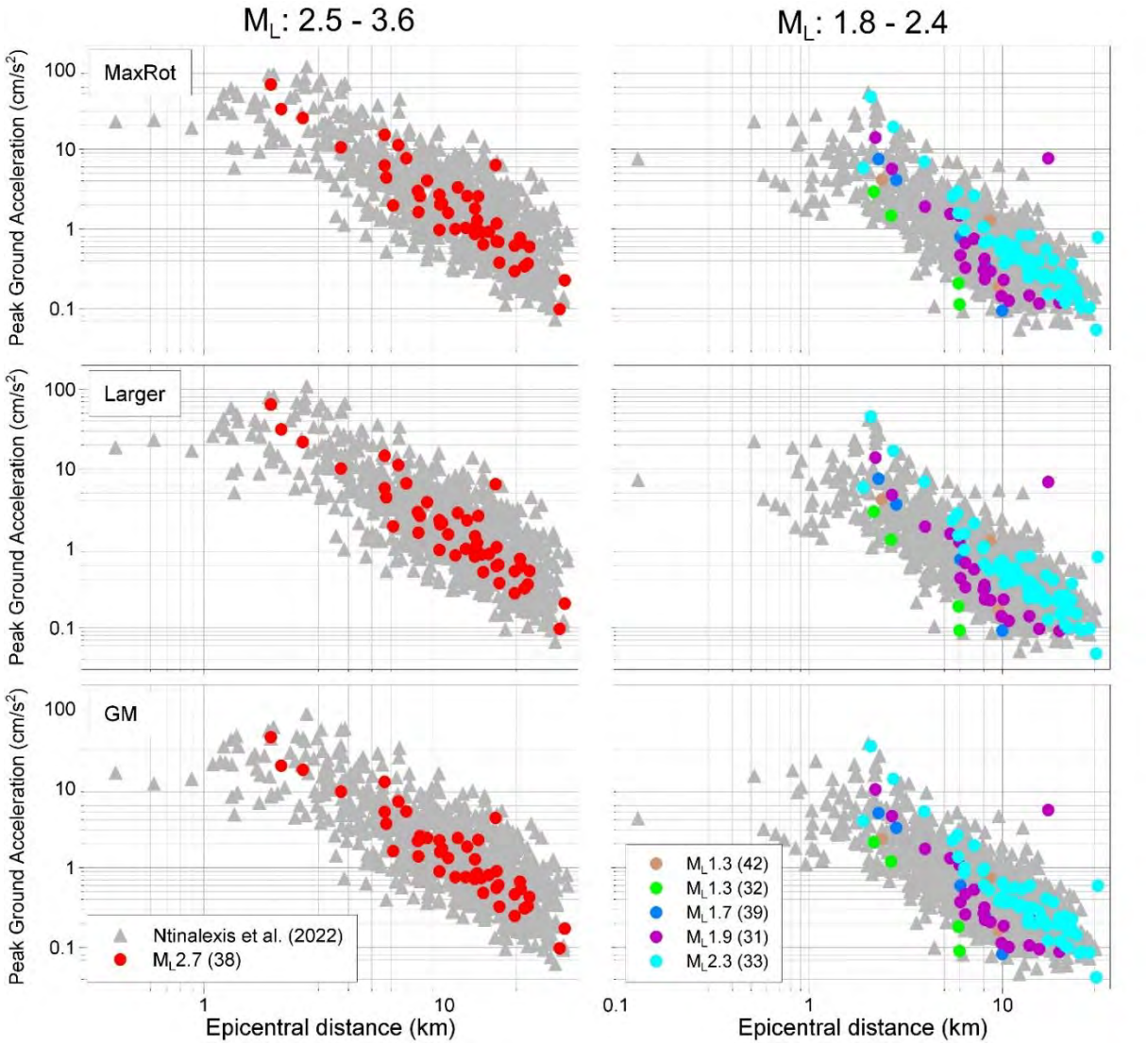

Figure 3.4 Horizontal components of PGA recorded during the Uithuizen earthquakes and previous earthquakes plotted against epicentral distance

The largest PGA and PGV values of each of the six events were recorded at the same station and component: station G610 and component H1 (NS). The largest PGA of the M_L2.7 event was 64.57 cm/s^2, which is the eighth-largest value that has been recorded by the KNMI networks since 2006, but significantly smaller than the largest PGA which was recorded at the EW component of the BGAR station during the M_L3.4 Zeerijp earthquake that occurred in January 2018, with a value of 108.68 cm/s^2. The largest PGV of the M_L2.7 event was 1.13 cm/s, the 23rd largest recorded since 2006 and also significantly smaller than the largest PGV recorded to date, a 3.46 cm/s on the NS component of the MID1 station during the August 2012 M_L3.6 Huizinge earthquake. The largest PGA and PGV values of the six Uithuizen events are presented in Table 3.2.

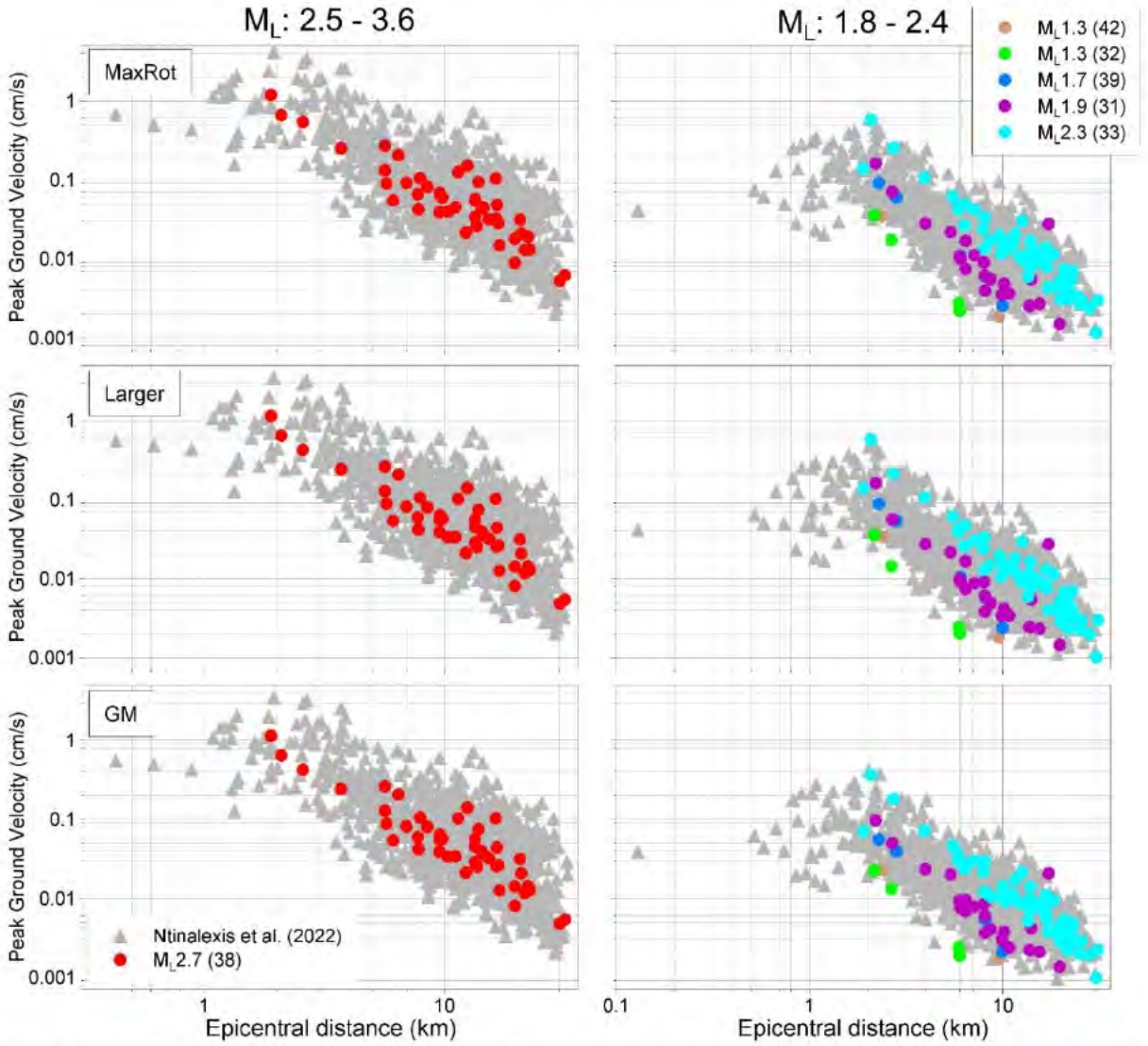

Figure 3.5 Horizontal components of PGV recorded during the Uithuizen earthquakes and previous earthquakes plotted against epicentral distance

Event	M_L	Max. PGA (cm/s²)	Max. PGV (cm/s)	R_{epi} (km)
42	1.3	4.39	0.034	2.37
39	1.7	7.23	0.088	2.28
38	2.7	64.57	1.130	1.90
33	2.3	45.35	0.570	2.08
32	1.3	2.91	0.035	2.16
31	1.9	13.90	0.161	2.20

Table 3.2 Largest as-recorded PGA and PGV values of the six events

From Figures 3.4 and 3.5, it is immediately apparent that the amplitudes of motion are consistent with previous earthquakes of comparable size. At the same time, the largest PGA values of the M_L2.3 and M_L2.7 events continue to stand out. Additionally, a recording from the M_L1.9 event also stands out, with larger than expected PGA and PGV values at 17 km from the epicentre. This is recording G340 and is plotted in Figure 3.6.

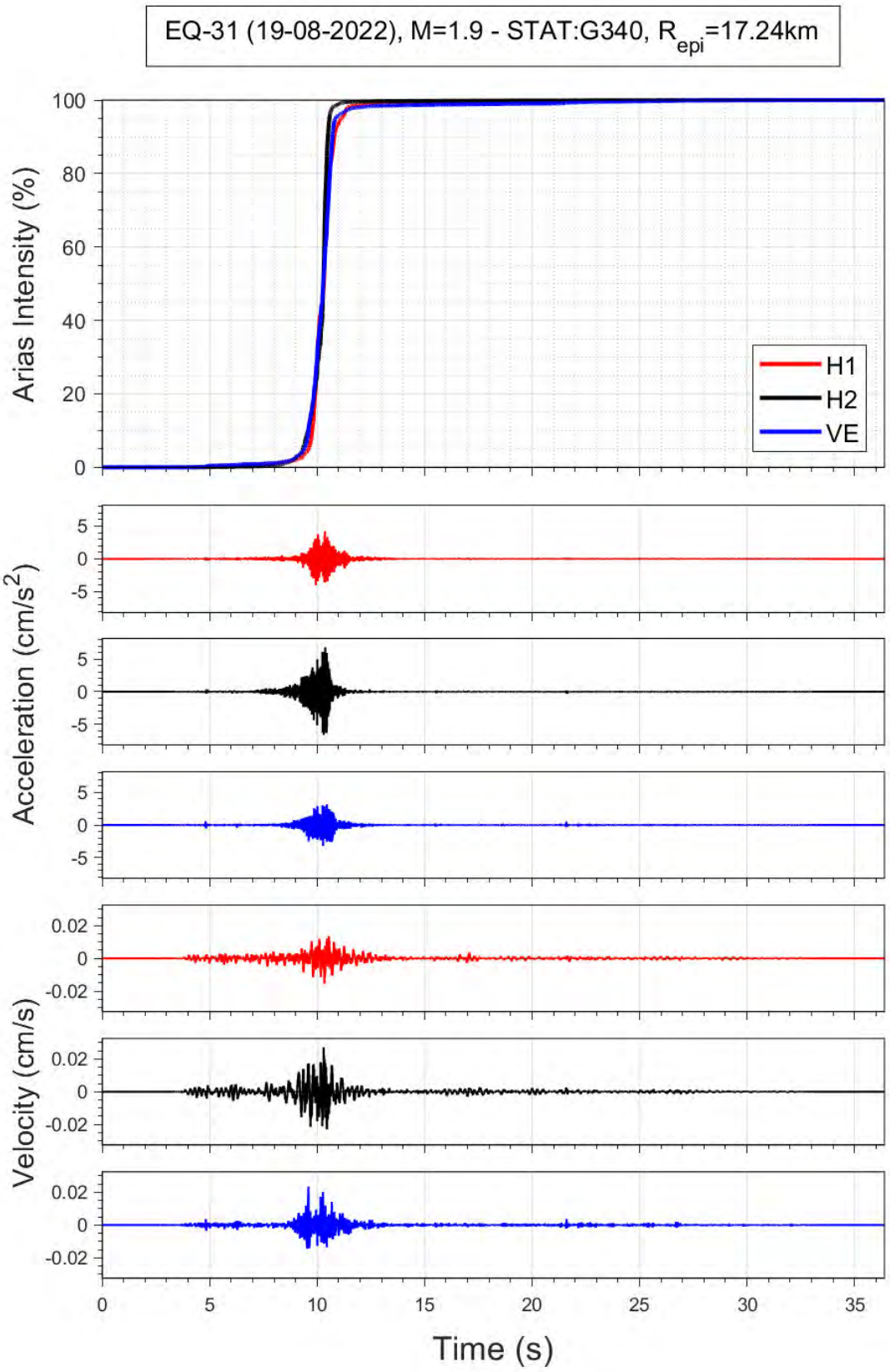

Figure 3.6 Horizontal components of acceleration and velocity recorded at the G340 station during event 31; the upper frame shows the accumulation of Arias intensity (energy) over time.

Figures 3.7 – 3.12 show the horizontal components of PGA and PGV obtained within 6 km of the epicentre, from which it can be appreciated that the very strong polarisation often observed in

Groningen recordings (*e.g.*, Ref. 40) is also apparent in records of these events, especially at stations G040 and G610. Additionally, the strong directivity of the ground-motions is also apparent, with significantly larger amplitudes recorded primarily to the south and secondarily to the east of the epicentres.

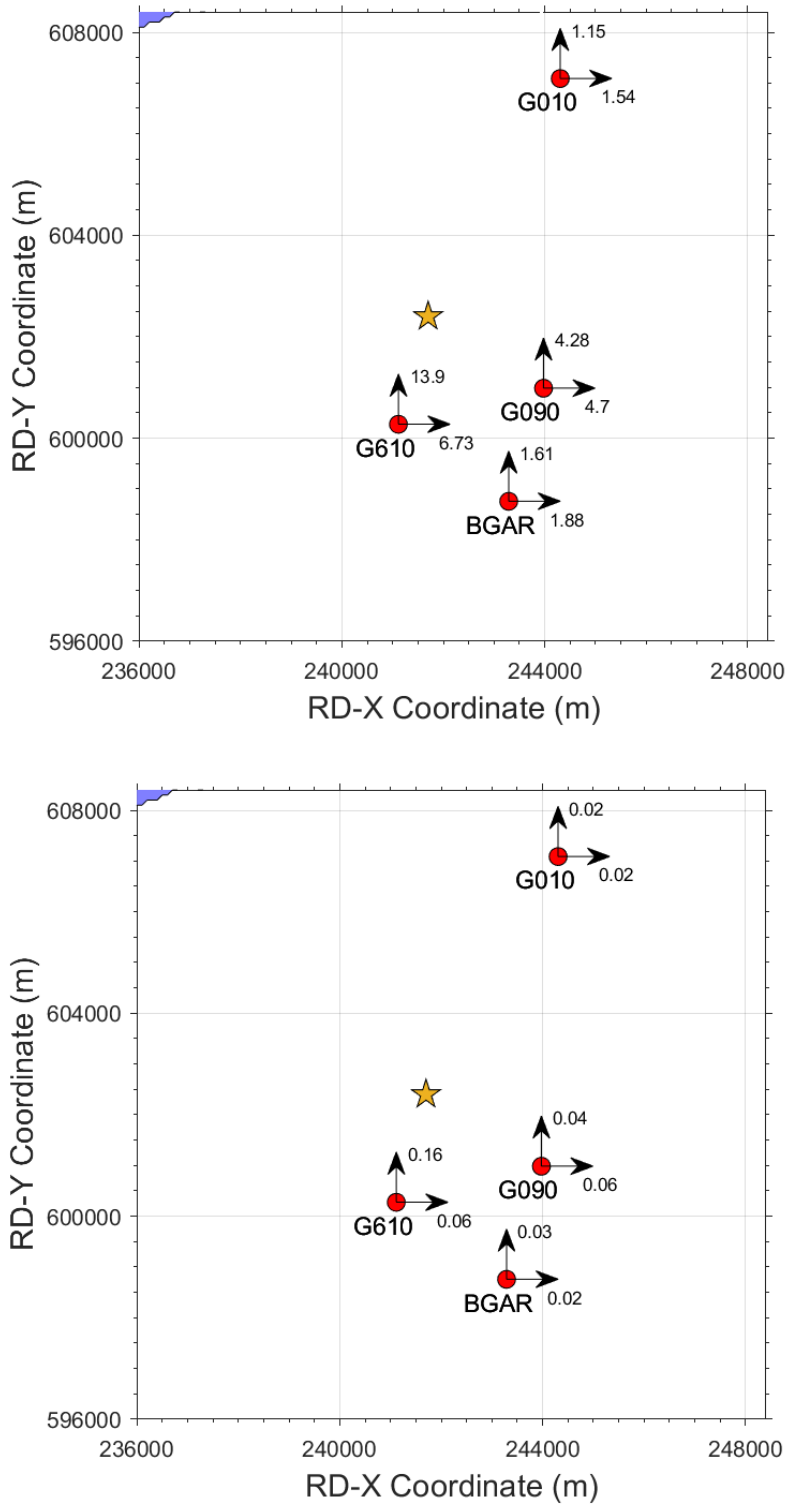

Figure 3.7 Horizontal components of PGA (upper) and PGV (lower) recorded during event 31 (M_L1.9) at epicentral distances of less than 6 km; units are cm/s² and cm/s, respectively.

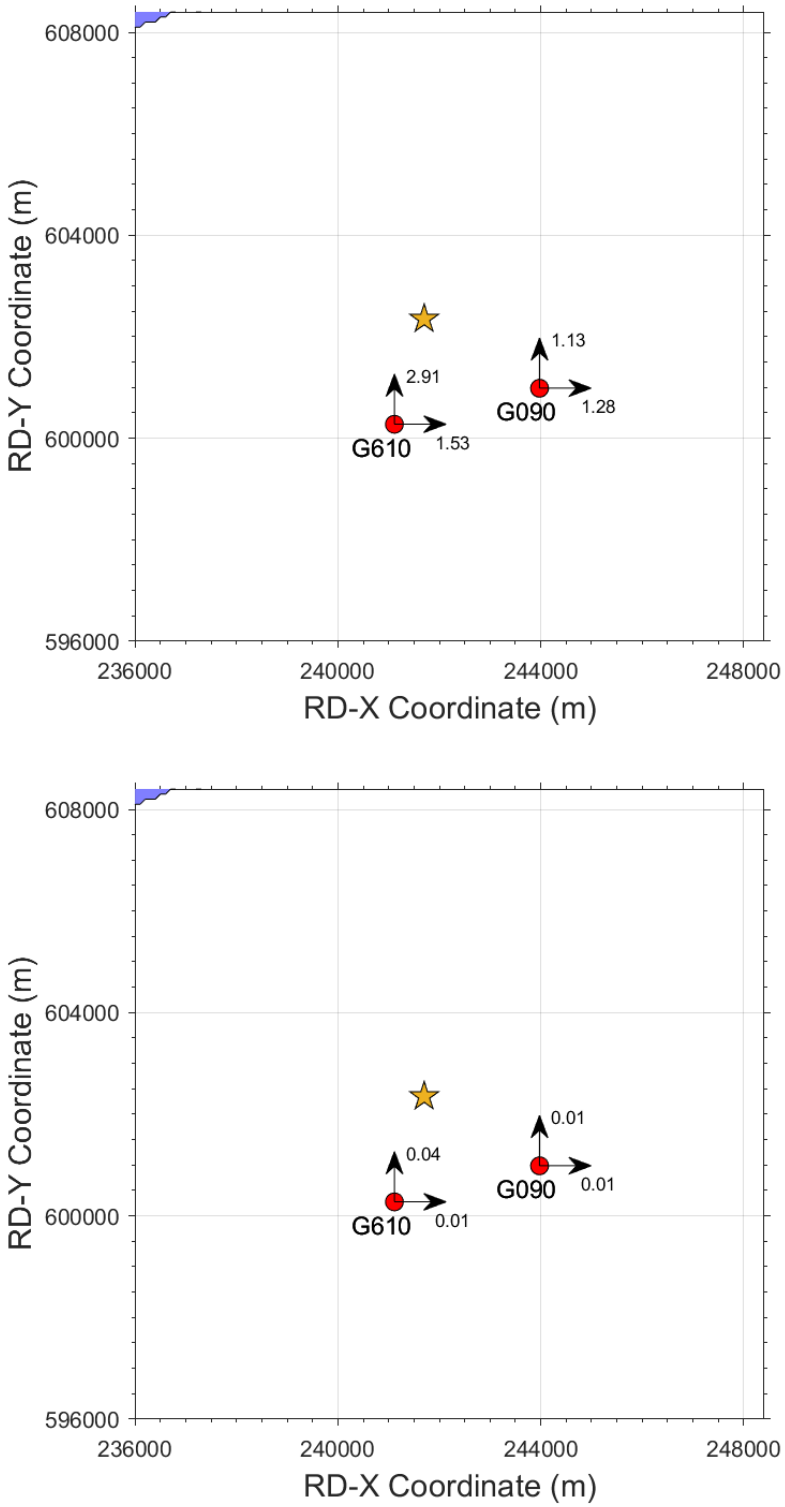

Figure 3.8 Horizontal components of PGA (upper) and PGV (lower) recorded during event 32 (M_L1.3) at epicentral distances of less than 6 km; units are cm/s^2 and cm/s, respectively.

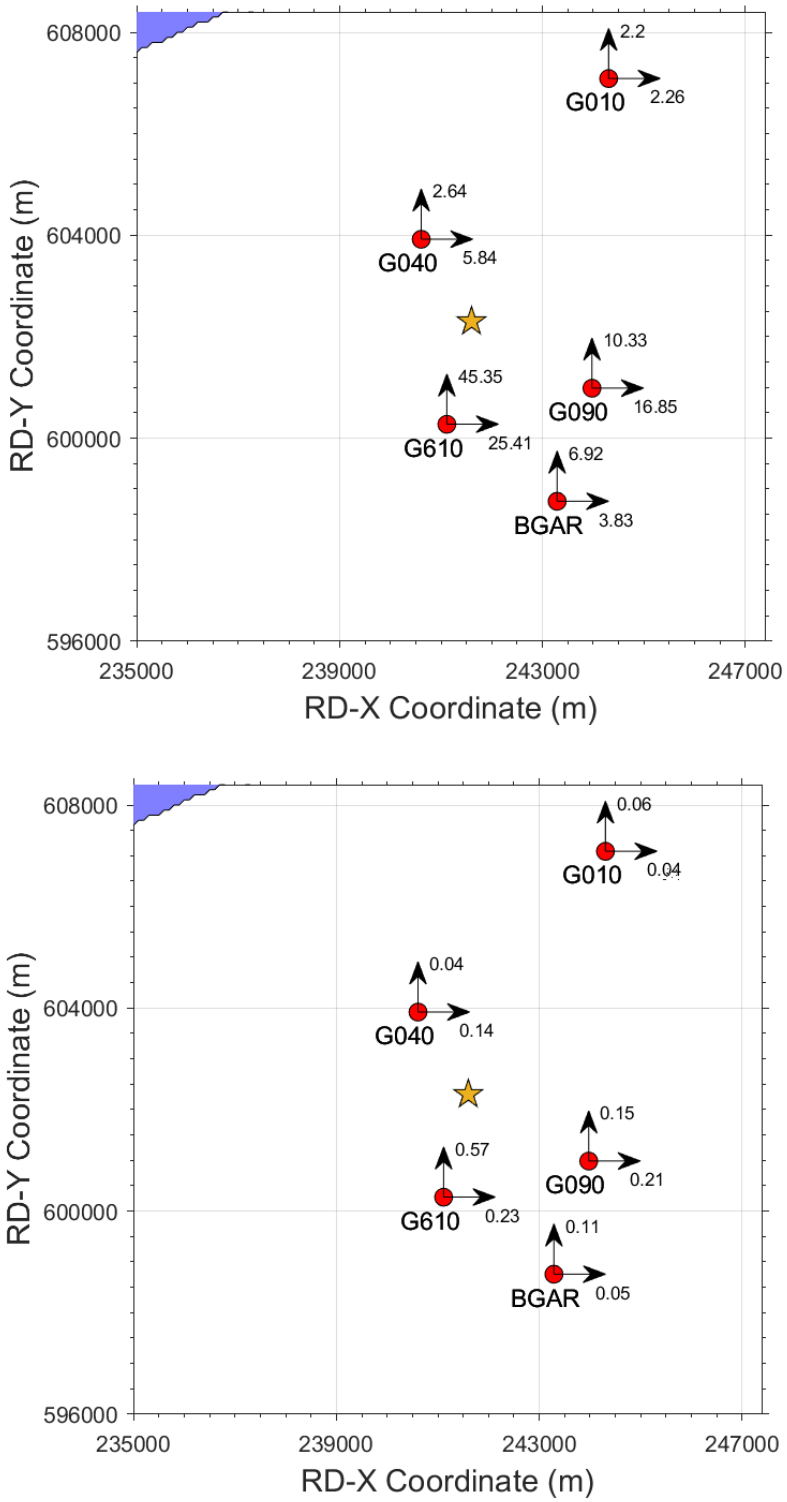

Figure 3.9 Horizontal components of PGA (upper) and PGV (lower) recorded during event 33 (M_L2.3) at epicentral distances of less than 6 km; units are cm/s^2 and cm/s, respectively.

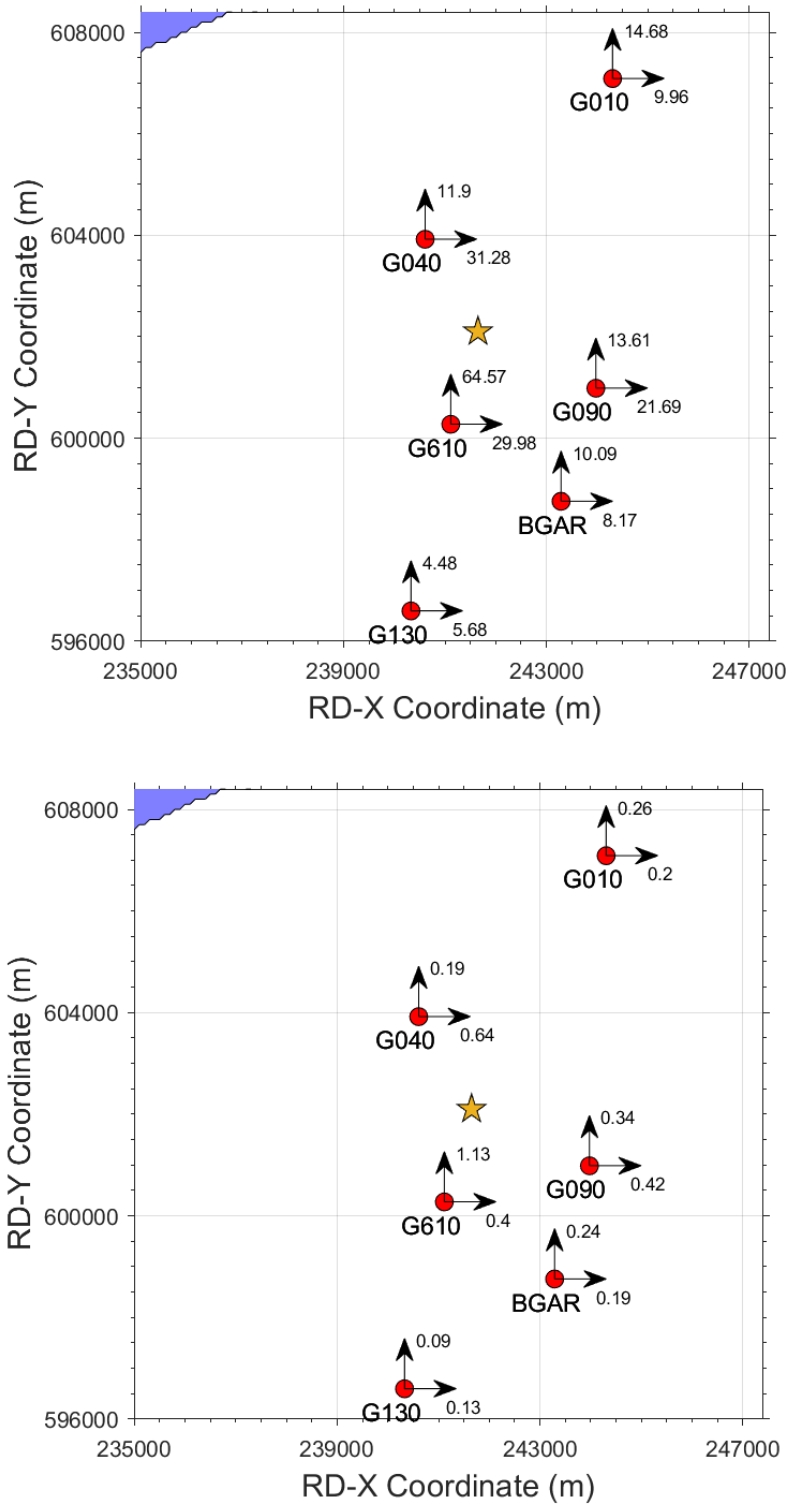

Figure 3.10 Horizontal components of PGA (upper) and PGV (lower) recorded during event 38 (M_L2.7) at epicentral distances of less than 6 km; units are cm/s^2 and cm/s, respectively.

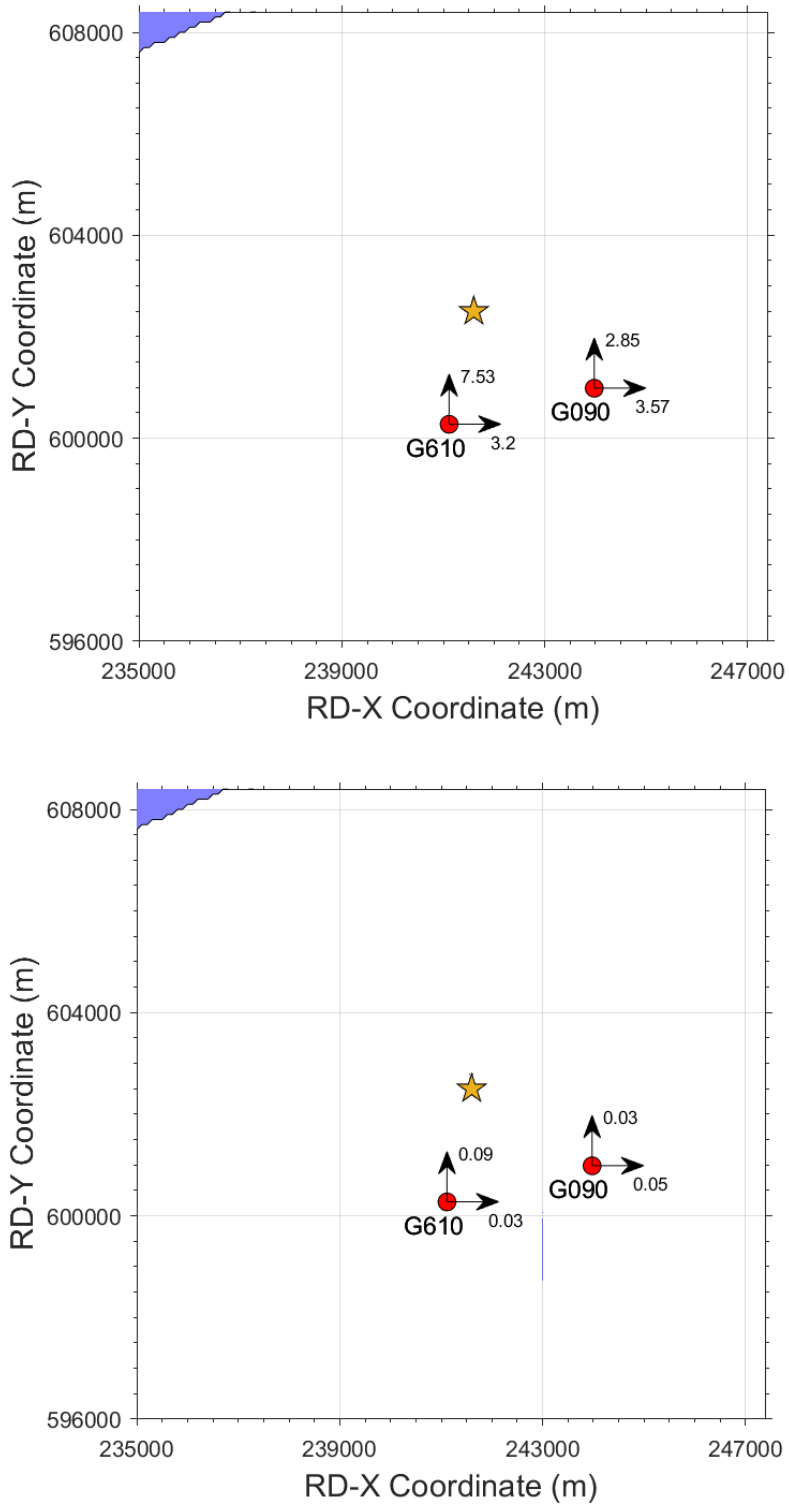

Figure 3.11 Horizontal components of PGA (upper) and PGV (lower) recorded during event 39 (M_L1.7) at epicentral distances of less than 6 km; units are cm/s^2 and cm/s, respectively.

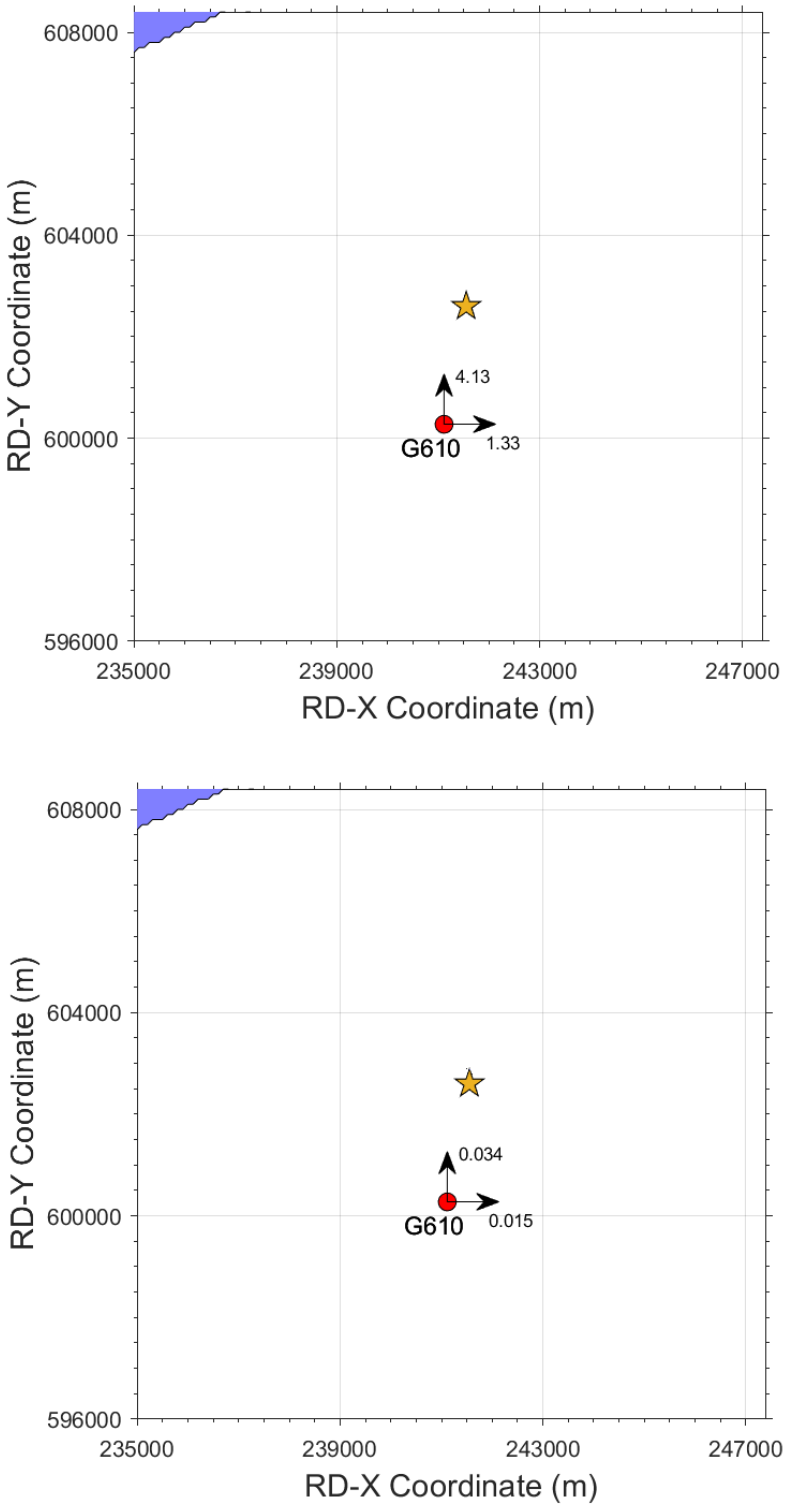

Figure 3.12 Horizontal components of PGA (upper) and PGV (lower) recorded during event 42 (M_L1.3) at epicentral distances of less than 6 km; units are cm/s^2 and cm/s, respectively.

As already shown in Figures 3.4 and 3.5, the amplitudes decay rapidly with distance although the effect of simultaneous arrivals of direct and critically refracted/reflected waves leads to an increase in amplitudes at some locations between 12 and 20 km from the epicentre. However, these effects do not lead to significant absolute amplitudes at those distances, and it is clear from Figures 3.7 – 3.12

that, outside the epicentral area, the motions are of very low amplitude: < 0.01*g* for PGA and < 0.1 cm/s for PGV.

3.3 Ground-Motion Durations

The maximum amplitude of ground shaking, whether represented by PGA or PGV, provides a simple indication of the strength of the motion but the potential for adverse effects—such as damage to masonry buildings or triggering liquefaction—also depends on the duration or number of cycles of the motion.

A feature that has been consistently observed in the Groningen ground motions is a very pronounced negative correlation between PGA and duration, with high amplitude motions consistently associated with shaking of very short duration (Ref. 38). The same pattern is observed in the recordings of the Uithuizen earthquakes, as shown in Figure 3.13. The shortest duration recorded during the Uithuizen events is only 0.435 seconds, is associated with a PGA of 11.20 cm/s^2 and belongs to the H1 component of station G030. The horizontal components of both acceleration and velocity from this station are shown in Figure 3.14, which also shows the build-up of Arias intensity (which is a measure of the energy in the motion) over time. The strong concentration of the energy in a single pulse of motion in the H1 component is immediately apparent. Durations of the signals recorded in the G610 station (Fig. 3.15), where the largest PGA and PGV values of all six events correspond, are slightly longer and range, on the H1 component, from 1.695 to 1.870 seconds. The reason, in this case, is a strong P-wave arrival about 1.5 seconds before the S-wave peak, which elongates the calculated durations (Figures 3.14 - 3.20).

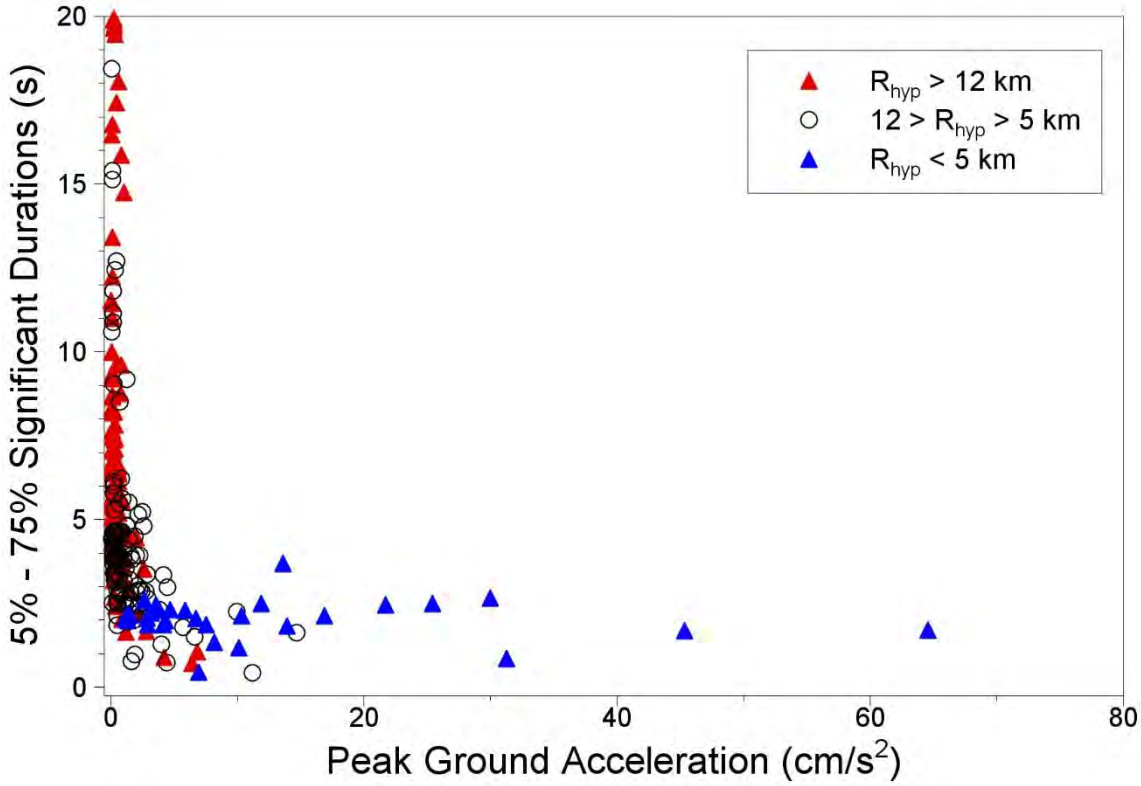

Figure 3.13 Pairs of PGA and significant duration for individual components of the Uithuizen records, with symbols indicating the rupture distance of the recording.

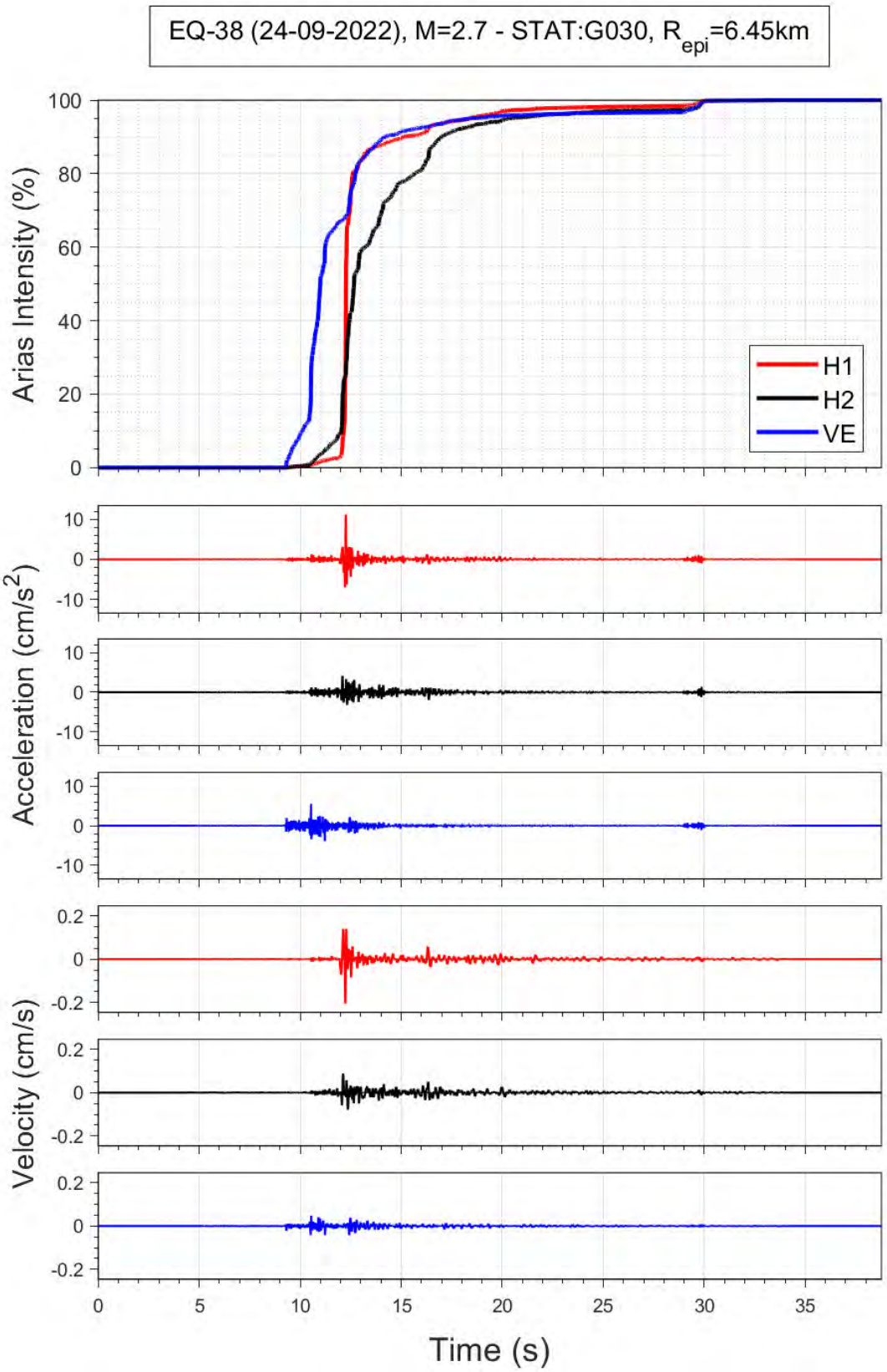

Figure 3.14 Horizontal components of acceleration and velocity recorded at the G030 station during event 38; the upper frame shows the accumulation of Arias intensity (energy) over time.

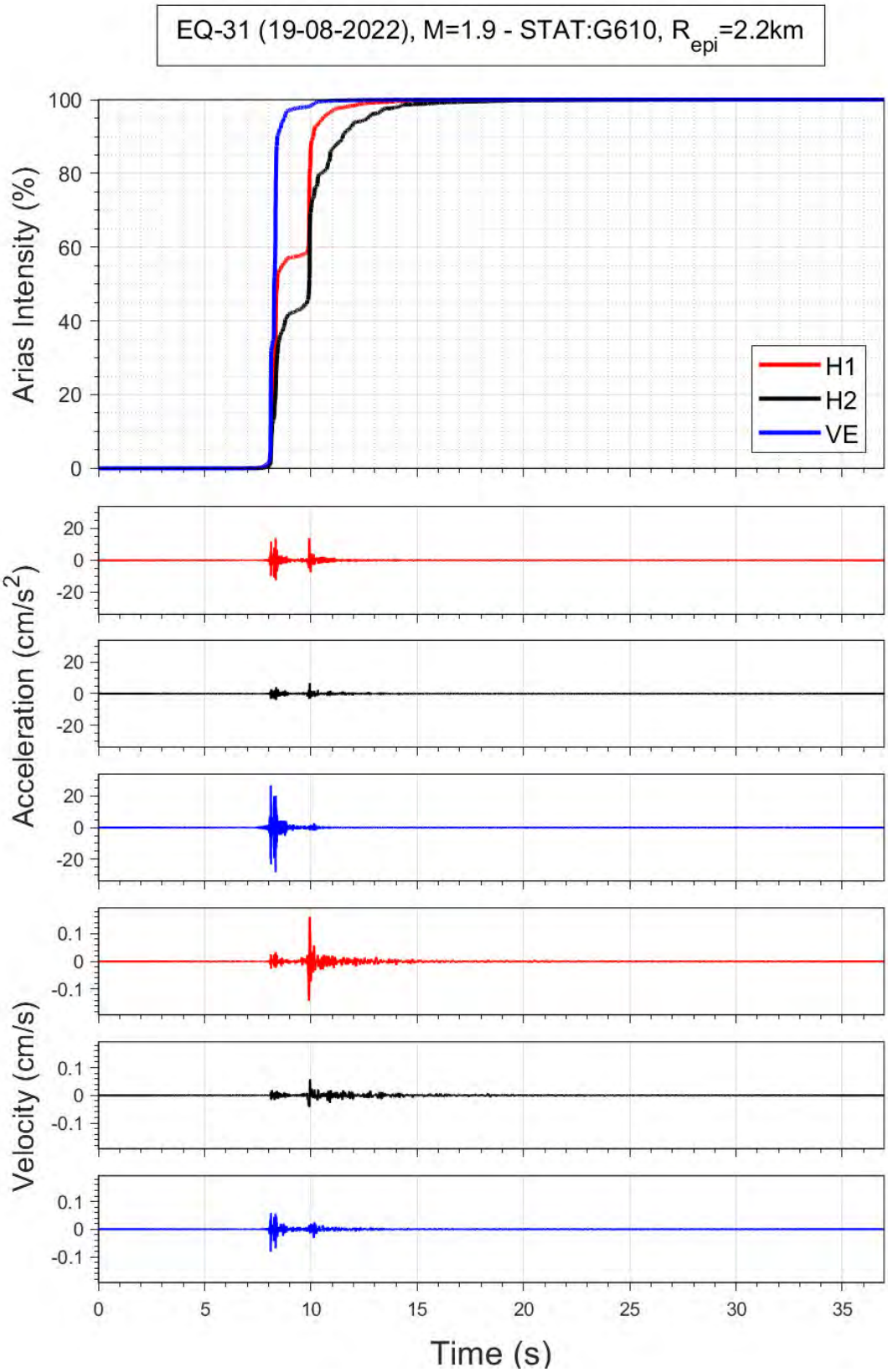

Figure 3.15 Horizontal components of acceleration and velocity recorded at the G610 station during event 31; the upper frame shows the accumulation of Arias intensity (energy) over time.

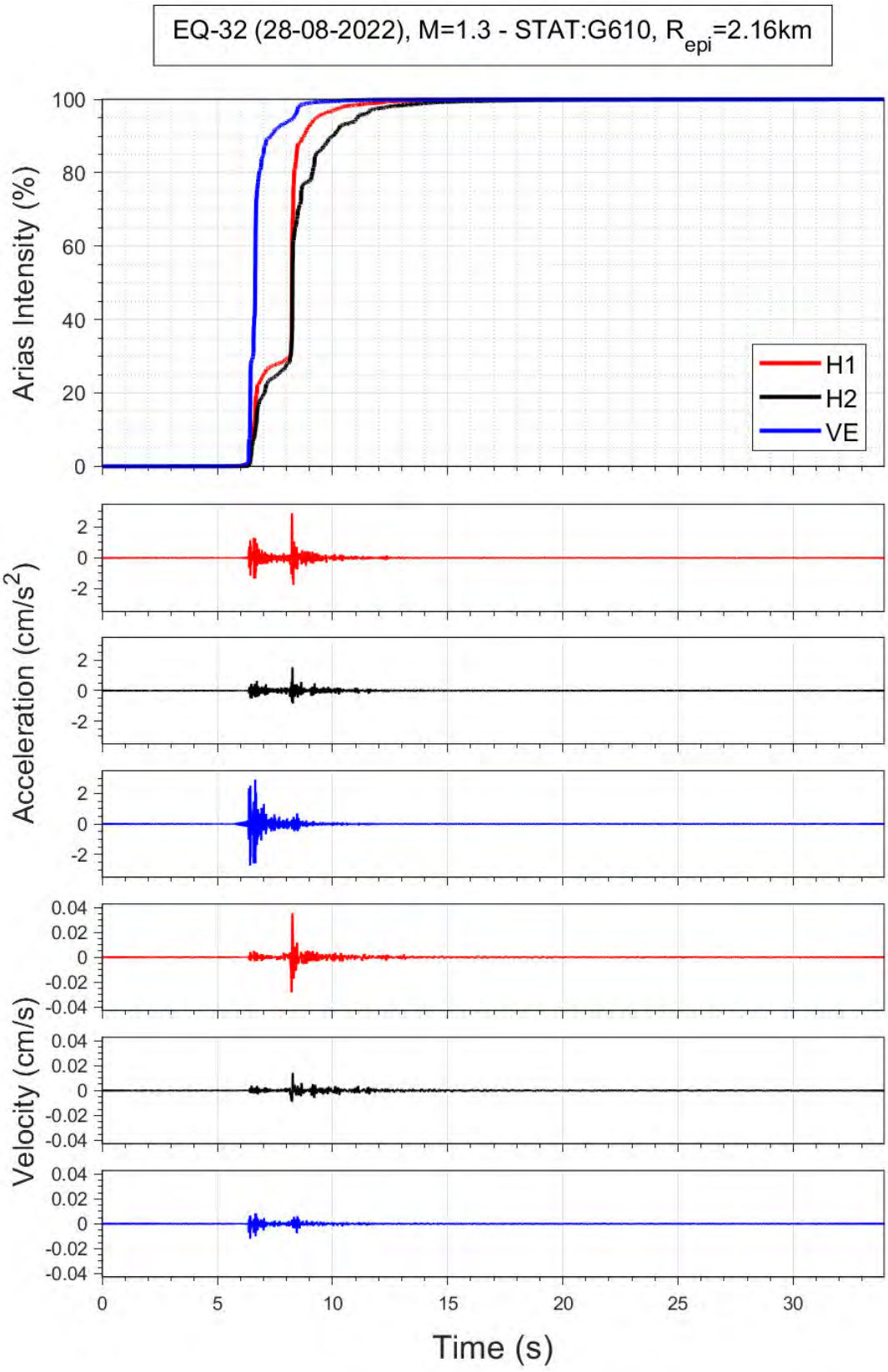

Figure 3.16 Horizontal components of acceleration and velocity recorded at the G610 station during event 32; the upper frame shows the accumulation of Arias intensity (energy) over time.

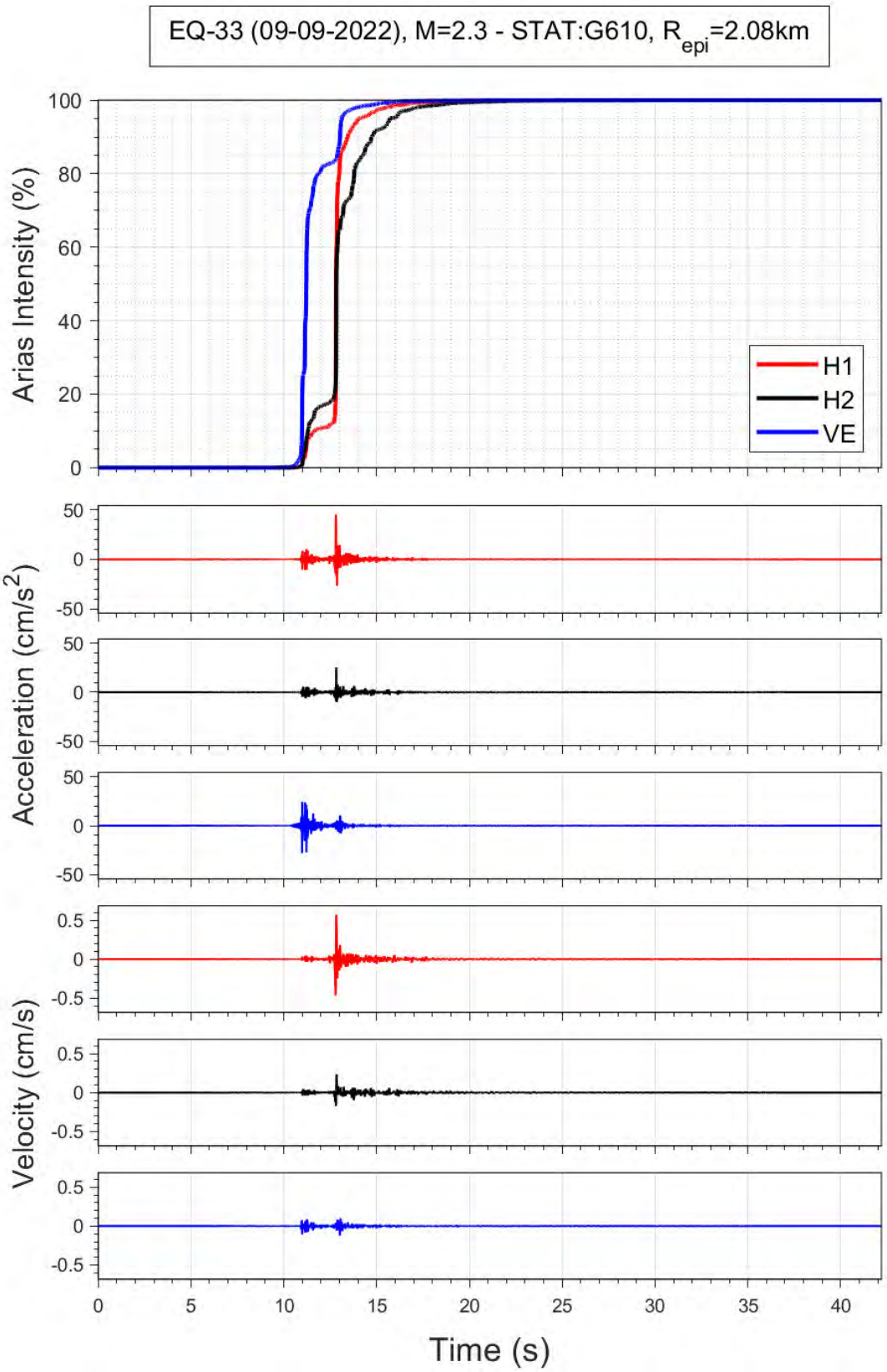

Figure 3.17 Horizontal components of acceleration and velocity recorded at the G610 station during event 33; the upper frame shows the accumulation of Arias intensity (energy) over time.

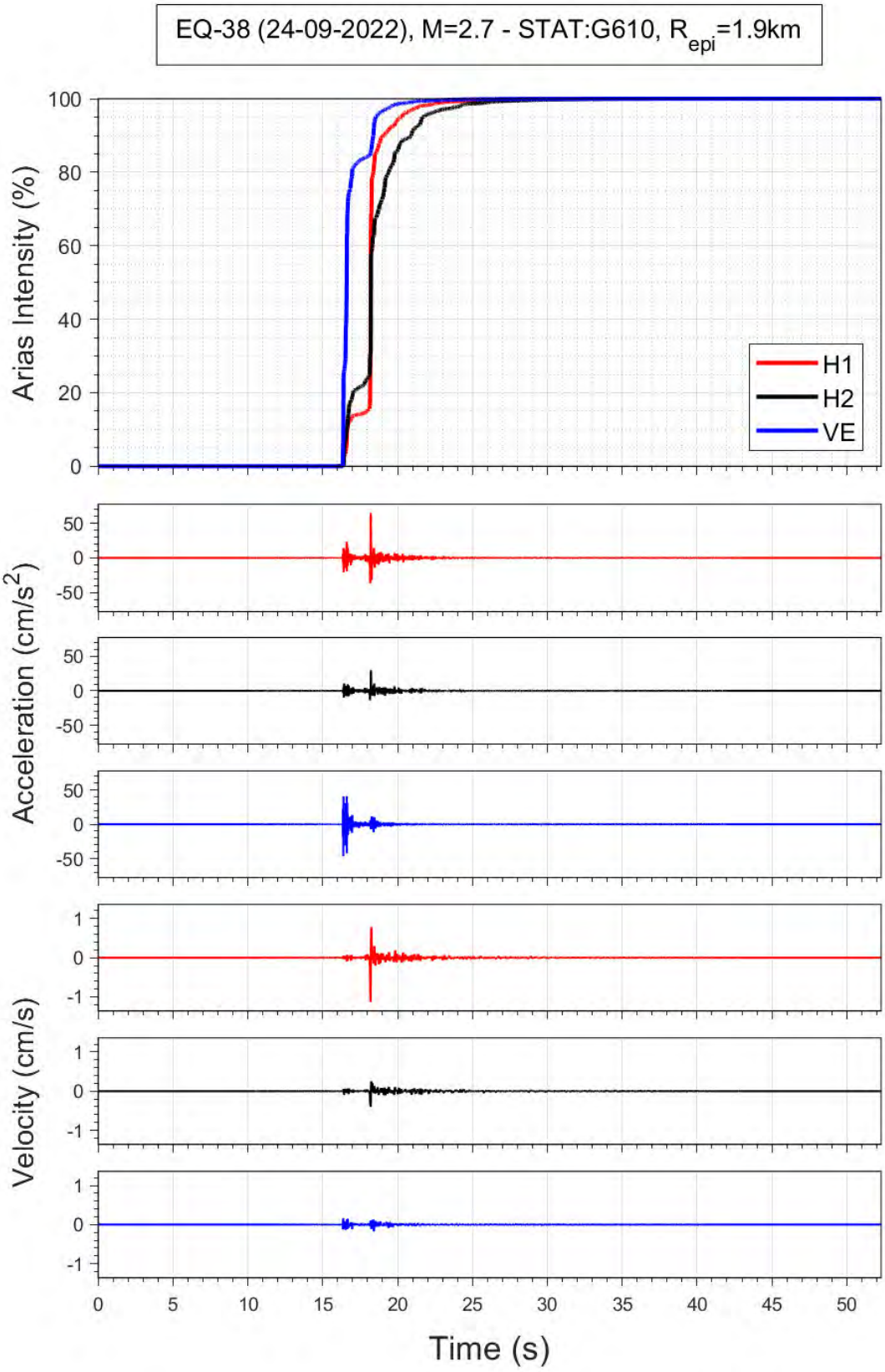

Figure 3.18 Horizontal components of acceleration and velocity recorded at the G610 station during event 38; the upper frame shows the accumulation of Arias intensity (energy) over time.

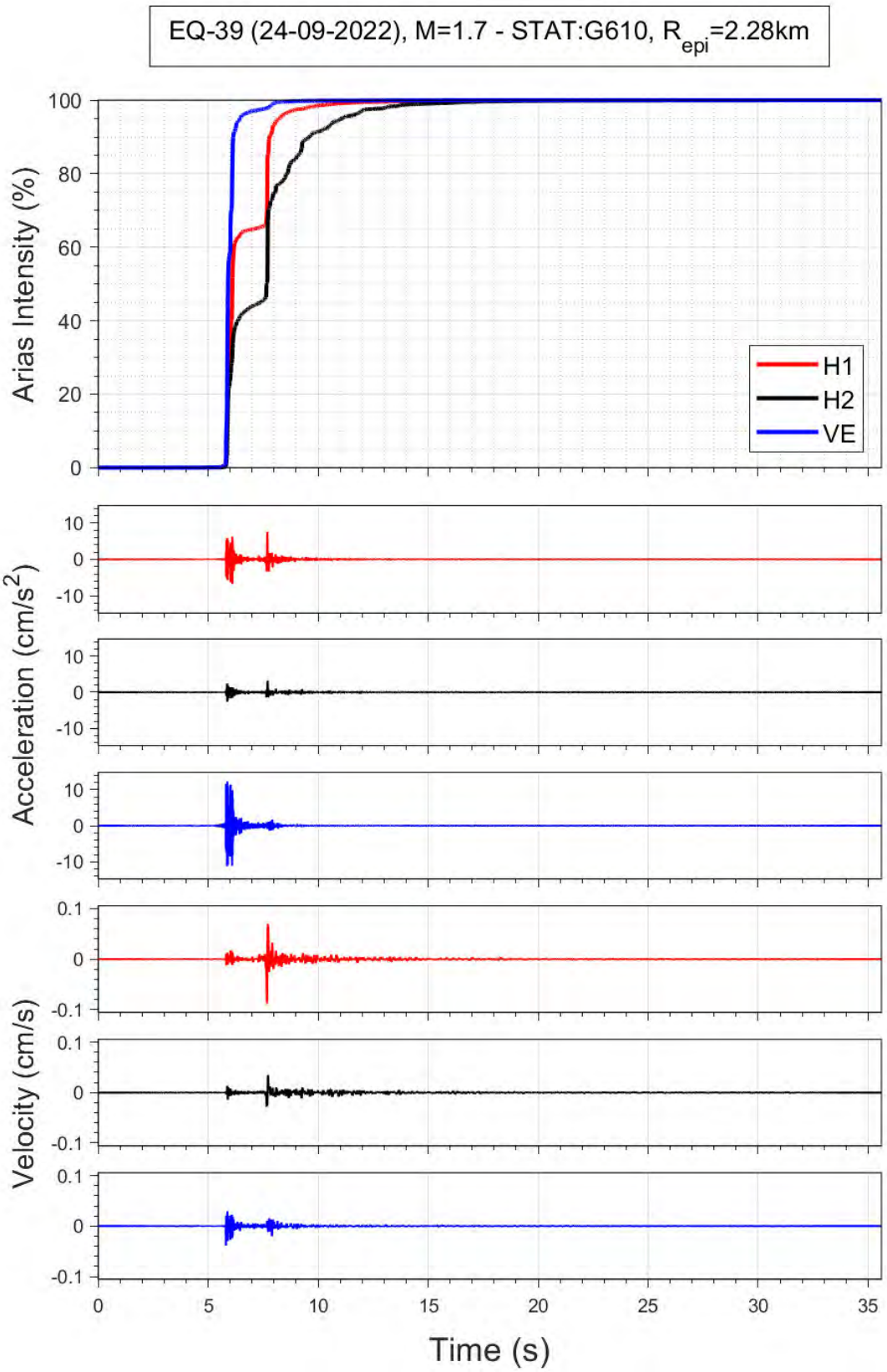

Figure 3.19 Horizontal components of acceleration and velocity recorded at the G610 station during event 39; the upper frame shows the accumulation of Arias intensity (energy) over time.

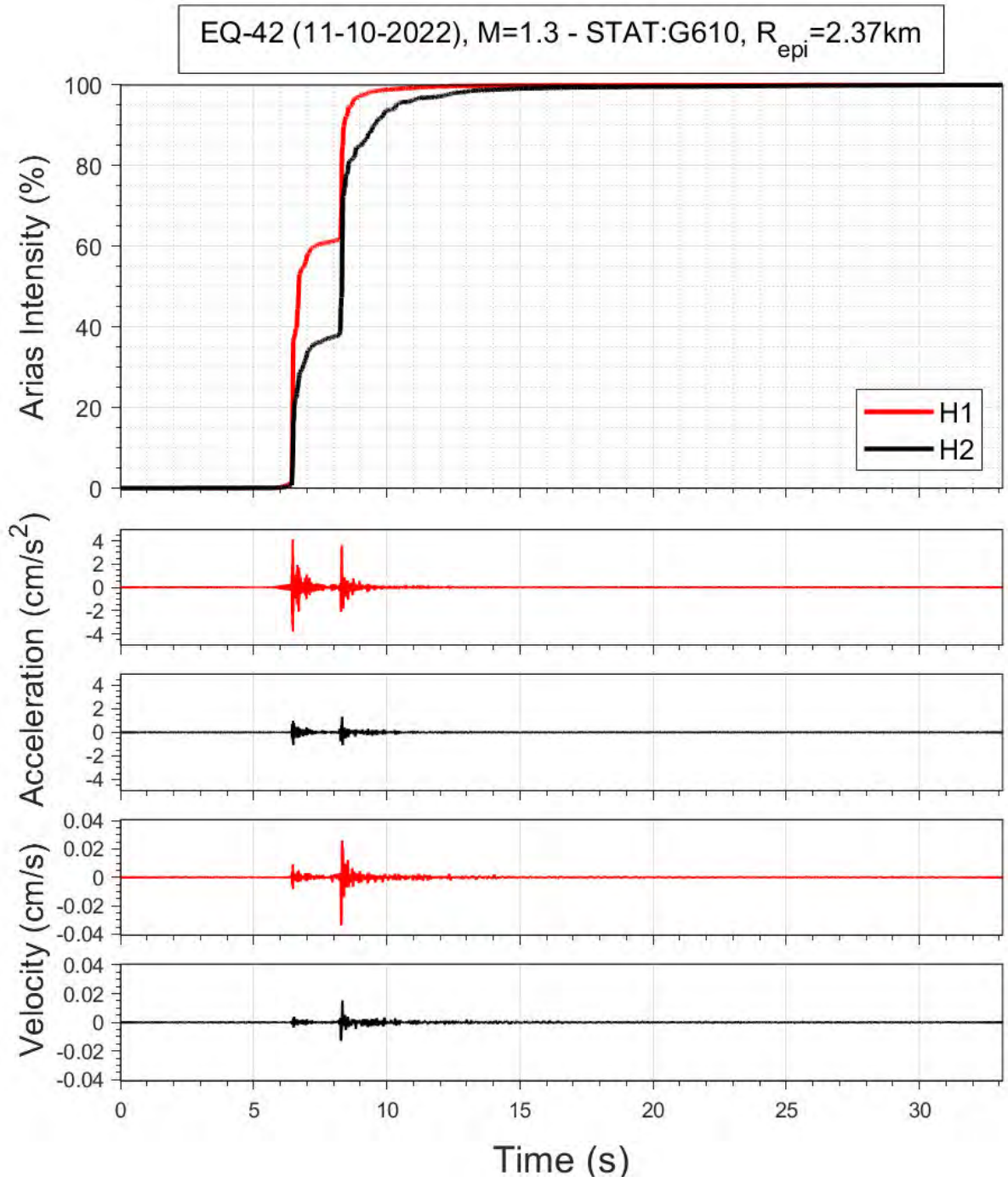

Figure 3.20 Horizontal components of acceleration and velocity recorded at the G610 station during event 42; the upper frame shows the accumulation of Arias intensity (energy) over time.

3.4 Spectral Accelerations and Comparison with Ground-Motion Models

Additional insight into the nature of the ground motions can be obtained from the 5%-damped acceleration response spectra and Fourier spectra. The spectra from the G610 recordings are shown in Figures 3.21 – 3.26. The spectral shapes are consistent with previous observations in the field. The divergence between the red and black curves in both frames shows that the horizontal polarisation of the recordings seen previously for PGA and PGV (Figures 3.7 – 3.12) persists across the entire range of usable response periods.

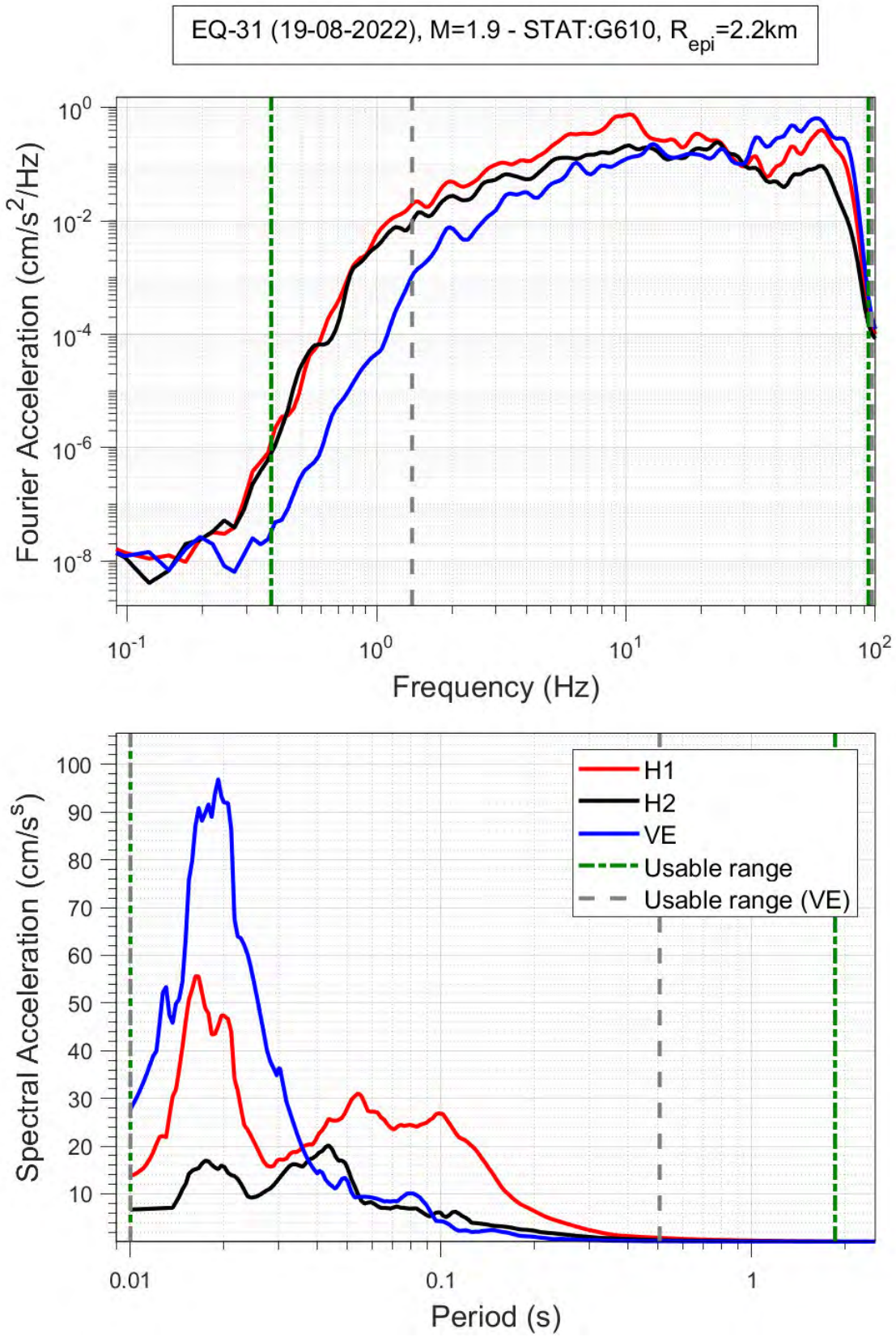

Figure 3.21 Fourier and response spectra from the G610 record of event 31

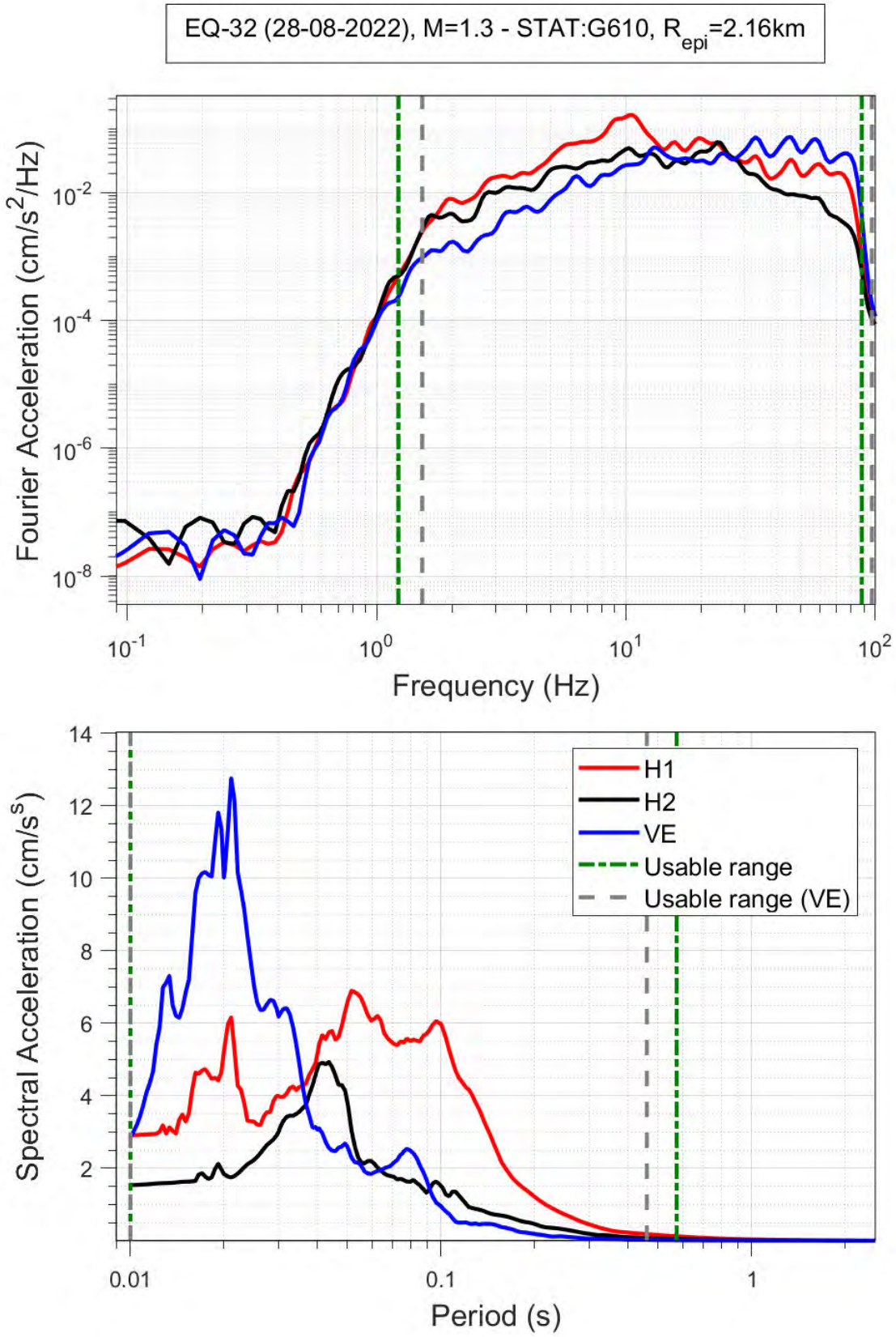

Figure 3.22 Fourier and response spectra from the G610 record of event 32

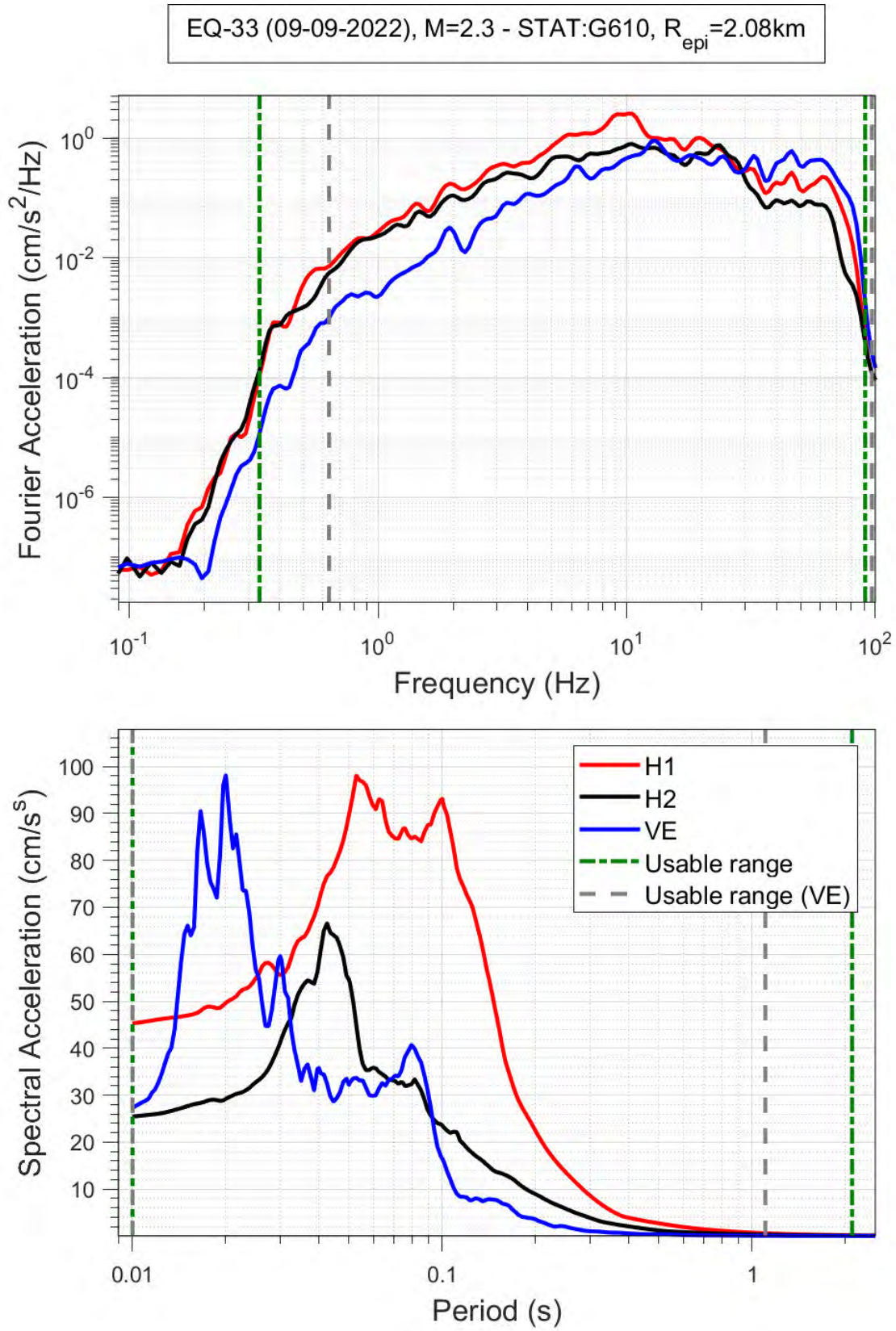

Figure 3.23 Fourier and response spectra from the G610 record of event 33

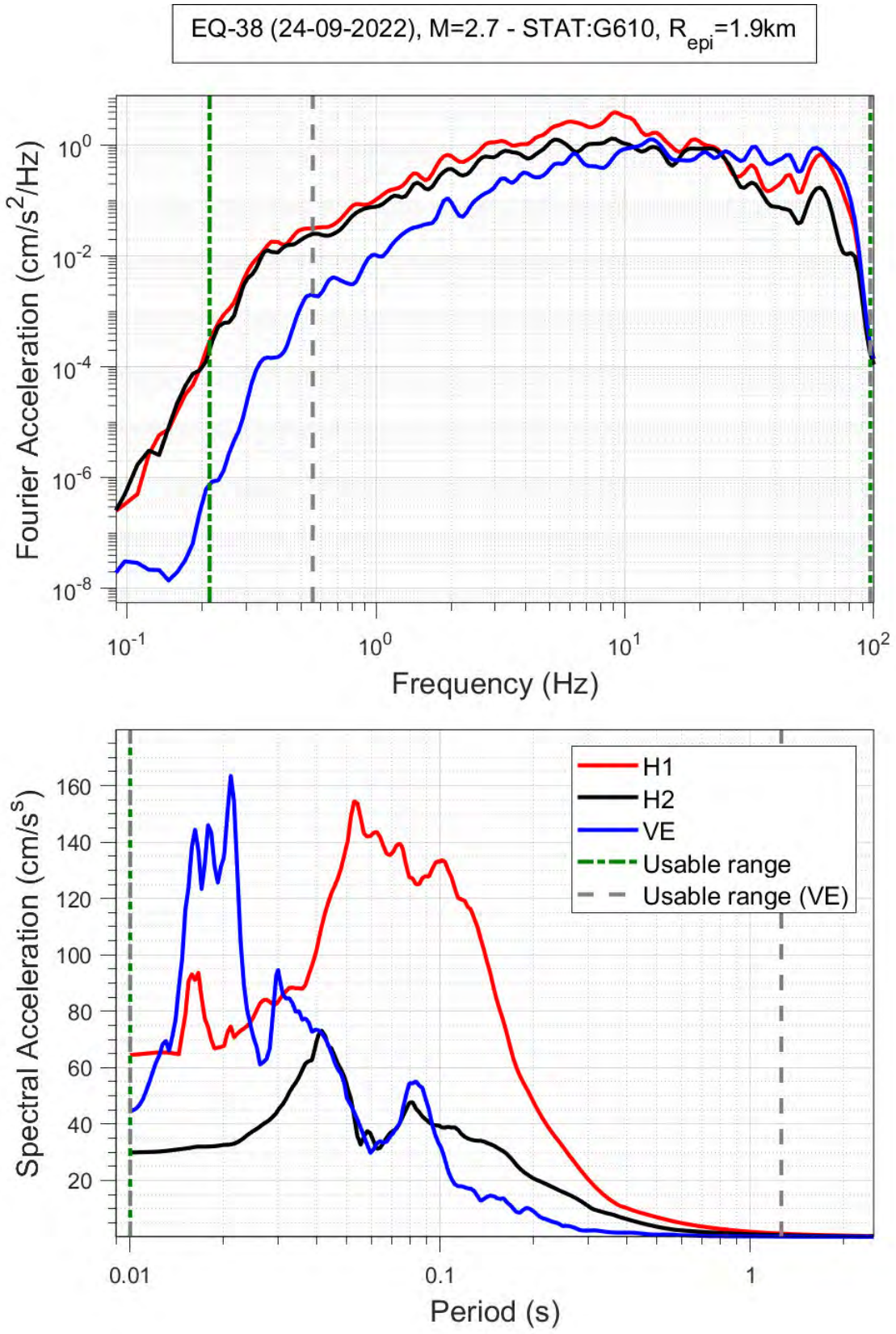

Figure 3.24 Fourier and response spectra from the G610 record of event 38

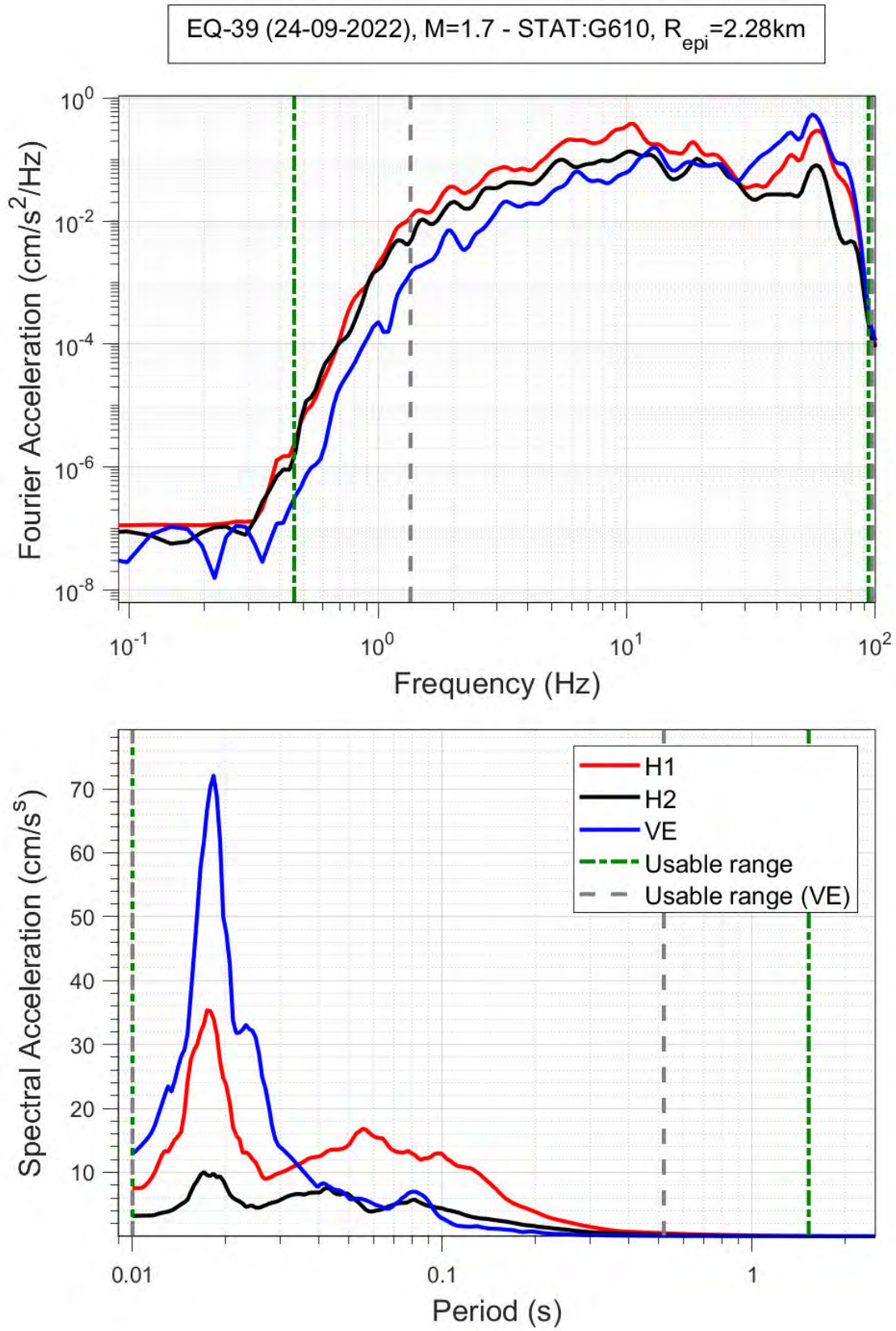

Figure 3.25 Fourier and response spectra from the G610 record of event 39

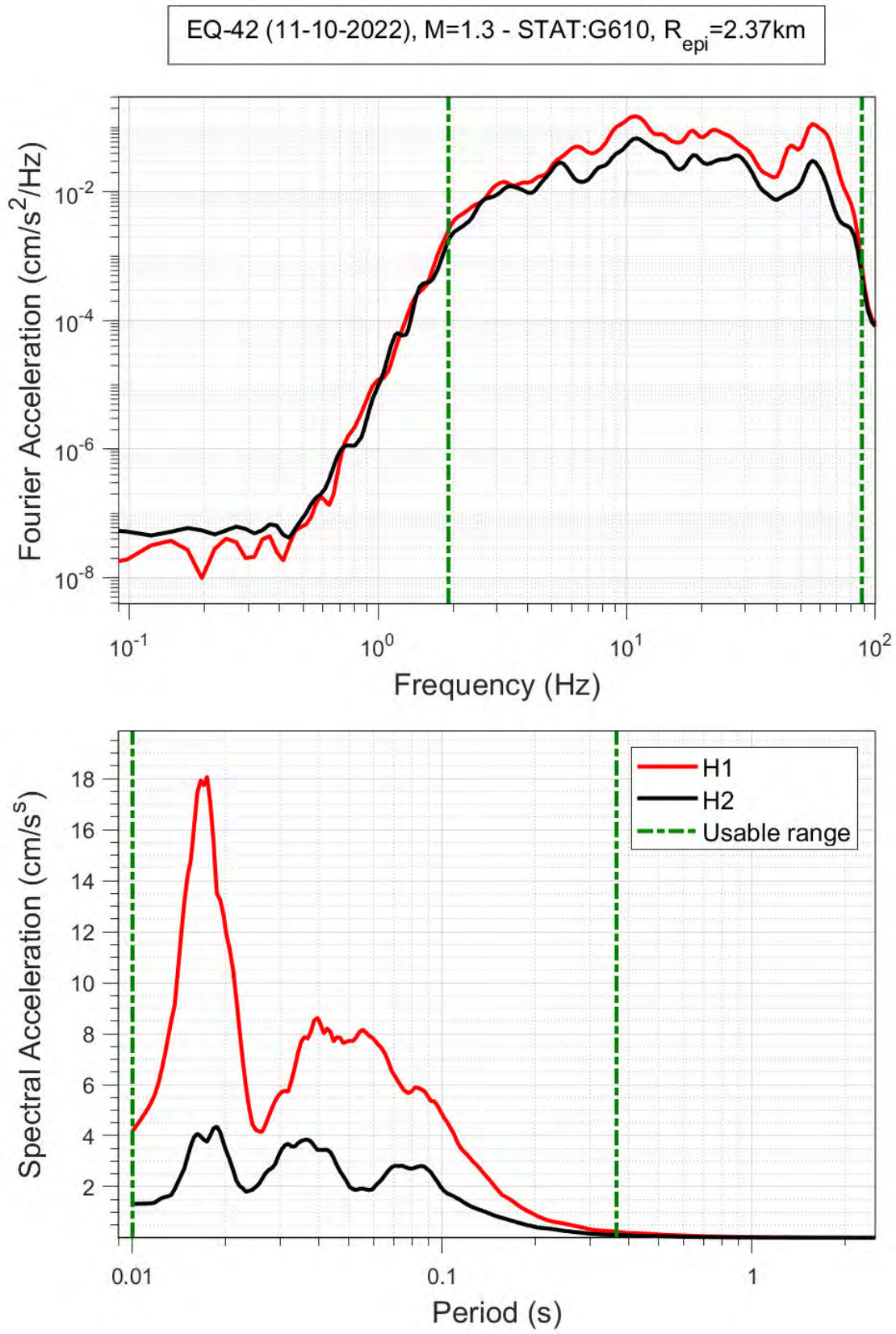

Figure 3.26 Fourier and response spectra from the G610 record of event 42

For this analysis, the key question of interest is whether the motions recorded in this earthquake are consistent with the current GMM and empirical PGV GMPEs being used in the Groningen field. The current GMM is the V7 GMM (Ref. 39) and event 38 is within its range of applicability (2.5 - 7.25) and

we have simply calculated the total residuals at the surface for different ground-motion parameters. In each case, the residual is the natural logarithm of the ratio of the observed (recorded) to the median predicted value, so a residual of 0.7 indicates that the recorded value was underestimated by a factor of 2 by the model and a residual of -0.7 would indicate over-prediction by a factor of 2. Figure 3.27 shows the residuals of spectral accelerations at 0.01 seconds with respect to the V7 GMM plotted against rupture distance. The scatter is very considerable but similar to the scatter of the data used in the V7 GMM development, while the residuals are centred above the zero line, which suggests an under-prediction by the model. A trend of the residuals with distance can be observed, with larger residuals observed at short distances. At longer periods (Figures 3.28 – 3.29), the scatter is smaller, however, the residuals are better centred on the zero line, indicating that the median predictions of the model provide an overall good fit to the data at those periods. It is important to note that the V7 GMM is calibrated to match the average spectral accelerations over the periods between 0.01 and 1 seconds, and not spectral accelerations at individual periods. The residuals with respect to the average spectral acceleration are shown in Figure 3.32, where it can be observed that the distance trend seen in the short periods is not present, and overall, the model under-predicts the recorded ground-motions, albeit only to a small degree.

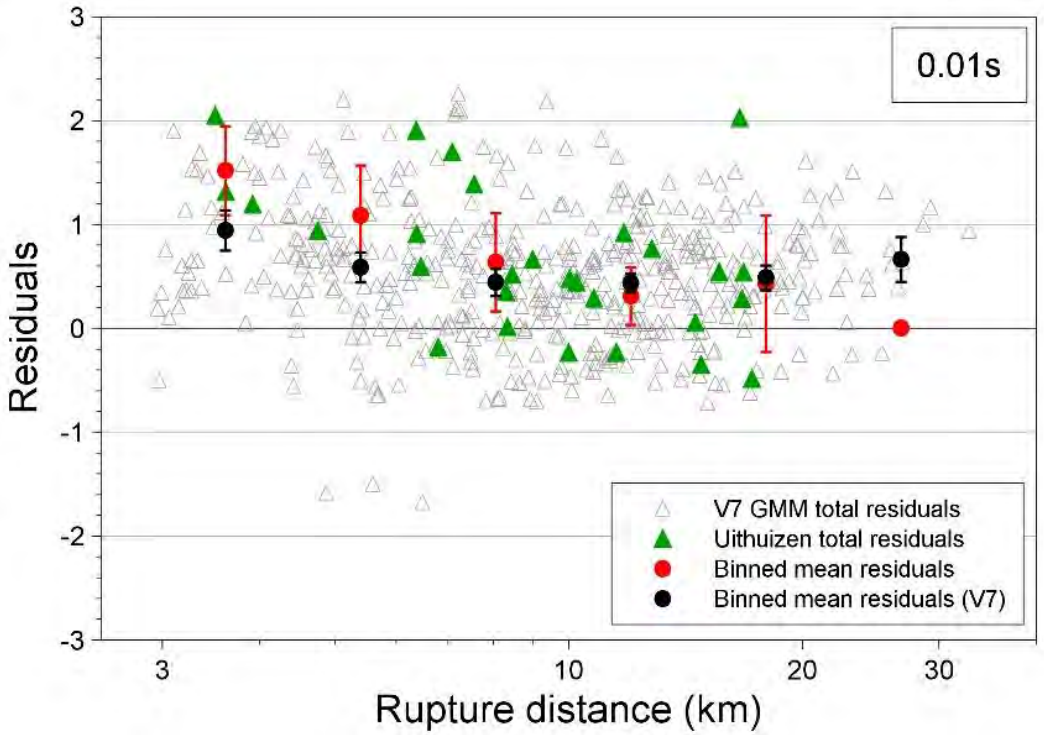

Figure 3.27 Residuals of Sa(T) with respect to the central branch of the V7 GMM at 0.01 seconds

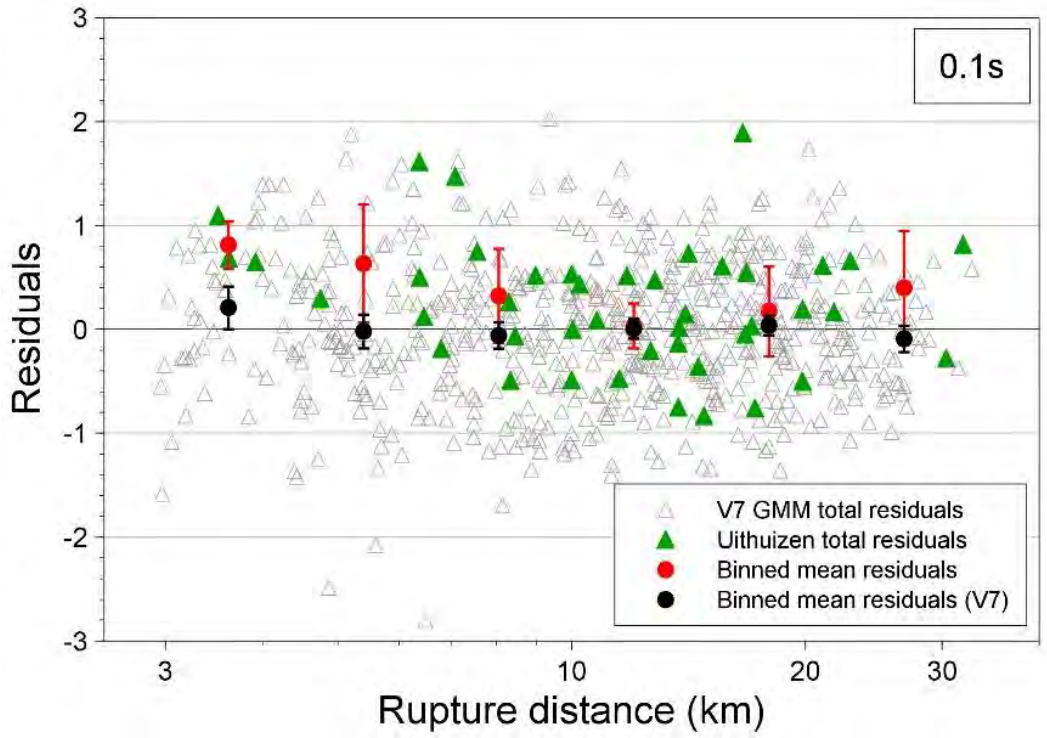

Figure 3.28 Residuals of Sa(T) with respect to the central branch of the V7 GMM at 0.1 seconds

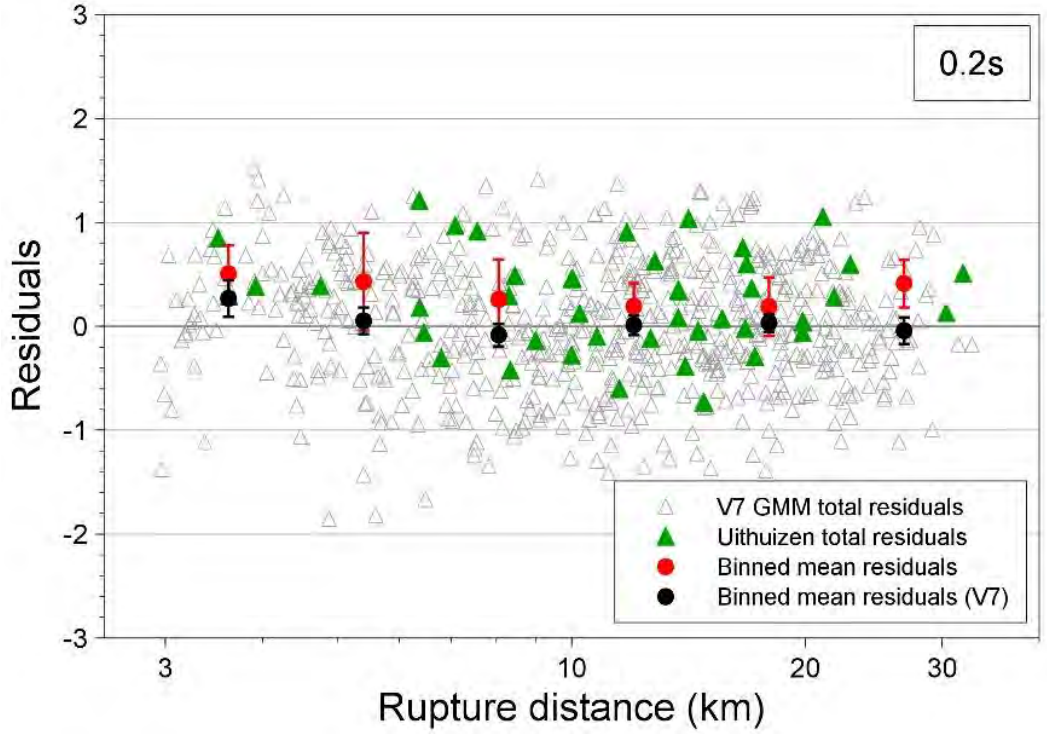

Figure 3.29 Residuals of Sa(T) with respect to the central branch of the V7 GMM at 0.2 seconds

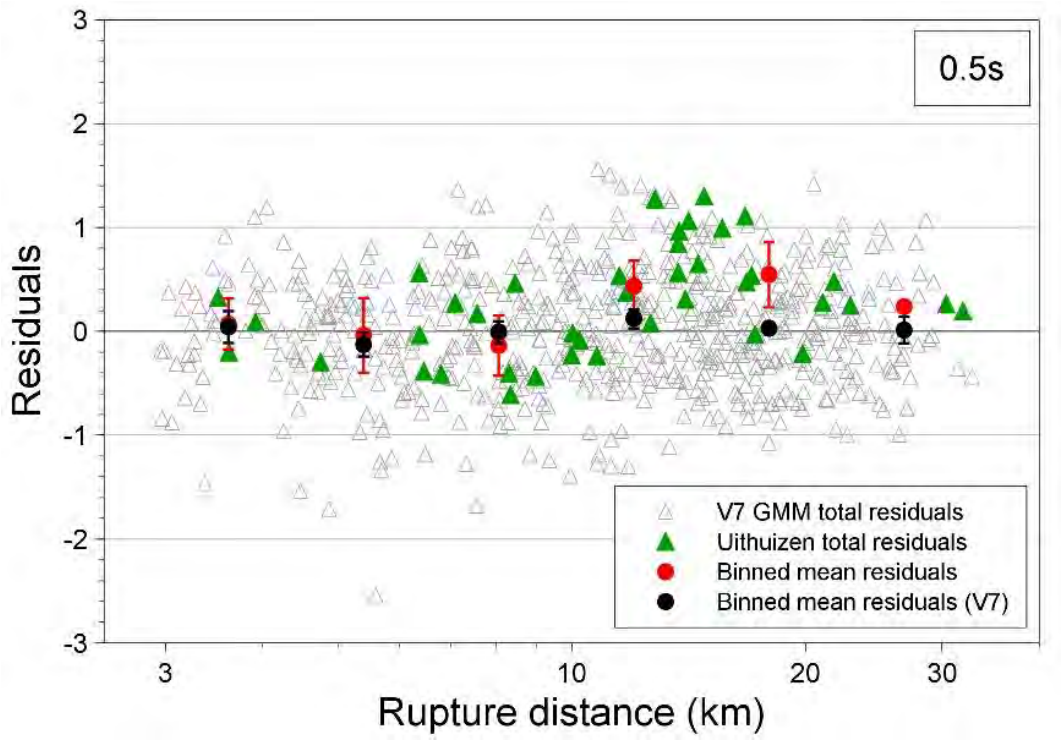

Figure 3.30 Residuals of Sa(T) with respect to the central branch of the V7 GMM at 0.5 seconds

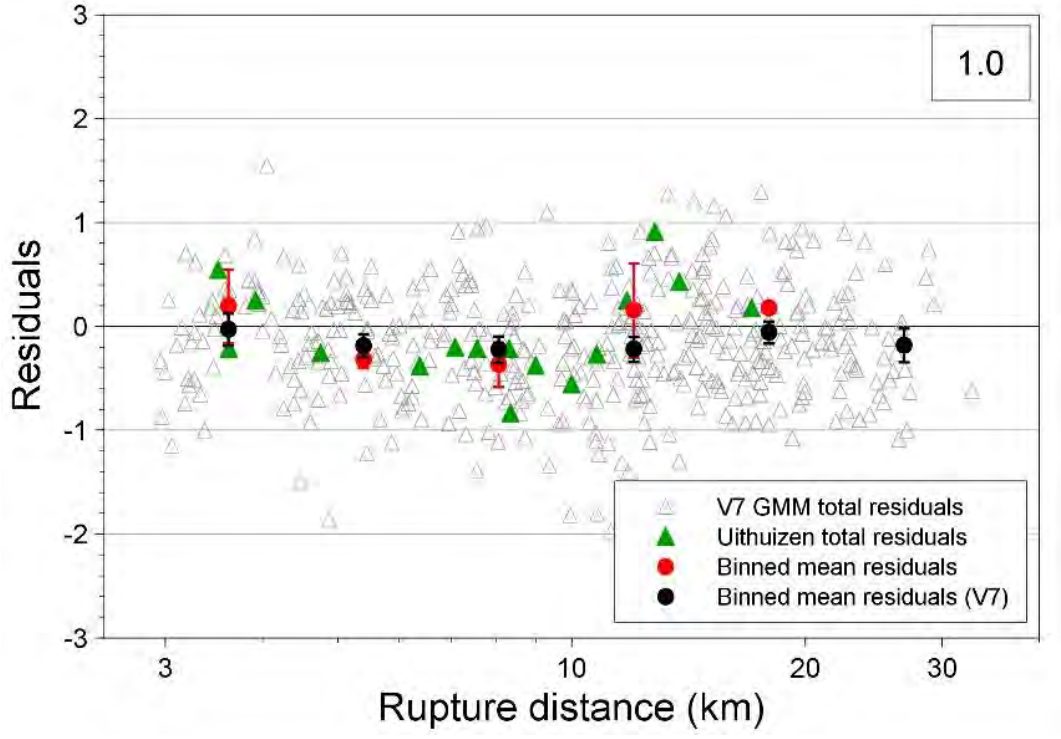

Figure 3.31 Residuals of Sa(T) with respect to the central branch of the V7 GMM at 1 second

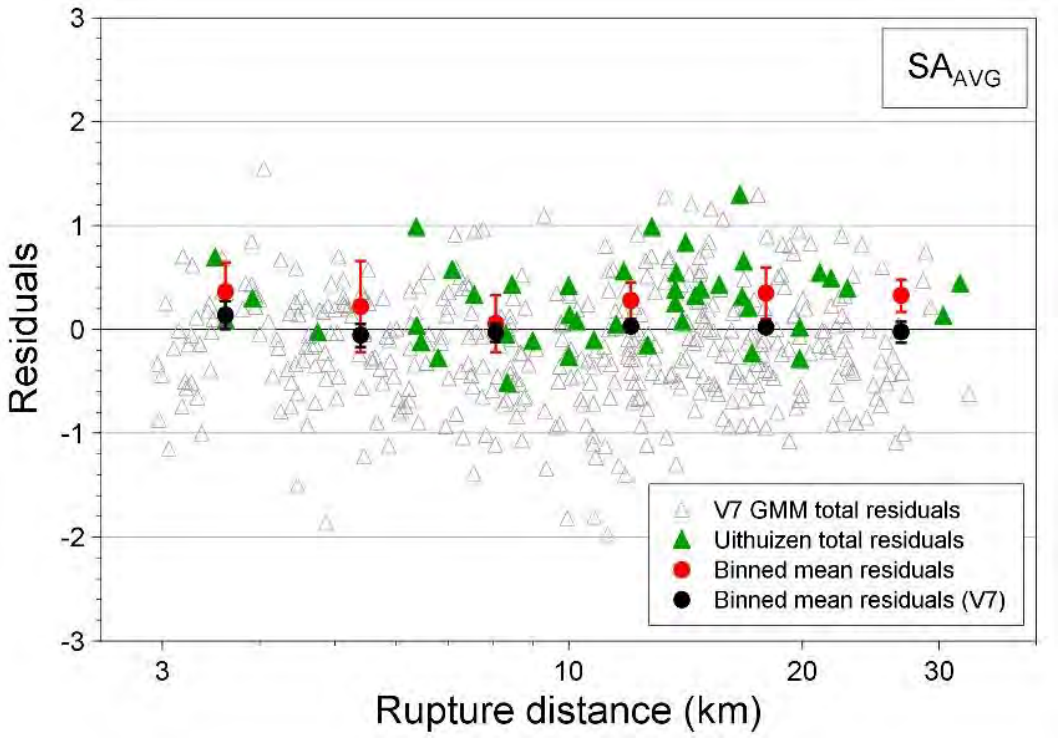

Figure 3.32 Residuals of period-averaged Sa with respect to the central branch of the V7 GMM

The V7 GMM superseded and replaced the V6 GMM (Ref. 41); the extensive additions, improvements and changes that the V7 GMM has in comparison to V6 are described in detail in Bommer *et al*. (Ref. 39). However, for completeness, and because the V6 GMM was used in the TNO-SDRA on which the current operational strategy for the Groningen field is based, we repeat the comparisons of Figures 3.27 – 3.32 for the V6 GMM in Figures 3.33 – 3.38 below. The observations that can be made are similar to those made for the V7 model residuals, with the distance trend at the short periods, however, being more prominent. The V6 database was not included in Figures 3.33 – 3.38 for comparison, as it was processed and compiled following different methods than the records of this event.

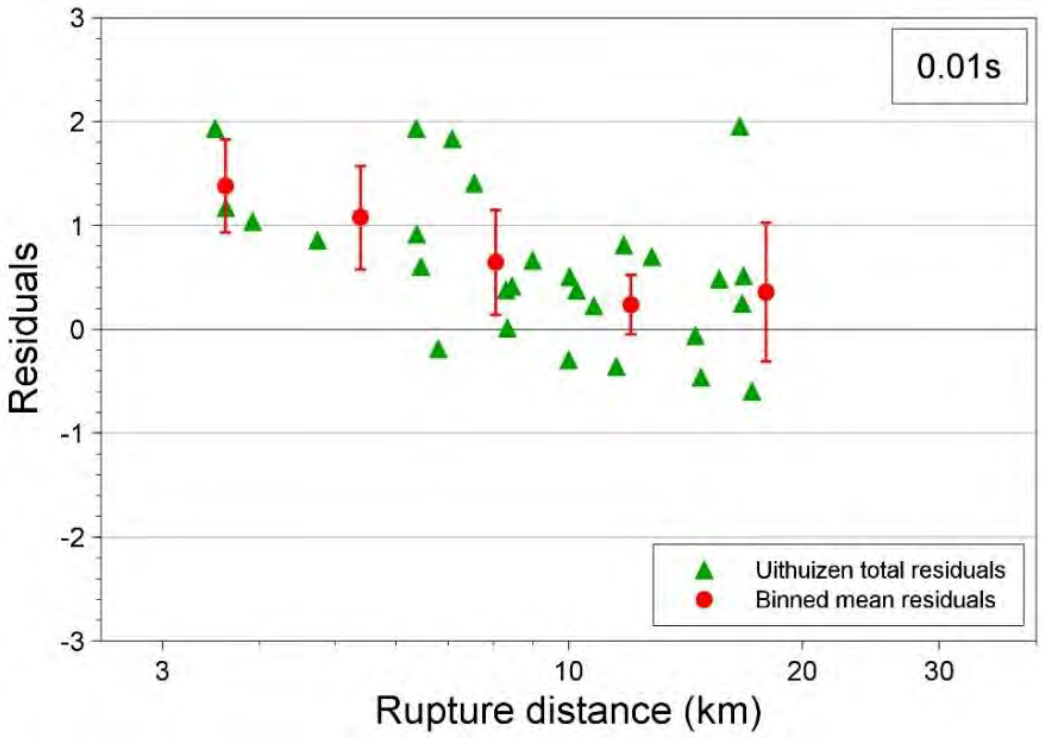

Figure 3.33 Residuals of Sa(T) with respect to the central branch of the V6 GMM at 0.01 seconds

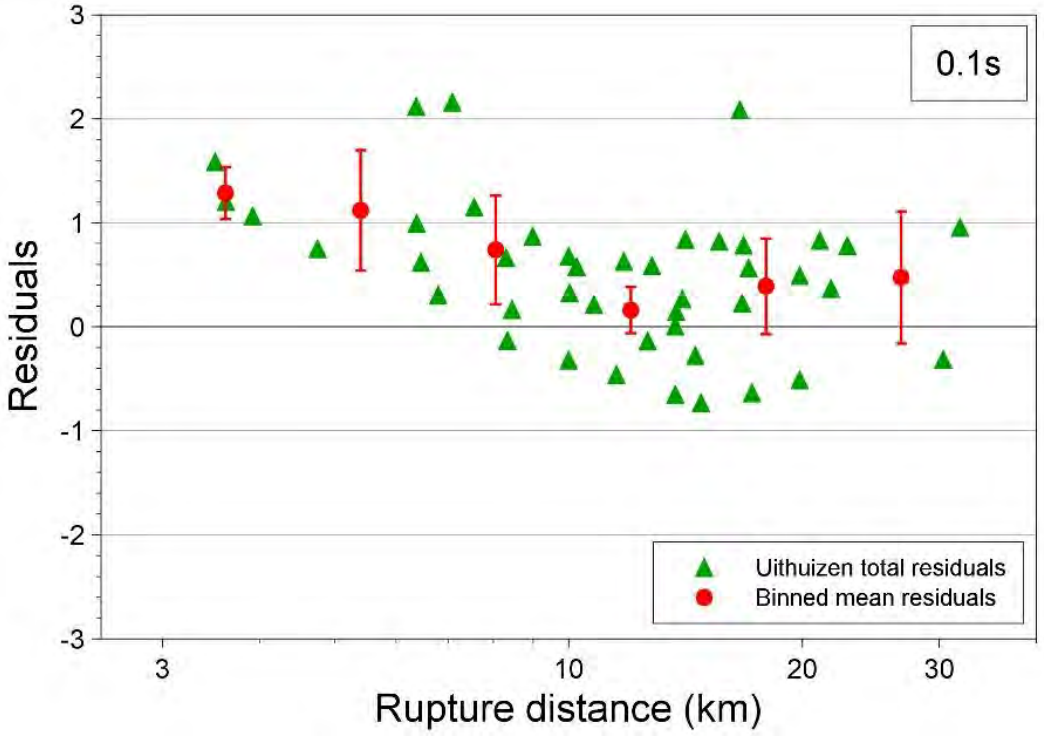

Figure 3.34 Residuals of Sa(T) with respect to the central branch of the V6 GMM at 0.1 seconds

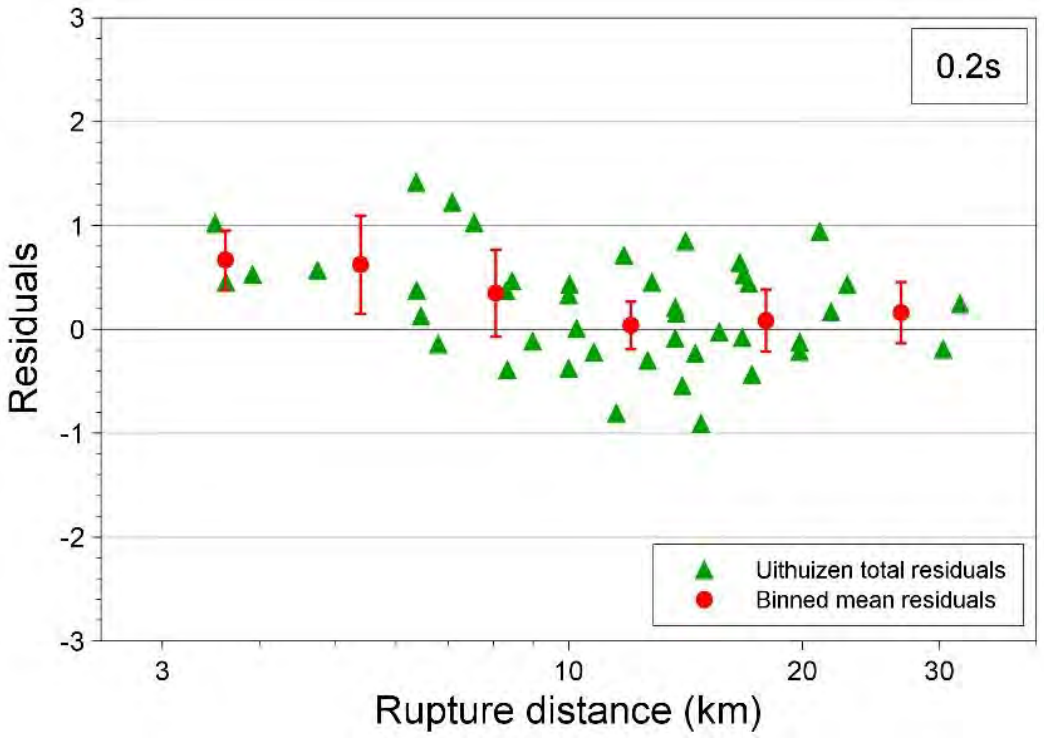

Figure 3.35 Residuals of Sa(T) with respect to the central branch of the V6 GMM at 0.2 seconds

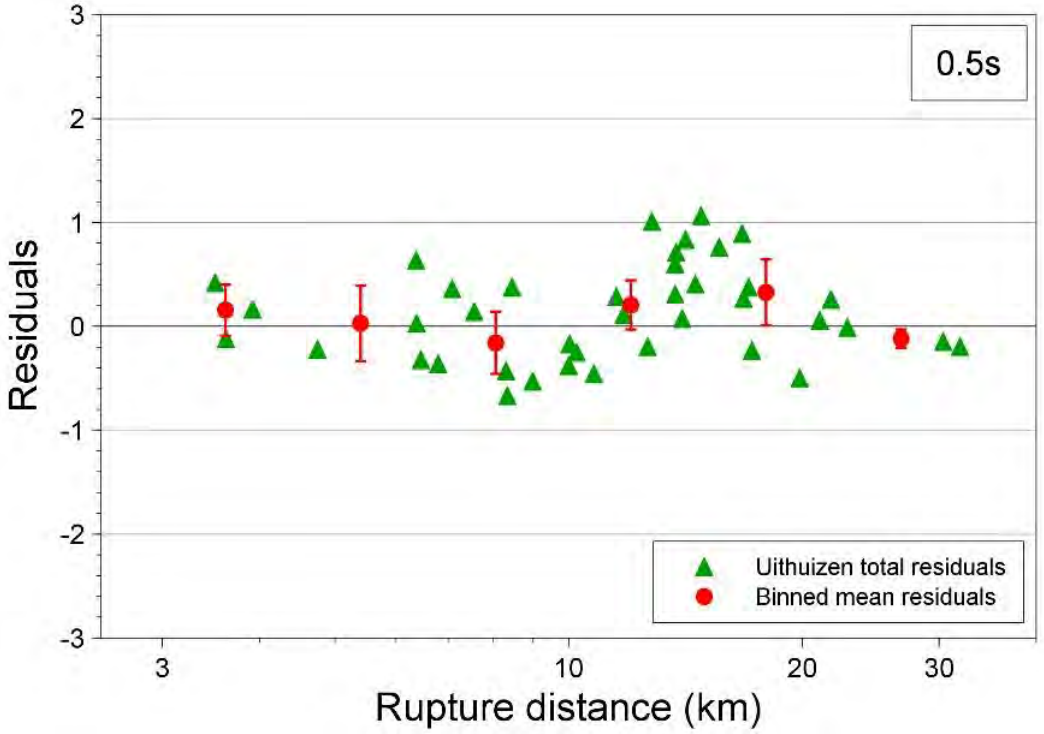

Figure 3.36 Residuals of Sa(T) with respect to the central branch of the V6 GMM at 0.5 seconds

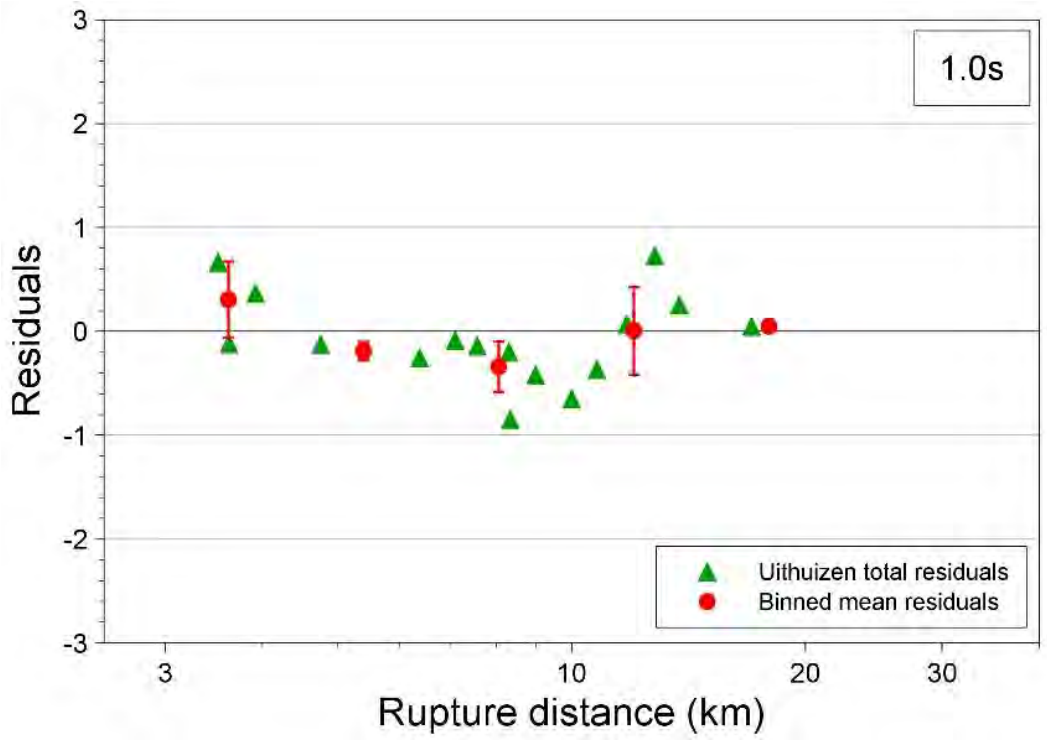

Figure 3.37 Residuals of Sa(T) with respect to the central branch of the V6 GMM at 1 second

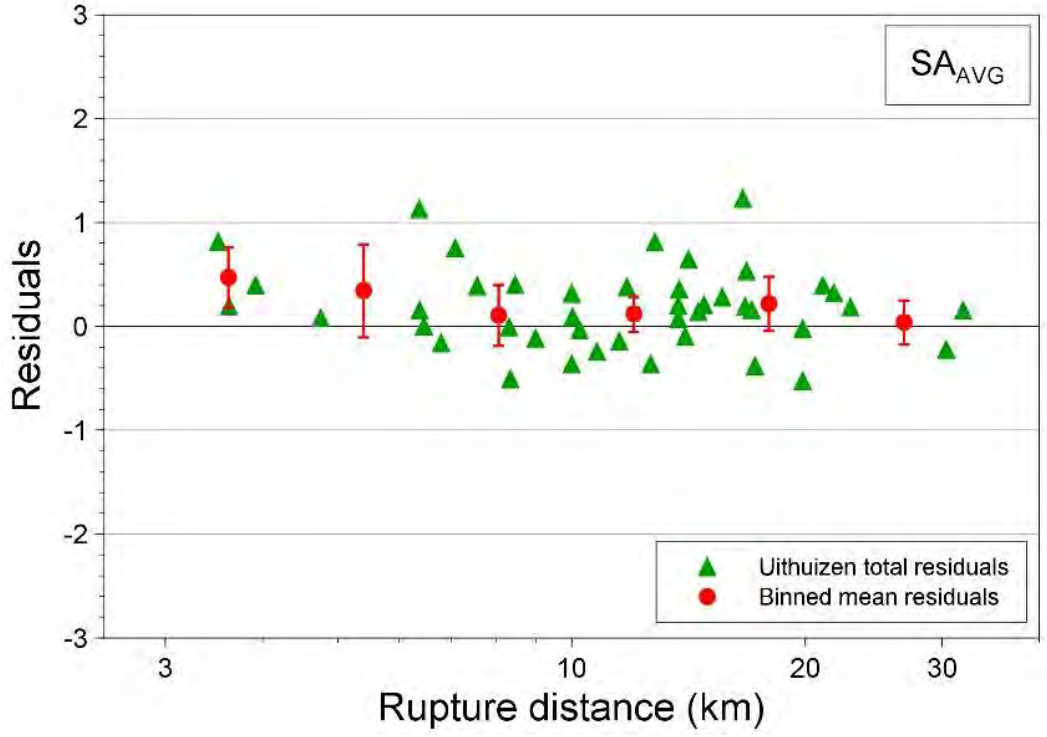

Figure 3.38 Residuals of period-averaged Sa with respect to the central branch of the V6 GMM

The current empirical PGV model was also developed in 2021 (Ref. 42). Events 31, 33 and 38 are within the applicability range of the GMPEs (M_L1.8-3.6), while event 39 is marginally outside; therefore, we have calculated the total, inter- and intra- event residuals for each of these four events. Figures 3.39 - 3.42 show the within-event model residuals of the three component definitions of PGV predicted by the GMPEs, plotted against hypocentral distance. In all cases, nearly all residuals of the Uithuizen

earthquake recordings are within two within-event standard deviations of the zero line, which suggests that the model captures well the variability of the data.

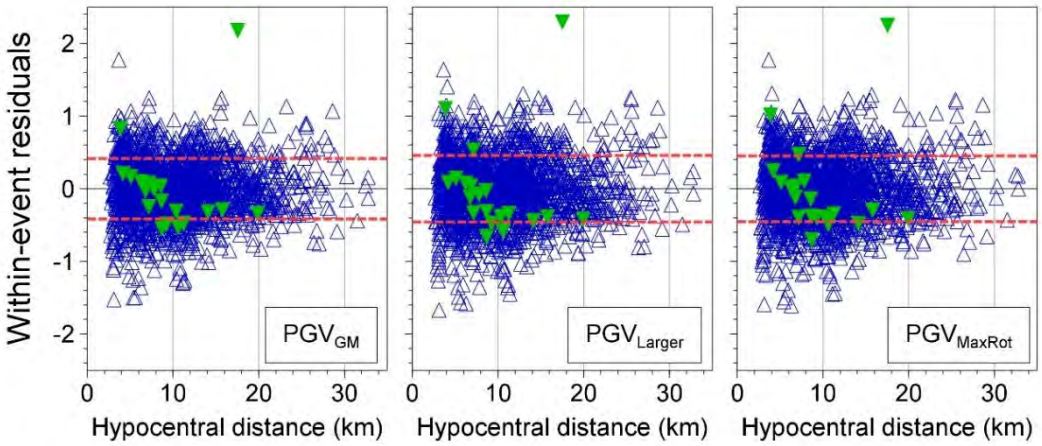

Figure 3.39 Event- and station-corrected within-event residuals of three component definitions of PGV with respect to the equations of the empirical PGV GMPE (Bommer et al., 2021) for event 31. Residuals of the Uithuizen earthquake recordings are shown in green and of other events in blue. The within-event standard deviation (φ_{SS}) is shown in red dashed lines.

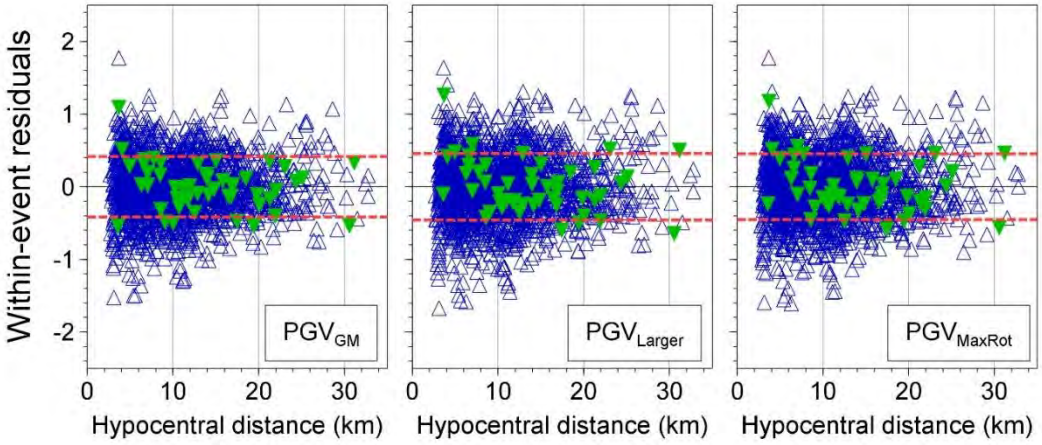

Figure 3.40 As with Figure 39, for event 33.

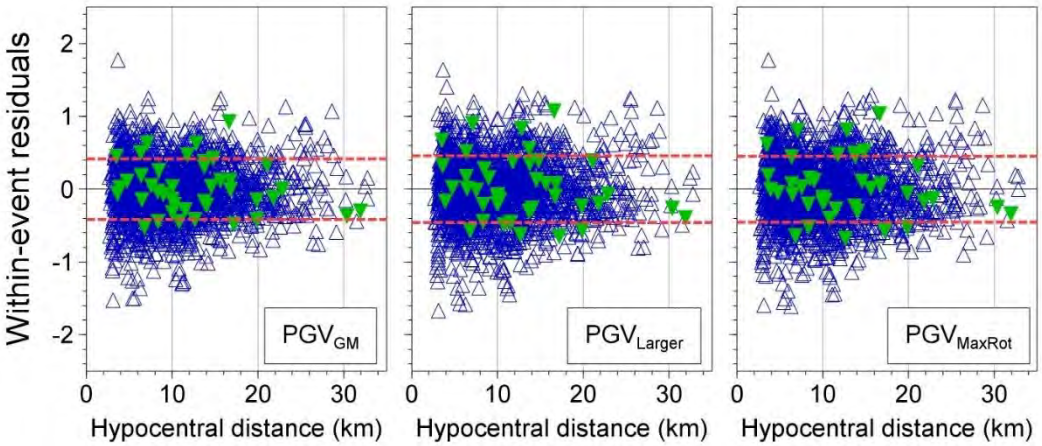

Figure 41. As with Figure 39, for event 38.

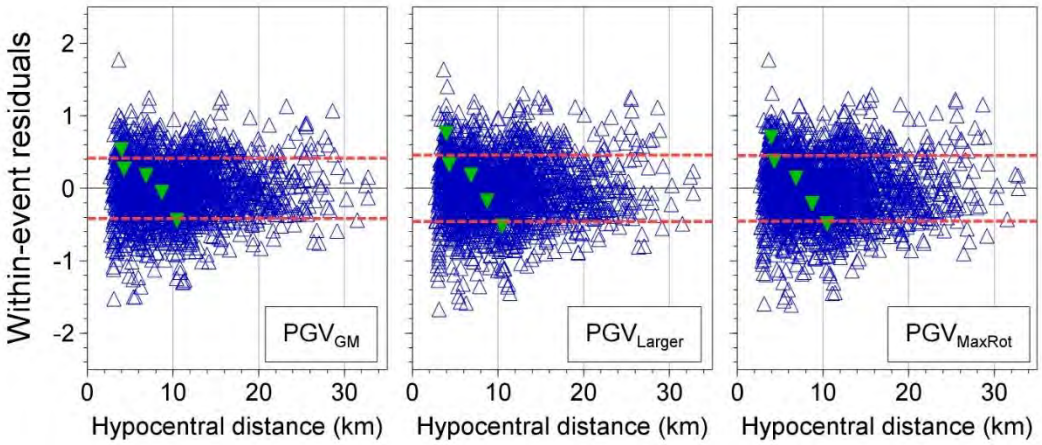

Figure 3.42 As with Figure 39, for event 39.

Figure 3.43 compares the inter-event residuals (event-terms) of the Uithuizen earthquakes to those of the previous events of the database. These event terms effectively represent the average offset of the recorded motions from each earthquake compared to the median prediction from the empirical model for the event magnitude, with a positive event-term indicating a stronger-than-average earthquake, a negative value a somewhat weaker-than-average earthquake. The event-terms of the Uithuizen earthquakes lie all within one standard deviation of the expected mean, indicating that the PGV values recorded are within the prediction range of the model.

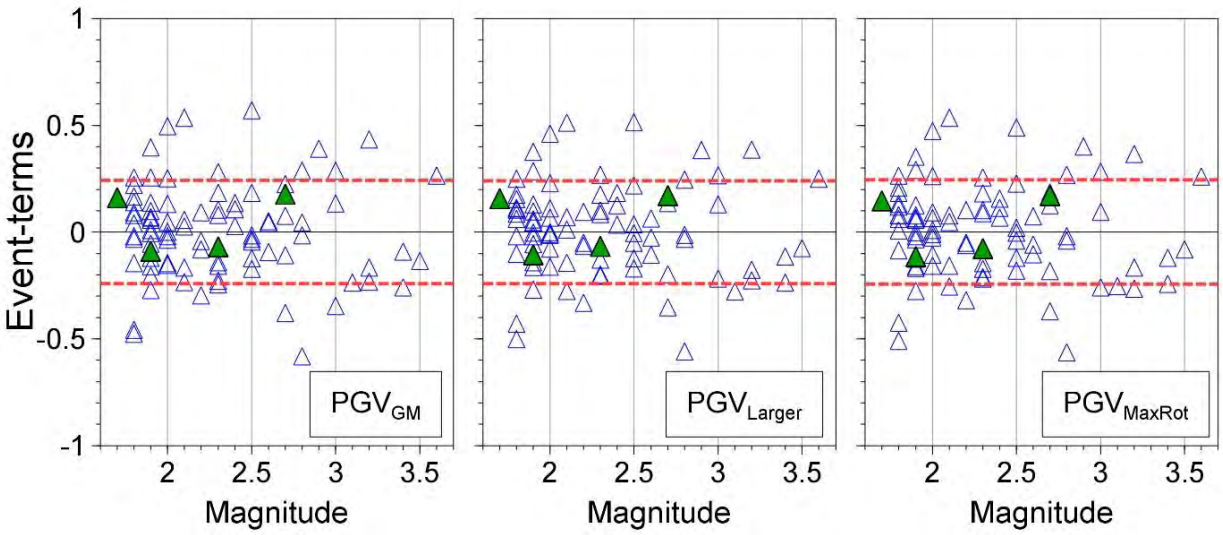

Figure 43 Inter-event residuals of three component definitions of PGV with respect to the equations of the empirical PGV GMPE (Bommer et al., 2021b). Residuals of the Uithuizen earthquake recordings are shown in green and of older events in blue. The inter-event standard deviation is shown in red dashed lines.

4 Conclusions

4.1 Event rate, epicentres and source mechanism

In August, September and October 2022 (19th August to 11th Oktober), eight earthquakes took place in a small area around the village of Uithuizen. Four of these earthquakes have magnitudes $M_L \geq 1.5$. During the equilibration of the reservoir pressure the earthquakes are expected to occur mainly to the North-West of Loppersum. The location of earthquakes near Uithuizen are consist with this. Remarkable is the very small area of some 500 m by 150 m, where seven of these earthquakes took place over a period of two months.

Based on locations of epicenters and source mechanism, the first two of these, although 9 days apart, had their epicentre most likely at the same fault.

On 24th September 2022 the monitoring level of the highest earthquake density for 'increased seismicity' was exceeded, when earthquake density reached 0.38 earthquake events per (year * km^2). With the earthquake on 11th October 2022, this monitoring level reached 0.46 earthquake events per (year * km^2) exceeding the monitoring level for 'strong seismicity'.

4.2 Ground Motions

The M_L 1.3-2.7 Uithuizen earthquakes of August, September and October 2022 have generated a large number of ground-motion recordings. The largest component of PGA recorded is 0.06 *g* and the largest value of PGV—which is generally considered a better indicator of the damage potential of the motion—recorded is 1.13 cm/s, which is significantly smaller than the largest value of the Groningen ground-motion database, the 3.46 cm/s recorded in the M_L3.6 2012Huizinge earthquake.

An important observation is that the motions recorded in the Uithuizen earthquakes are broadly consistent with the predictions from the empirical PGV GMPEs used to assess damage claims.

While the ground-motions recorded during the M_L2.7 event appear to be, on average, lower than those recorded in previous events of similar magnitudes (Figures 3.2 and 3.3), the V7 and V6 GMM ground-motion models, which are currently deployed in the seismic hazard and risk modelling for Groningen, under-predict the amplitudes by a small degree. A possible explanation for this can be found when examining the location of the epicentre with respect to the recording networks (Figure 3.1) and the direction of the largest amplitudes (Figures 3.7 - 3.12). The majority of recording stations is located southeast of the epicentres, which coincides with the direction of the largest amplitudes. Conversely, the number of stations in the opposite direction is small. This could likely lead to a biased recording sampling of the radiation pattern of the event, with areas with larger amplitudes being over-sampled.

References

1. Analyse seismiciteit, Nov 2016.
2. Rapportage recente aardbevingen Wirdum en Garsthuizen 2016/2017, NAM, Mar 2017.
3. Gaswinning Groningen Periodieke rapportage ontwikkeling seismiciteit - Volgens artikel 5, lid 3 van het Instemmingsbesluit winningsplan Groningenveld Rapportage 1 mei 2017, NAM, May 2017.
4. Ground Motions from the ML 2.6 Slochteren Earthquake of 27th May 2017, June 2017.
5. Special Report on the earthquake density and activity rate following the earthquakes in Appingedam (ML=1.8) and Scharmer (ML=1.5) in August 2017, NAM, Sept 2017.
6. Rapportage Seismiciteit Groningen - 1 Nov 2017, NAM, Nov 2017.
7. Special Report on the Loppersum earthquakes – December 2017, Taco den Bezemer and Jan van Elk, NAM, Dec 2017.
8. Special Report on the Zeerijp Earthquake, Taco den Bezemer and Jan van Elk, NAM, Jan 2018.
9. Short special report Exceedance Activity Rate February 2018, NAM, Feb 2018.
10. Rapportage Seismiciteit Groningen - 1 Juni 2018, NAM, July 2018.
11. Rapportage Seismiciteit Groningen - 1 November 2018, NAM, Nov 2018.
12. Periodieke rapportage Seismiciteit Groningen - Mei 2019, Jan van Elk and Dirk Doorkhof, NAM, May 2019.
13. Special Report - Westerwijtwerd Earthquake - 22nd May 2019, Jan van Elk and Dirk Doorkhof, NAM, May 2019.
14. Analyse overschrijding MRP-grenswaarde Aardbevingsdichtheid 9 september 2019, NAM, NAM, Sept 2019.
15. Rapportage seismiciteit Groningen - November 2019, NAM, NAM, Nov 2019.
16. Rapportage artikel 6, tweede lid, Vaststellingsbesluit Groningen gas veld 2019 - 2020, NAM, NAM, Dec 2019.
17. Analyse overschrijding aardbevingsdichtheid - 3 december 2019, NAM, NAM, Dec 2019.
18. Rapportage Seismiciteit Groningen - mei 2020, NAM, NAM, Apr 2020.
19. Special Report on the Zijldijk ML 2.5 Earthquake of 2nd May 2020, Jan van Elk, NAM, May 2020.
20. Special Report on the Loppersum ML 2.7 Earthquake of 14th June 2020, Jan van Elk, Dirk Doornhof and Jeroen Uilenreef, NAM, Aug 2020.
21. Rapportage Groningen gasveld Artikel 52H Mijnbouwwet Gasjaar 2019/2020, NAM, Nov 2020.
22. Periodieke rapportage seismiciteit Groningen - 1 november 2020, NAM, NAM, Nov 2020.
23. Rapportage Seismiciteit Groningen - mei 2021, NAM, NAM, May 2021.
24. Periodieke rapportage seismiciteit Groningen - 1 november 2021, NAM, NAM, Oct 2021.
25. Special Report on the Zeerijp Earthquake Swarm starting 4th October 2021, Jan van Elk and Jeroen Uilenreef, NAM, Oct 2021.
26. Rapportage Groningengasveld artikel 52h Mijnbouwwet gasjaar 2020-2021, NAM, NAM, Oct 2021.
27. 48-uur brief voor de Garrelsweer aardbeving aan SodM, NAM, NAM, Nov 2021.
28. 48-uur brief voor de Garrelsweer aardbeving aan ministerie EZK, NAM, NAM, Nov 2021.
29. Special Report on the Garrelsweer Earthquake 16th November 2021 with Magnitude ML = 3.2, Jan van Elk and Jeroen Uilenreef, NAM, Nov 2021.
30. Supplement to Special Report on the Zeerijp Earthquake Swarm starting 4th October 2021, Jan van Elk and Jeroen Uilenreef, NAM, Nov 2021.
31. Periodieke rapportage seismiciteit Groningen - 1 mei 2022, Jan van Elk and Jeroen Uilenreef, NAM, May 2022.
32. Appendix bij het Meet- en Regelprotocol Groningen – Cases, NAM, June 2017, NAM, June 2017.
33. Appendix bij het Meet- en Regelprotocol Groningen – Cases, NAM, June 2017, NAM, June 2017.
34. Meet- en Regelprotocol Groningen, NAM, June 2017.
35. Meet- en Regelprotocol Groningen, NAM, June 2017.
36. Technisch Addendum bij het Meet- en Regelprotocol Groningen, NAM, June 2017.
37. Technisch Addendum bij het Meet- en Regelprotocol Groningen, NAM, June 2017.
38. Bommer, J.J., B. Dost, B. Edwards, P.J. Stafford, J. van Elk, D. Doornhof & M. Ntinalexis (2016). Developing an application-specific ground-motion model for induced seismicity. Bulletin of the Seismological Society of America 106(1), 158-173.
39. Bommer, J.J., B. Edwards, P.P. Kruiver, A. Rodriguez-Marek, P.J. Stafford, M. Ntinalexis, E. Ruigrok & B. Dost (2022a). V7 Ground-Motion Model for Induced Seismicity in the Groningen Gas Field. Revision 1, 20 February 2022, 273 pp.
40. Bommer, J.J., P.J. Stafford, B. Edwards, B. Dost, E. van Dedem, A. Rodriguez-Marek, P. Kruiver, J. van Elk, D. Doornhof & M. Ntinalexis (2017). Framework for a ground-motion model for induced seismic hazard and risk analysis in the Groningen gas field, The Netherlands. Earthquake Spectra 33(2), 481-498.
41. Bommer, J.J., B. Edwards, P.P. Kruiver, A. Rodriguez-Marek, P.J. Stafford, B. Dost, M. Ntinalexis, E. Ruigrok & J. Spetzler (2019). V6 Ground-Motion Model for Induced Seismicity in the Groningen Gas Field. Revision 1, 19 December 2019, 196 pp.
42. Bommer, J. J., P. J. Stafford, and M. Ntinalexis (2021). Empirical Equations for the Prediction of Peak Ground Velocity due to Induced Earthquakes in the Groningen Gas Field, 10 March 2019
43. Bommer, J.J., P.J. Stafford, E. Ruigrok, A. Rodriguez-Marek, M. Ntinalexis, P. P. Kruiver, B. Edwards, B. Dost, and J. van Elk, (2022b). Ground Motion Prediction Models for Induced Earthquakes in the Groningen Gas Field, the Netherlands. Journal of Seismology, under review
44. Dost, B., E. Ruigrok & J. Spetzler (2017). Development of probabilistic seismic hazard assessment for the Groningen gas field. Netherlands Journal of Geoscience 96, s235–s245.
45. Edwards, B. & M. Ntinalexis (2021). Usable bandwidth of weak-motion data: application to induced seismicity in the Groningen Gas Field, the Netherlands. Journal of Seismology, doi: 10.1007/s10950-021-10010-7.

46. Ntinalexis, M., J.J. Bommer, E. Ruigrok, B. Edwards, R. Pinho, B. Dost, A.A. Correia, J. Uilenreef, P.J. Stafford & J. van Elk (2019). Ground-motion networks in the Groningen field: usability and consistency of surface recordings. Journal of Seismology 23(6), 1233-1253.
47. Ntinalexis, M., P.P. Kruiver, J.J. Bommer, E. Ruigrok, A. Rodriguez-Marek, B. Edwards, R. Pinho, J. Spetzler, E. Obando Hernandez, M. Pefkos, M. Bahrampouri, E.P. van Onselen, B. Dost, B., and J. van Elk (2022). A database of ground-motion recordings, site profiles, and amplification factors from the Groningen gas field in the Netherlands. Earthquake Spectra, under review.

Appendix A FWI analysis of the earthquake near Uithuizen on the 19th August 2022 with a magnitude of 1.9

Event 31 - Uithuizen
19 August 2022 05:49:14

13 September 2022

Induced Seismicity Taskforce

Disclaimer

- The results presented in this report have been automatically generated using an unconstrained full waveform, event location and moment tensor inversion workflow, developed by the Induced Seismicity Taskforce at Shell.
- These results have not been previously reviewed.
- For questions related to the results then you should contact:
  - Chris Willacy (Christopher.Willacy@Shell.com) or
  - Jan-Willem Blokland (Jan-Willem.Blokland@Shell.com)

Event summary

The event happened at:

Date	19 August 2022
Time	05:49:14.266485

The event is located at:

Location	Uithuizen
Northing (m)	602400
Easting (m)	241700
Depth (m)	3200

The source characteristics are:

	Solution 1	Solution 2
Strike angle (degree)	130.87	317.38
Dip angle (degree)	46.25	60.21
Rake angle (degree)	-95.89	-85.10
Isotropic (percentage)	-22.74	-22.74
CLVD (percentage)	26.32	26.32
Magnitude M_{L}	1.90	1.90

Magnitude summary

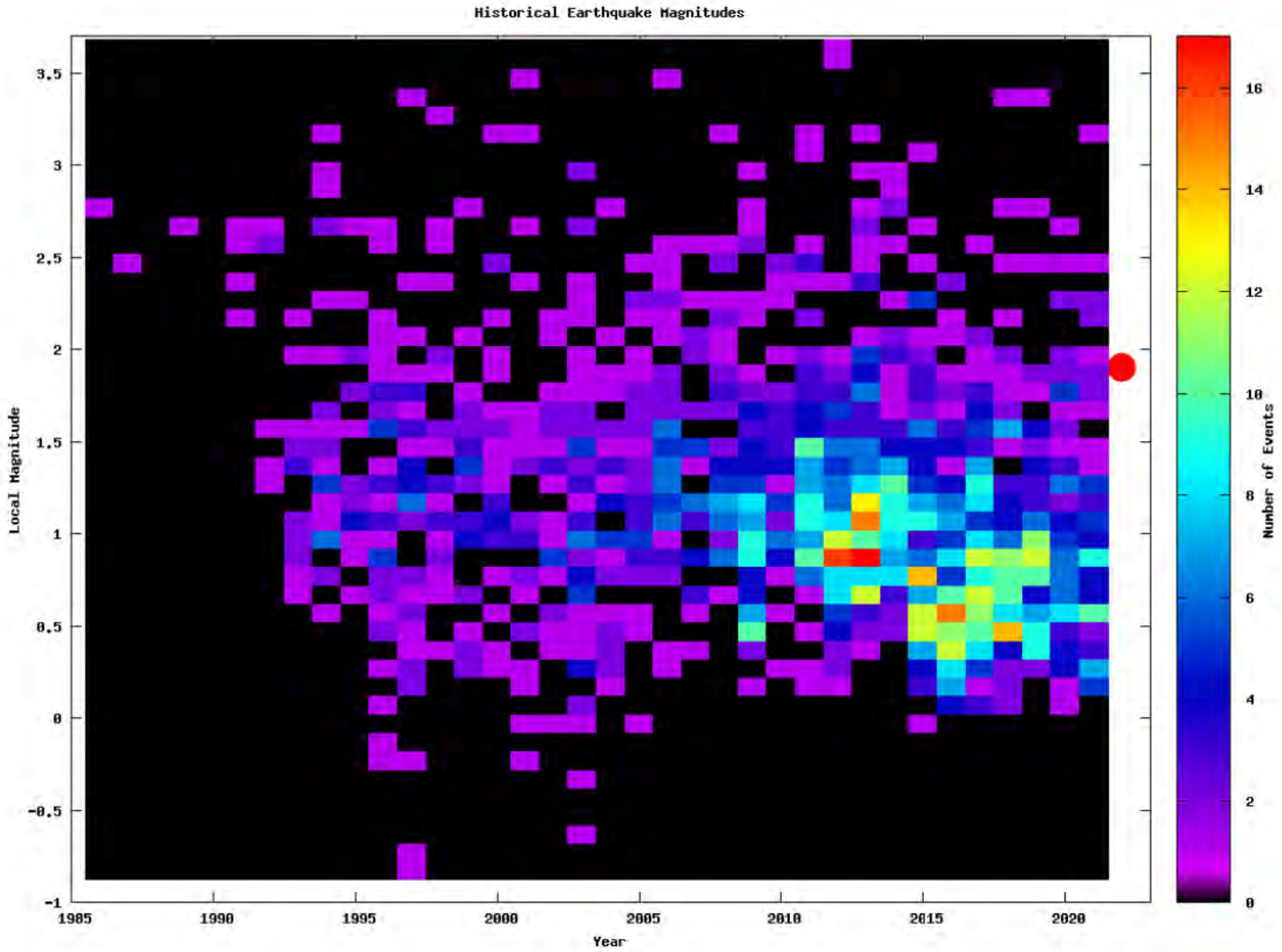

Regional and historical map

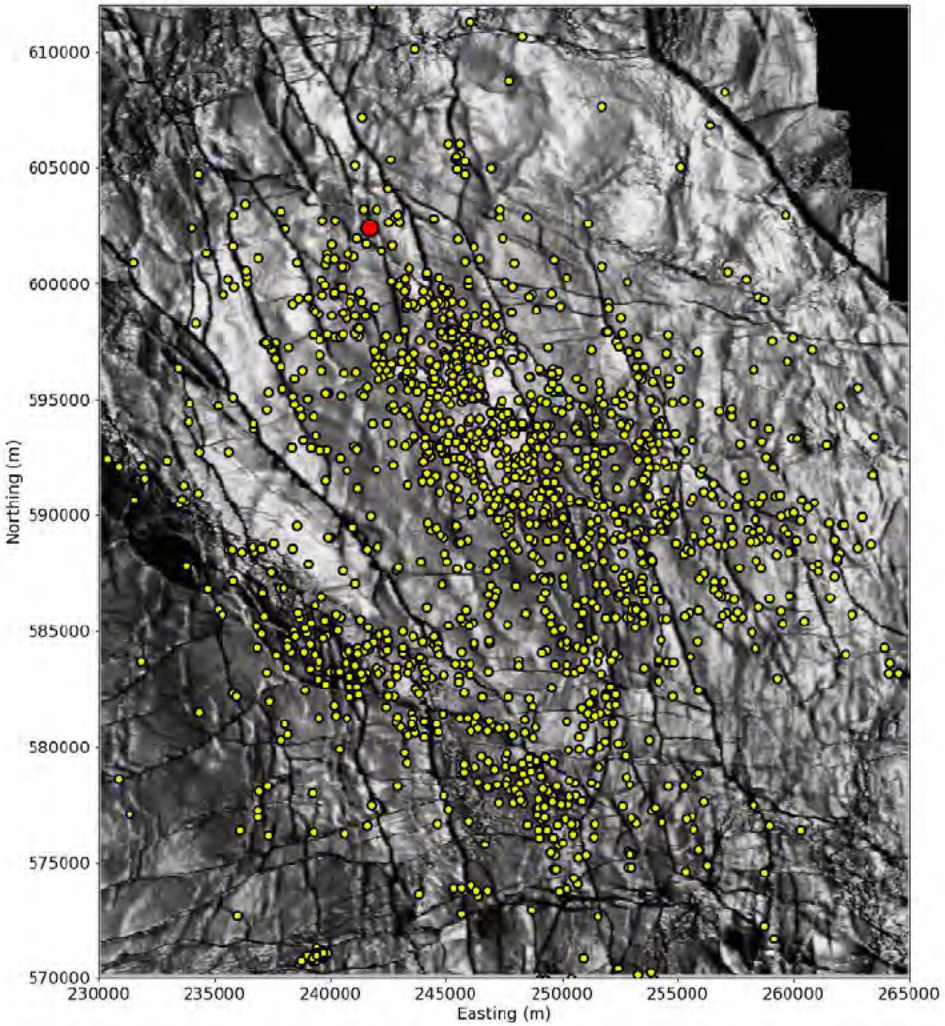

Event depth summary

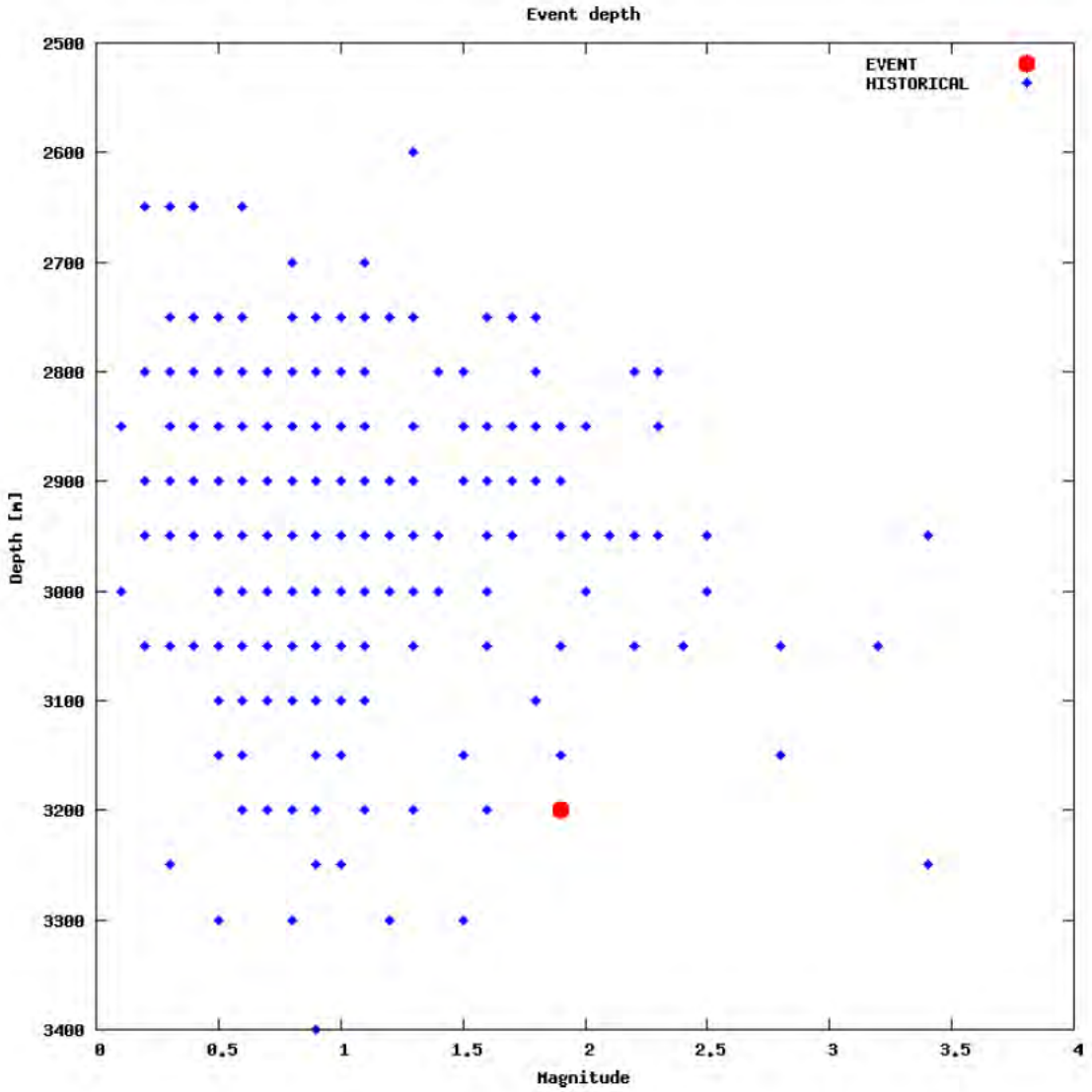

Event location - Map

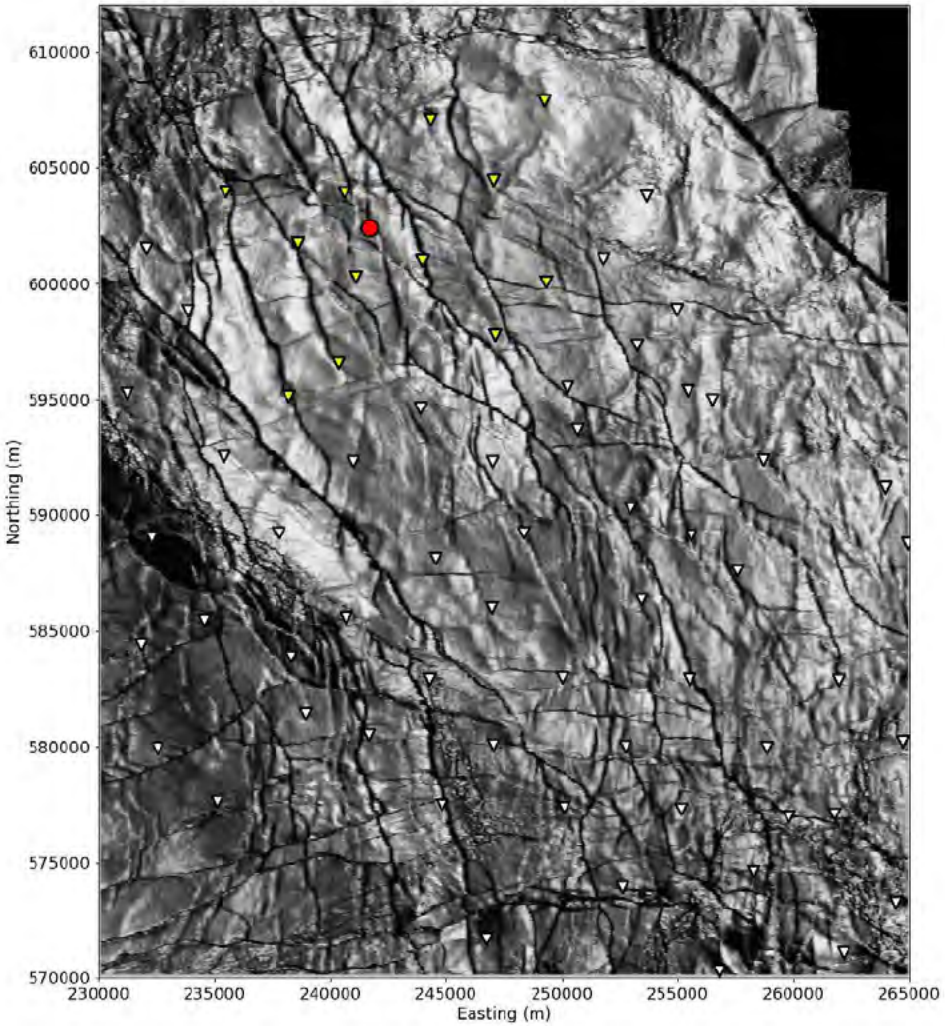

Event location and depth

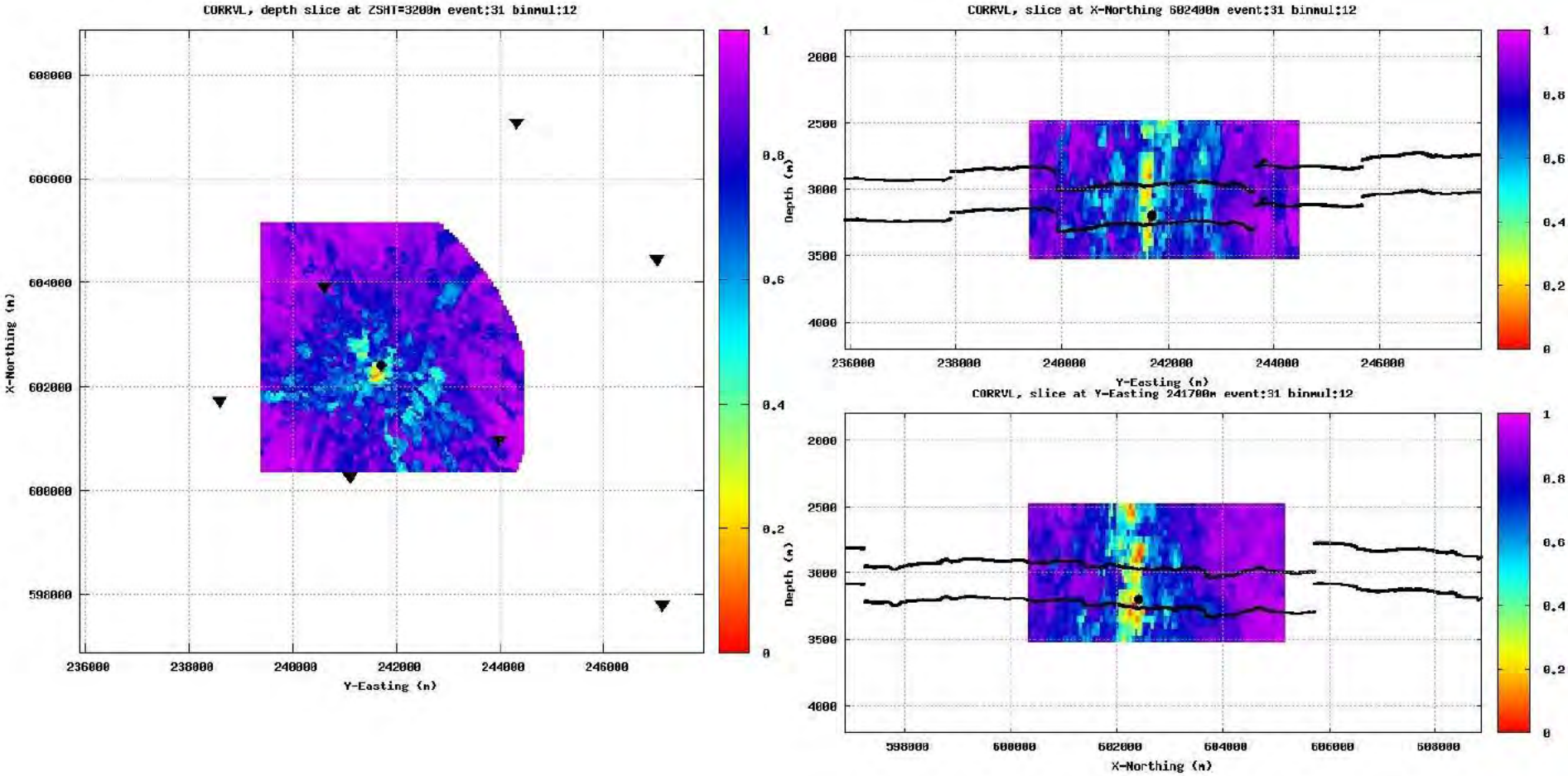

Moment tensor

Double-coupled part

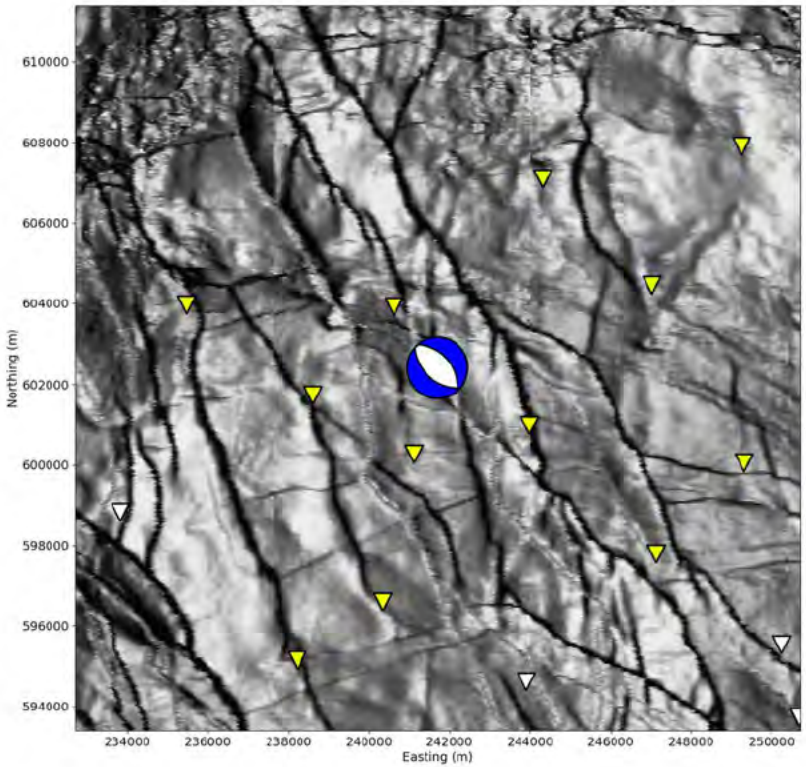

Full

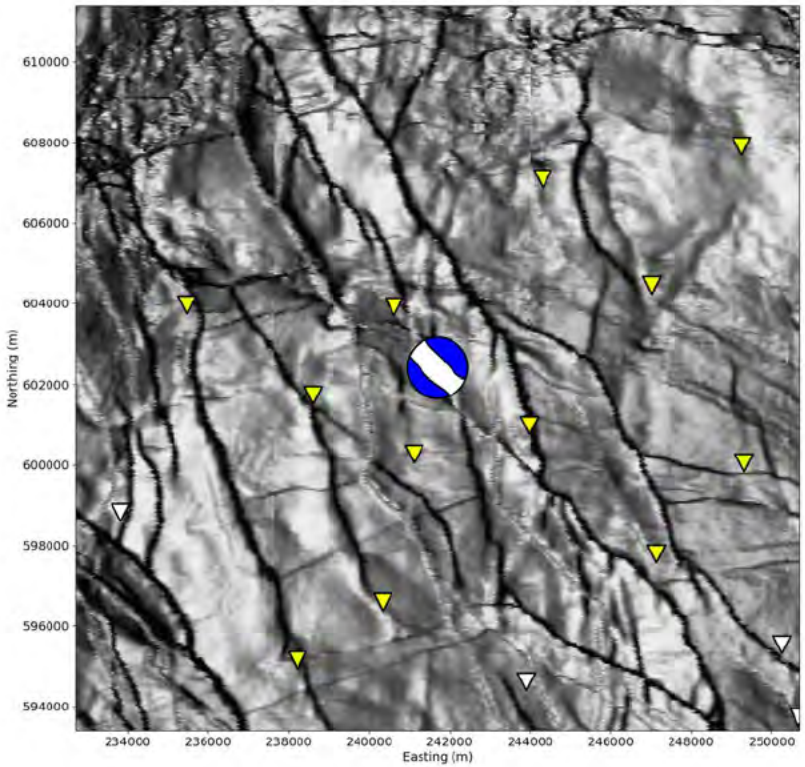

Moment Tensor: Decomposition

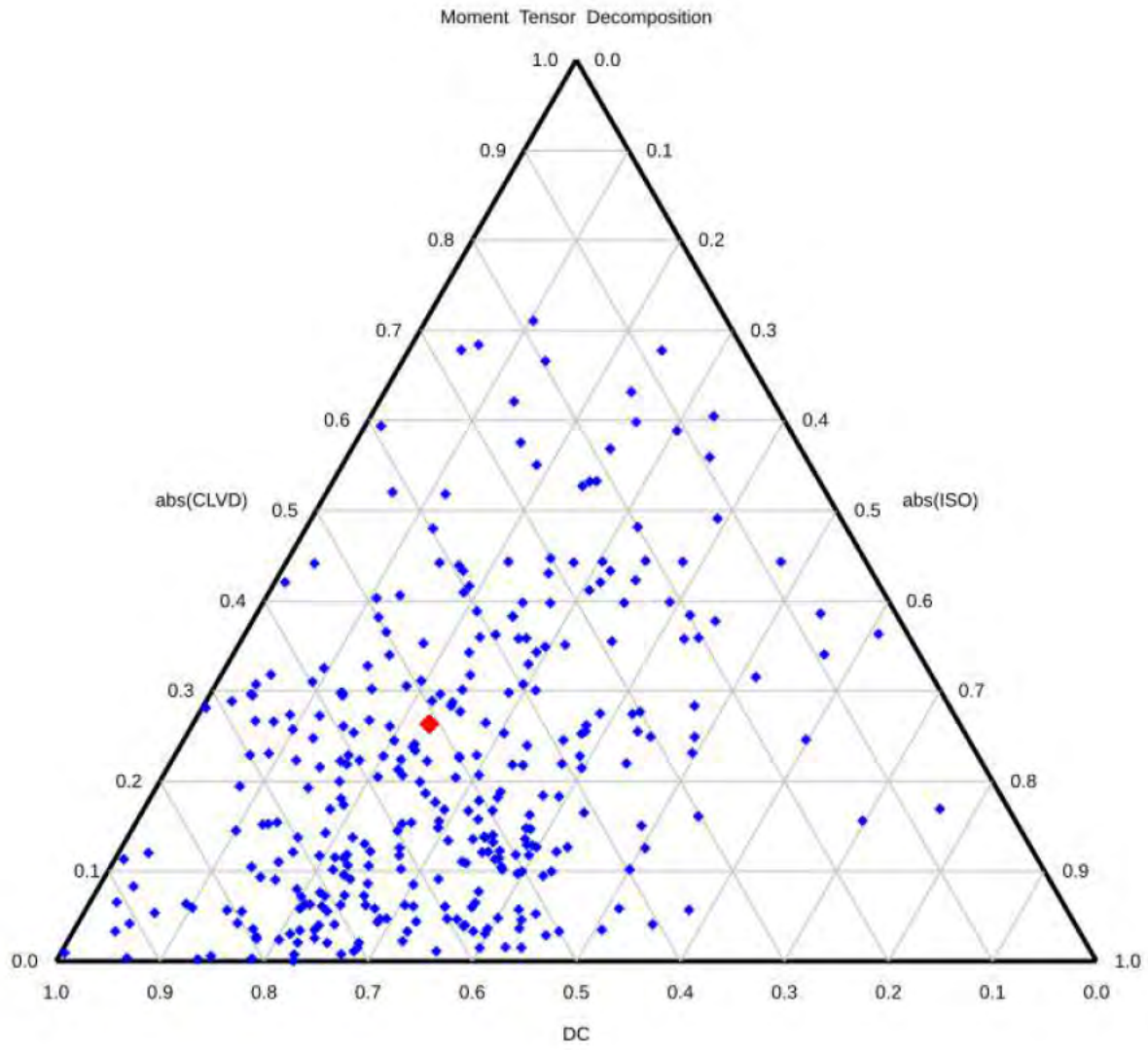

Field data traces

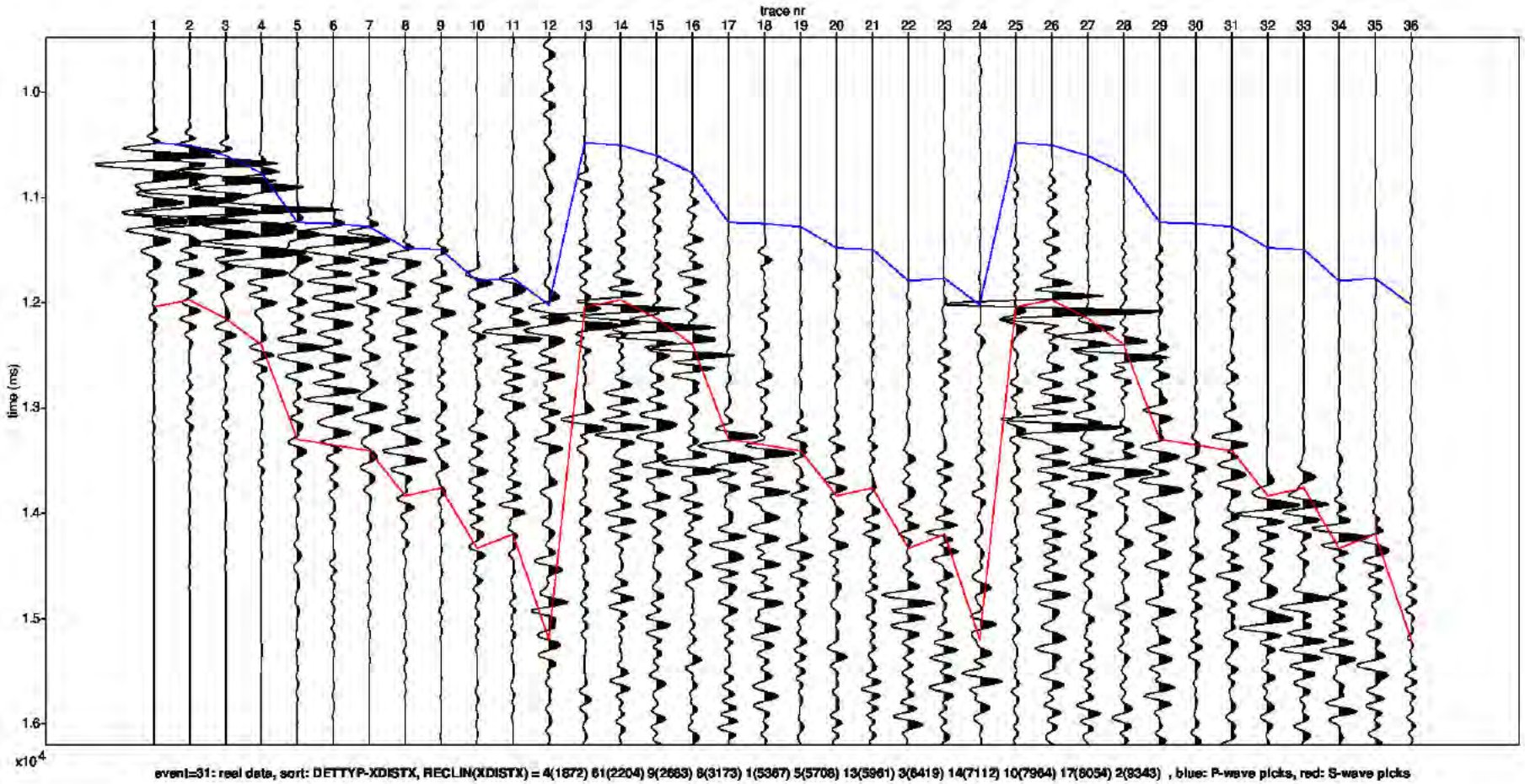

Modelled data traces

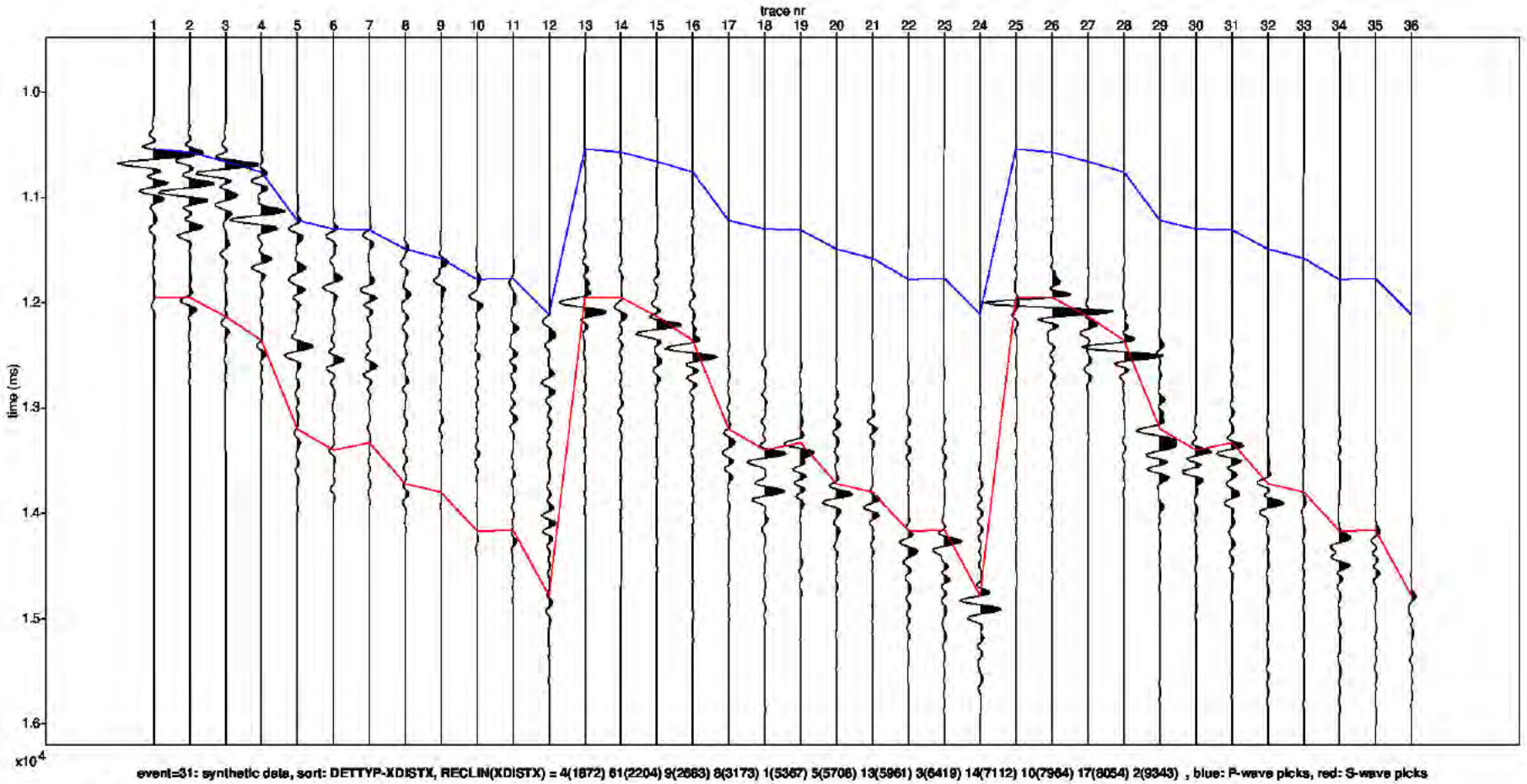

Appendix - Figure Captions

Page

3 Detailed parameter summary for the event. Both primary and secondary focal plane solutions are provided from the moment tensor inversion.

4 Magnitude summary. Prior years are displayed as a “heat map” where the number of events for a given magnitude is displayed per grid cell. The current event is displayed in red.

5 Regional map showing the historical events from KNMI (1986-2019) in blue and the location of the current event in red.

6 Event depth summary. Depths from our automatic workflow (2018-2020) are shown in blue and the current event depth is shown in red. The resolution of the vertical grid is 50m.

7 Event location details for the current event, superimposed on the top Rotliegend depth horizon. Station locations as shown as inverted triangles. Blue triangles are the actual stations used to locate the event whose epicentre is shown by the red dot.

8 QC displays extracted from the objective function for the current event location. The colour attribute displayed is 1 minus the normalized cross correlation between observed and synthetic waveforms. Station locations are shown as black inverted triangles on the map and the event location is shown by the black dot (left plot). The west to east and north to south vertical profiles are shown on the right. The top and base reservoir are shown for reference as black lines.

Appendix - Figure Captions (continued)

Page

9 Moment tensor inversion results for the event. The double couple portion of the moment tensor is shown on the left and the full moment tensor is displayed on the right. Station locations used in the inversion are shown as inverted triangles.

10 Ternary diagram showing the moment tensor decompositions into relative double-couple(DC), isotropic (ISO) and compensated linear vector dipole (CLVD) contributions. The automatic Shell events (2018-2020) are shown in blue and the current event is highlighted in red.

11 Observed traces for each station and each component. The automatic picks for the P- and S-waves are indicated by the blue and red lines respectively.

12 Modelled waveform data for each station and each component. The automatic picks for the P- and S-waves are indicated by the blue and red lines respectively.

Appendix B FWI analysis of the earthquake near Uithuizen on the 28th August 2022 with a magnitude of 1.3

Event 32 - Uithuizen
28 August 2022 03:18:59

30 August 2022

Induced Seismicity Taskforce

Disclaimer

- The results presented in this report have been automatically generated using an unconstrained full waveform, event location and moment tensor inversion workflow, developed by the Induced Seismicity Taskforce at Shell.
- These results have not been previously reviewed.
- For questions related to the results then you should contact:
  - Chris Willacy (Christopher.Willacy@Shell.com) or
  - Jan-Willem Blokland (Jan-Willem.Blokland@Shell.com)

Event summary

The event happened at:

Date	28 August 2022
Time	03:18:59.096896

The event is located at:

Location	Uithuizen
Northing (m)	602350
Easting (m)	241700
Depth (m)	3250

The source characteristics are:

	Solution 1	Solution 2
Strike angle (degree)	127.65	324.16
Dip angle (degree)	42.01	54.16
Rake angle (degree)	-103.37	-79.00
Isotropic (percentage)	-13.09	-13.09
CLVD (percentage)	9.58	9.58
Magnitude M_{L}	1.30	1.30

Magnitude summary

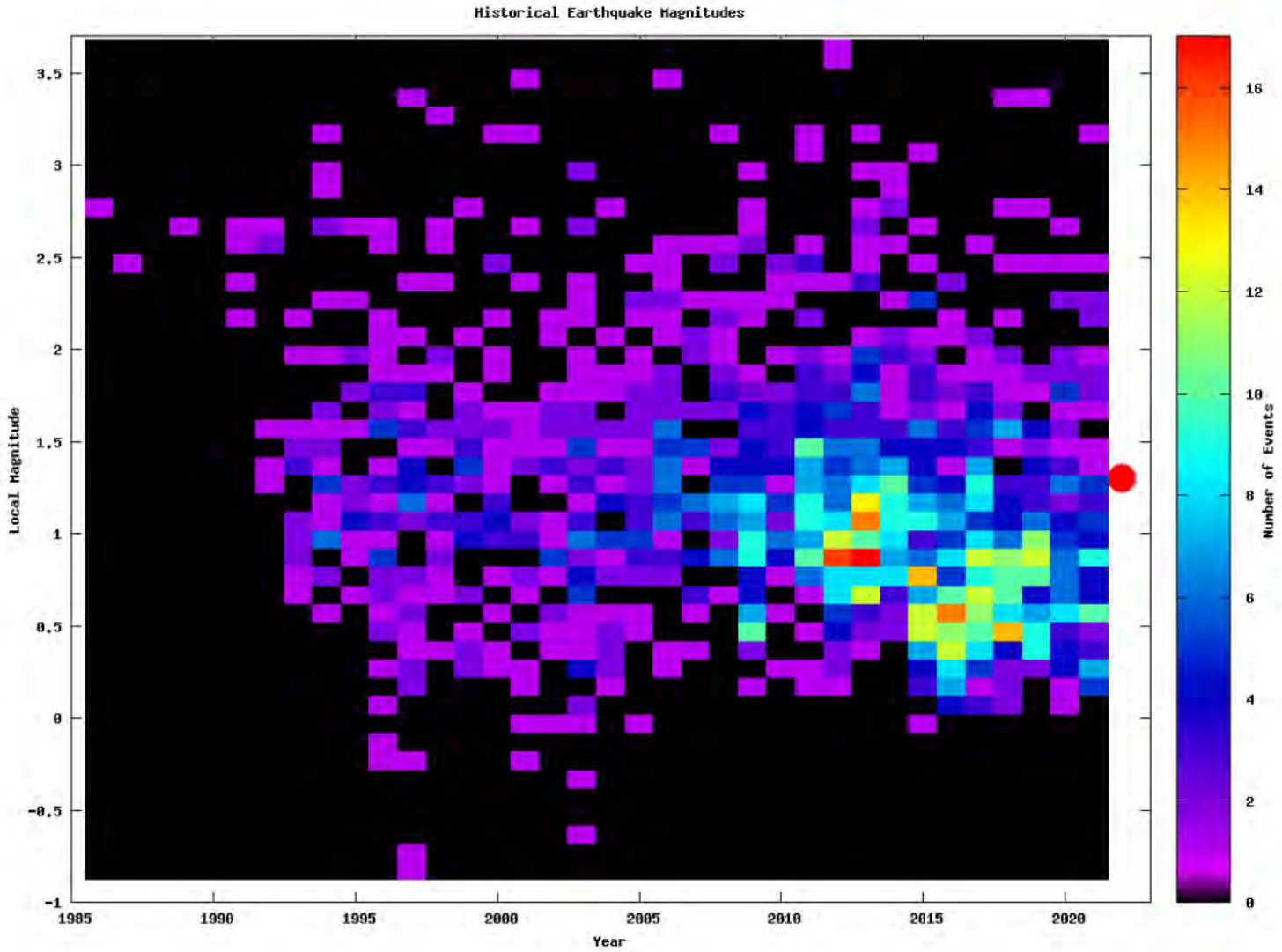

Regional and historical map

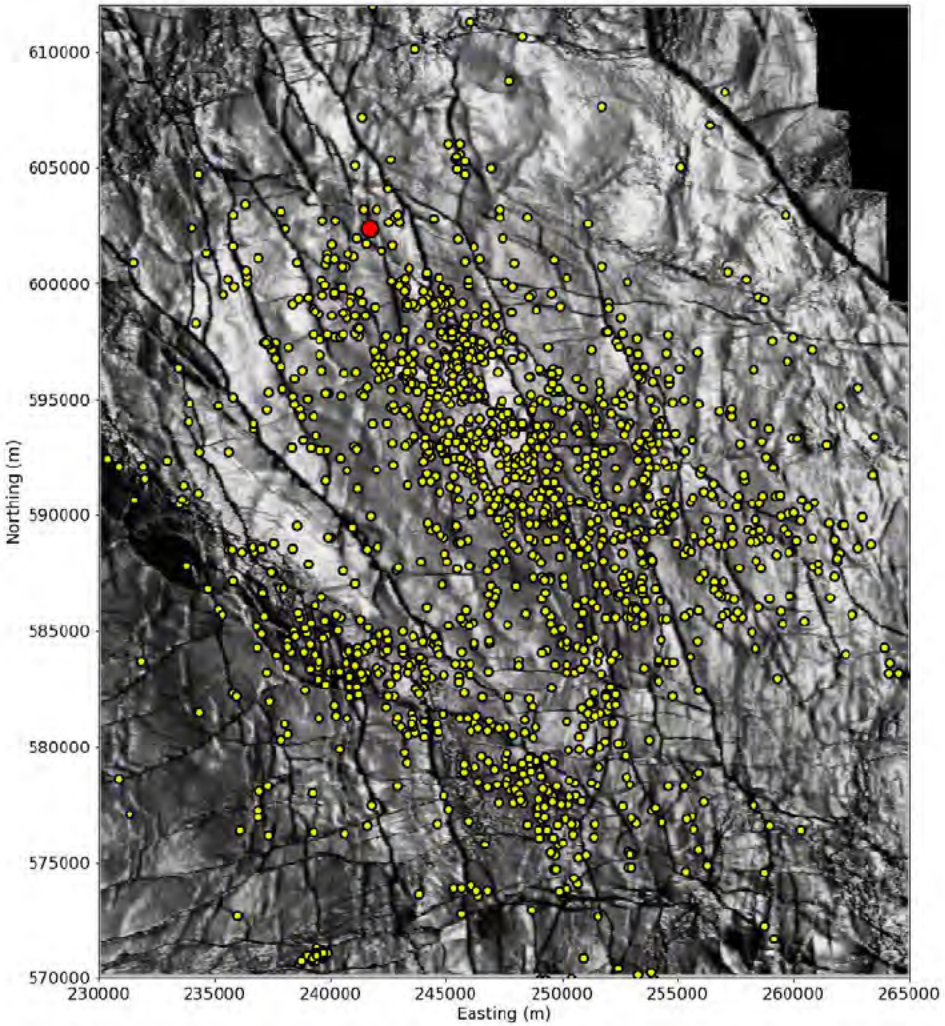

Event depth summary

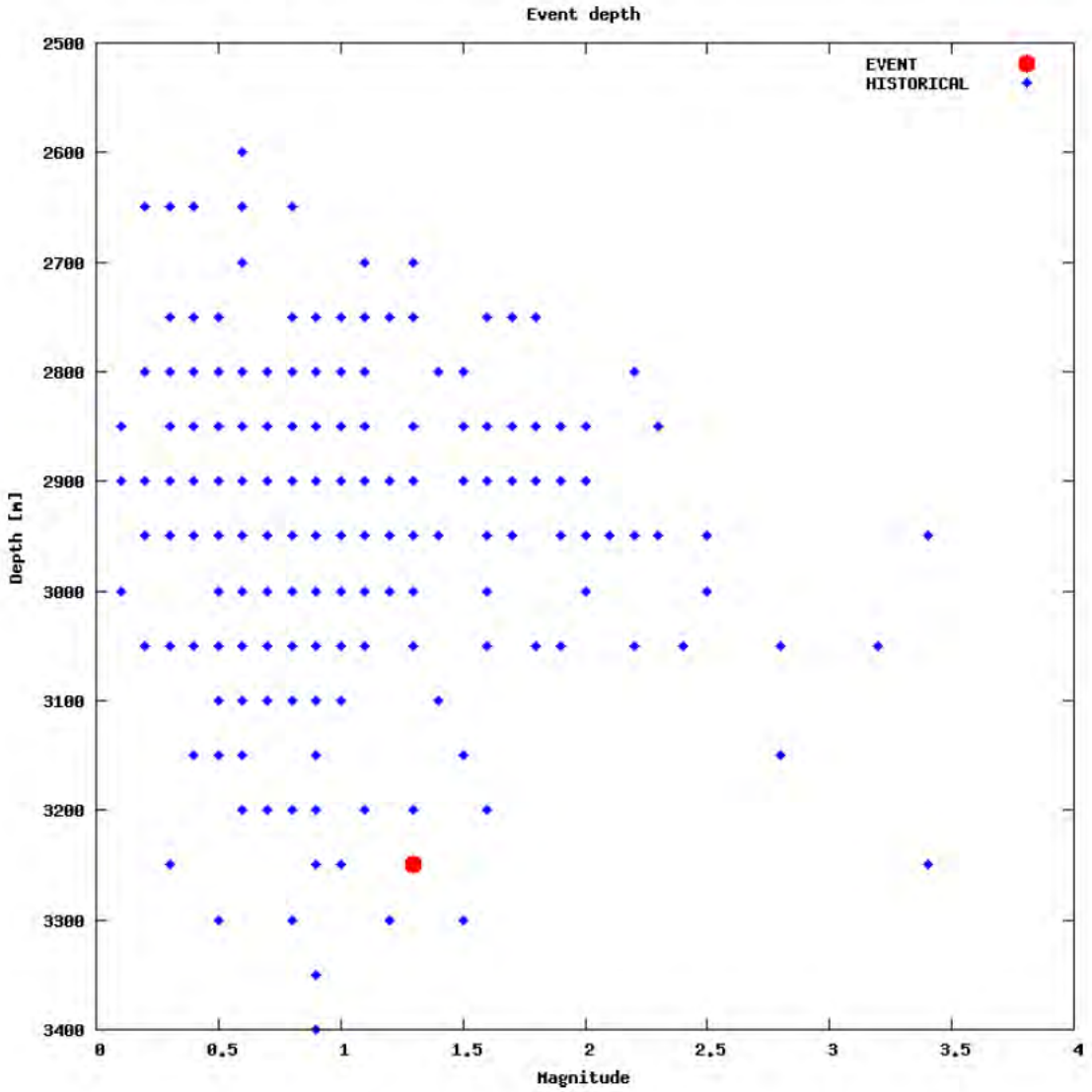

Event location - Map

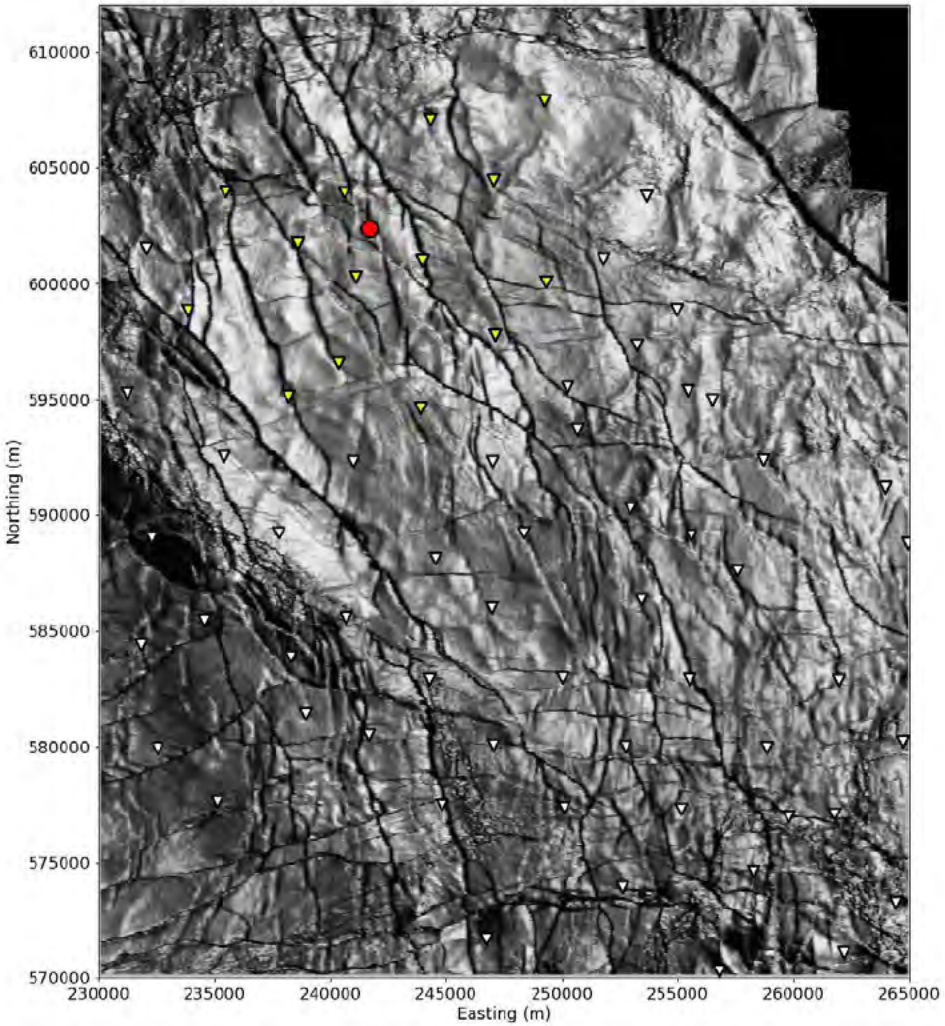

Event location and depth (initial)

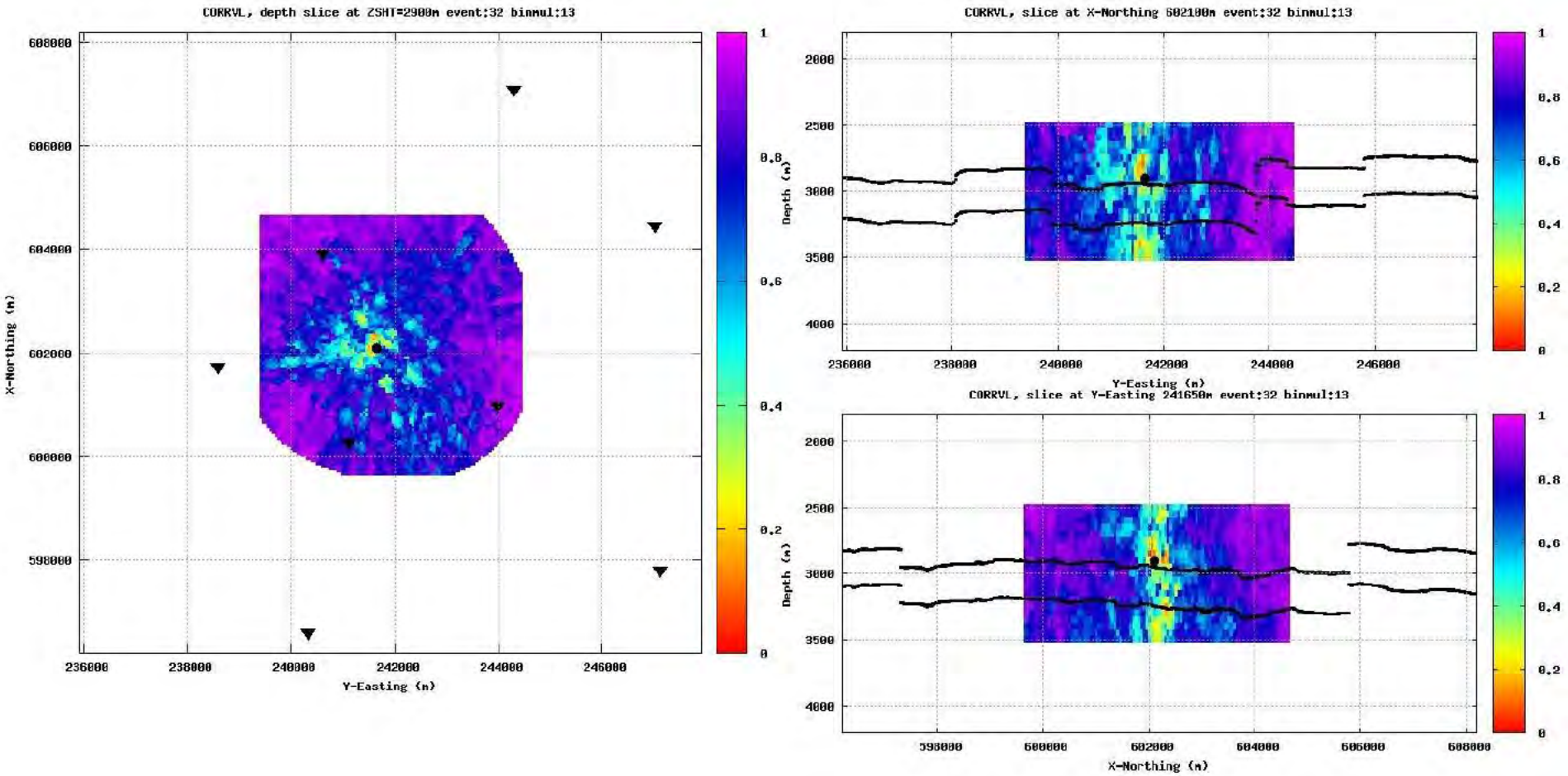

Event location and depth (alternative)

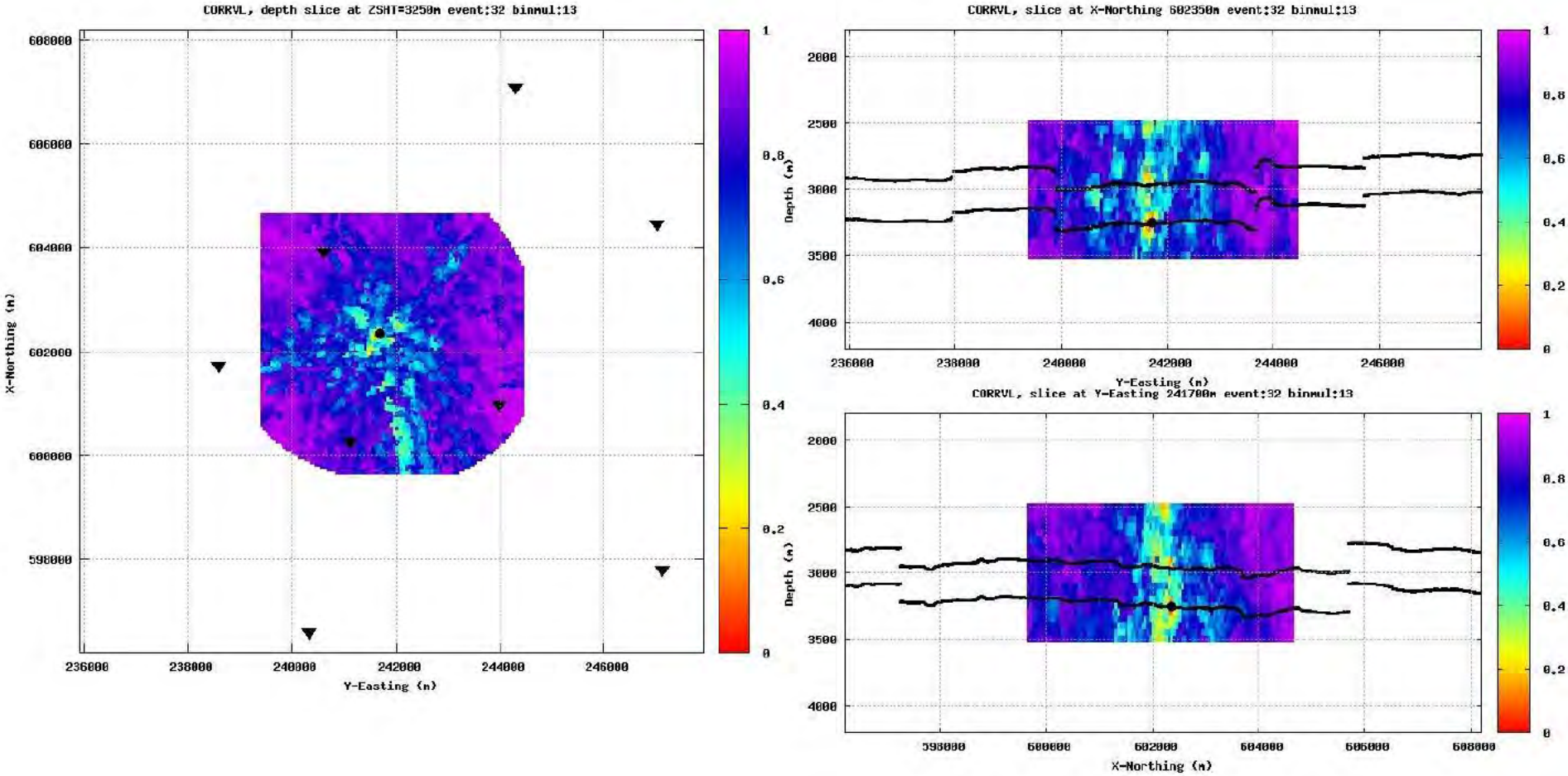

Moment tensor

Double-coupled part

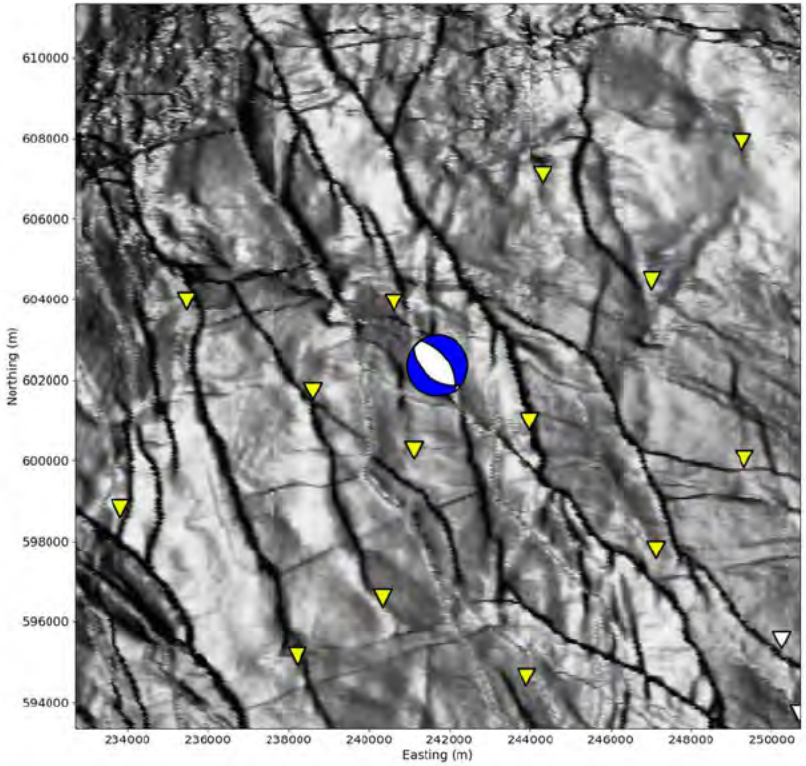

Full

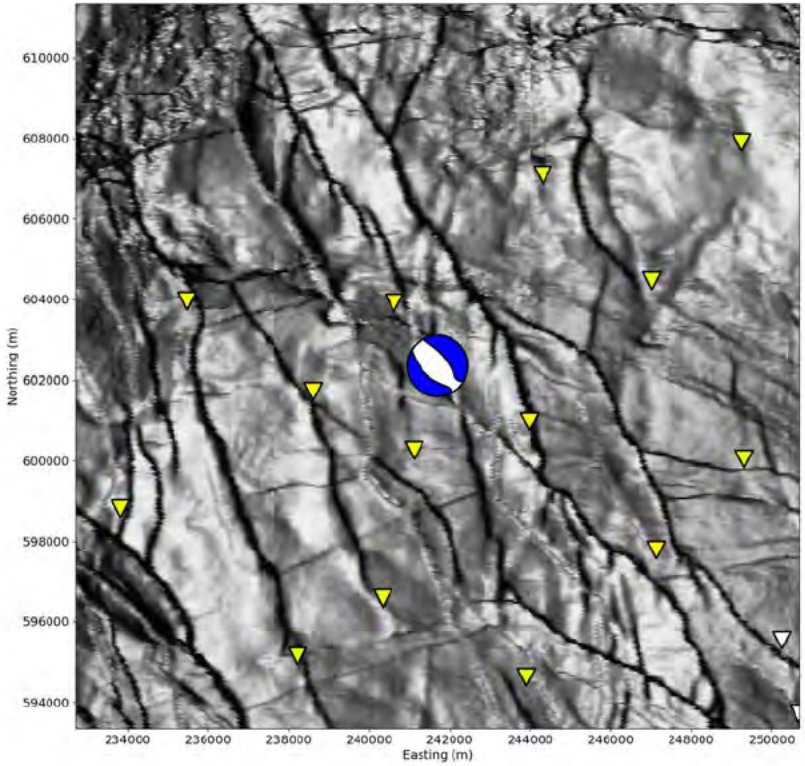

Moment Tensor: Decomposition

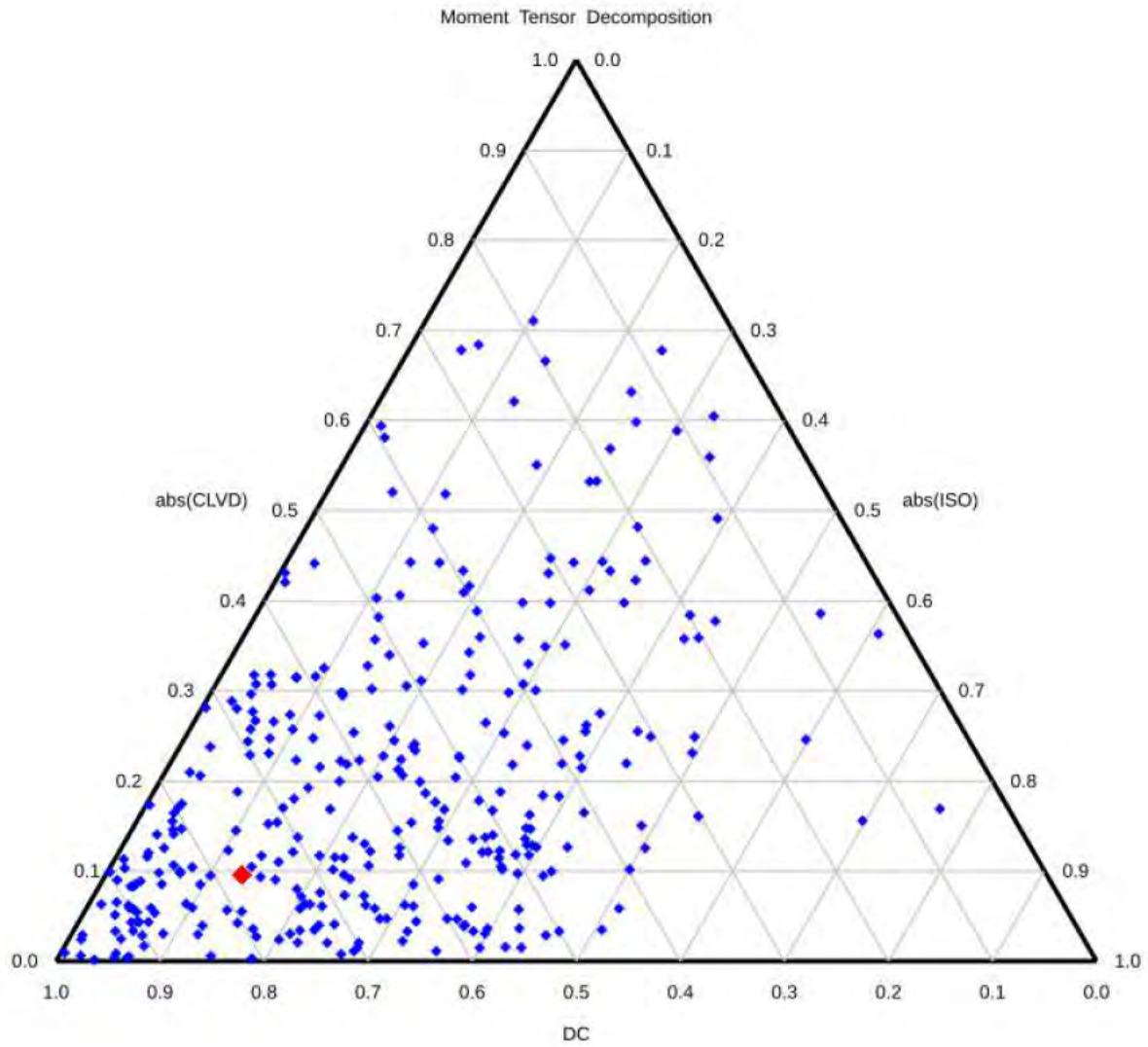

Field data traces

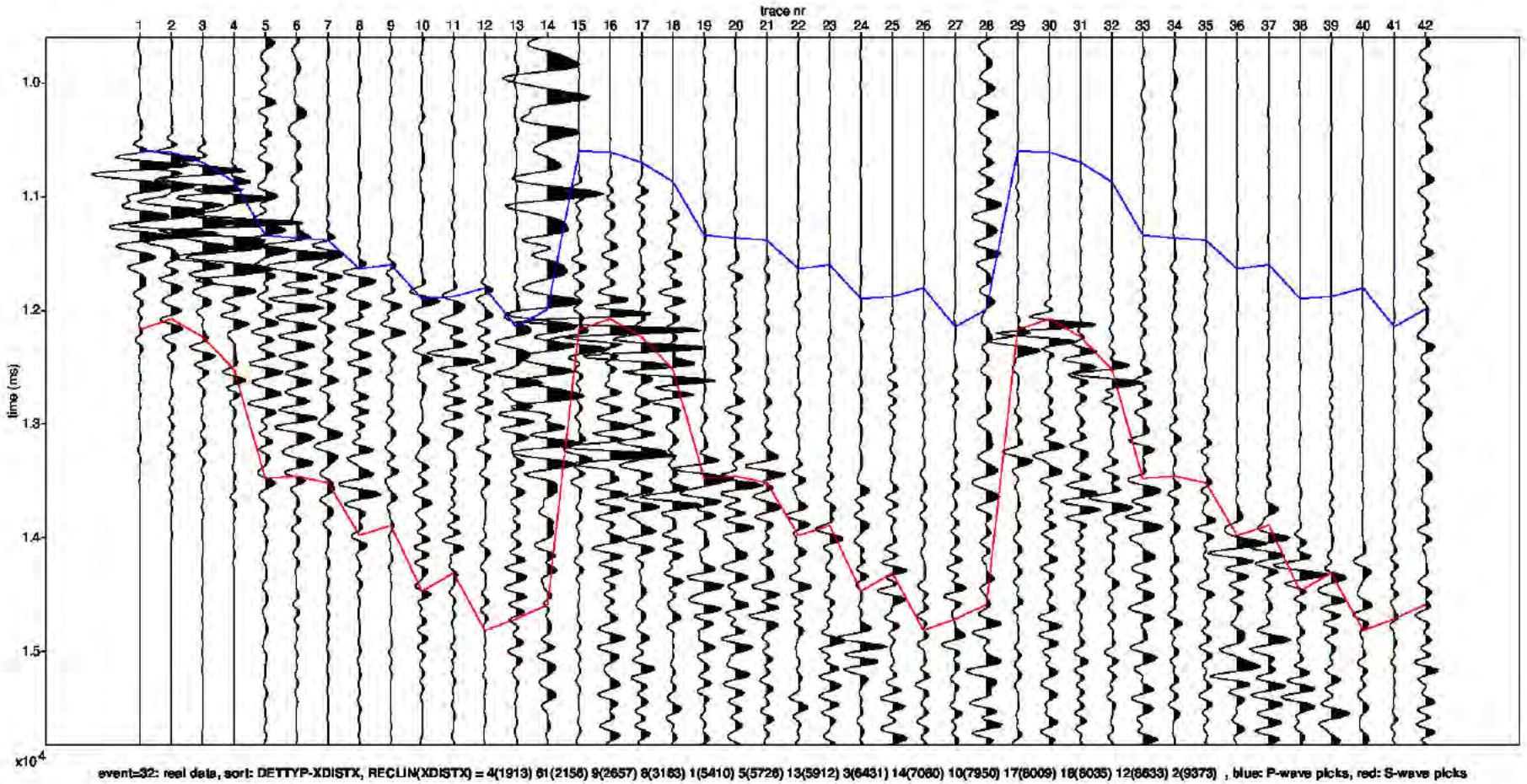

Modelled data traces

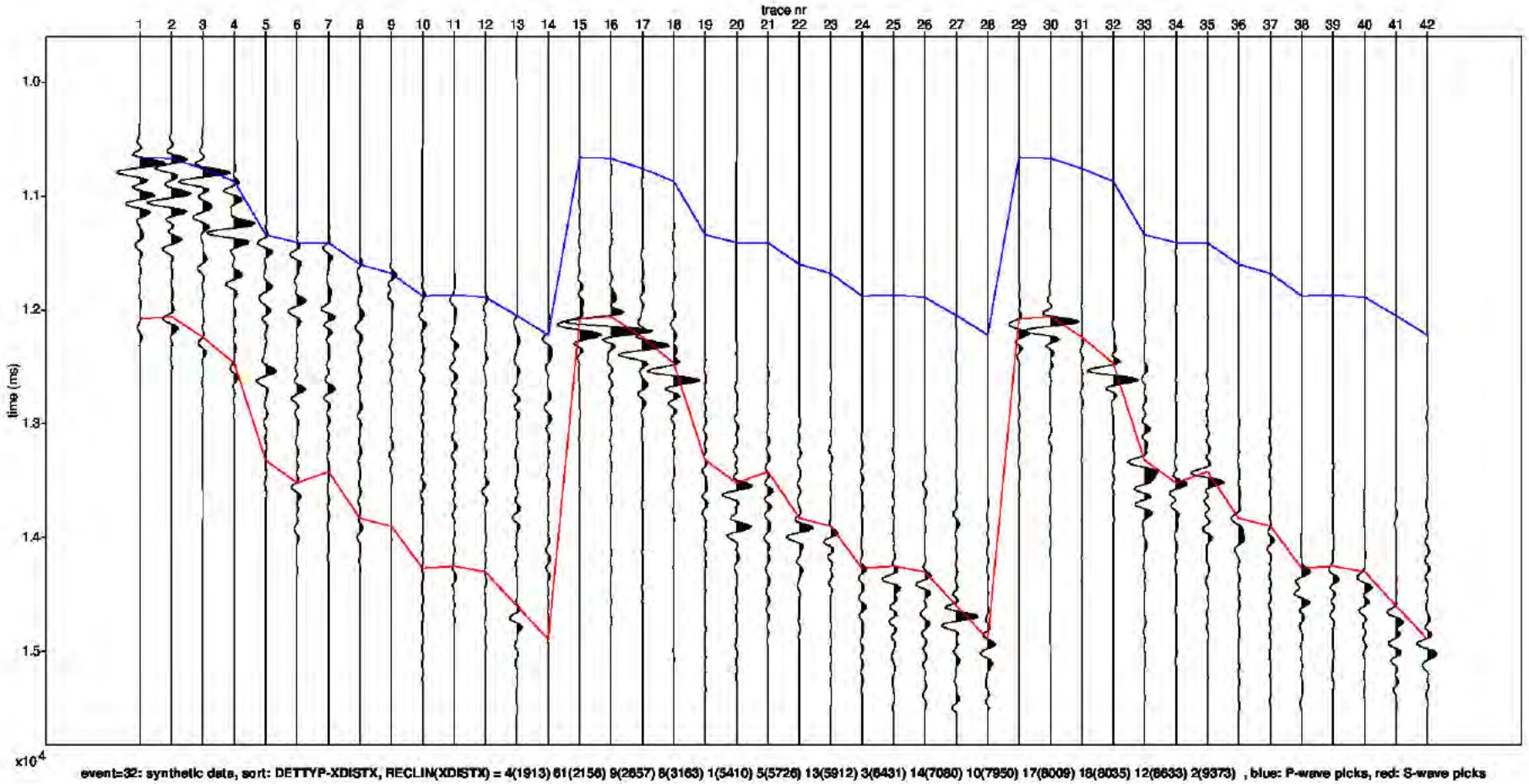

Appendix - Figure Captions

Page

3 Detailed parameter summary for the event. Both primary and secondary focal plane solutions are provided from the moment tensor inversion.

4 Magnitude summary. Prior years are displayed as a “heat map” where the number of events for a given magnitude is displayed per grid cell. The current event is displayed in red.

5 Regional map showing the historical events from KNMI (1986-2019) in blue and the location of the current event in red.

6 Event depth summary. Depths from our automatic workflow (2018-2020) are shown in blue and the current event depth is shown in red. The resolution of the vertical grid is 50m.

7 Event location details for the current event, superimposed on the top Rotliegend depth horizon. Station locations as shown as inverted triangles. Blue triangles are the actual stations used to locate the event whose epicentre is shown by the red dot.

8 QC displays extracted from the objective function for the initial event location. The colour attribute displayed is 1 minus the normalized cross correlation between observed and synthetic waveforms. Station locations are shown as black inverted triangles on the map and the event location is shown by the black dot (left plot). The west to east and north to south vertical profiles are shown on the right. The top and base reservoir are shown for reference as black lines.

Appendix - Figure Captions (continued)

Page

9 QC displays extracted from the objective function for the alternative event location. The colour attribute displayed is 1 minus the normalized cross correlation between observed and synthetic waveforms. Station locations are shown as black inverted triangles on the map and the event location is shown by the black dot (left plot). The west to east and north to south vertical profiles are shown on the right. The top and base reservoir are shown for reference as black lines.

10 Moment tensor inversion results for the event. The double couple portion of the moment tensor is shown on the left and the full moment tensor is displayed on the right. Station locations used in the inversion are shown as inverted triangles.

11 Ternary diagram showing the moment tensor decompositions into relative double-couple(DC), isotropic (ISO) and compensated linear vector dipole (CLVD) contributions. The automatic Shell events (2018-2020) are shown in blue and the current event is highlighted in red.

12 Observed traces for each station and each component. The automatic picks for the P- and S-waves are indicated by the blue and red lines respectively.

13 Modelled waveform data for each station and each component. The automatic picks for the P- and S-waves are indicated by the blue and red lines respectively.

Appendix C FWI analysis of the earthquake near Uithuizen on the 9th September 2022 with a magnitude of 2.3

Initially KNMI estimated the magnitude of this earthquake at 2.4 and revised this later to 2.3. This report was completed before this revision of the magnitude and therefore still states the initial estimate of the magnitude.

Event 33 - Uithuizen
09 September 2022 00:39:11

9 September 2022

Induced Seismicity Taskforce

Disclaimer

- The results presented in this report have been automatically generated using an unconstrained full waveform, event location and moment tensor inversion workflow, developed by the Induced Seismicity Taskforce at Shell.
- These results have not been previously reviewed.
- For questions related to the results then you should contact:
  - Chris Willacy (Christopher.Willacy@Shell.com) or
  - Jan-Willem Blokland (Jan-Willem.Blokland@Shell.com)

Event summary

The event happened at:

Date	09 September 2022
Time	00:39:11.622820

The event is located at:

Location	Uithuizen
Northing (m)	602300
Easting (m)	241600
Depth (m)	3050

The source characteristics are:

	Solution 1	Solution 2
Strike angle (degree)	317.67	169.41
Dip angle (degree)	48.81	40.92
Rake angle (degree)	-110.22	-66.60
Isotropic (percentage)	13.38	13.38
CLVD (percentage)	-8.82	-8.82
Magnitude M_{L}	2.40	2.40

Magnitude summary

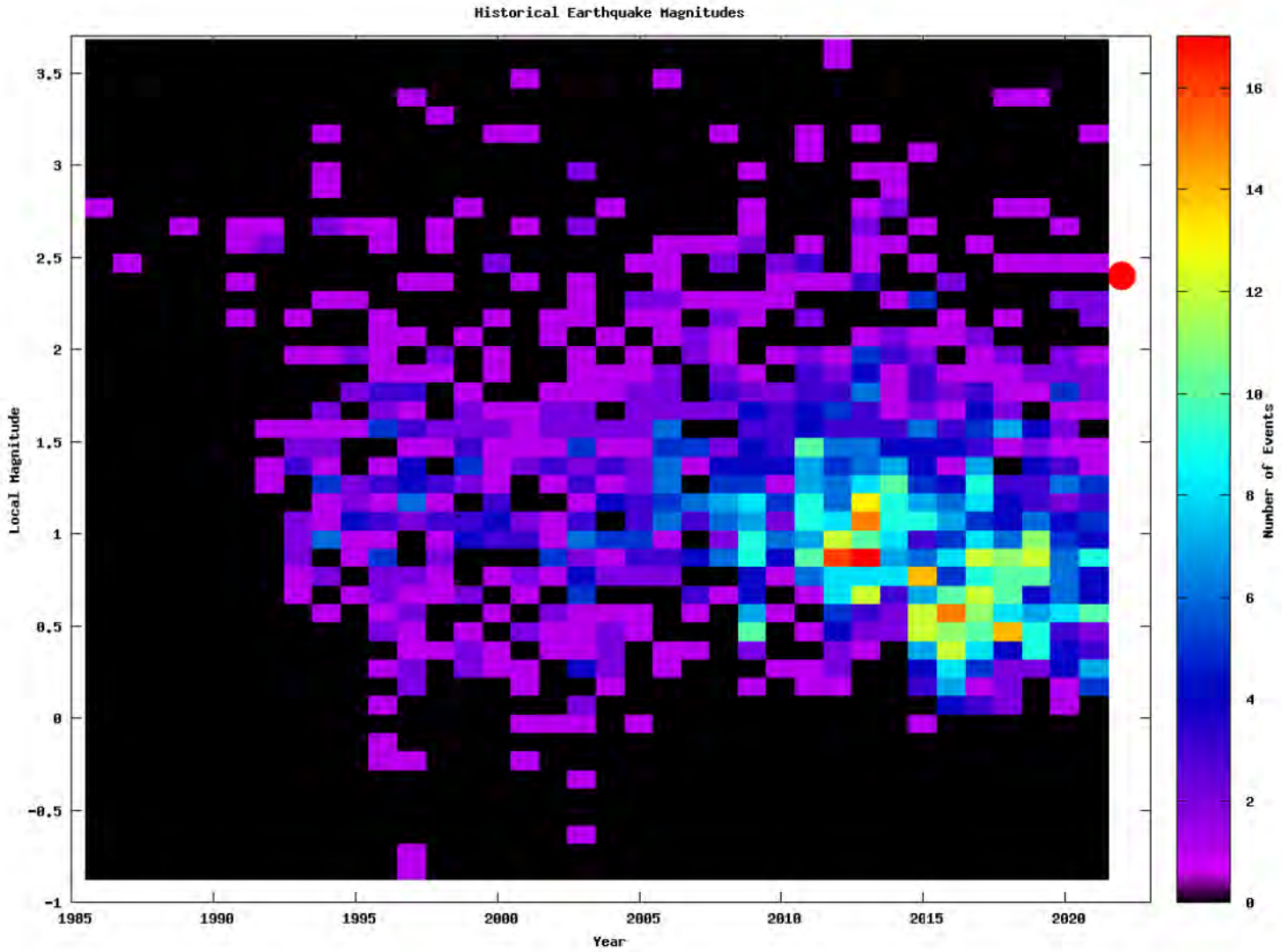

Regional and historical map

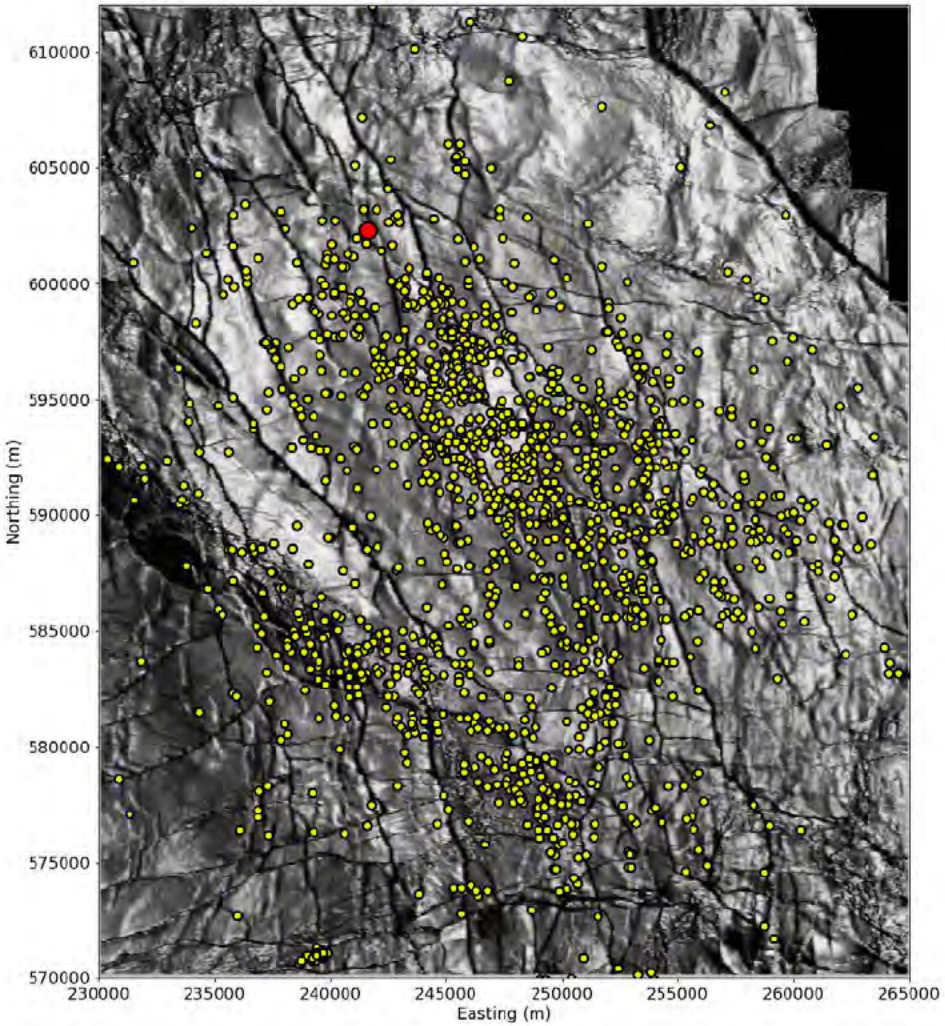

Event depth summary

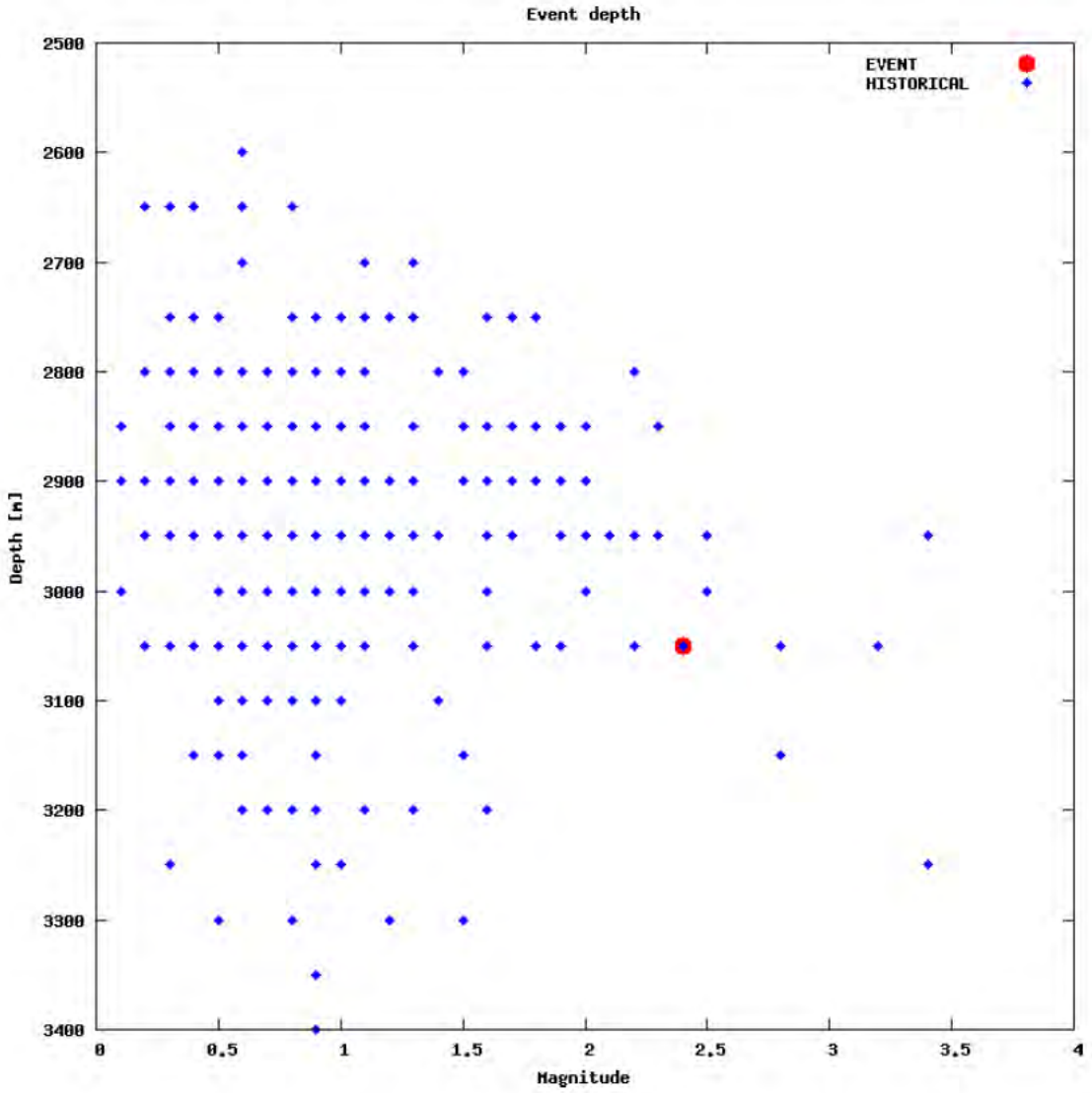

Event location - Map

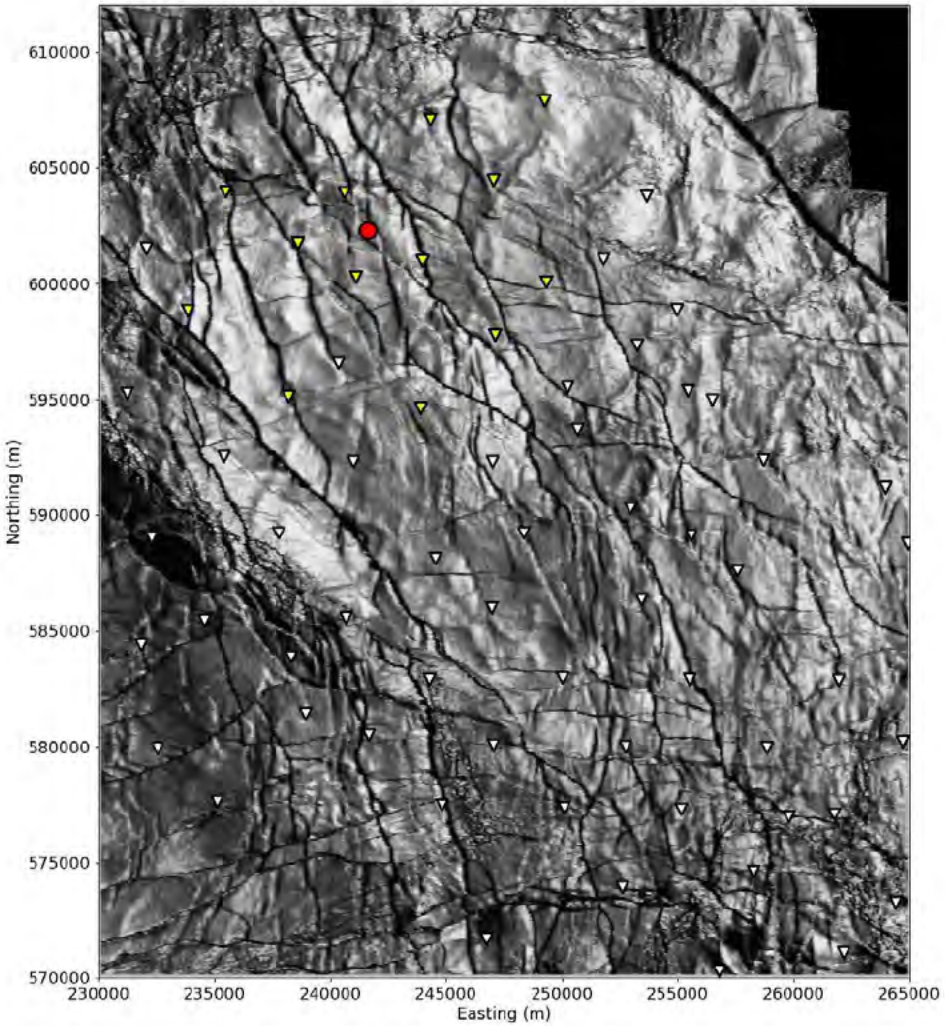

Event location and depth (initial)

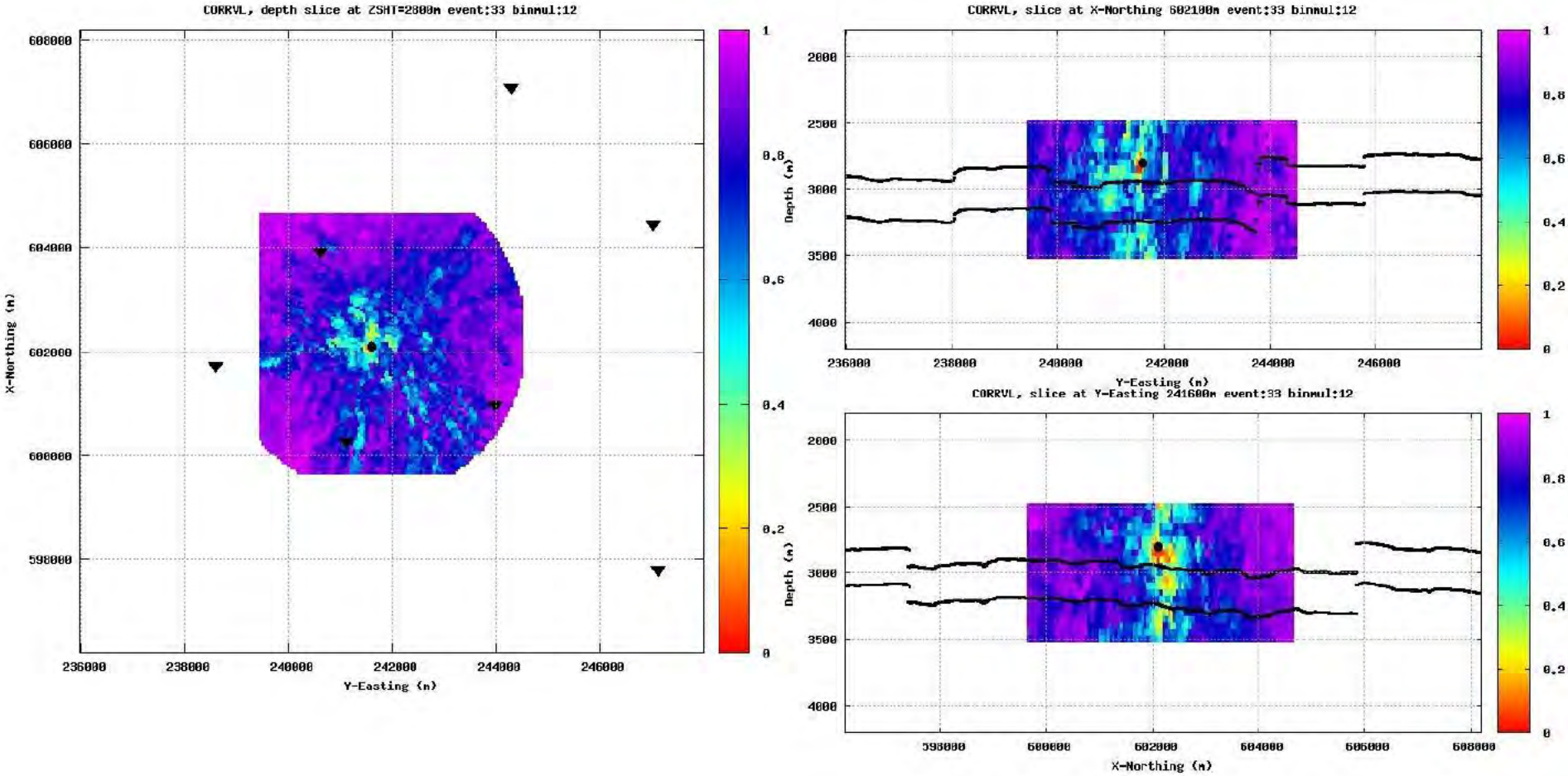

Event location and depth (alternative)

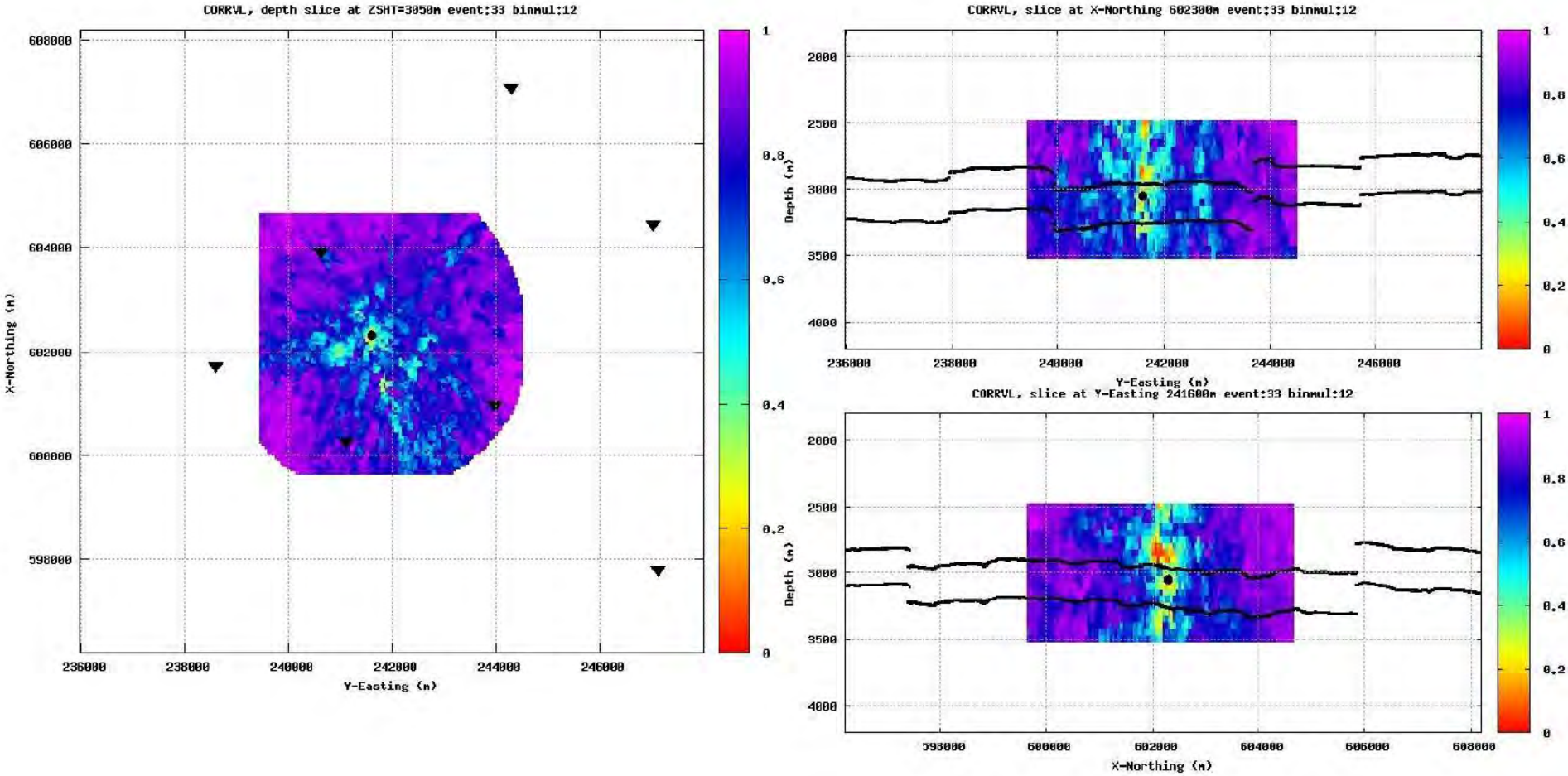

Moment tensor

Double-coupled part

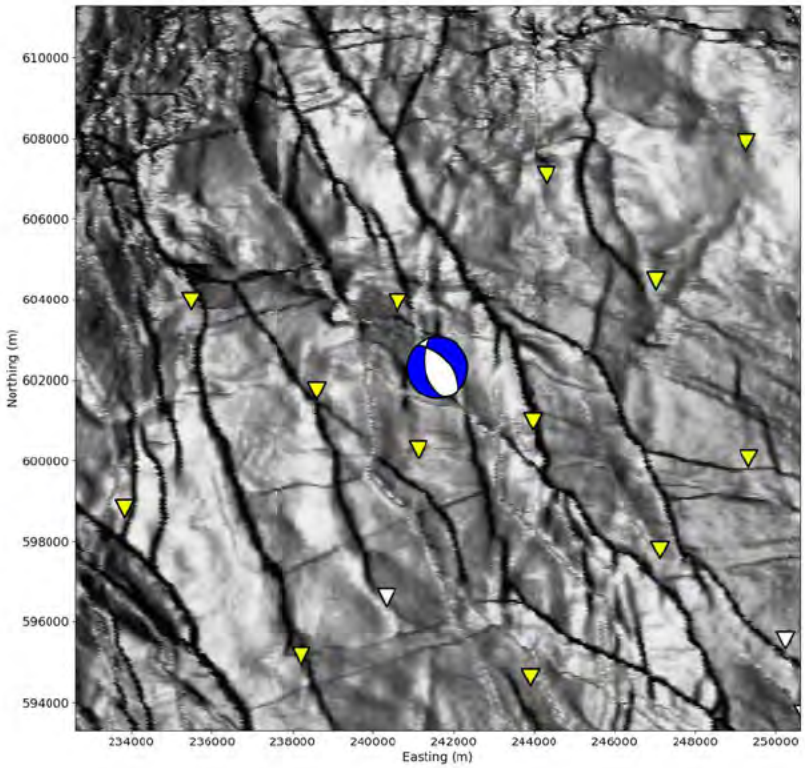

Full

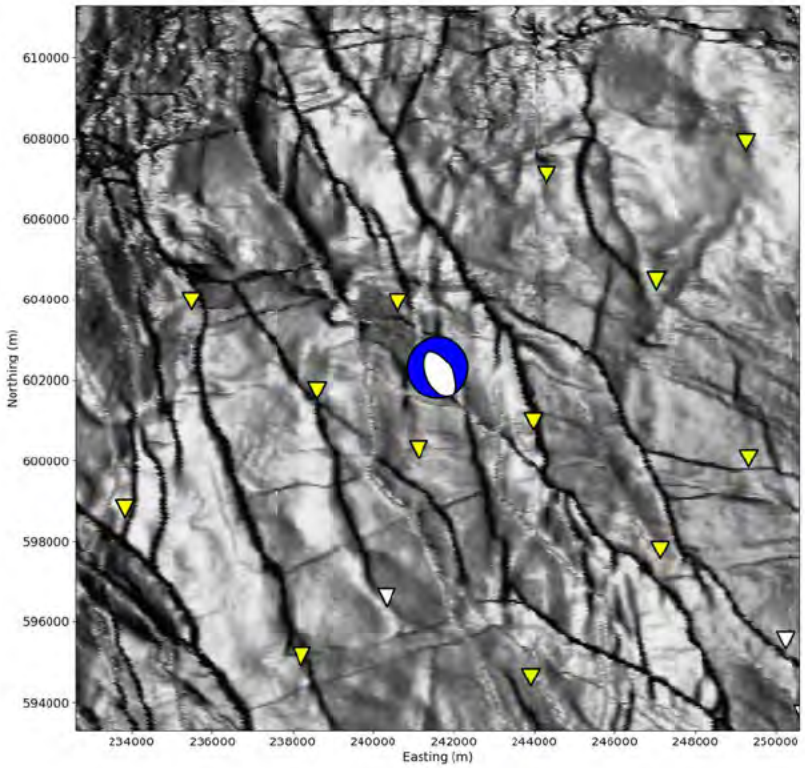

Moment Tensor: Decomposition

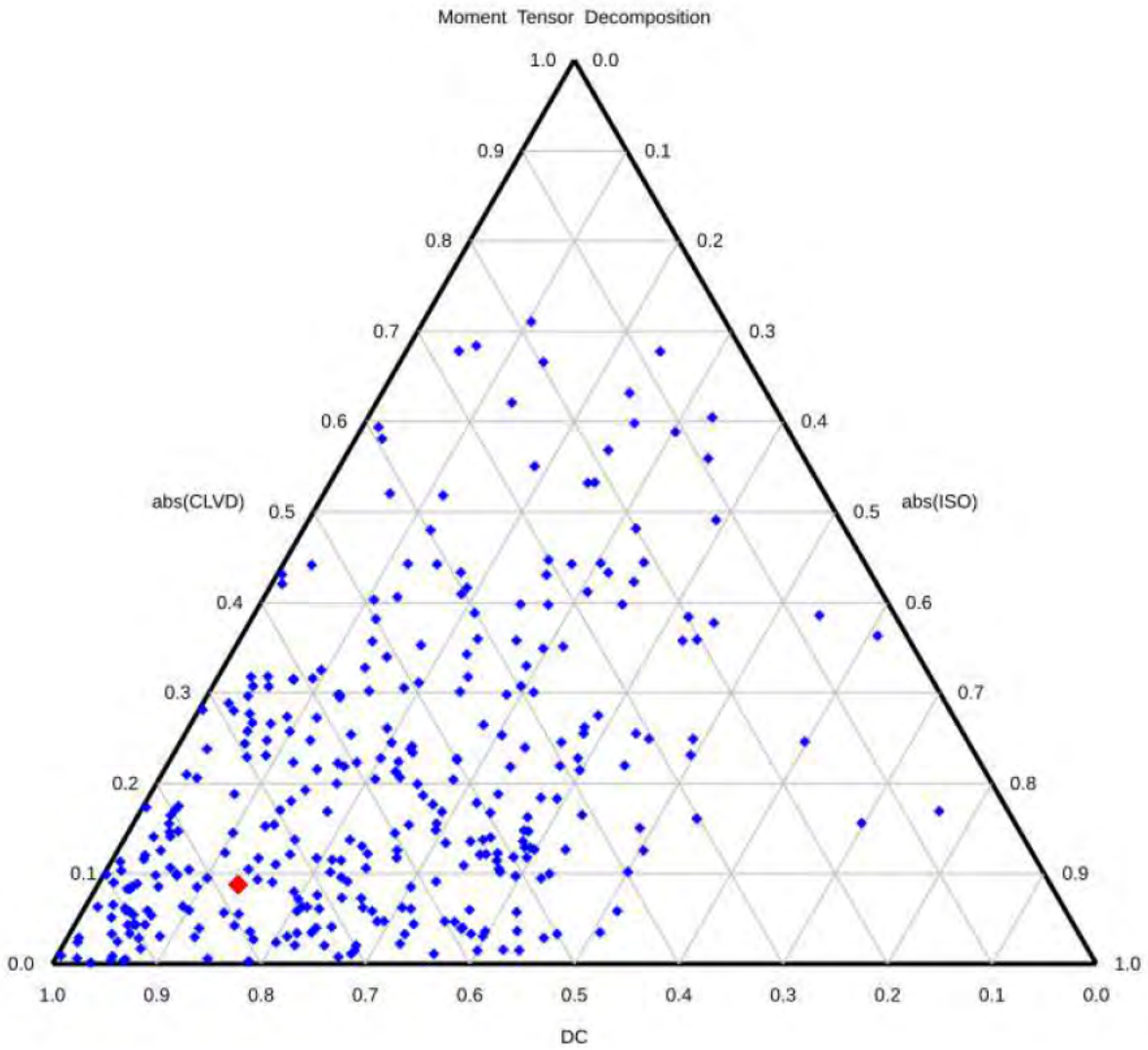

Field data traces

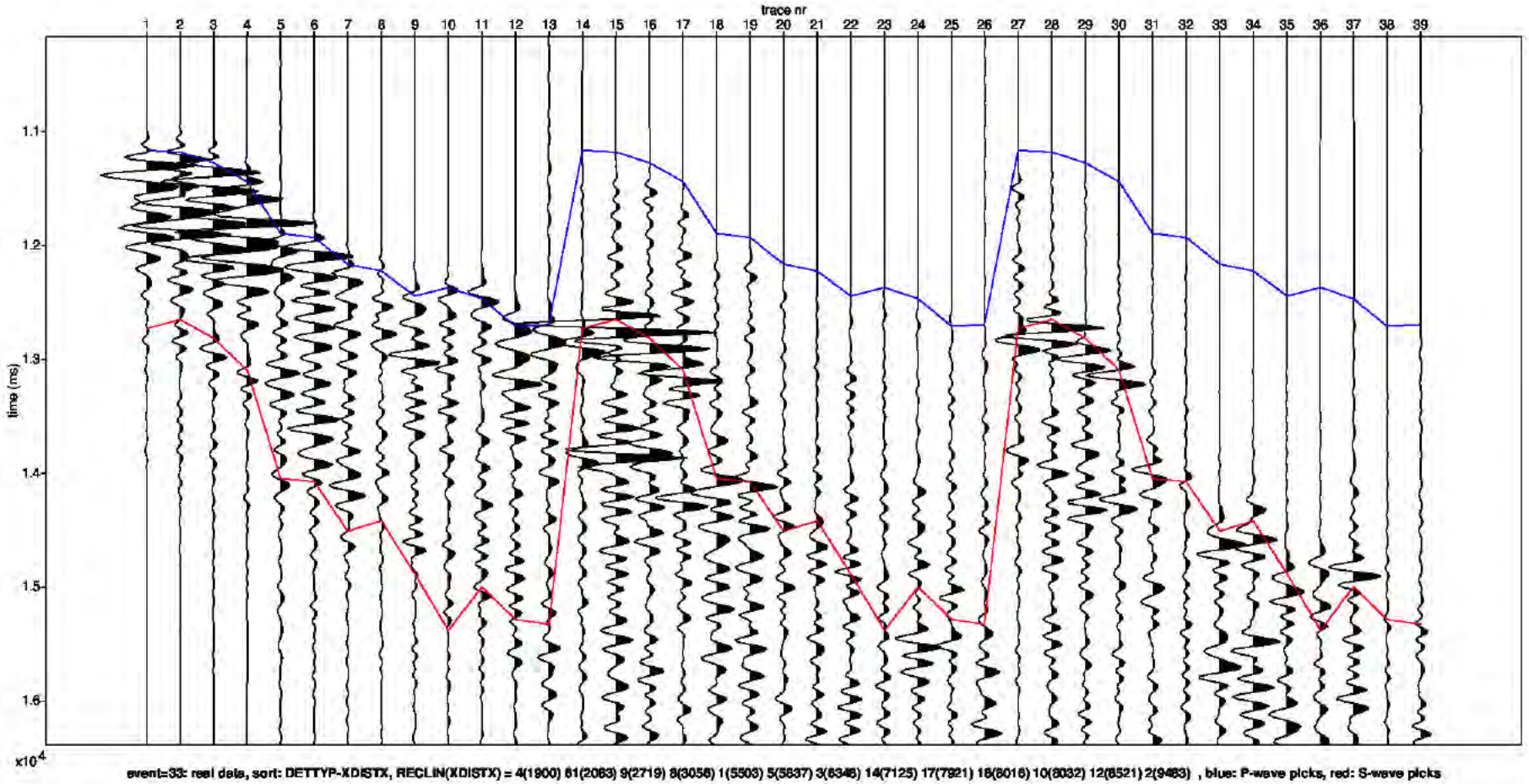

Modelled data traces

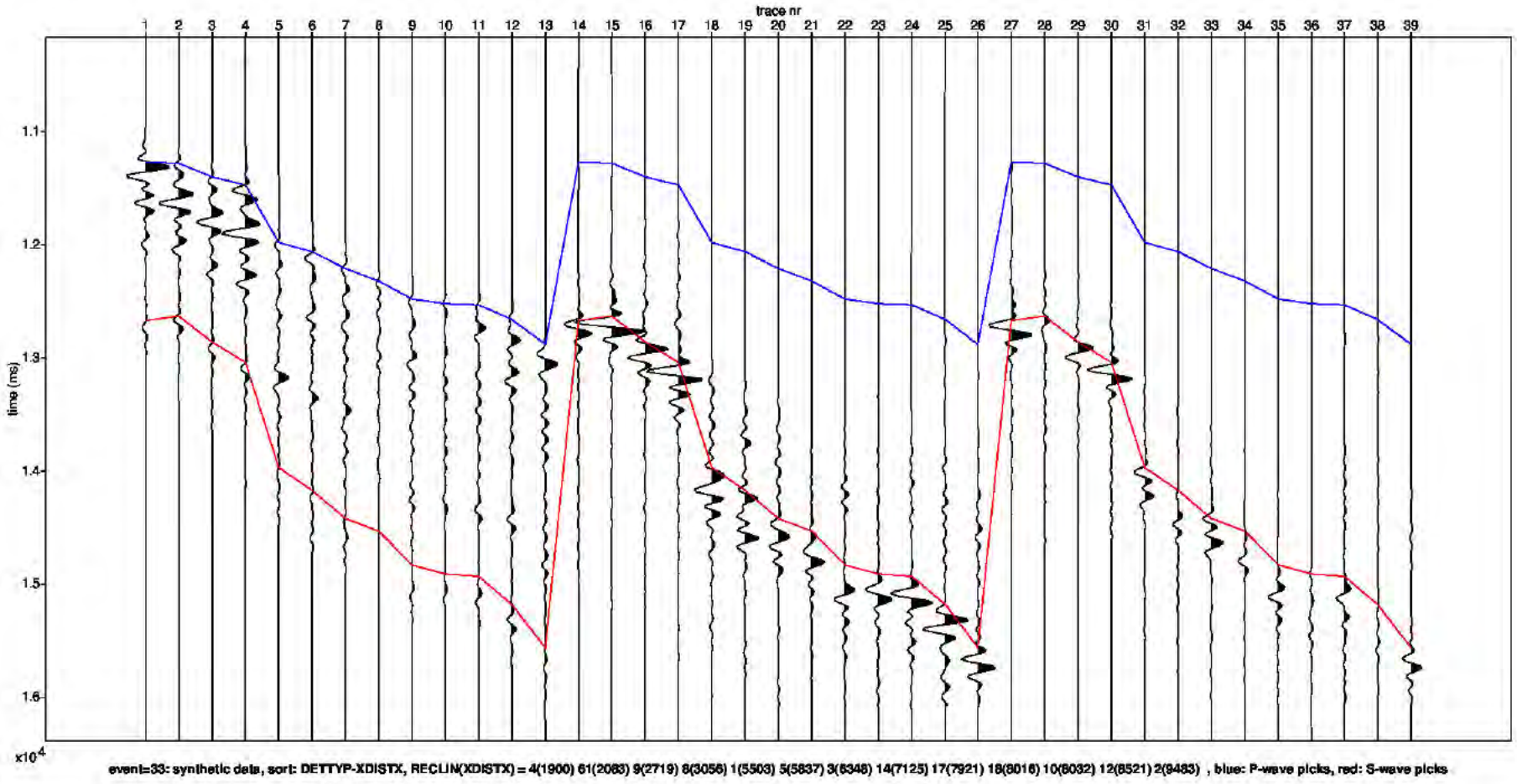

Appendix - Figure Captions

Page

3 Detailed parameter summary for the event. Both primary and secondary focal plane solutions are provided from the moment tensor inversion.

4 Magnitude summary. Prior years are displayed as a “heat map” where the number of events for a given magnitude is displayed per grid cell. The current event is displayed in red.

5 Regional map showing the historical events from KNMI (1986-2019) in blue and the location of the current event in red.

6 Event depth summary. Depths from our automatic workflow (2018-2020) are shown in blue and the current event depth is shown in red. The resolution of the vertical grid is 50m.

7 Event location details for the current event, superimposed on the top Rotliegend depth horizon. Station locations as shown as inverted triangles. Blue triangles are the actual stations used to locate the event whose epicentre is shown by the red dot.

8 QC displays extracted from the objective function for the initial event location. The colour attribute displayed is 1 minus the normalized cross correlation between observed and synthetic waveforms. Station locations are shown as black inverted triangles on the map and the event location is shown by the black dot (left plot). The west to east and north to south vertical profiles are shown on the right. The top and base reservoir are shown for reference as black lines.

Appendix - Figure Captions (continued)

Page

9 QC displays extracted from the objective function for the alternative event location. The colour attribute displayed is 1 minus the normalized cross correlation between observed and synthetic waveforms. Station locations are shown as black inverted triangles on the map and the event location is shown by the black dot (left plot). The west to east and north to south vertical profiles are shown on the right. The top and base reservoir are shown for reference as black lines.

10 Moment tensor inversion results for the event. The double couple portion of the moment tensor is shown on the left and the full moment tensor is displayed on the right. Station locations used in the inversion are shown as inverted triangles.

11 Ternary diagram showing the moment tensor decompositions into relative double-couple(DC), isotropic (ISO) and compensated linear vector dipole (CLVD) contributions. The automatic Shell events (2018-2020) are shown in blue and the current event is highlighted in red.

12 Observed traces for each station and each component. The automatic picks for the P- and S-waves are indicated by the blue and red lines respectively.

13 Modelled waveform data for each station and each component. The automatic picks for the P- and S-waves are indicated by the blue and red lines respectively.

Appendix D FWI analysis of the earthquake near Uithuizen on the 18th September 2022 with a magnitude of 0.8

Event 34 - Uithuizen
18 September 2022 04:10:00

20 September 2022

Induced Seismicity Taskforce

Disclaimer

- The results presented in this report have been automatically generated using an unconstrained full waveform, event location and moment tensor inversion workflow, developed by the Induced Seismicity Taskforce at Shell.
- These results have not been previously reviewed.
- For questions related to the results then you should contact:
  - Chris Willacy (Christopher.Willacy@Shell.com) or
  - Jan-Willem Blokland (Jan-Willem.Blokland@Shell.com)

Event summary

The event happened at:

Date	18 September 2022
Time	04:10:00.700118

The event is located at:

Location	Uithuizen
Northing (m)	602150
Easting (m)	240750
Depth (m)	3000

The source characteristics are:

	Solution 1	Solution 2
Strike angle (degree)	319.65	201.65
Dip angle (degree)	50.16	34.64
Rake angle (degree)	-122.02	-44.26
Isotropic (percentage)	-20.50	-20.50
CLVD (percentage)	-30.83	-30.83
Magnitude M_{L}	0.80	0.80

Magnitude summary

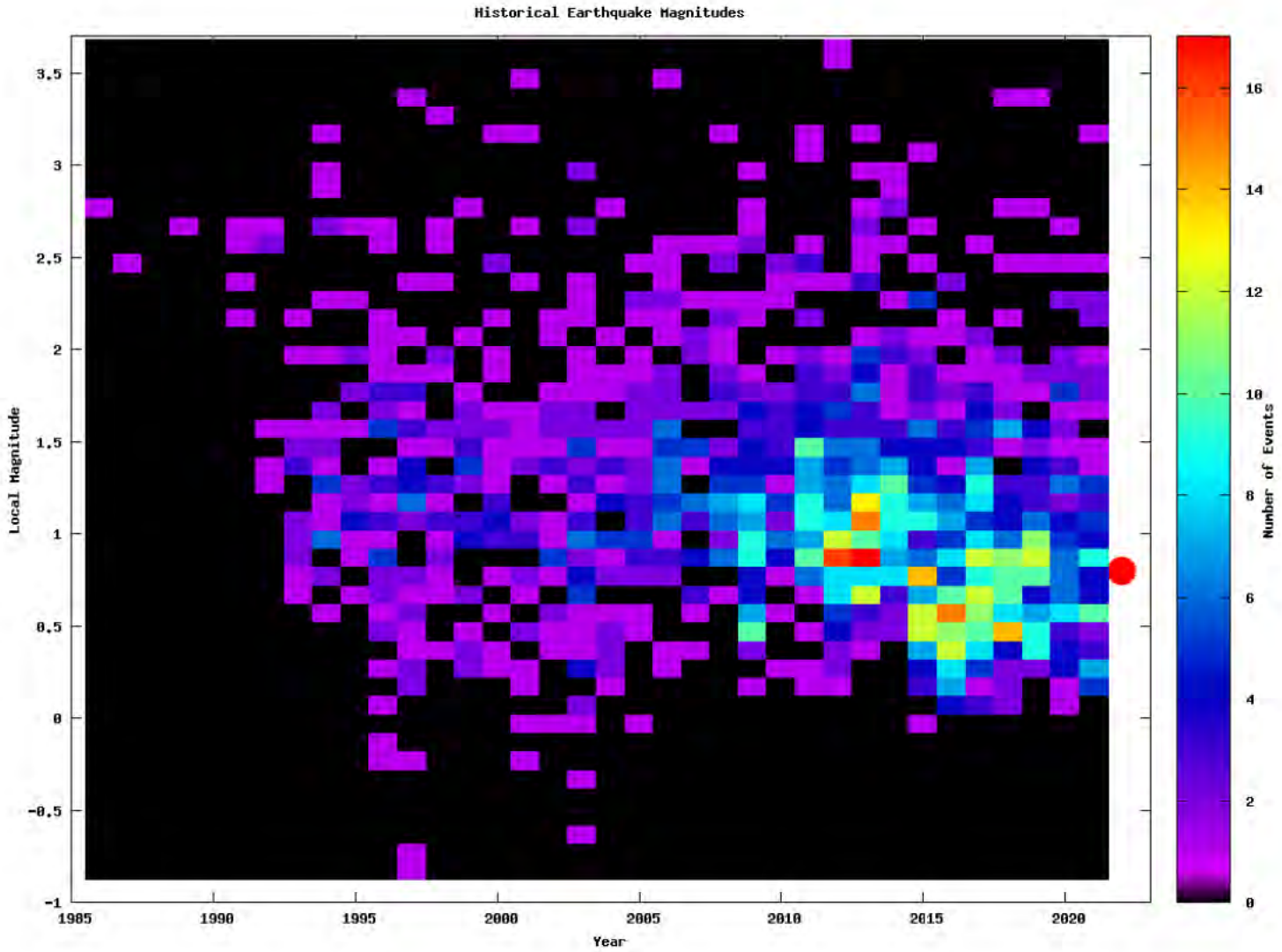

Regional and historical map

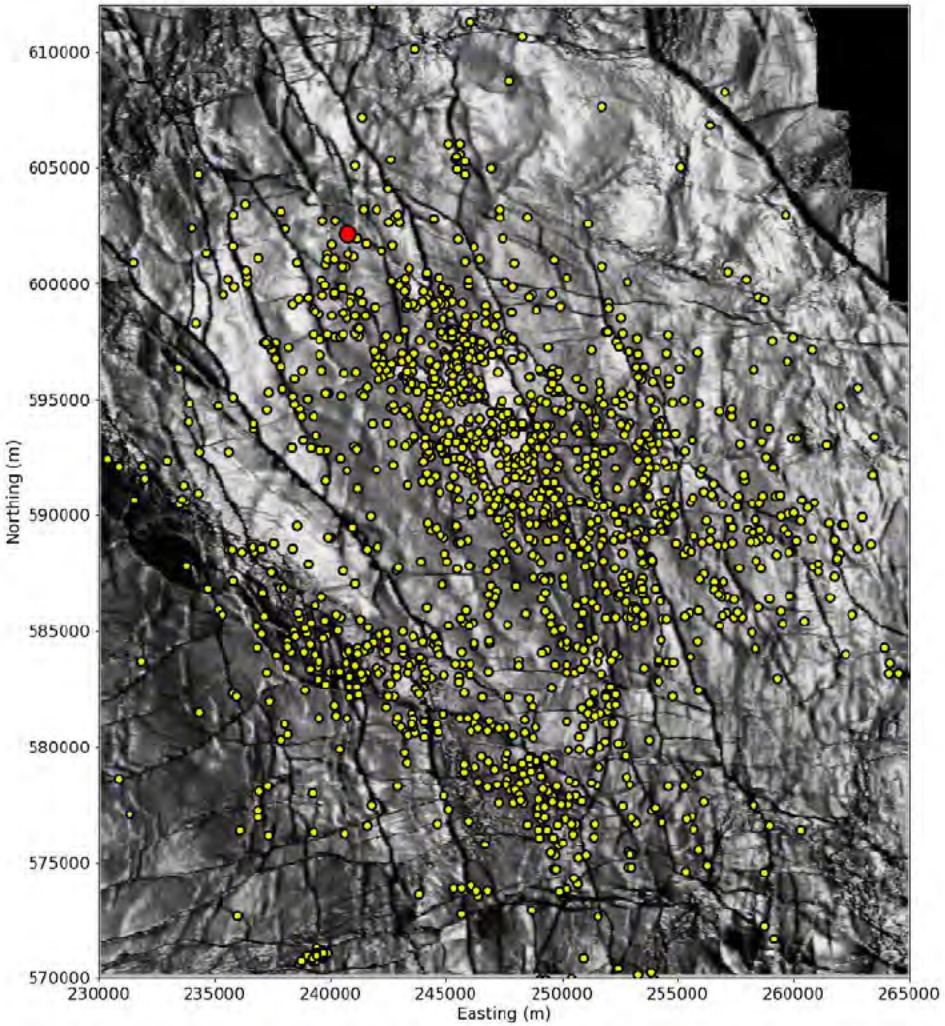

Event depth summary

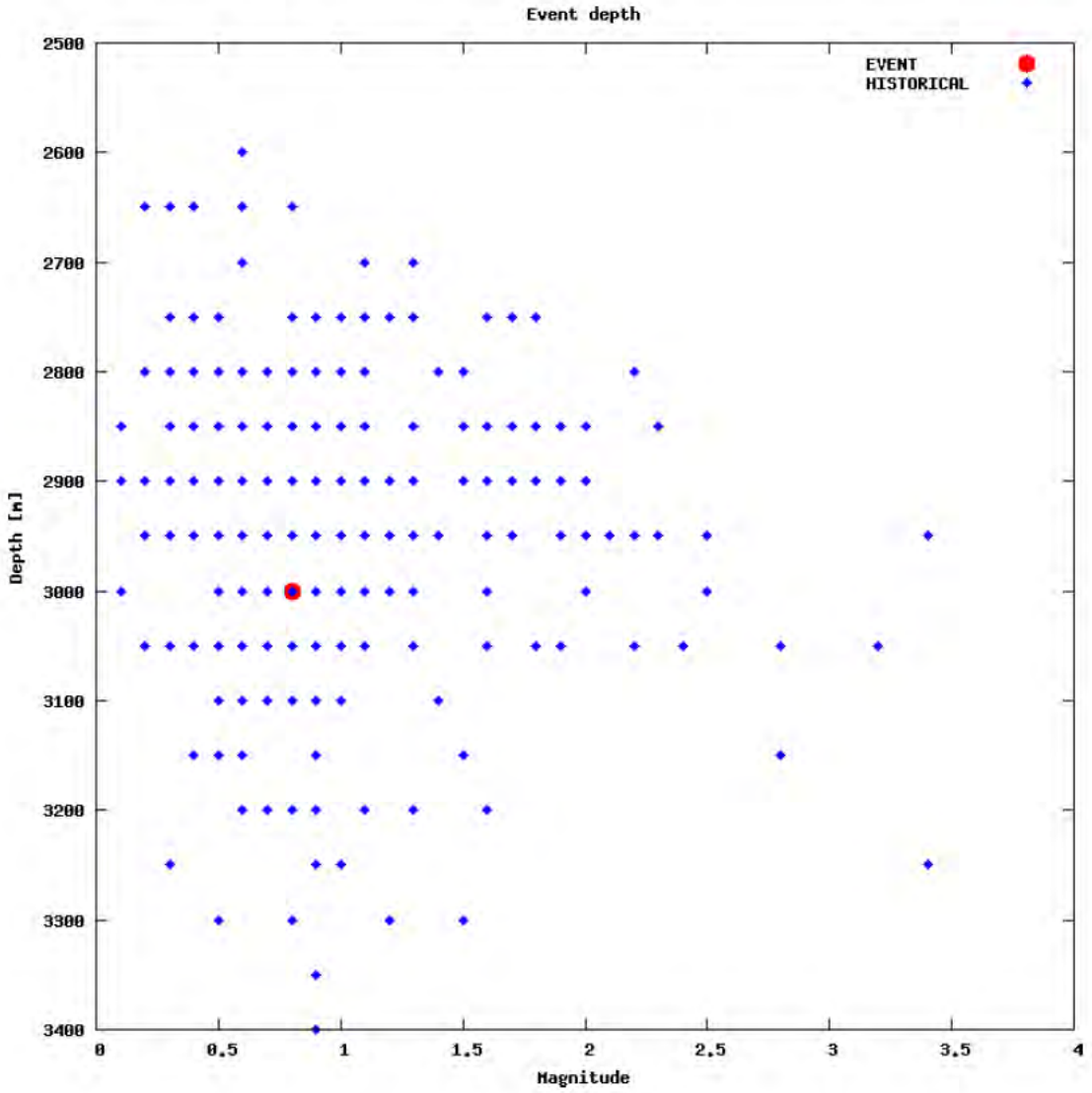

Event location - Map

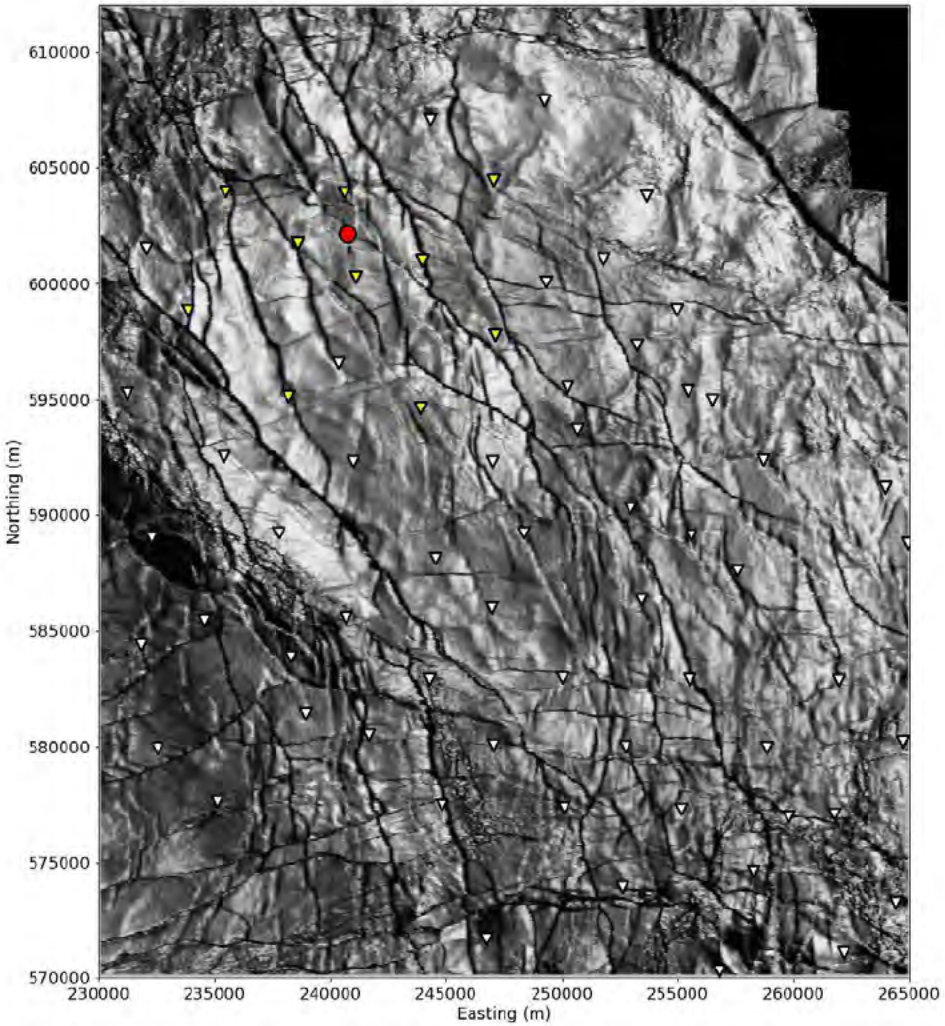

Event location and depth (initial)

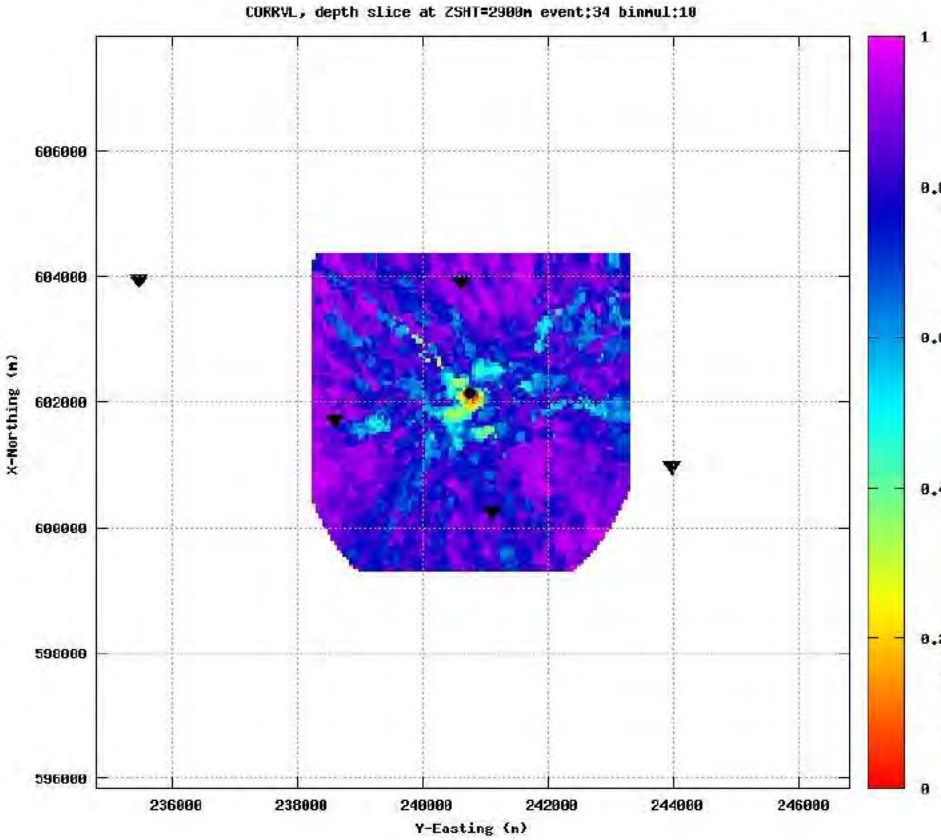

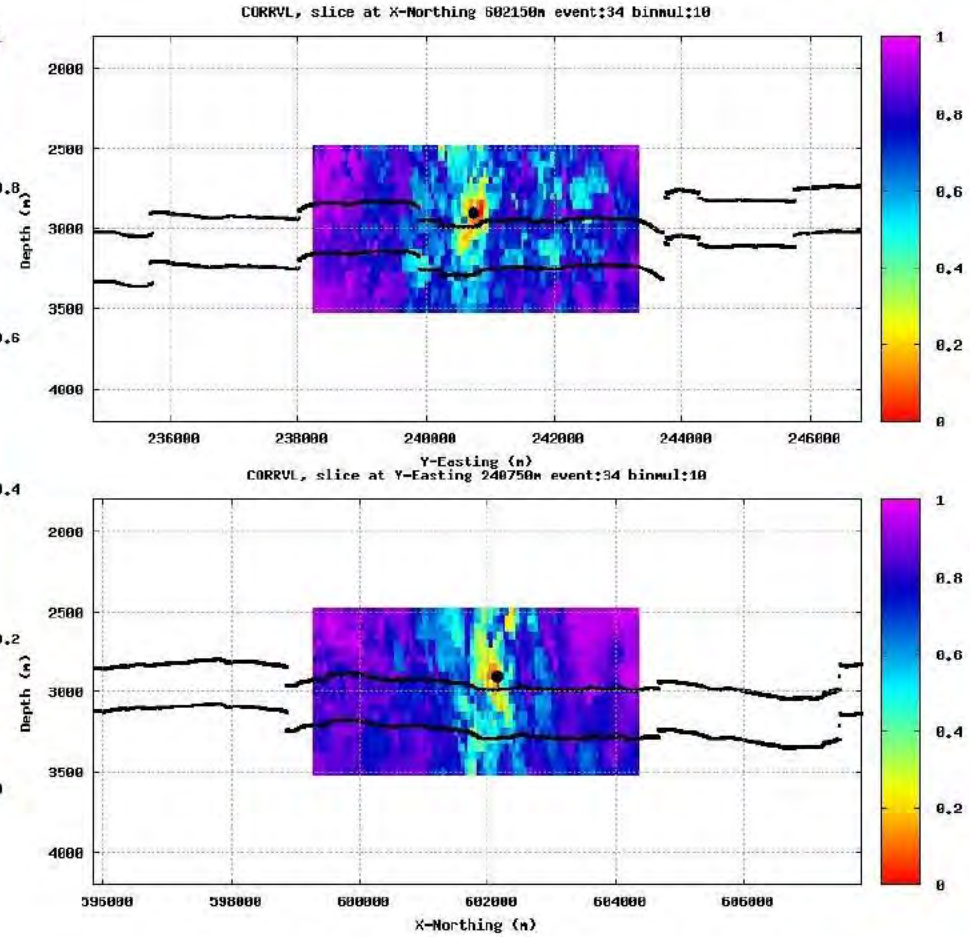

Event location and depth (alternative)

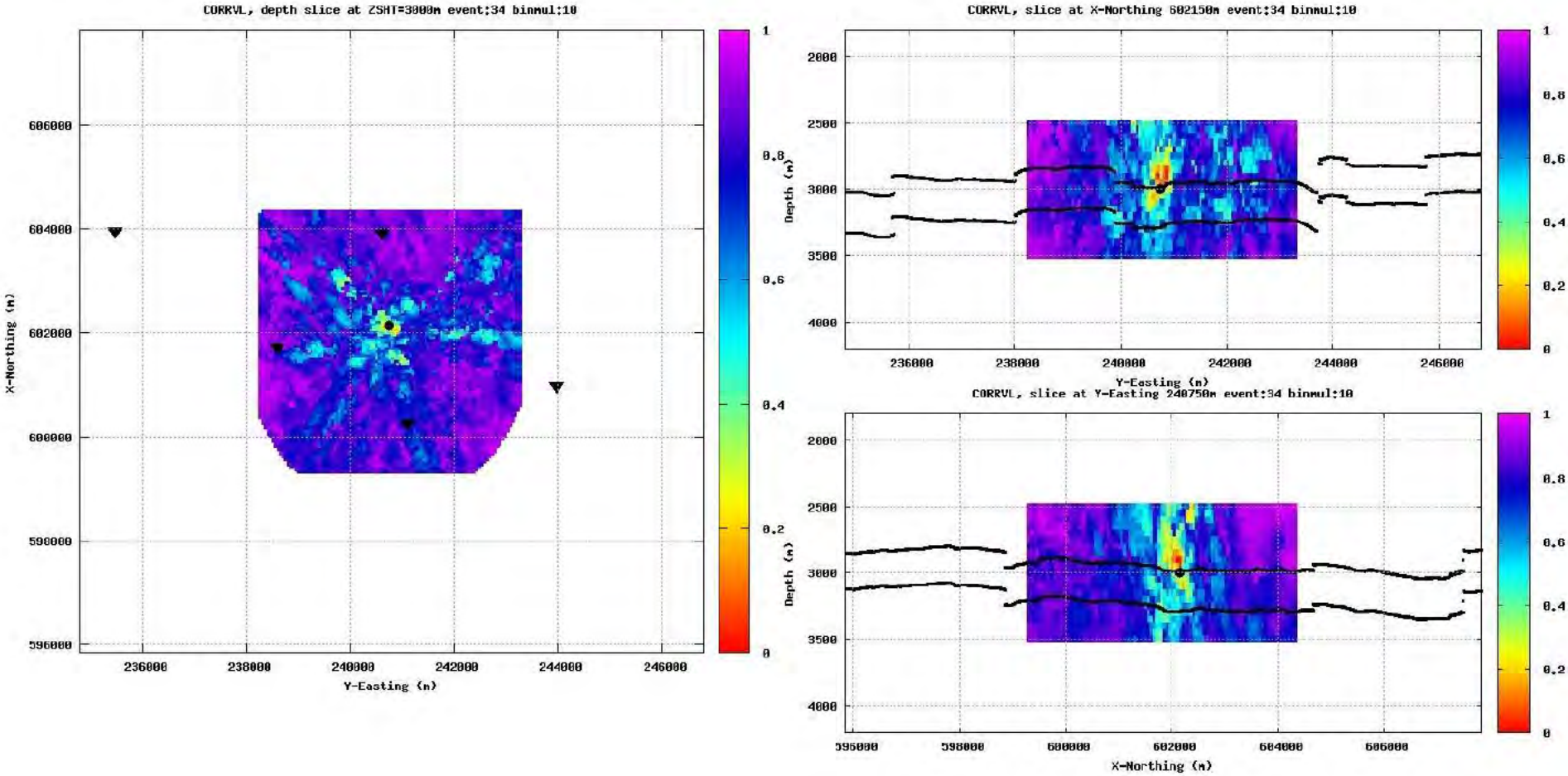

Moment tensor

Double-coupled part

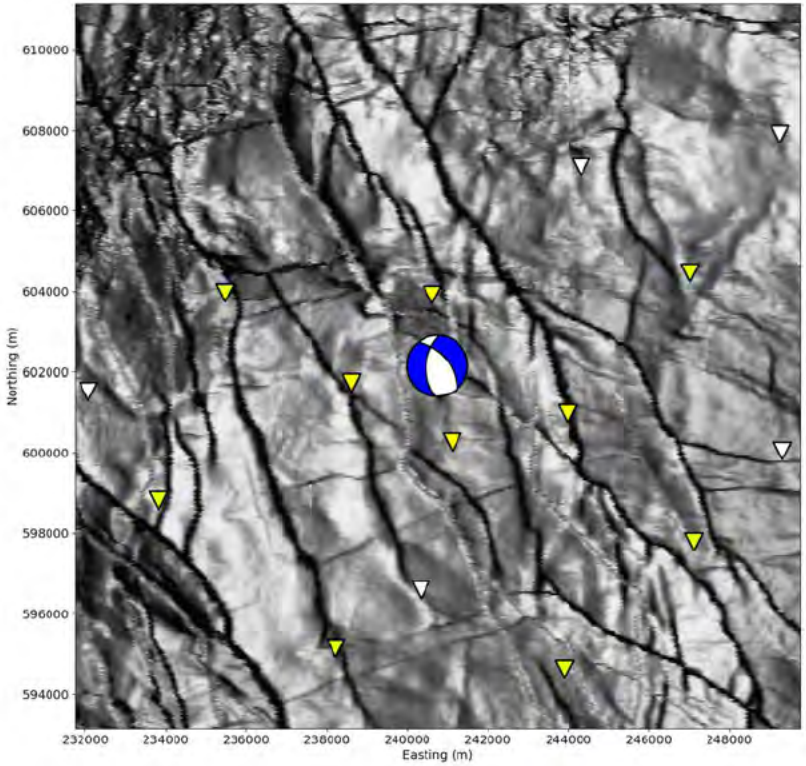

Full

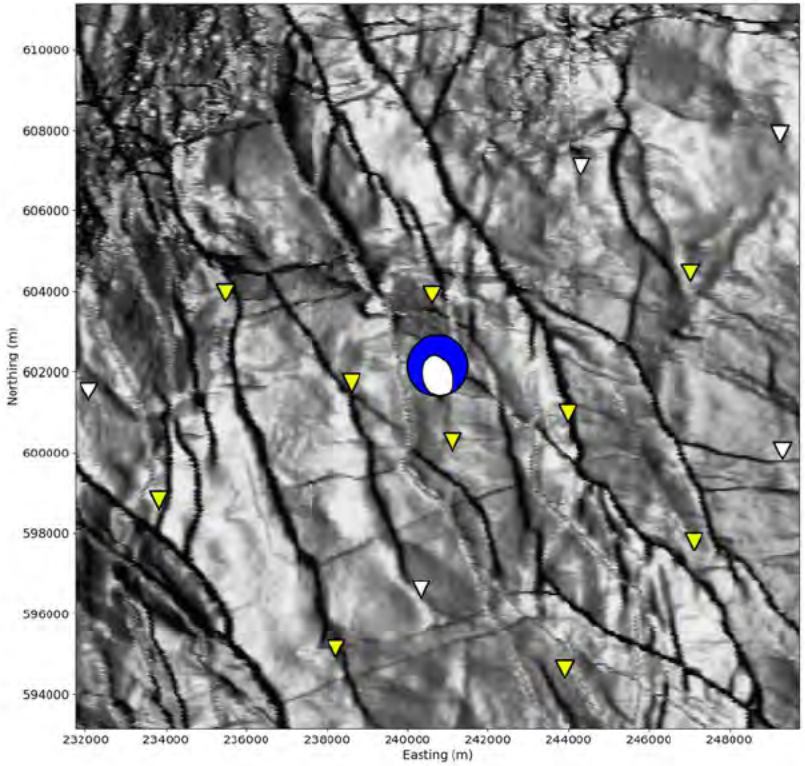

Moment Tensor: Decomposition

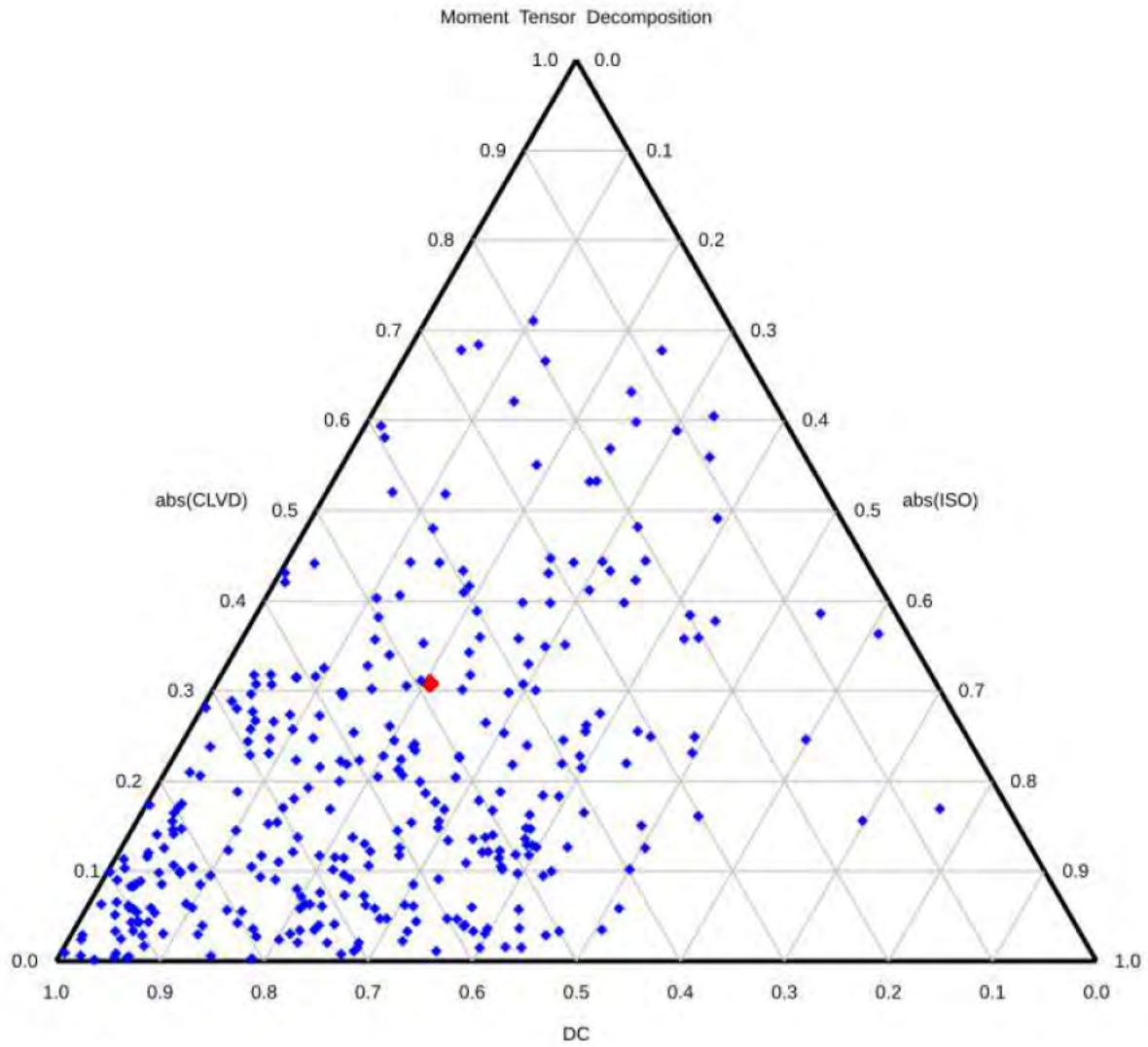

Field data traces

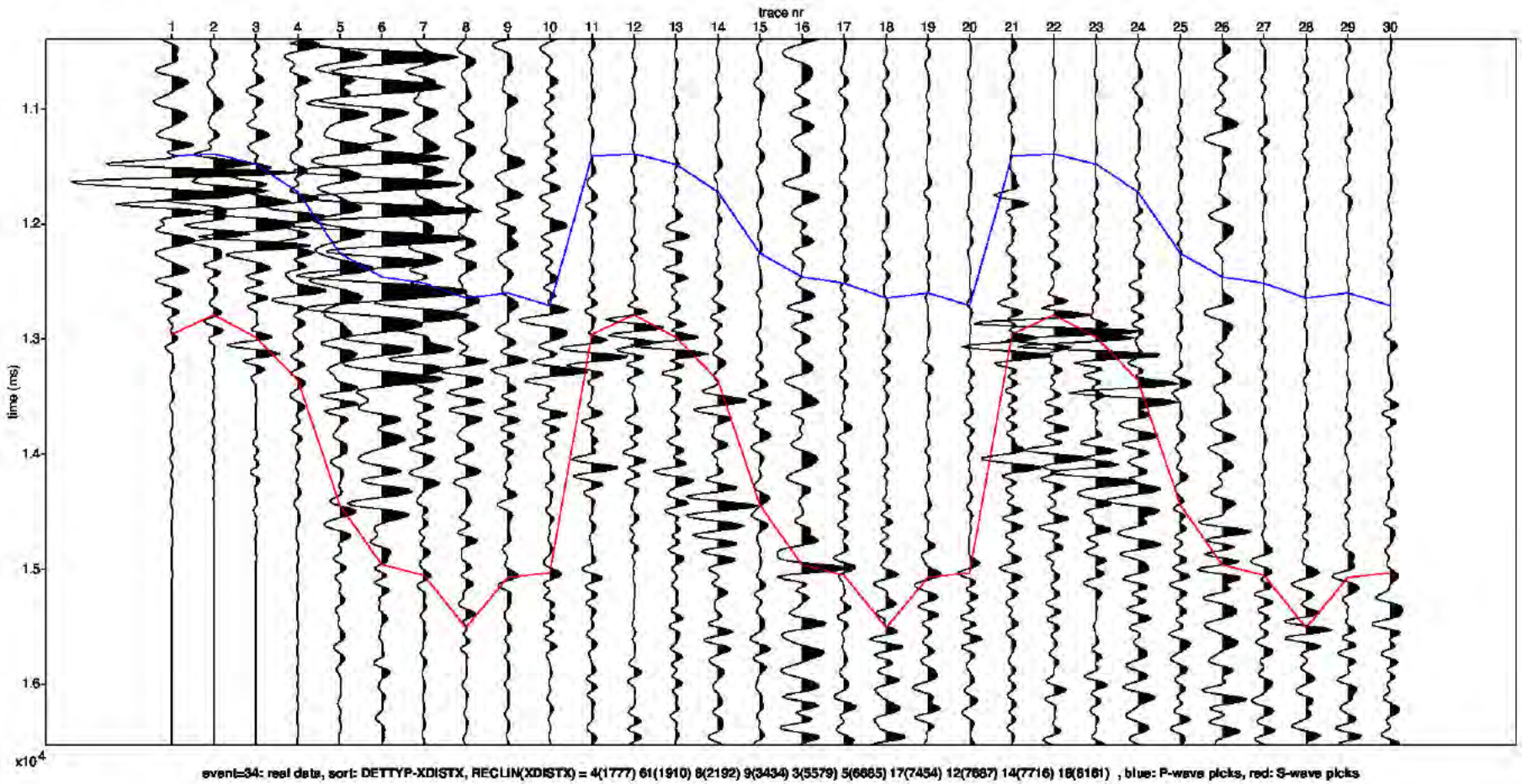

Modelled data traces

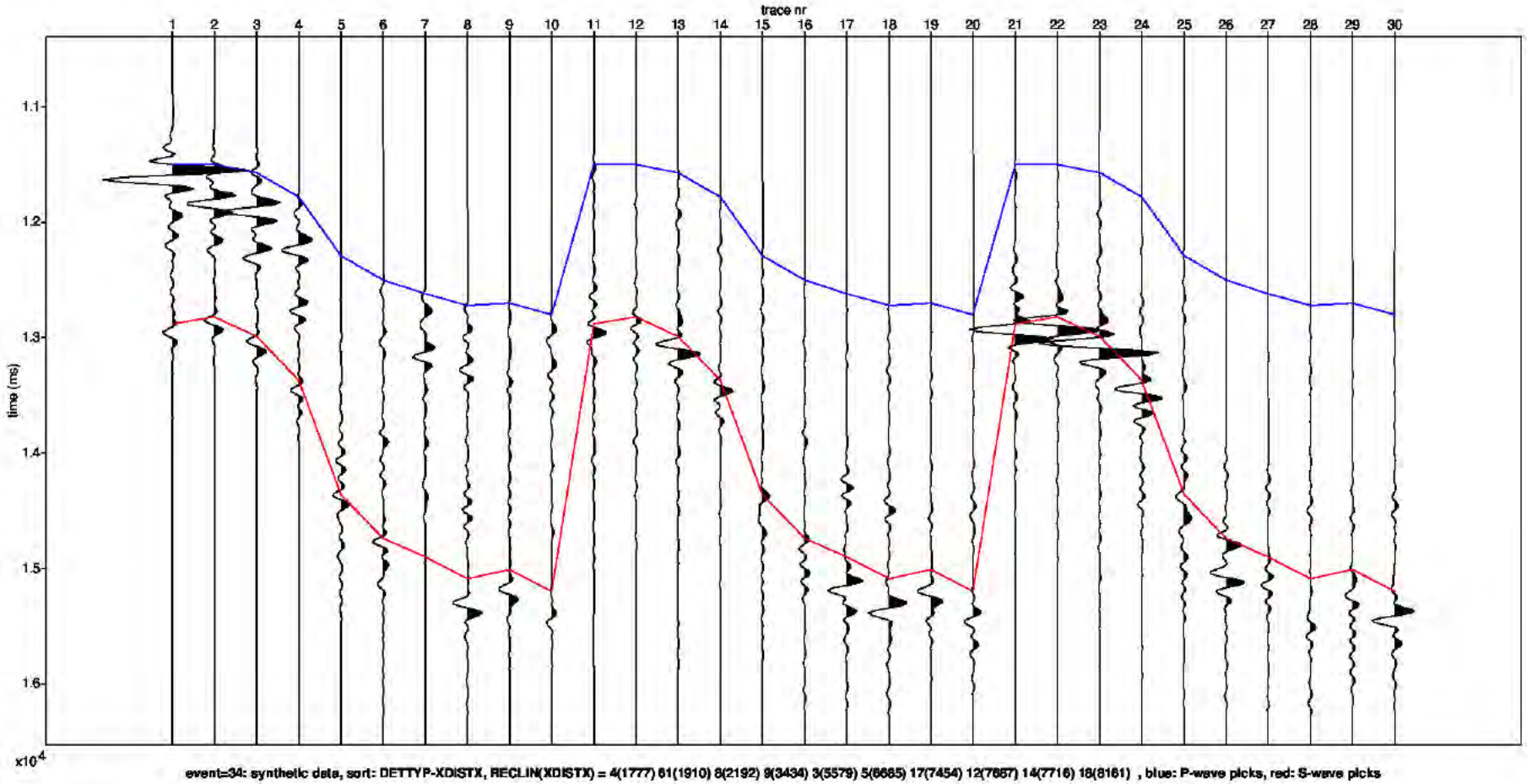

Appendix - Figure Captions

Page

3 Detailed parameter summary for the event. Both primary and secondary focal plane solutions are provided from the moment tensor inversion.

4 Magnitude summary. Prior years are displayed as a “heat map” where the number of events for a given magnitude is displayed per grid cell. The current event is displayed in red.

5 Regional map showing the historical events from KNMI (1986-2019) in blue and the location of the current event in red.

6 Event depth summary. Depths from our automatic workflow (2018-2020) are shown in blue and the current event depth is shown in red. The resolution of the vertical grid is 50m.

7 Event location details for the current event, superimposed on the top Rotliegend depth horizon. Station locations as shown as inverted triangles. Blue triangles are the actual stations used to locate the event whose epicentre is shown by the red dot.

8 QC displays extracted from the objective function for the initial event location. The colour attribute displayed is 1 minus the normalized cross correlation between observed and synthetic waveforms. Station locations are shown as black inverted triangles on the map and the event location is shown by the black dot (left plot). The west to east and north to south vertical profiles are shown on the right. The top and base reservoir are shown for reference as black lines.

Appendix - Figure Captions (continued)

Page

9 QC displays extracted from the objective function for the alternative event location. The colour attribute displayed is 1 minus the normalized cross correlation between observed and synthetic waveforms. Station locations are shown as black inverted triangles on the map and the event location is shown by the black dot (left plot). The west to east and north to south vertical profiles are shown on the right. The top and base reservoir are shown for reference as black lines.

10 Moment tensor inversion results for the event. The double couple portion of the moment tensor is shown on the left and the full moment tensor is displayed on the right. Station locations used in the inversion are shown as inverted triangles.

11 Ternary diagram showing the moment tensor decompositions into relative double-couple(DC), isotropic (ISO) and compensated linear vector dipole (CLVD) contributions. The automatic Shell events (2018-2020) are shown in blue and the current event is highlighted in red.

12 Observed traces for each station and each component. The automatic picks for the P- and S-waves are indicated by the blue and red lines respectively.

13 Modelled waveform data for each station and each component. The automatic picks for the P- and S-waves are indicated by the blue and red lines respectively.

Appendix E FWI analysis of the earthquake near Uithuizen on the 24th September 2022 with a magnitude of 2.7

Event 38 - Uithuizen
24 September 2022 10:20:39

26 September 2022

Induced Seismicity Taskforce

Disclaimer

- The results presented in this report have been automatically generated using an unconstrained full waveform, event location and moment tensor inversion workflow, developed by the Induced Seismicity Taskforce at Shell.
- These results have not been previously reviewed.
- For questions related to the results then you should contact:
  - Chris Willacy (Christopher.Willacy@Shell.com) or
  - Jan-Willem Blokland (Jan-Willem.Blokland@Shell.com)

Event summary

The event happened at:

Date	24 September 2022
Time	10:20:39.055255

The event is located at:

Location	Uithuizen
Northing (m)	602100
Easting (m)	241650
Depth (m)	2950

The source characteristics are:

	Solution 1	Solution 2
Strike angle (degree)	298.10	162.60
Dip angle (degree)	40.89	39.71
Rake angle (degree)	-117.84	-61.42
Isotropic (percentage)	27.57	27.57
CLVD (percentage)	-24.99	-24.99
Magnitude M_{L}	2.70	2.70

Magnitude summary

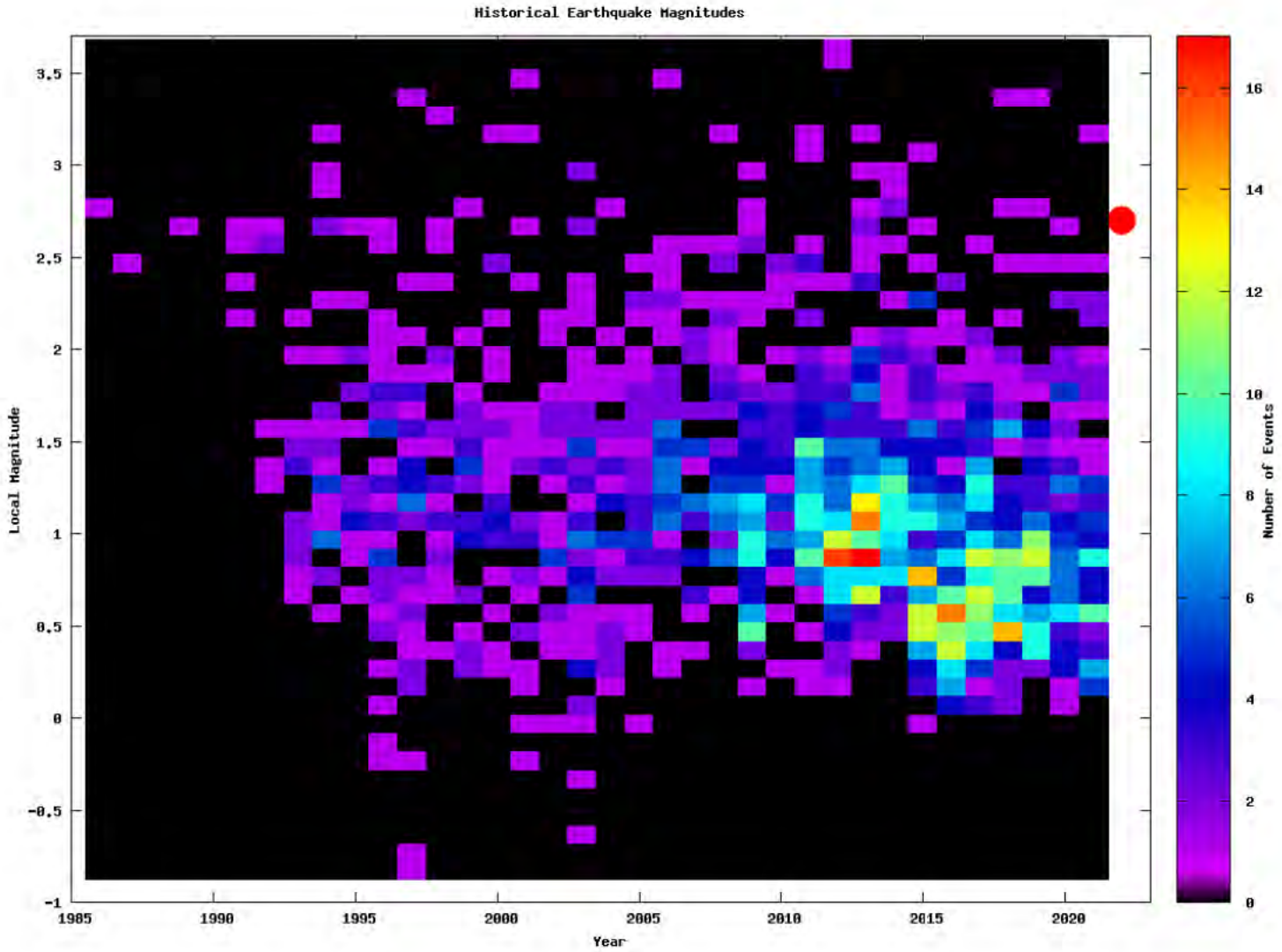

Regional and historical map

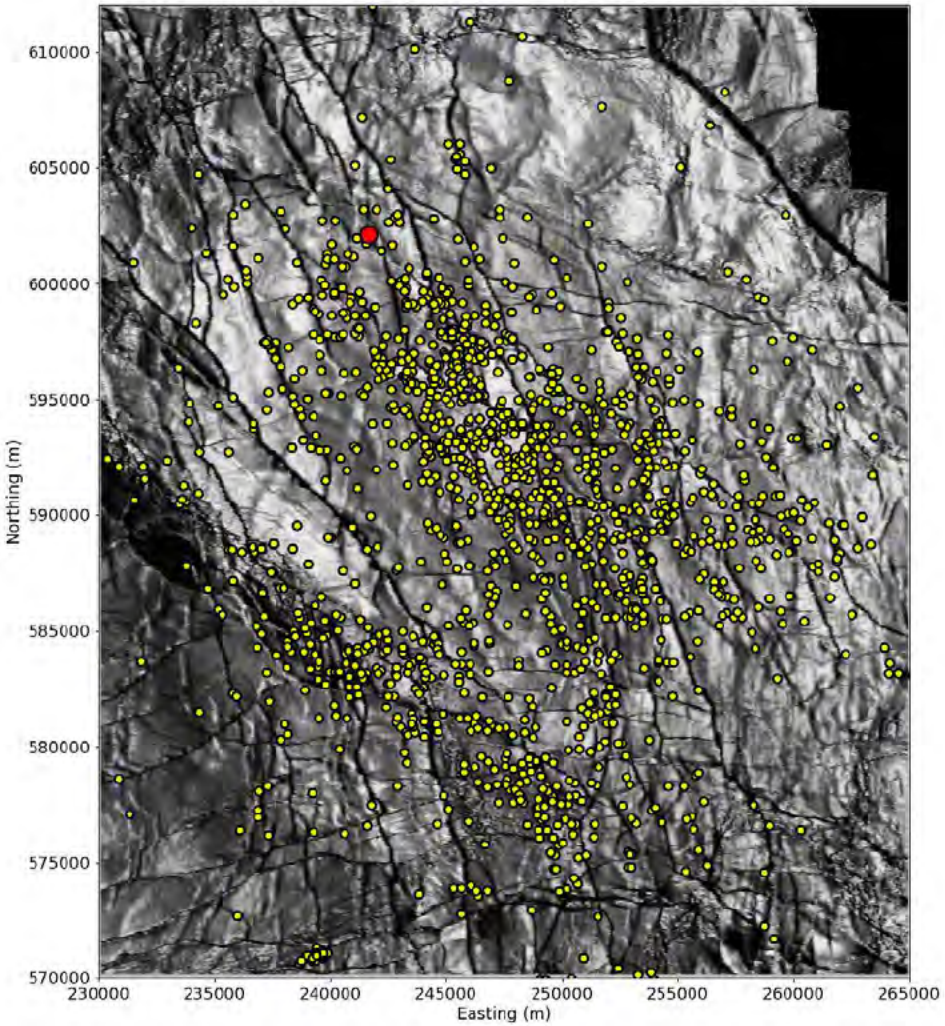

Event depth summary

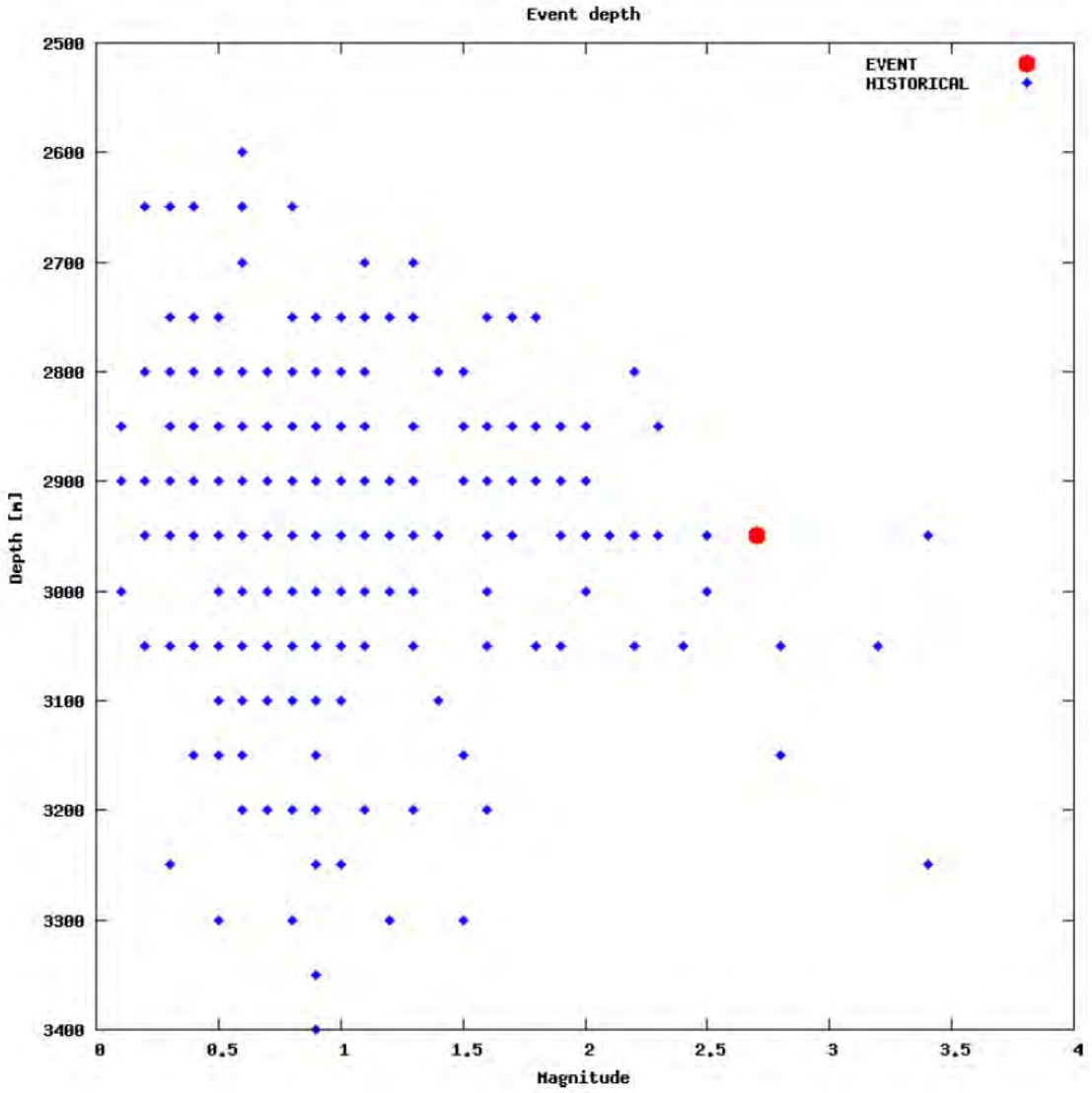

Event location - Map

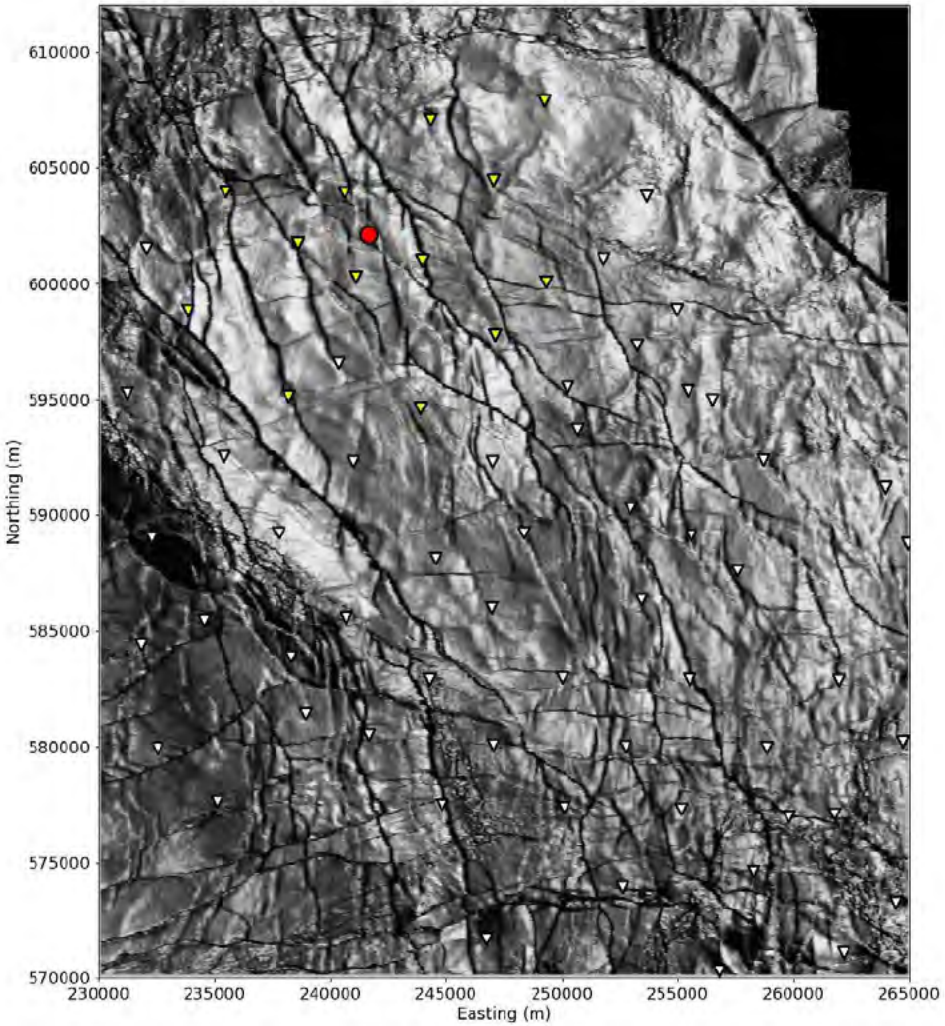

Event location and depth (initial)

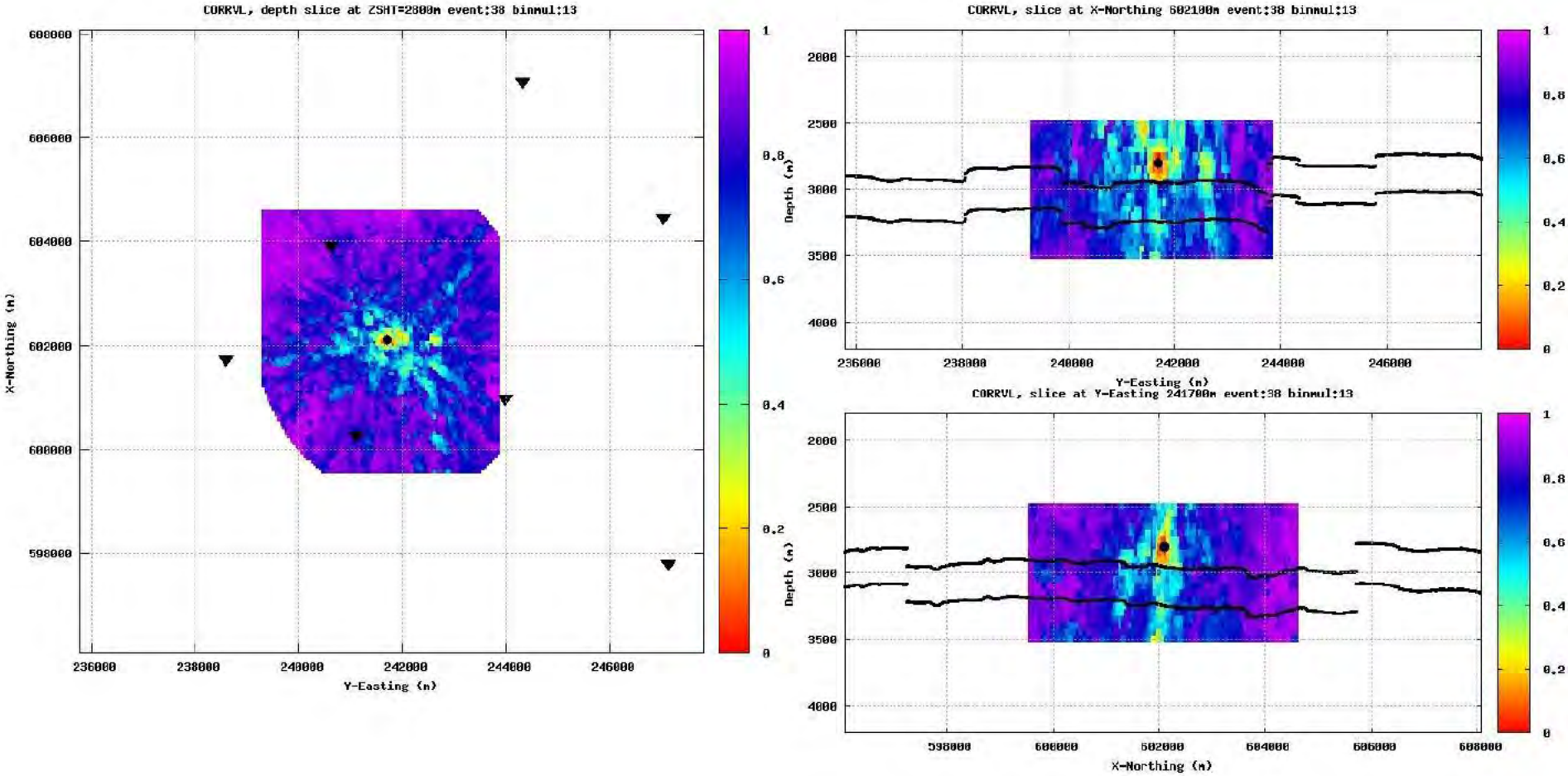

Event location and depth (alternative)

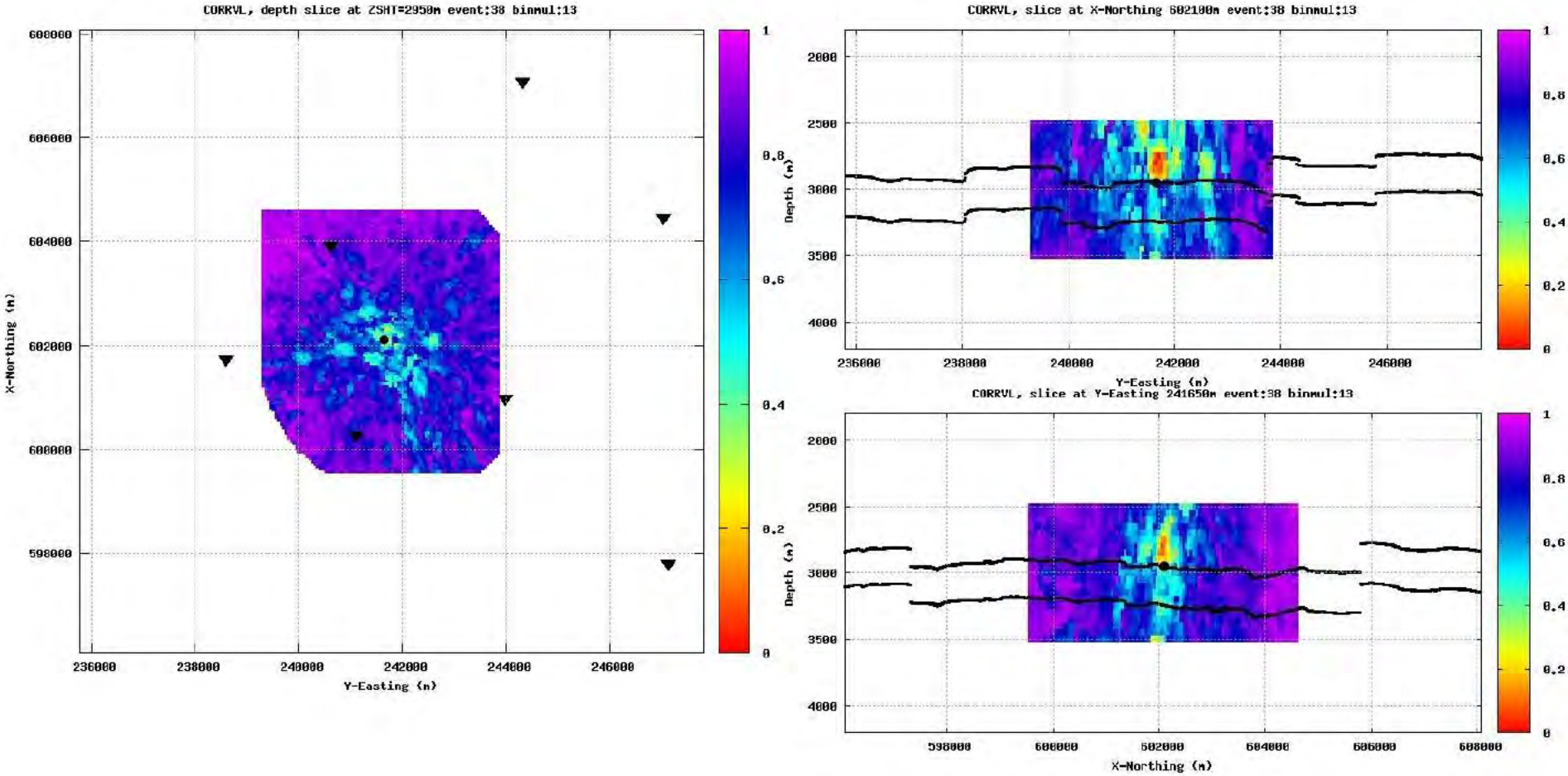

Moment tensor

Double-coupled part

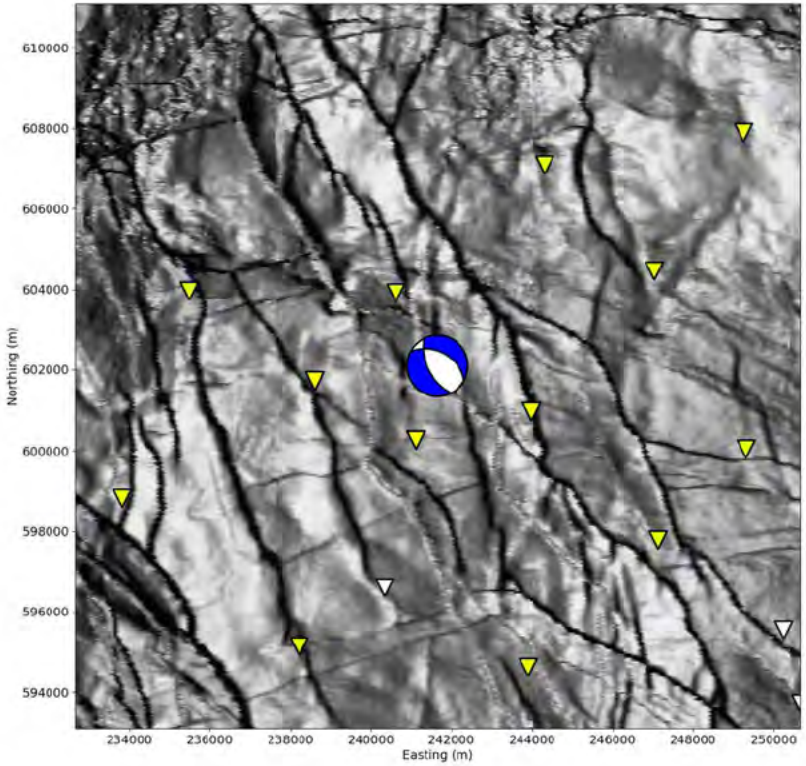

Full

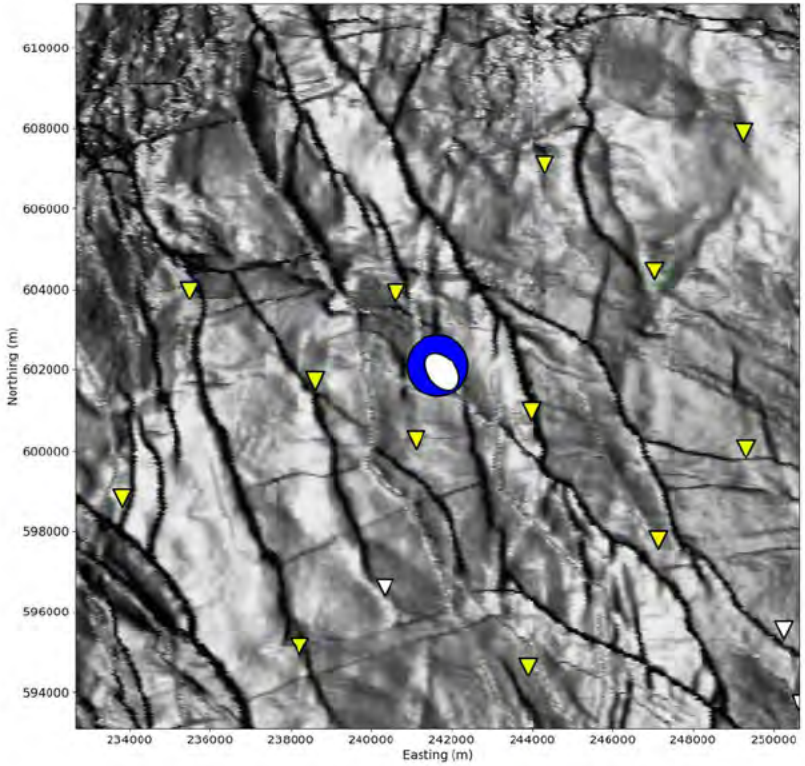

Moment Tensor: Decomposition

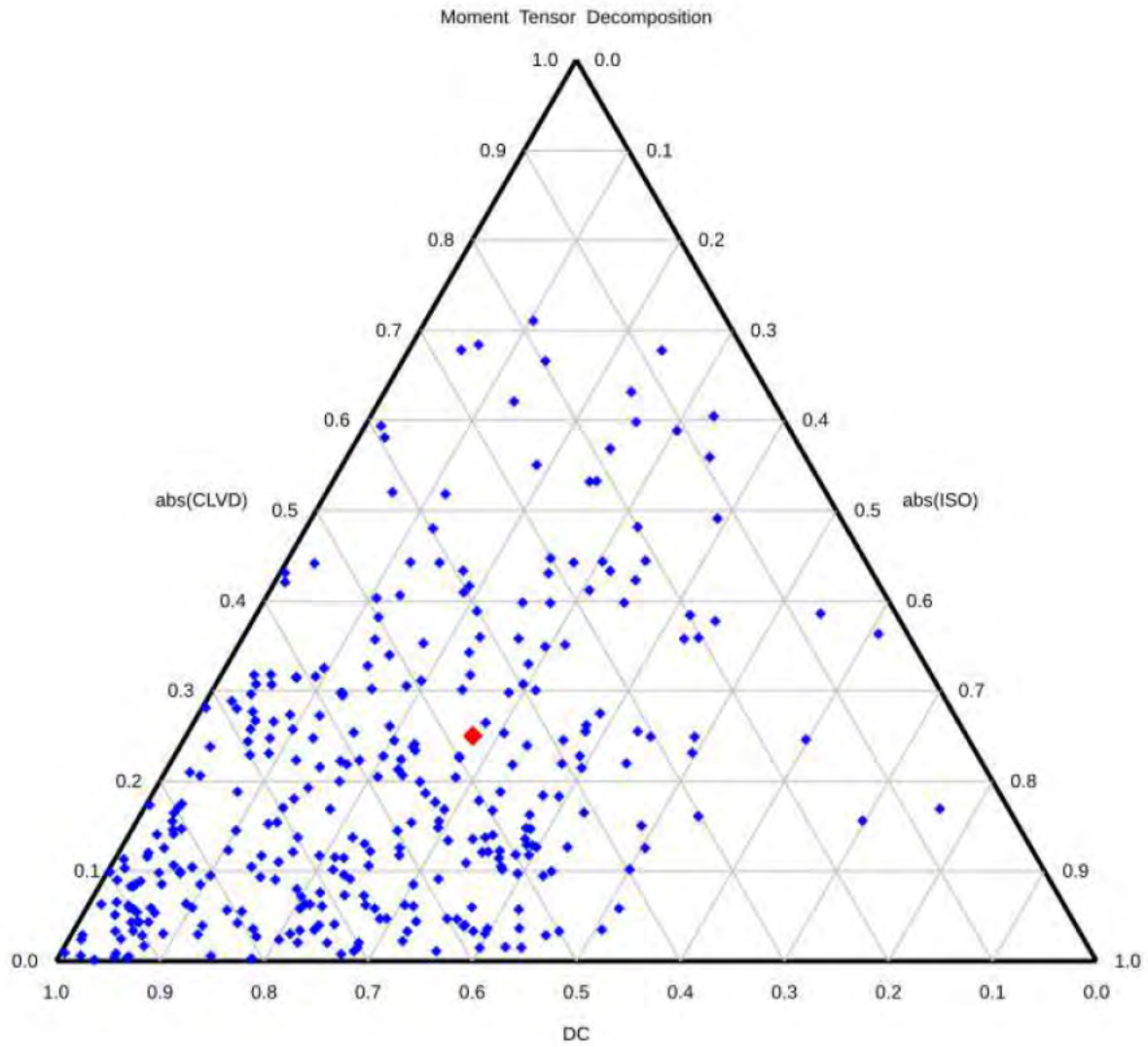

Field data traces

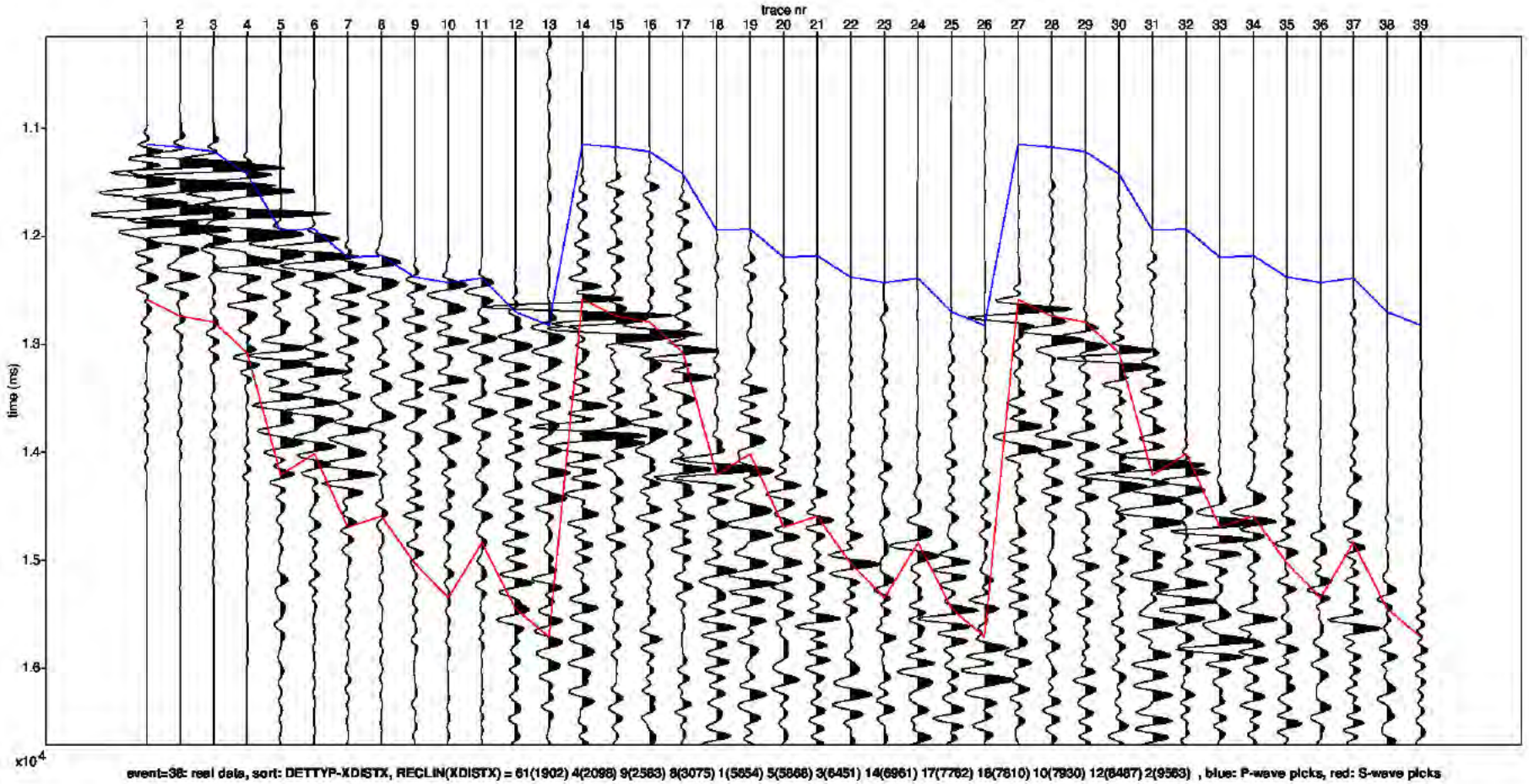

Modelled data traces

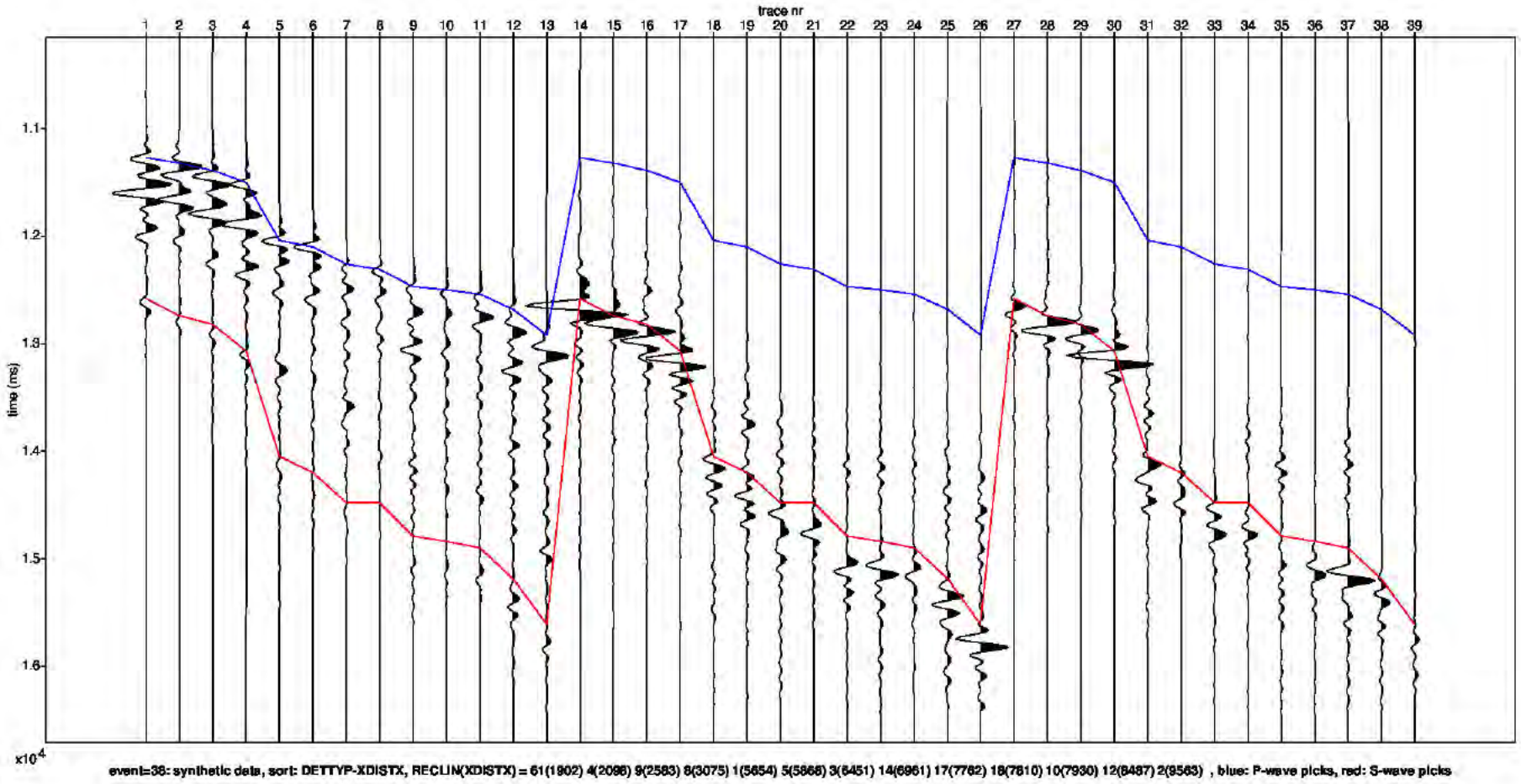

Appendix - Figure Captions

Page

3 Detailed parameter summary for the event. Both primary and secondary focal plane solutions are provided from the moment tensor inversion.

4 Magnitude summary. Prior years are displayed as a “heat map” where the number of events for a given magnitude is displayed per grid cell. The current event is displayed in red.

5 Regional map showing the historical events from KNMI (1986-2019) in blue and the location of the current event in red.

6 Event depth summary. Depths from our automatic workflow (2018-2020) are shown in blue and the current event depth is shown in red. The resolution of the vertical grid is 50m.

7 Event location details for the current event, superimposed on the top Rotliegend depth horizon. Station locations as shown as inverted triangles. Blue triangles are the actual stations used to locate the event whose epicentre is shown by the red dot.

8 QC displays extracted from the objective function for the initial event location. The colour attribute displayed is 1 minus the normalized cross correlation between observed and synthetic waveforms. Station locations are shown as black inverted triangles on the map and the event location is shown by the black dot (left plot). The west to east and north to south vertical profiles are shown on the right. The top and base reservoir are shown for reference as black lines.

Appendix - Figure Captions (continued)

Page

9 QC displays extracted from the objective function for the alternative event location. The colour attribute displayed is 1 minus the normalized cross correlation between observed and synthetic waveforms. Station locations are shown as black inverted triangles on the map and the event location is shown by the black dot (left plot). The west to east and north to south vertical profiles are shown on the right. The top and base reservoir are shown for reference as black lines.

10 Moment tensor inversion results for the event. The double couple portion of the moment tensor is shown on the left and the full moment tensor is displayed on the right. Station locations used in the inversion are shown as inverted triangles.

11 Ternary diagram showing the moment tensor decompositions into relative double-couple(DC), isotropic (ISO) and compensated linear vector dipole (CLVD) contributions. The automatic Shell events (2018-2020) are shown in blue and the current event is highlighted in red.

12 Observed traces for each station and each component. The automatic picks for the P- and S-waves are indicated by the blue and red lines respectively.

13 Modelled waveform data for each station and each component. The automatic picks for the P- and S-waves are indicated by the blue and red lines respectively.

Appendix F FWI analysis of the earthquake near Uithuizen on the 24th September 2022 with a magnitude of 1.7

Event 39 - Uithuizen
24 September 2022 11:37:29

26 September 2022

Induced Seismicity Taskforce

Disclaimer

- The results presented in this report have been automatically generated using an unconstrained full waveform, event location and moment tensor inversion workflow, developed by the Induced Seismicity Taskforce at Shell.
- These results have not been previously reviewed.
- For questions related to the results then you should contact:
  - Chris Willacy (Christopher.Willacy@Shell.com) or
  - Jan-Willem Blokland (Jan-Willem.Blokland@Shell.com)

Event summary

The event happened at:

Date	24 September 2022
Time	11:37:29.588478

The event is located at:

Location	Uithuizen
Northing (m)	602500
Easting (m)	241600
Depth (m)	3250

The source characteristics are:

	Solution 1	Solution 2
Strike angle (degree)	150.27	334.41
Dip angle (degree)	41.00	45.18
Rake angle (degree)	-92.95	-87.28
Isotropic (percentage)	-12.39	-12.39
CLVD (percentage)	-7.76	-7.76
Magnitude M_{L}	1.70	1.70

Magnitude summary

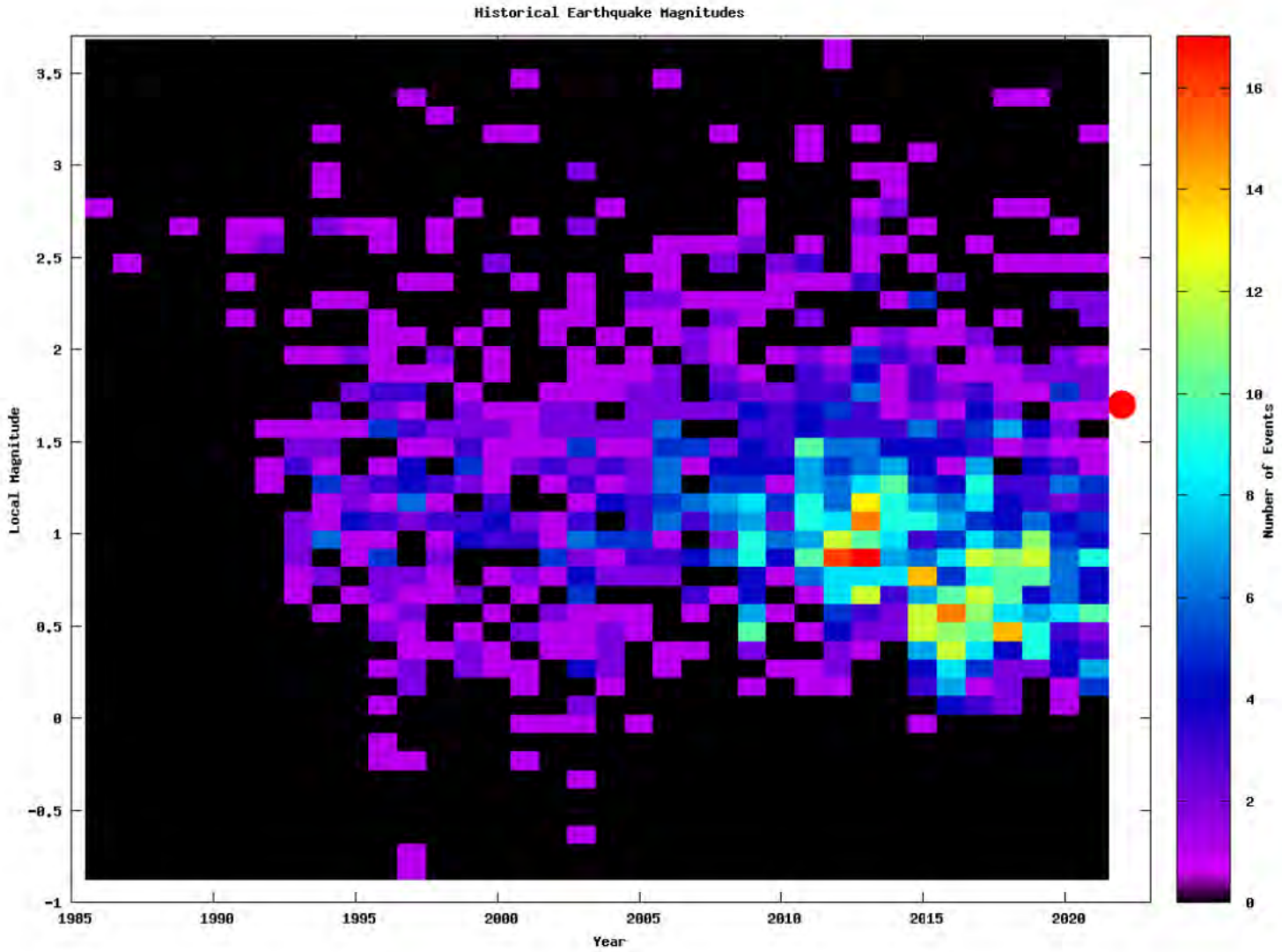

Regional and historical map

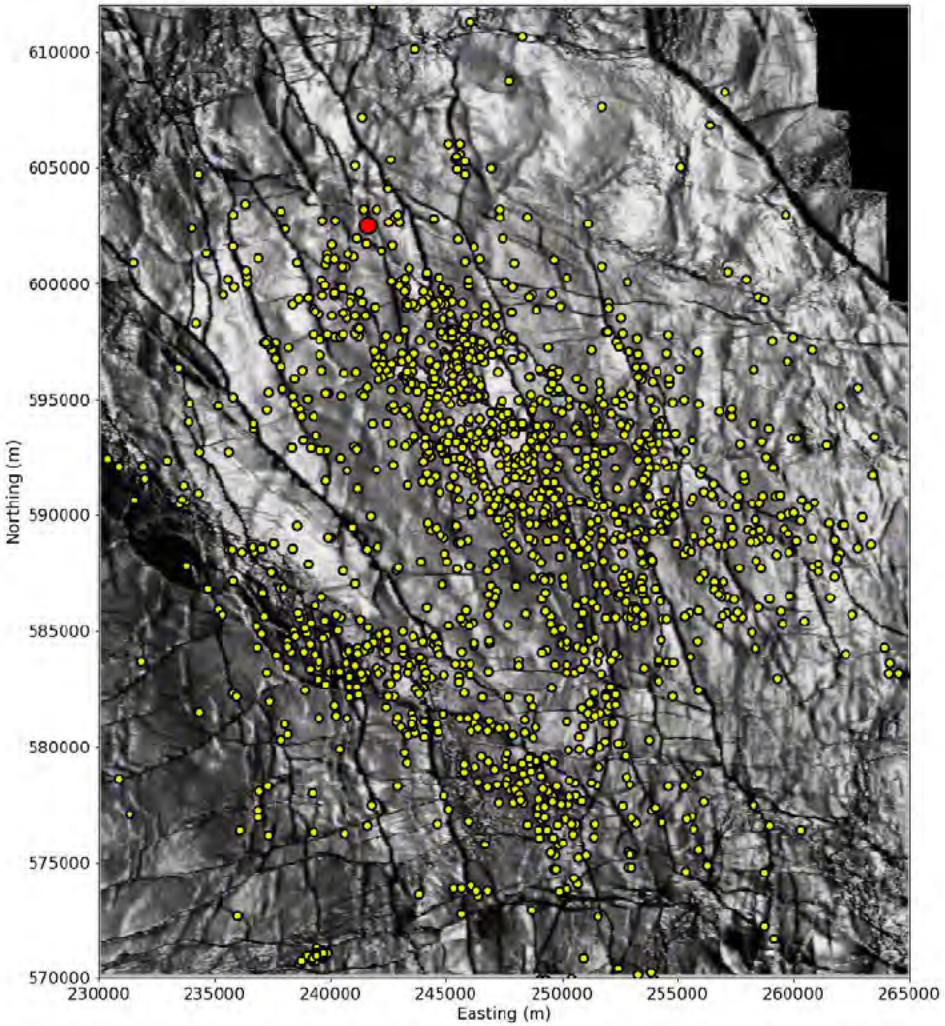

Event depth summary

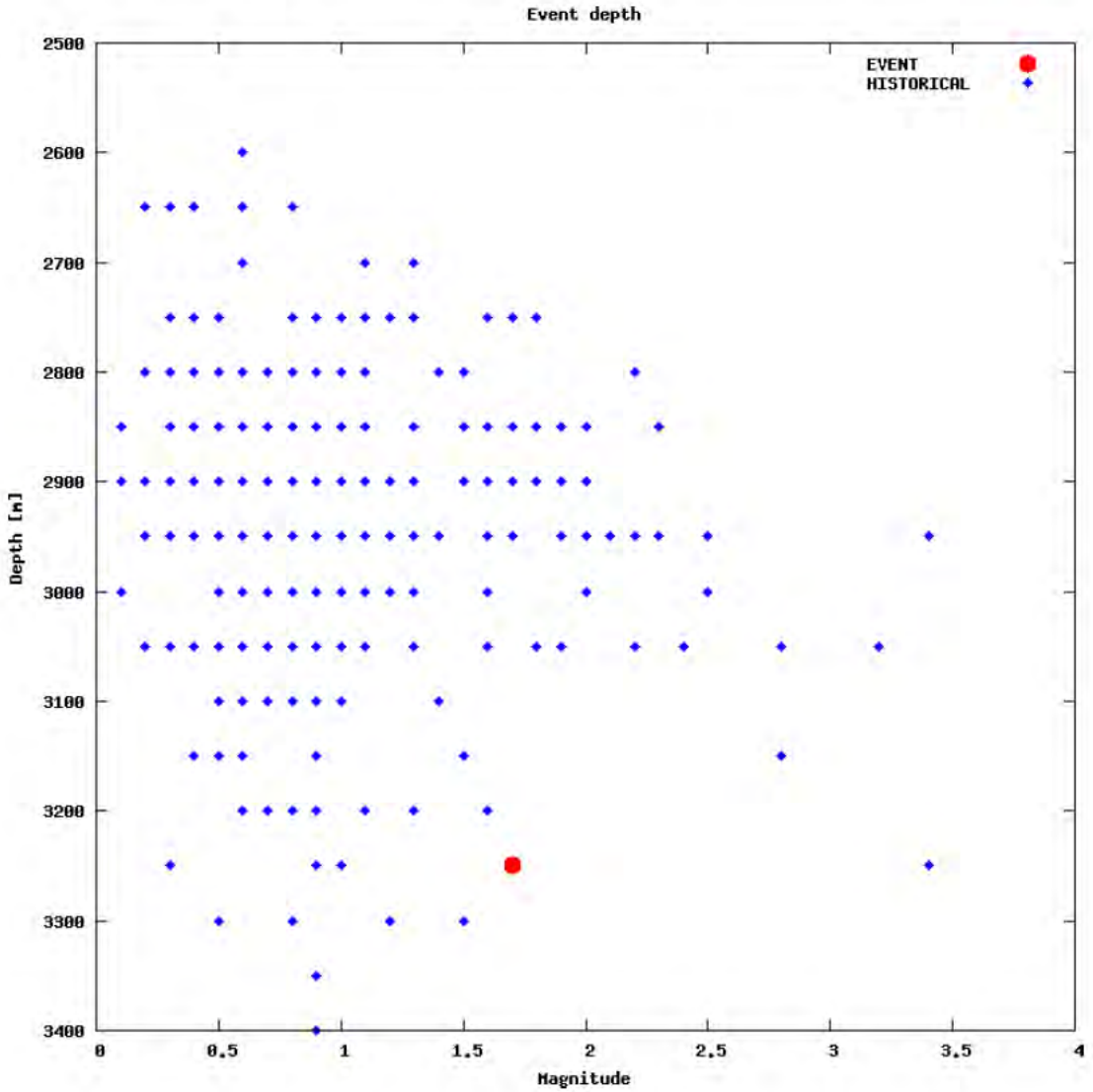

Event location - Map

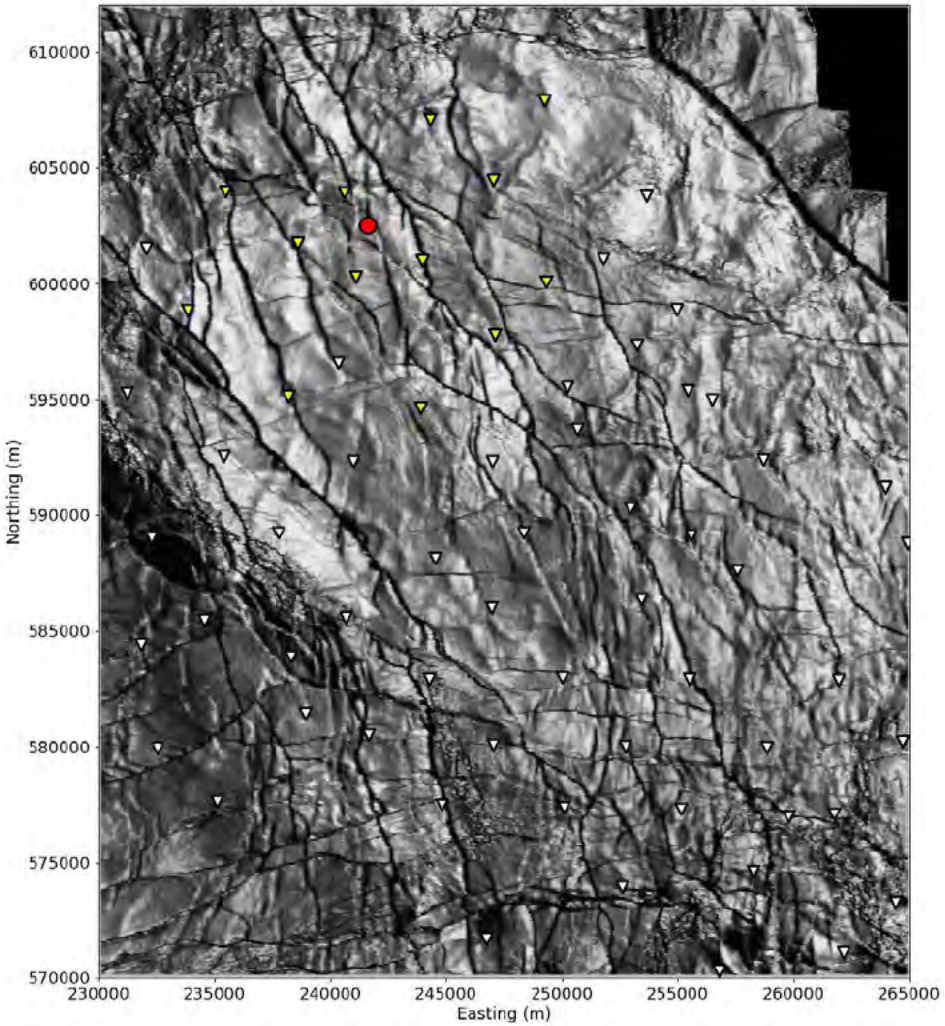

Event location and depth (initial)

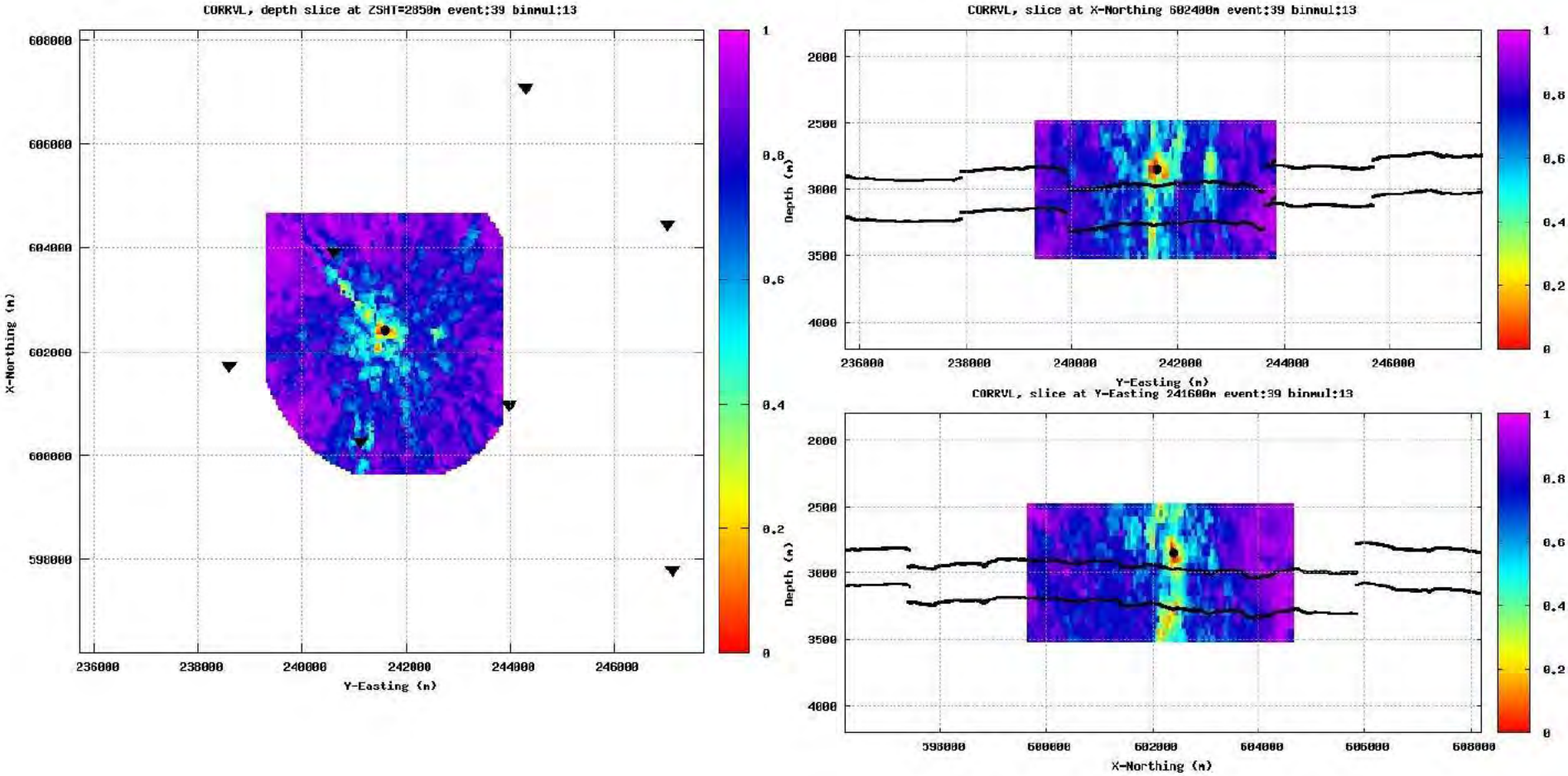

Event location and depth (alternative)

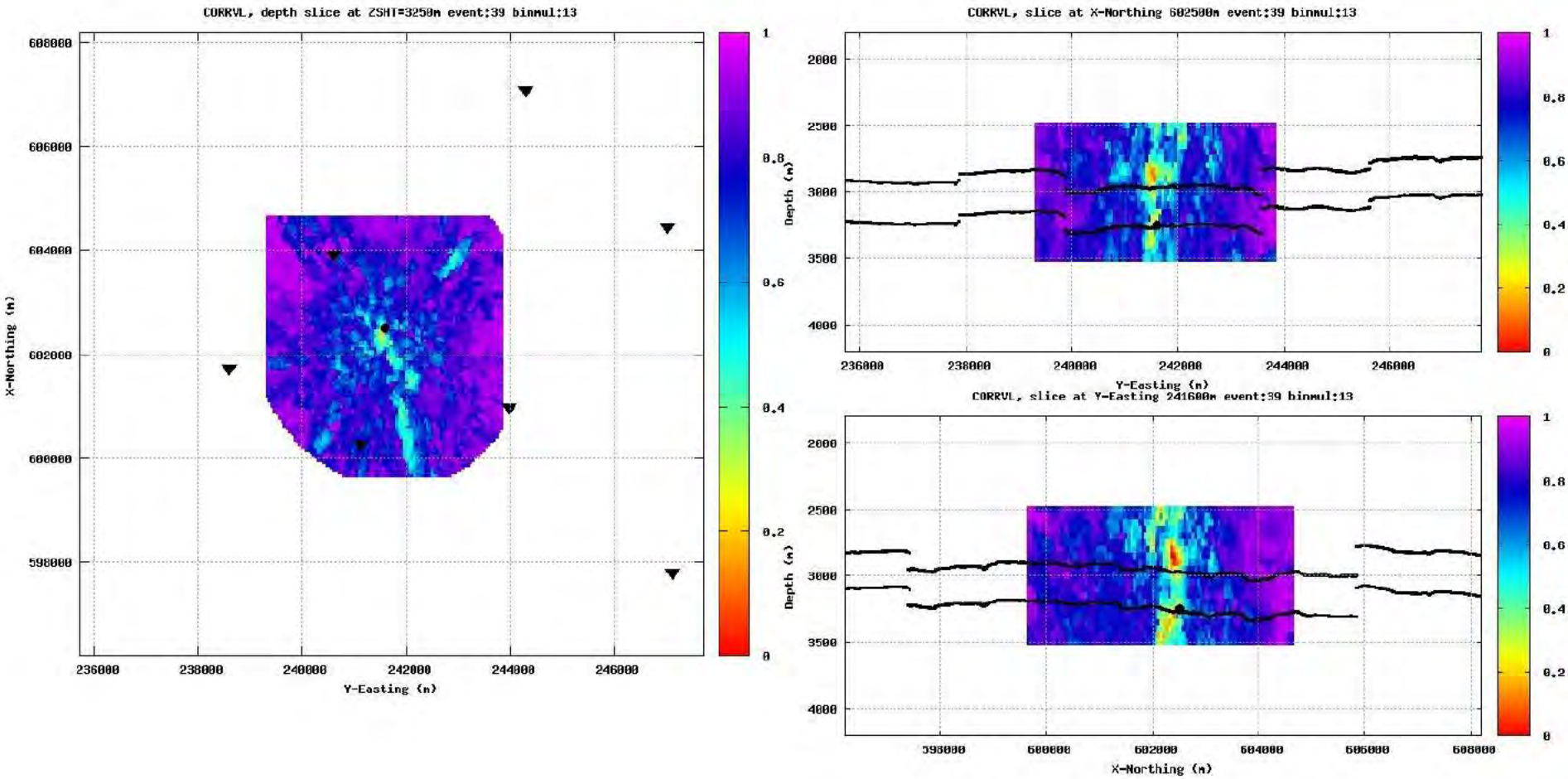

Moment tensor

Double-coupled part

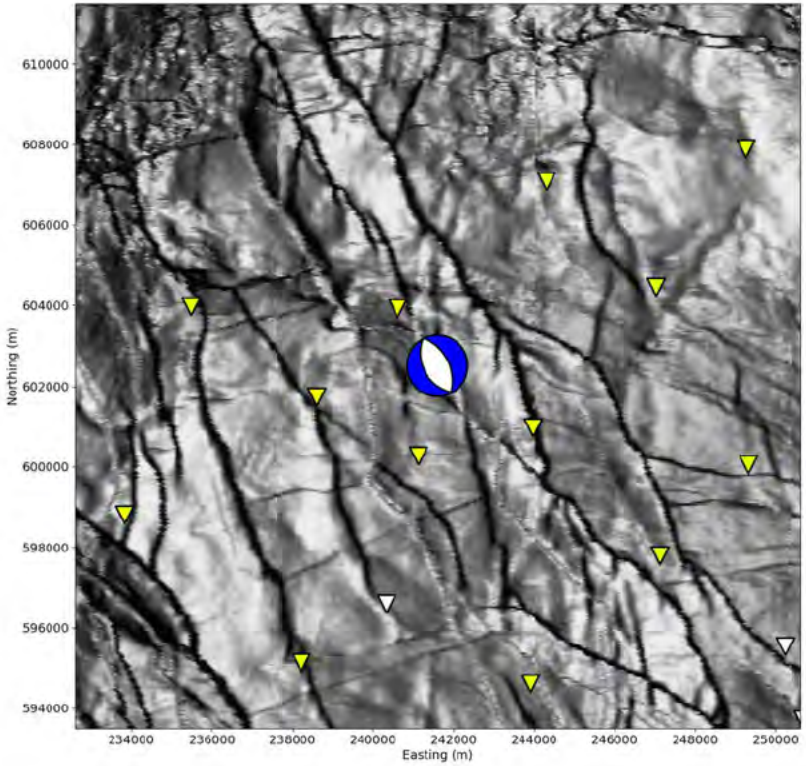

Full

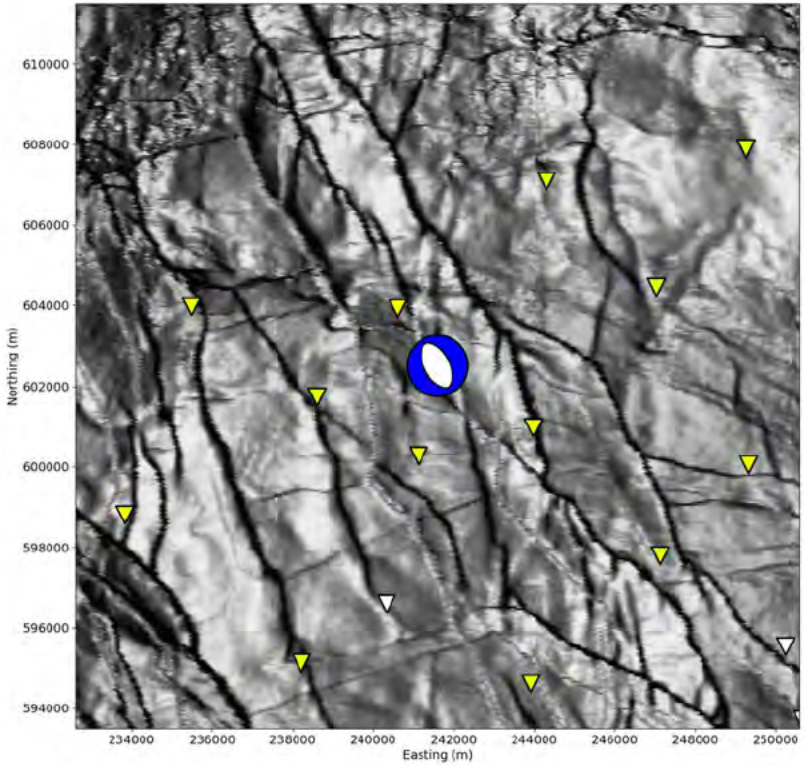

Moment Tensor: Decomposition

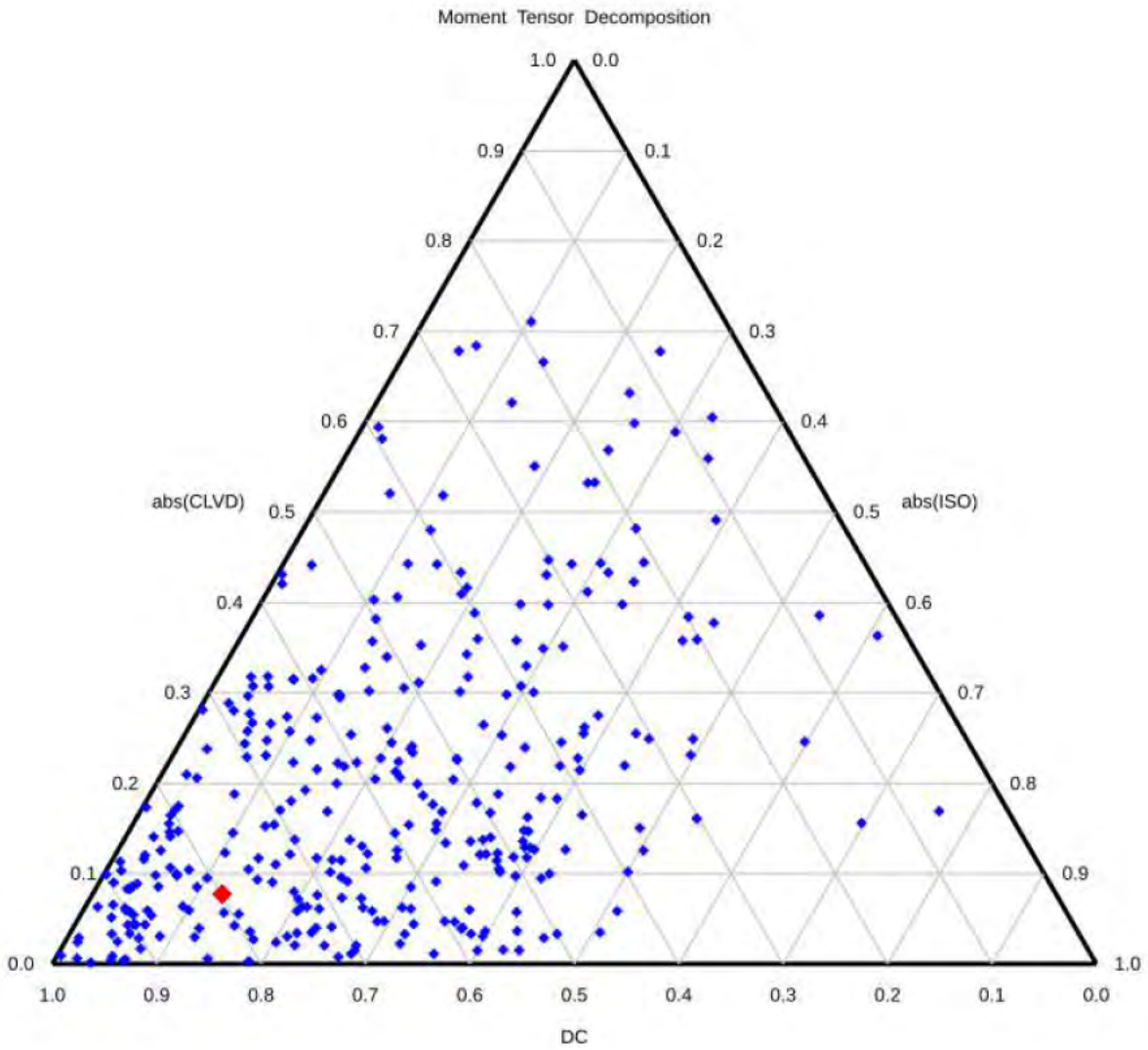

Field data traces

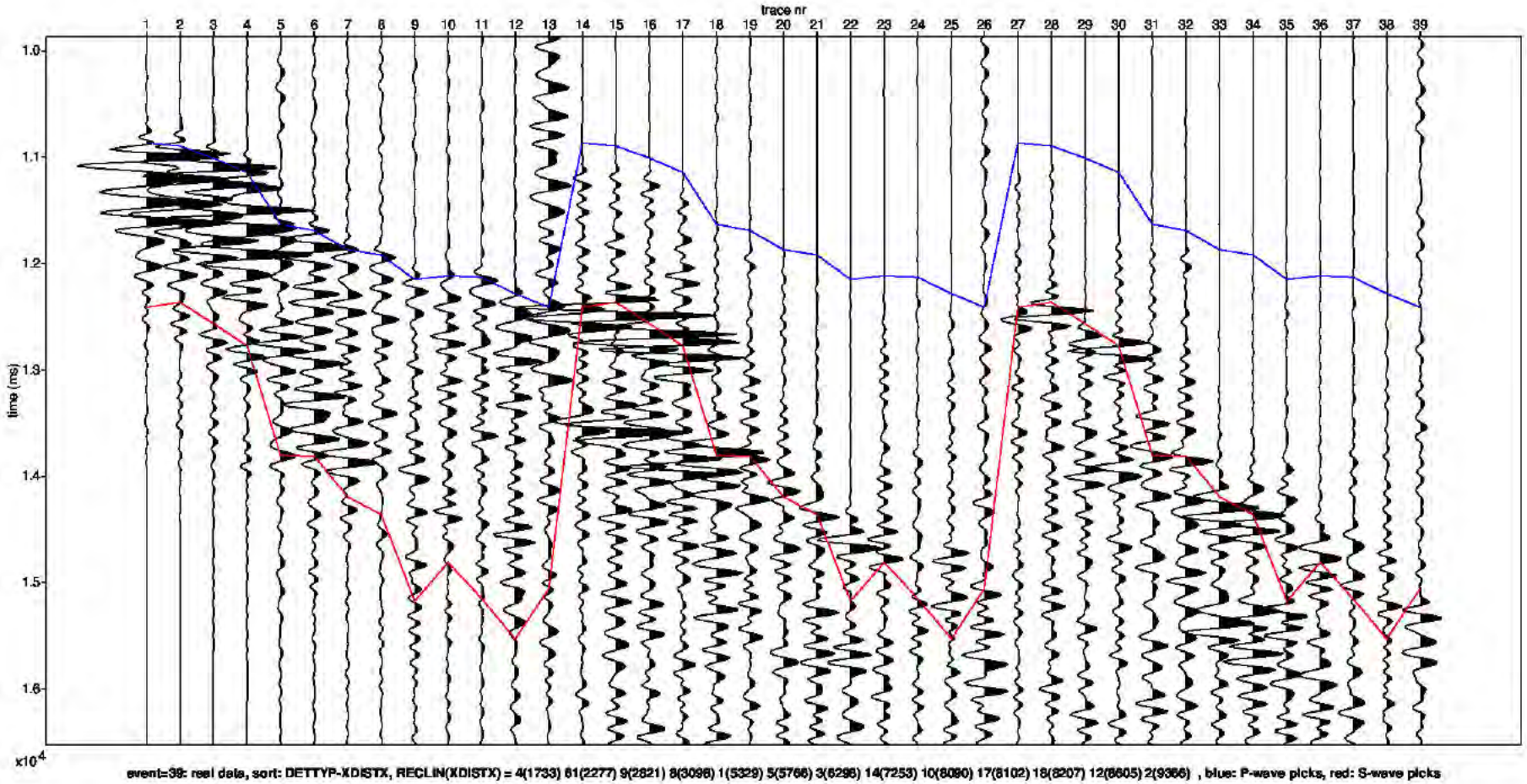

Modelled data traces

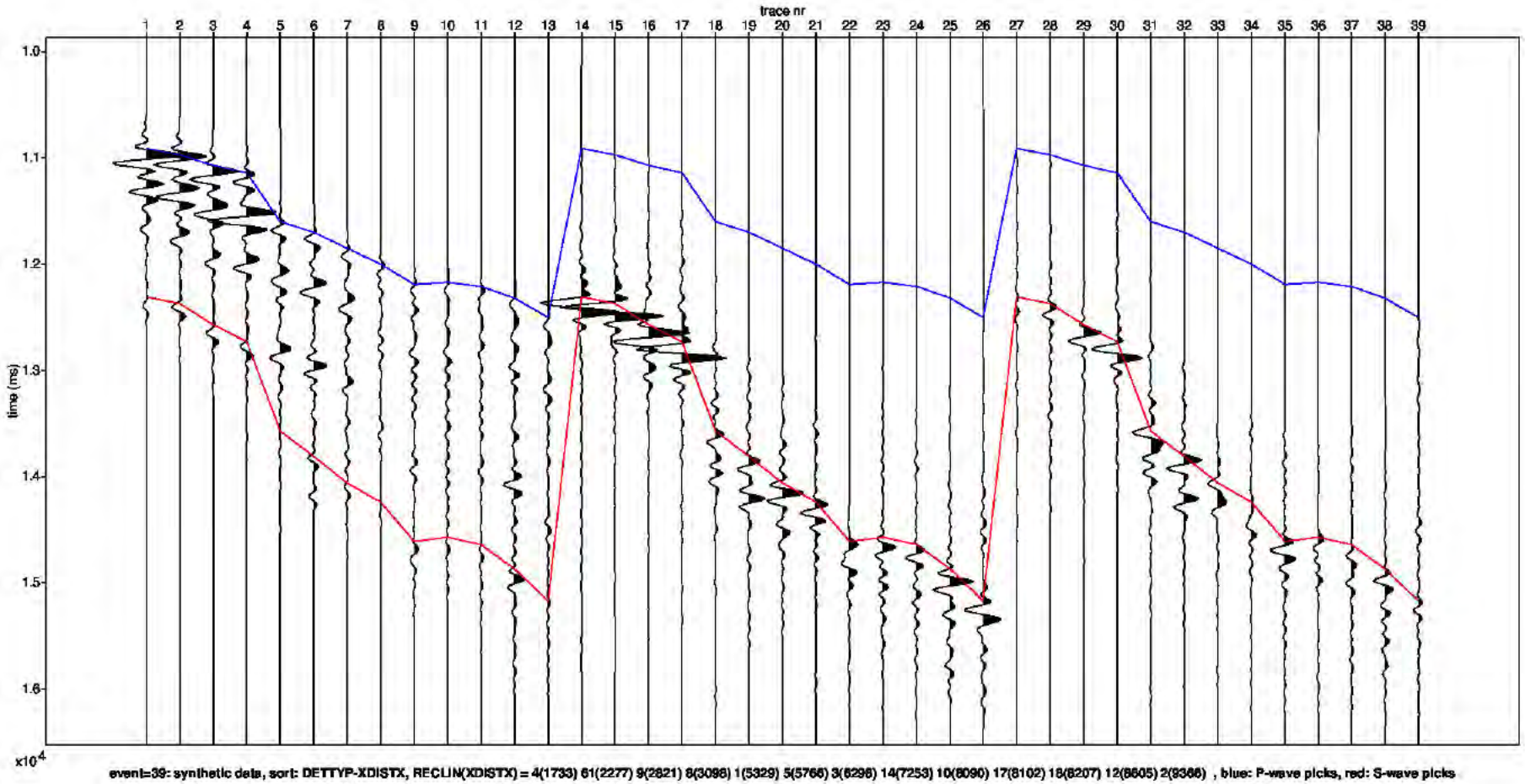

Appendix - Figure Captions

Page

3 Detailed parameter summary for the event. Both primary and secondary focal plane solutions are provided from the moment tensor inversion.

4 Magnitude summary. Prior years are displayed as a “heat map” where the number of events for a given magnitude is displayed per grid cell. The current event is displayed in red.

5 Regional map showing the historical events from KNMI (1986-2019) in blue and the location of the current event in red.

6 Event depth summary. Depths from our automatic workflow (2018-2020) are shown in blue and the current event depth is shown in red. The resolution of the vertical grid is 50m.

7 Event location details for the current event, superimposed on the top Rotliegend depth horizon. Station locations as shown as inverted triangles. Blue triangles are the actual stations used to locate the event whose epicentre is shown by the red dot.

8 QC displays extracted from the objective function for the initial event location. The colour attribute displayed is 1 minus the normalized cross correlation between observed and synthetic waveforms. Station locations are shown as black inverted triangles on the map and the event location is shown by the black dot (left plot). The west to east and north to south vertical profiles are shown on the right. The top and base reservoir are shown for reference as black lines.

Appendix - Figure Captions (continued)

Page

9 QC displays extracted from the objective function for the alternative event location. The colour attribute displayed is 1 minus the normalized cross correlation between observed and synthetic waveforms. Station locations are shown as black inverted triangles on the map and the event location is shown by the black dot (left plot). The west to east and north to south vertical profiles are shown on the right. The top and base reservoir are shown for reference as black lines.

10 Moment tensor inversion results for the event. The double couple portion of the moment tensor is shown on the left and the full moment tensor is displayed on the right. Station locations used in the inversion are shown as inverted triangles.

11 Ternary diagram showing the moment tensor decompositions into relative double-couple(DC), isotropic (ISO) and compensated linear vector dipole (CLVD) contributions. The automatic Shell events (2018-2020) are shown in blue and the current event is highlighted in red.

12 Observed traces for each station and each component. The automatic picks for the P- and S-waves are indicated by the blue and red lines respectively.

13 Modelled waveform data for each station and each component. The automatic picks for the P- and S-waves are indicated by the blue and red lines respectively.

Appendix G FWI analysis of the earthquake near Uithuizen on the 11th October 2022 with a magnitude of 1.3

Event 42 - Uithuizen
11 October 2022 15:36:39

12 October 2022

Induced Seismicity Taskforce

Disclaimer

- The results presented in this report have been automatically generated using an unconstrained full waveform, event location and moment tensor inversion workflow, developed by the Induced Seismicity Taskforce at Shell.
- These results have not been previously reviewed.
- For questions related to the results then you should contact:
  - Chris Willacy (Christopher.Willacy@Shell.com) or
  - Jan-Willem Blokland (Jan-Willem.Blokland@Shell.com)

Event summary

The event happened at:

Date	11 October 2022
Time	15:36:39.576970

The event is located at:

Location	Uithuizen
Northing (m)	602600
Easting (m)	241550
Depth (m)	3050

The source characteristics are:

	Solution 1	Solution 2
Strike angle (degree)	133.22	334.01
Dip angle (degree)	45.91	65.73
Rake angle (degree)	-110.01	-74.36
Isotropic (percentage)	-38.63	-38.63
CLVD (percentage)	24.08	24.08
Magnitude M_{L}	1.30	1.30

Magnitude summary

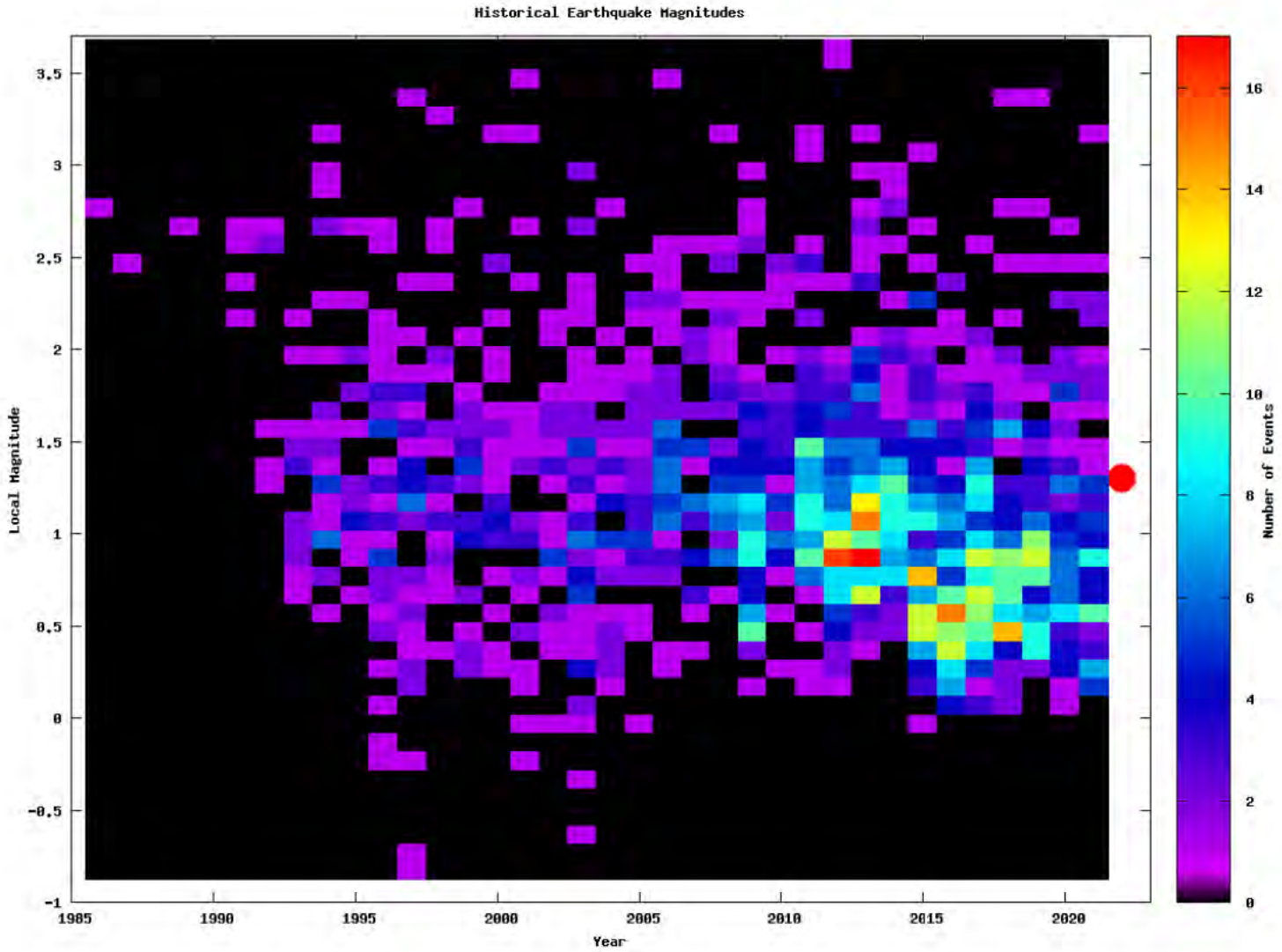

Regional and historical map

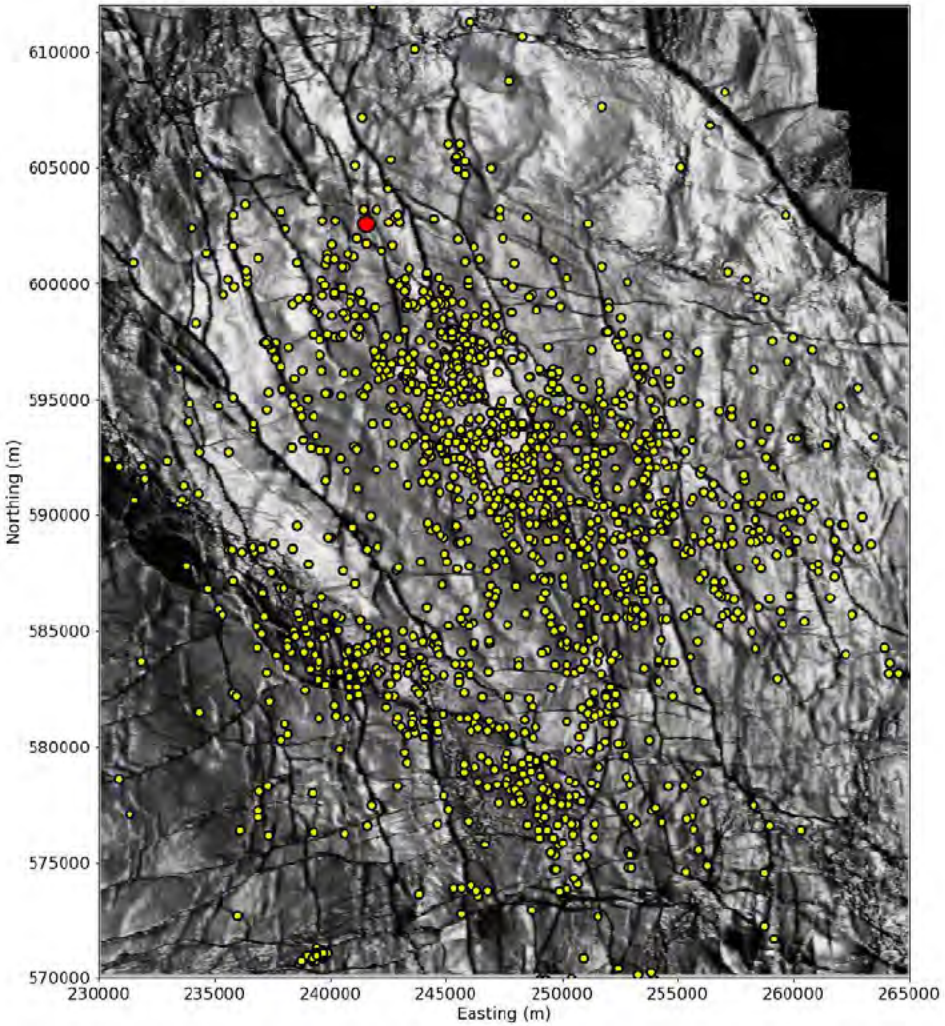

Event depth summary

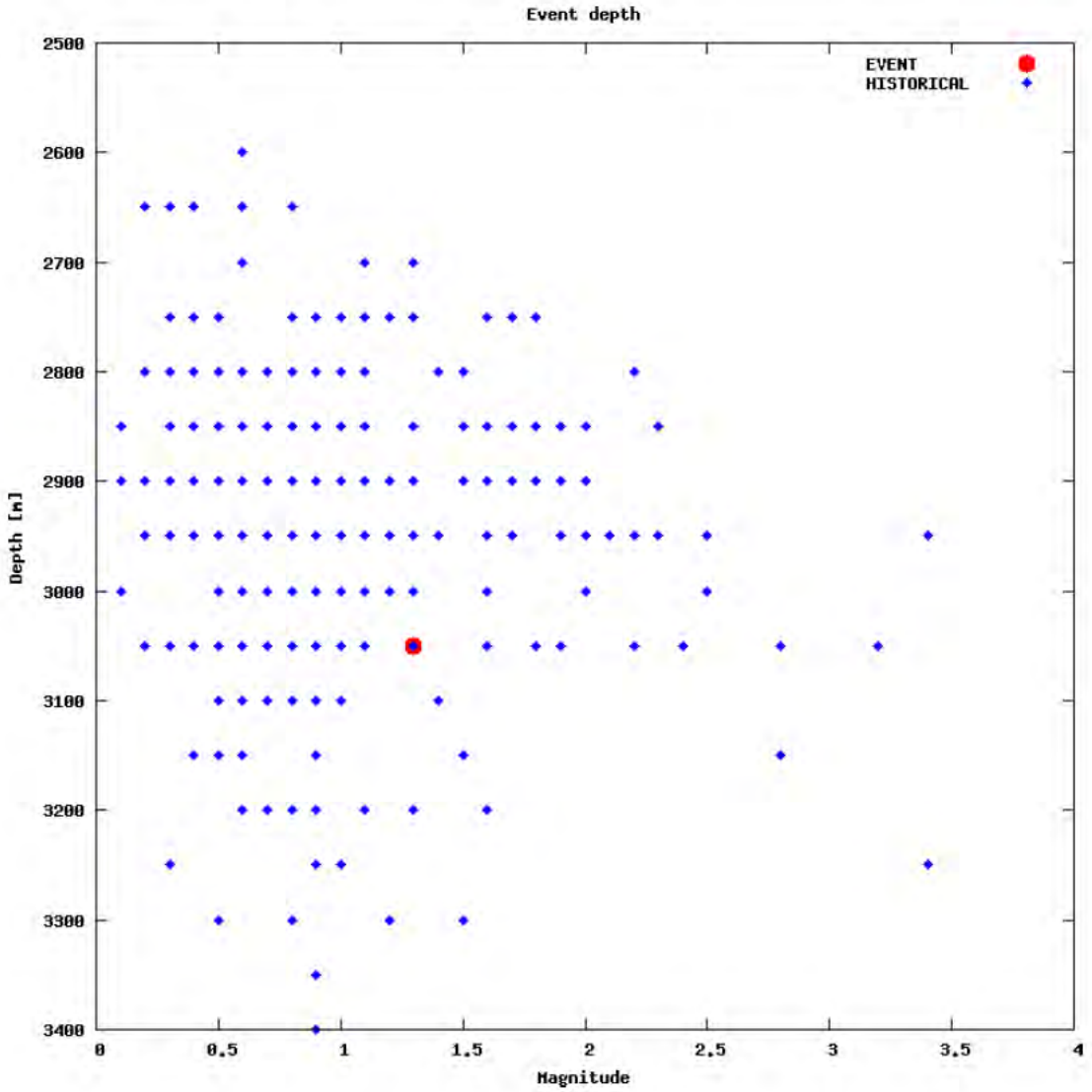

Event location - Map

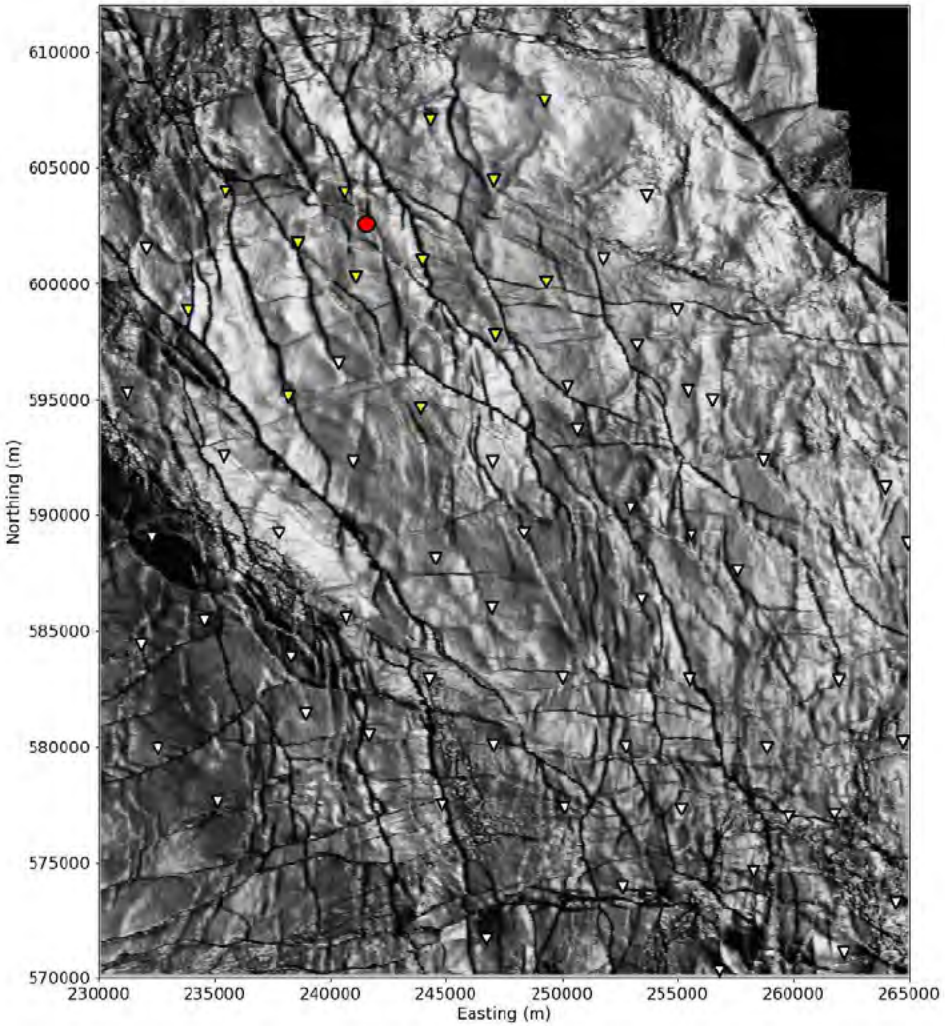

Event location and depth (initial)

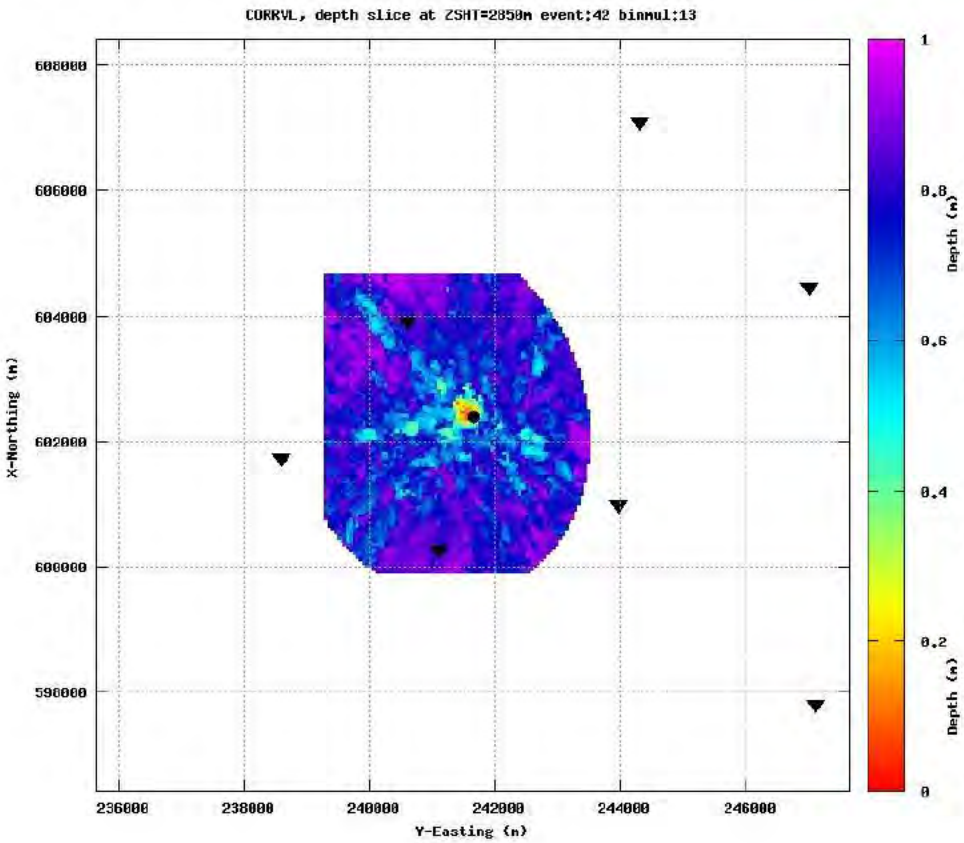

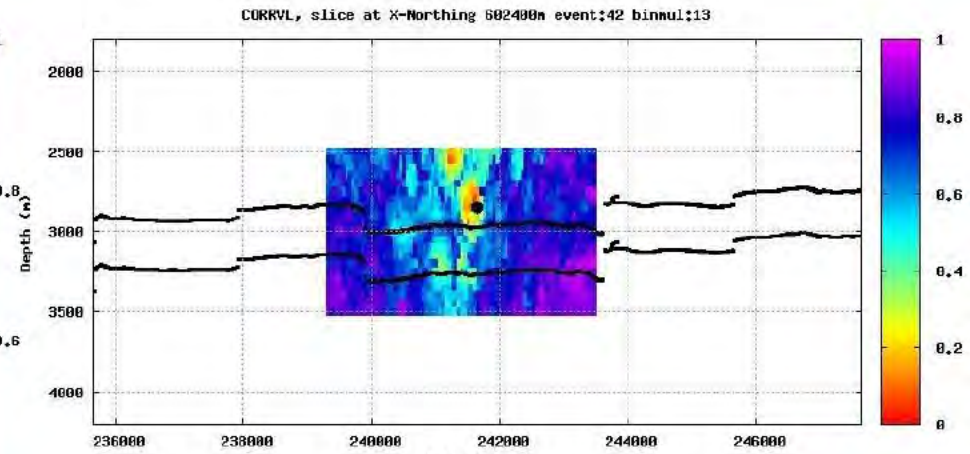

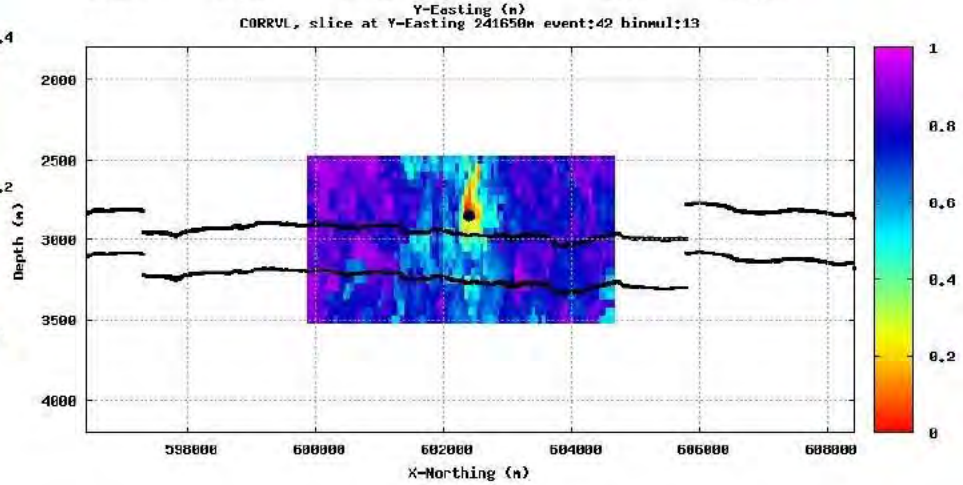

Event location and depth (alternative)

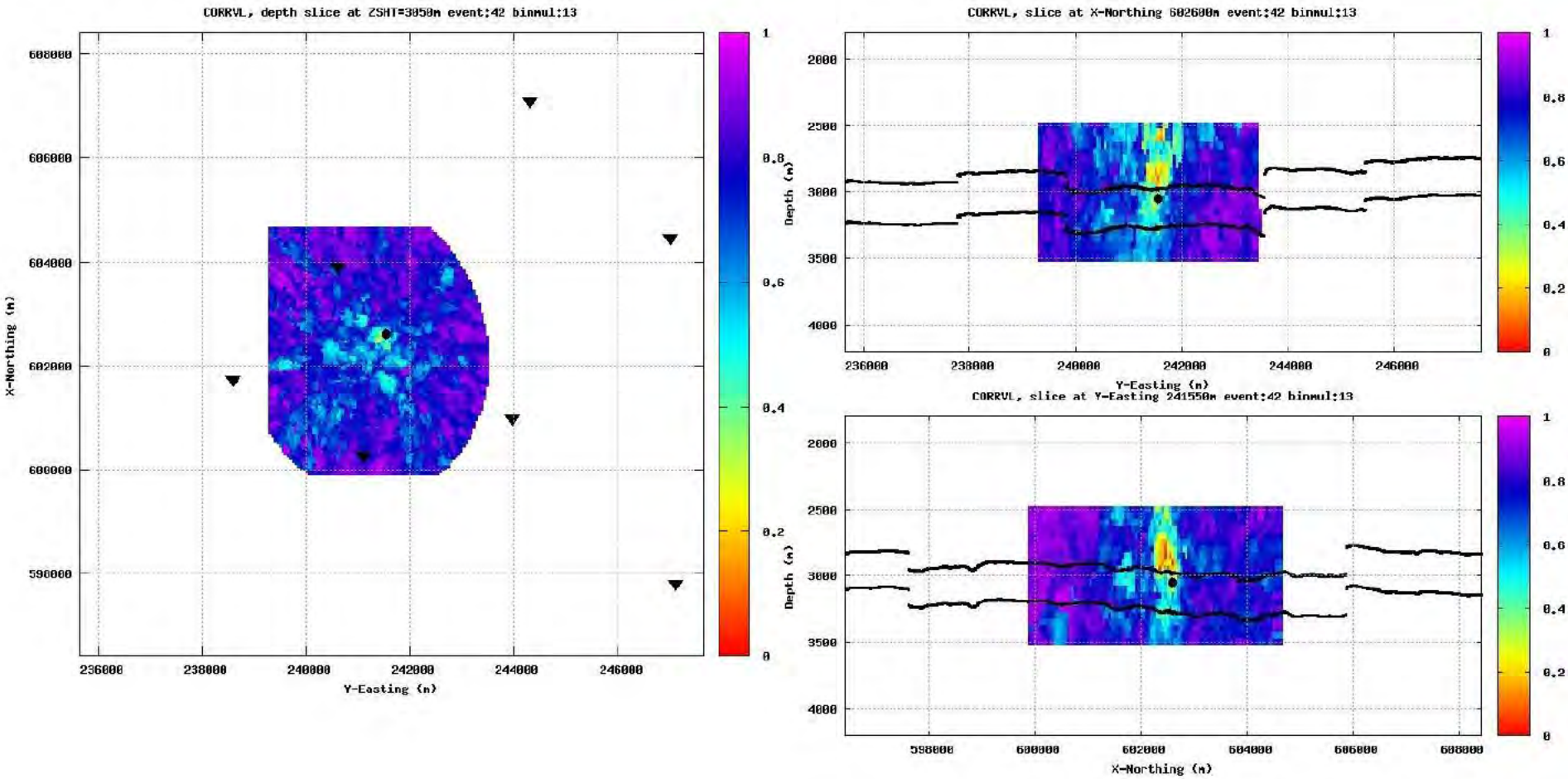

Moment tensor

Double-coupled part

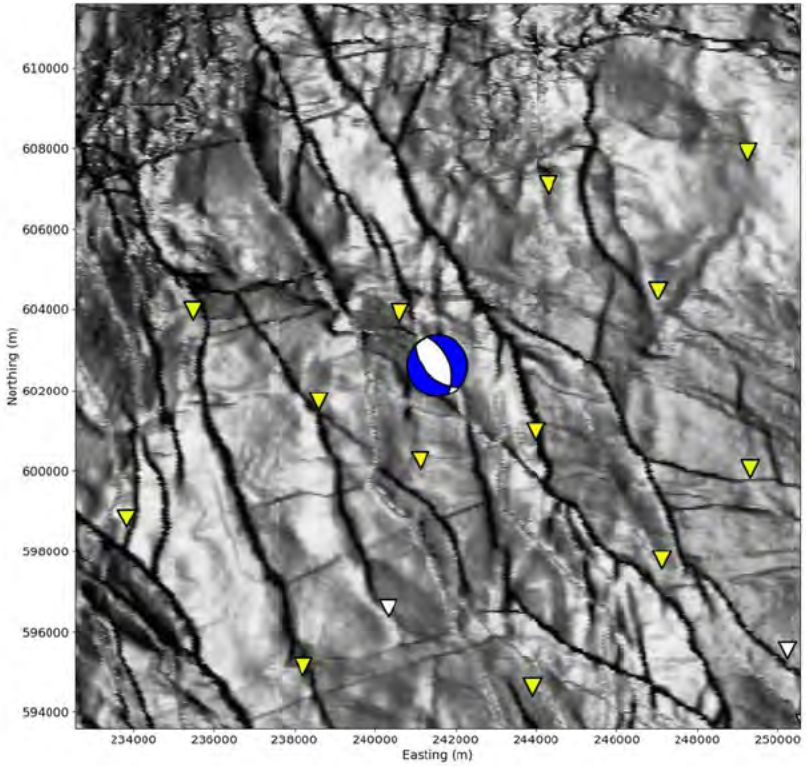

Full

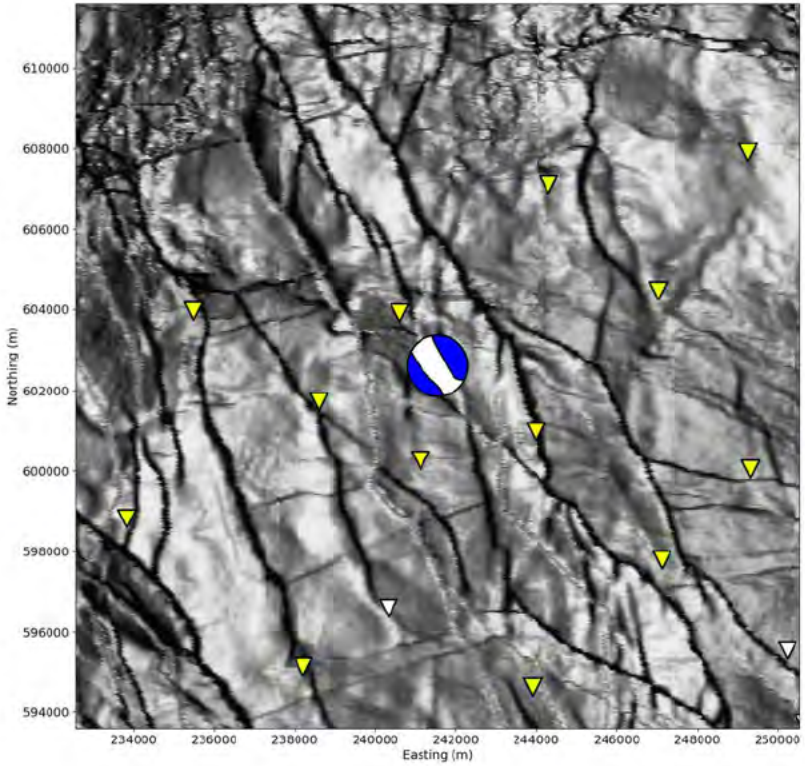

Moment Tensor: Decomposition

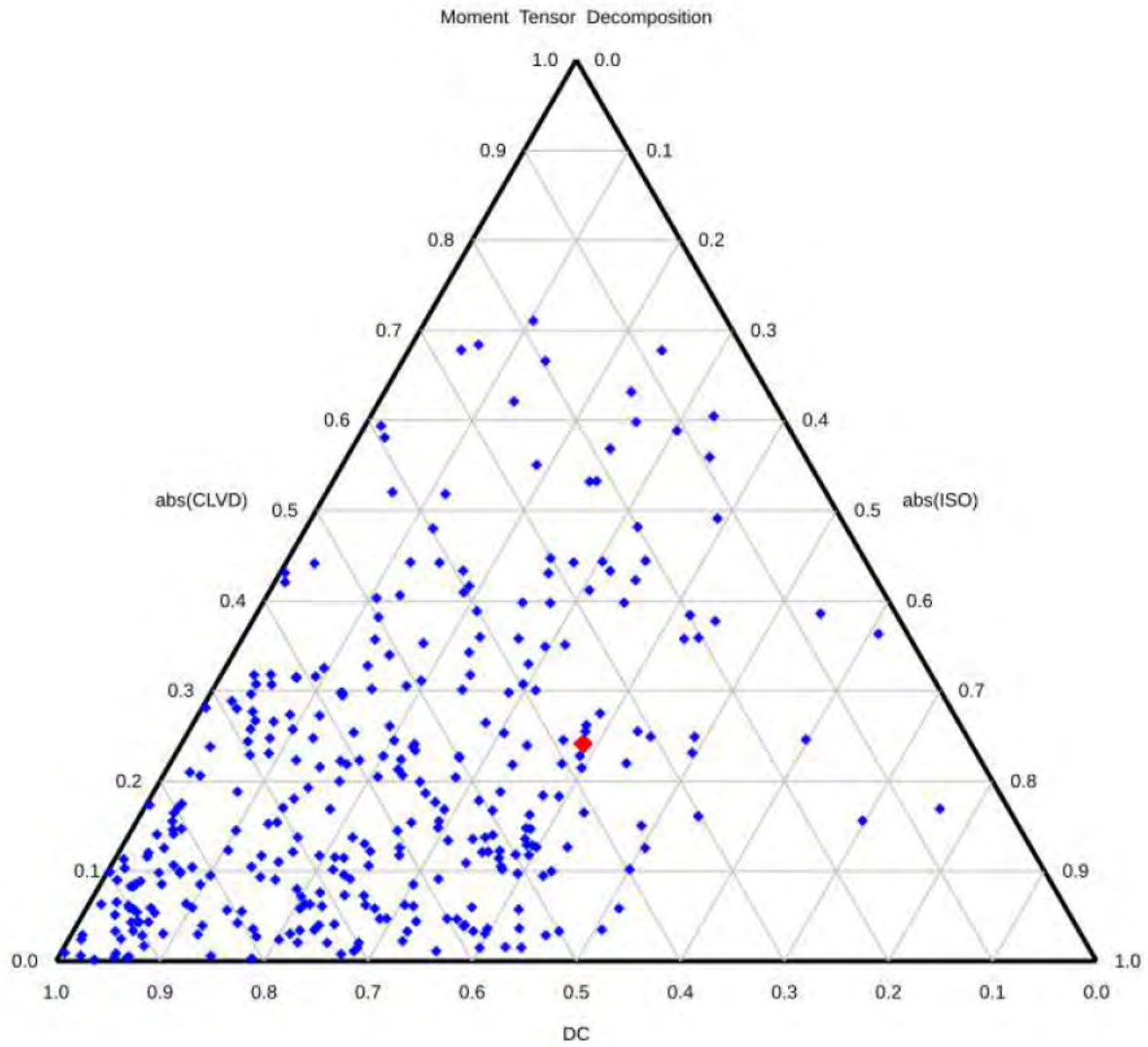

Field data traces

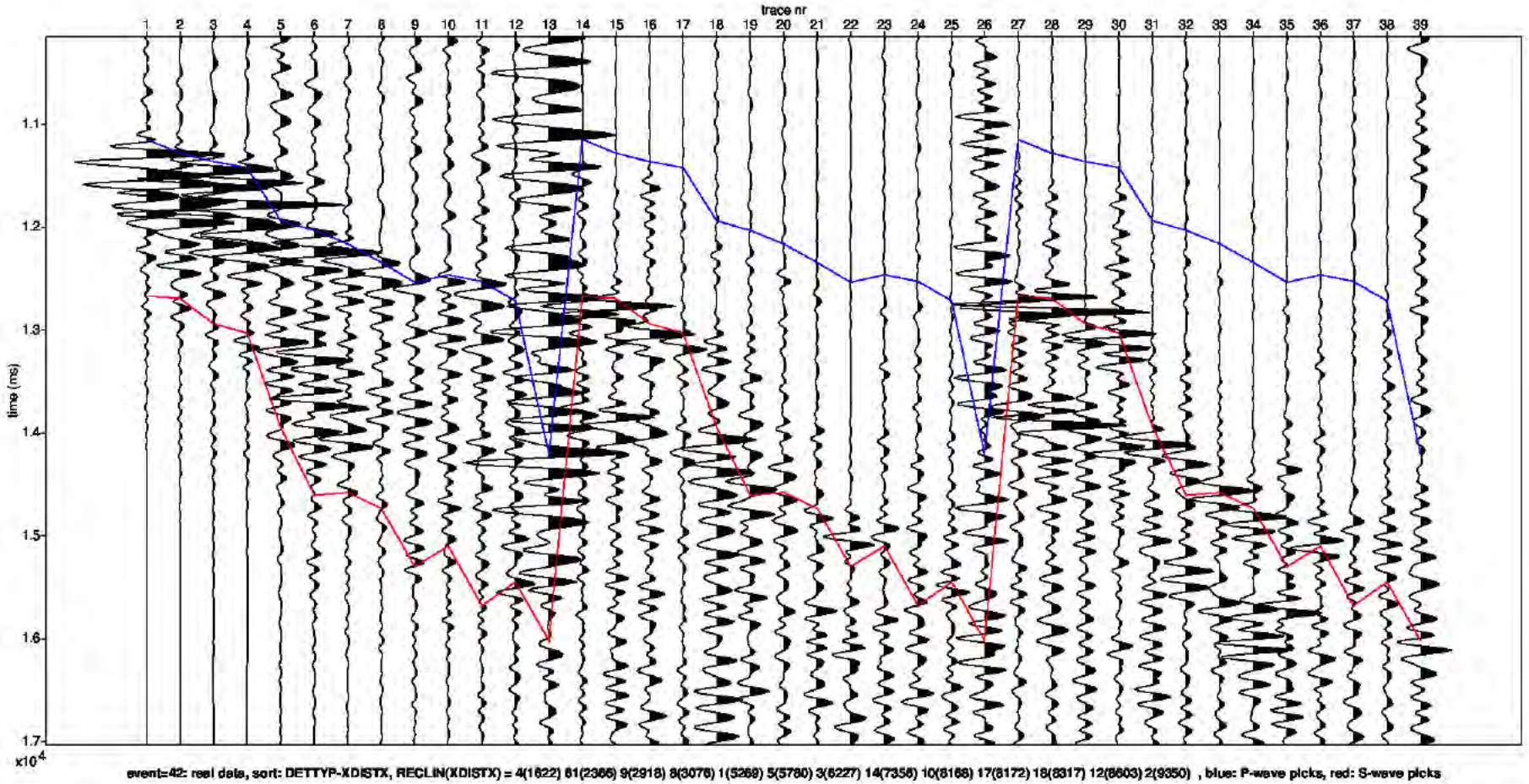

Modelled data traces

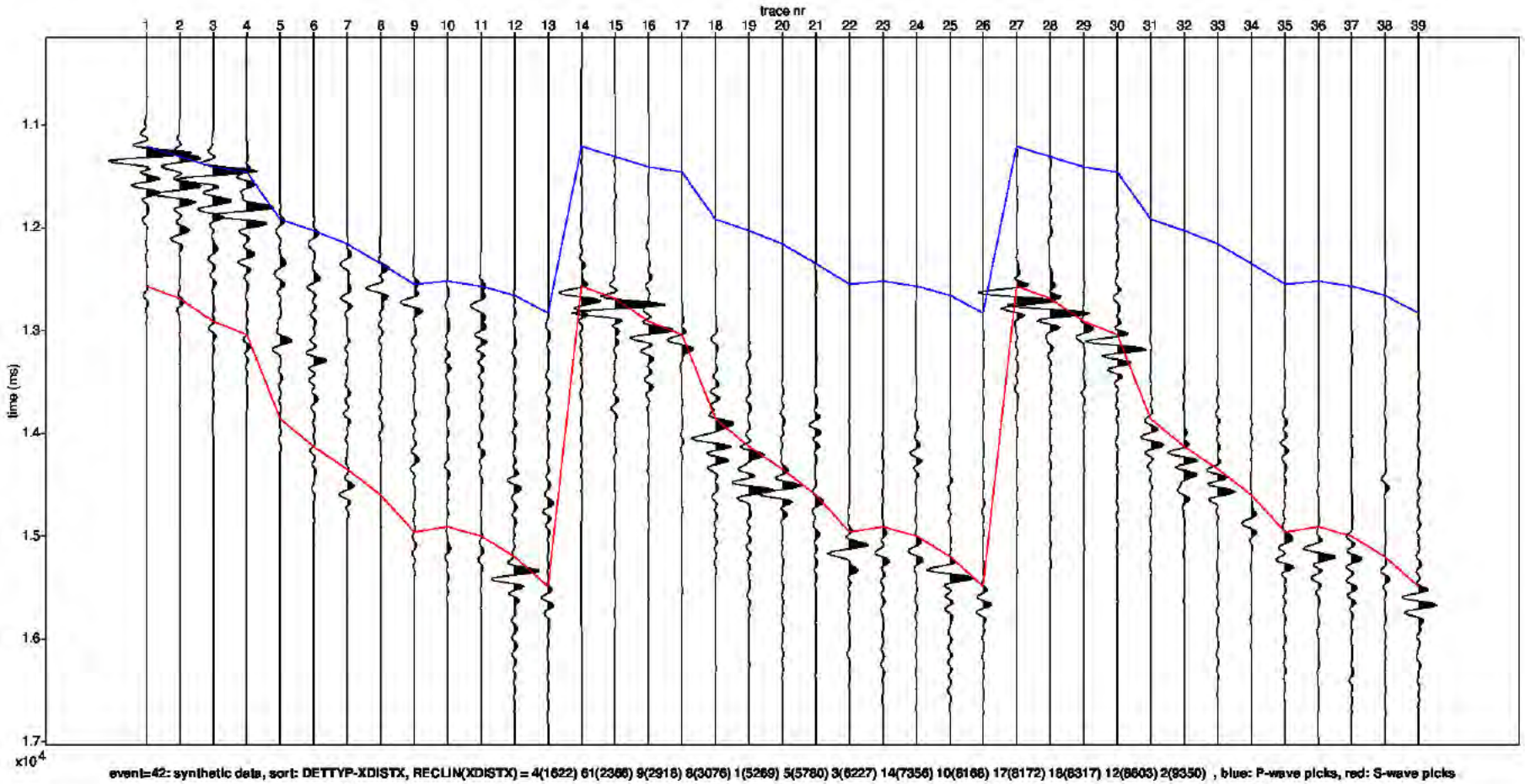

Appendix - Figure Captions

Page

3 Detailed parameter summary for the event. Both primary and secondary focal plane solutions are provided from the moment tensor inversion.

4 Magnitude summary. Prior years are displayed as a “heat map” where the number of events for a given magnitude is displayed per grid cell. The current event is displayed in red.

5 Regional map showing the historical events from KNMI (1986-2019) in blue and the location of the current event in red.

6 Event depth summary. Depths from our automatic workflow (2018-2020) are shown in blue and the current event depth is shown in red. The resolution of the vertical grid is 50m.

7 Event location details for the current event, superimposed on the top Rotliegend depth horizon. Station locations as shown as inverted triangles. Blue triangles are the actual stations used to locate the event whose epicentre is shown by the red dot.

8 QC displays extracted from the objective function for the initial event location. The colour attribute displayed is 1 minus the normalized cross correlation between observed and synthetic waveforms. Station locations are shown as black inverted triangles on the map and the event location is shown by the black dot (left plot). The west to east and north to south vertical profiles are shown on the right. The top and base reservoir are shown for reference as black lines.

Appendix - Figure Captions (continued)

Page

9 QC displays extracted from the objective function for the alternative event location. The colour attribute displayed is 1 minus the normalized cross correlation between observed and synthetic waveforms. Station locations are shown as black inverted triangles on the map and the event location is shown by the black dot (left plot). The west to east and north to south vertical profiles are shown on the right. The top and base reservoir are shown for reference as black lines.

10 Moment tensor inversion results for the event. The double couple portion of the moment tensor is shown on the left and the full moment tensor is displayed on the right. Station locations used in the inversion are shown as inverted triangles.

11 Ternary diagram showing the moment tensor decompositions into relative double-couple(DC), isotropic (ISO) and compensated linear vector dipole (CLVD) contributions. The automatic Shell events (2018-2020) are shown in blue and the current event is highlighted in red.

12 Observed traces for each station and each component. The automatic picks for the P- and S-waves are indicated by the blue and red lines respectively.

13 Modelled waveform data for each station and each component. The automatic picks for the P- and S-waves are indicated by the blue and red lines respectively.

NAM